ABSTRACT

Title of Dissertation: ARSENIC(III) SPECIATION IN SULFIDIC- AND CARBONATE-CONTAINING WATERS; THIOARSENITES AS LIGANDS FOR Ag(I), Pb(II) AND Hg(II)

Carla Sue Neuberger, Doctor of Philosophy, 2004

Dissertation Directed By: Professor George R. Helz
Department of Chemistry and Biochemistry

This dissertation has two objectives; the first is to investigate speciation of three d^{10} metals (Ag(I), Hg(II) and Pb(II)) in sulfidic solutions containing As(III) to determine if thioarsenite could act as a ligand for the metals. Second, a hypothesis that As(III) forms strong complexes with bicarbonate is investigated.

The solubility of As in sulfidic solutions (10^{-4}-10^{-3} M) equilibrated with As_2S_3+S at near-neutral pH (6.95-7.95) was measured and compared to the solubility of As in binary and ternary assemblages. Three species, $AsS(HS)(OH)^-$, $As(OH)_3$ and $H_2As_3S_6^-$, explain As speciation: $0.5As_2S_3 + 3H_2O \Leftrightarrow As(OH)_3 + 1.5H_2S$, pK=12.58, $1.5As_2S_3 + 1.5H_2S \Leftrightarrow H_2As_3S_6^- + H^+$, pK=6.20±0.77 and $0.5As_2S_3 + H_2O + 0.5H_2S \Leftrightarrow AsS(HS)(OH)^- + H^+$ pK=8.74±0.09.

The solubility of As and Ag in sulfidic solutions (10^{-4}-10^{-3} M) equilibrated with two Ag-As-S assemblages at near-neutral pH (6.89-8.37) was measured. The As

species that explained As_2S_3+S solubility also explained solubilities in the Ag-As-S system.

The silver solubility was explained by six species: $0.5Ag_2S_{(s)} + 1.5\ HS^- + 0.5\ H^+ \Leftrightarrow Ag(HS)_2^-$, pK=0.406±0.41; $Ag_2S_{(s)} + 2\ HS^- \Leftrightarrow Ag_2S(HS)_2^{2-}$, pK=4.78; $0.5Ag_2S_{(s)} + 0.5\ HS^- + 0.5\ H^+ \Leftrightarrow Ag(HS)$ pK=2.11±0.21; $0.5Ag_2S_{(s)} + Cl^- + 0.5\ HS^- + 0.5\ H^+ \Leftrightarrow Ag(Cl)(HS)^-$, pK=-1.09±0.20; $0.5Ag_2S_{(s)} + (x-1)S° + 0.5\ HS^- \Leftrightarrow AgS_x^- + 0.5\ H^+$, pK=8.51±0.19 and $Ag^+ + AsS(HS)(OH)^- \Leftrightarrow AgAsS(HS)(OH)^o$, pK=-17.17 ±0.20.

As shown by the last equilibrium expressions, dithioarsenite ($AsS(HS)(OH)^-$) is a strong ligand for Ag(I). Two other ternary systems, HgS+As_2S_3+S and PbS+As_2S_3+S, were investigated but the solubility of Hg^{2+} and Pb^{2+} were not significantly enhanced when arsenic was present. The order of stability of the metal-thioarsenite complexes agrees with predictions by Tossell (2000). The ΔG_F^o of natural orpiment was calculated to be -80.8±1.6.

The solubility of As_2O_3 in concentrated bicarbonate solutions at near-neutral pH is enhanced to a small, but statistically significant degree compared to the solubility in chloride solutions of the same ionic strength. This effect is attributed to one complex: $As(OH)_3 + HCO_3^- \Leftrightarrow As(OH)_2CO_3^-$, pK=0.57±0.15. The small constant suggests that As(III)-carbonate complexes will be negligible at carbonate concentrations found in nature.

ARSENIC(III) SPECIATION IN SULFIDIC- AND CARBONATE-CONTAINING WATERS; THIOARSENITES AS LIGANDS FOR Ag(I), Pb(II) AND Hg(II)

By

Carla Sue Neuberger

Dissertation submitted to the Faculty of the Graduate School of the
University of Maryland, College Park, in partial fulfillment
of the requirements for the degree of
Doctor of Philosophy
2004

Advisory Committee:
Professor George R. Helz, Chair/Advisor
Professor Neil Blough
Professor Allen Davis
Professor Bryan Eichhorn
Professor John Tossell

ACKNOWLEDGEMENTS

This work would not have been possible with the contributions and support of some very special people.

I would first like to than my husband, Brett, who has given me so much love and support throughout the years. Without his constant encouragement and patience I could not have completed my degree.

I would also like to thank my advisor, Dr. George Helz, for his guidance and insight. He is truly the best mentor I have ever had and his devotion to learning is inspiring.

I would also like to thank my family, Paula, Bill, Sean and James, for their love and support over the years.

I would also like to thank Mr. Mike Nabozny, who was an undergraduate student that helped complete the ternary studies involving HgS.

Many thanks go to the people at the University of Maryland who allowed me to use their laboratory space and equipment: Professor Allen Davis, Department of Civil and Environmental Engineering, for allowing me to use his Atomic Absorption Spectrophotometer; Professor Ann Wylie, Department of Geology, for her help with polishing and ore microscopy and Dr. Phil Piccoli, Department of Geology, for his help with electron microscopy.

TABLE OF CONTENTS

TABLE OF CONTENTS iii

LIST OF TABLES vii

LIST OF FIGURES x

Chapter I. Introduction 1

I.A. The Problem of Metal-Thioarsenite Interactions in Sulfidic Systems 1
I.A.1. Cu-Thioarsenite Complexing 1
I.A.2. Synergistic Solubilization Involving As, Pb, Hg, or Ag 3

I.B. Plan for This Dissertation 4

I.C. Metals in the Environment 5
I.C.1. Some Sulfidic Environments where Metals Could Interact 5
I.C.2. Arsenic 11
I.C.2.1. Sources and Toxicity 11
I.C.2.2. The Bangladesh/West Bengal Problem 13
I.C.2.3. Speciation of Arsenic in Seawater and Freshwater Systems 15
I.C.2.4. Speciation of As in Sulfidic Solutions 17
I.C.3. Lead 19
I.C.3.1. Sources and Toxicity 19
I.C.3.2. Lead in Aquatic Systems 20
I.C.3.3. Speciation of Pb in Sulfidic Solutions 21
I.C.4. Mercury 22
I.C.4.1. Sources and Toxicity 22
I.C.4.2. Mercury in Aquatic Systems 23
I.C.4.3. Speciation of Hg in Sulfidic Solutions 23
I.C.5. Silver 25
I.C.5.1. Sources and Toxicity 25
I.C.5.2. Silver in Aquatic Systems 27
I.C.5.3. Speciation of Ag in Sulfidic Solutions 28
I.C.5.4. The Ag-As-S System 30

Chapter II. As, Ag, Pb and Hg Solubility in Sulfidic Solutions 33

II.A. Introduction 33
II.A.1. Aim of Study 33

II.B. Methodology 34
II.B.1. Characterization of Materials 34
II.B.1.1. Characterization of Starting and Reacted Materials Containing As_2S_3, PbS and HgS 34

II.B.1.2. Synthesis and Characterization of Ag_2S, Ag_3AsS_3 and $AgAsS_2$ 47
II.B.1.2.1. Characterization of Ag_2S 47
II.B.1.2.2. Synthesis and Characterization of $AgAsS_2$ and Ag_3AsS_3 49
II.B.2. Mineral Dissolution 62
II.B.2.1. As_2S_3, As_2S_3+S, HgS+As_2S_3+S, PbS+As_2S_3+S, Ag Assemblage A and B in Sulfidic Solutions 62
II.B.3. Sample Analysis 65
II.B.4. Fitting/Modeling Strategy 72
II.B.4.1. Dissolution of As_2S_3, As_2S_3+S, HgS+As_2S_3+S and PbS+As_2S_3+S in Sulfidic Solutions 72
II.B.4.2. Modeling of the Activity of Sulfur in Experiments Containing As_2S_3 in Various Solutions of Polysulfides 74
II.B.5. Equilibration Rates and General Observations for Lead, Arsenic, Silver and Mercury 75

II.C. Results 79
II.C.1. Dissolution of Mineral Assemblages in Sulfidic Solutions 79
II.C.1.1. Dissolution of As_2S_3, As_2S_3+S, HgS+As_2S_3+S, PbS+As_2S_3+S, Ag Assemblage A and Ag Assemblage B 79
II.C.1.2. Dissolution of As_2S_3 in Various Polysulfide Solutions 88

II.D. Discussion 89
II.D.1 Speciation of Arsenic in Experiments with As_2S_3, As_2S_3+S, PbS+As_2S_3+S, HgS+As_2S_3+S, Ag Assemblage A and Ag Assemblage B in Sulfidic Solutions 89
II.D.1.1. Speciation of Arsenic in Experiments Containing As_2S_3 in Sulfidic Solution 89
II.D.1.2. Speciation of Arsenic in Experiments Containing As_2S_3, As_2S_3+S, PbS+As_2S_3+S, HgS+As_2S_3+S, Ag Assemblage A and Ag Assemblage B in Sulfidic Solutions 92
II.D.1.3. Free Energy of Formation for As_2S_3 104
II.D.2. Speciation of d^{10} Metals in Sulfidic Solutions Equilibrated with Silver, Lead, Mercury, Sulfur and Arsenic 106
II.D.2.1. Speciation of Silver in Sulfidic Solutions Equilibrated with Ag_2S, Ag_2S+S 107
II.D.2.1.1 Evidence for the $Ag(Cl)(HS)^-$ Species 112
II.D.2.1.2. Evidence for Polysulfide Species 114
II.D.2.1.3. Speciation Diagram for Ag_2S-S System 118
II.D.2.1.4. Two versus Three Coordination for Ag 121
II.D.2.2. Speciation of Silver in Sulfidic Solutions Equilibrated with Arsenic .122
II.D.2.2.1. Role of Sulfur in Ag Assemblage A and B Experiments 122
II.D.2.2.2. Silver Speciation in Sulfidic Solutions Equilibrated with Ag Assemblage A and Ag Assemblage B 125
II.D.2.2.3. Proposed Structure for $AgAsS(HS)(OH)^o$ and Silver Speciation Diagram 129
II.D.2.3. Speciation of Lead and Mercury in Sulfidic Solutions Equilibrated with PbS+As_2S_3+S or Hg+As_2S_3+S 131

II.D.2.3.1. Speciation of Mercury in Sulfidic Solutions Equilibrated with $HgS+As_2S_3+S$ 131
II.D.2.3.2. Speciation of Pb in Sulfidic Solutions Equilibrated with $PbS+As_2S_3+S$ 137
II.D.3. Critical Evaluation of Work 137

II.E. Conclusions 138

Chapter III. The Solubility of As_2O_3 in Carbonate Solutions 142

III.A. Introduction 142

III.B. Methodology 144
III.B.1. Materials 144
III.B.1.1. Recrystallization and Characterization of As_2O_3 144
III.B.1.2. Gasses and Solutions of Runs 148
III.B.1.3. Analytical Reagents and Standardization 149
III.B.1.3.1. PAO 149
III.B.1.3.2. PAO Standardization 149
III.B.1.3.3. Synthesis and Standardization of 0.05 M I_2 150
III.B.2. Experimental Procedures 150
III.B.2.1. Experimental Setup 150
III.B.3. Sampling 152
III.B.4. Analysis 152

III.C. Results 153
III.C.1. Measurement of Reversibility of Recrystallized As_2O_3 153
III.C.2. Solubility of Recrystallized As_2O_3 155
III.C.3. Identification of As-carbonate species from Raman Spectra 157

III.D. Discussion 160
III.D.1. Solubility Measurements 160
III.D.2. Determination of As-Carbonate Equilibrium Constant Expressions 161
III.D.3. Comparison of Carbonate Species through Computer Modeling 163
III.D.4. Comparison of $As(OH)_3$ Solubility with Previous Literature Values 166
III.D.5. Significance for As(III) in Natural Waters 167

Chapter IV. Conclusions 169

IV.A. Understanding As Chemistry in Sulfidic- and Carbonate-Containing Systems 169

IV.B. Future Work 173

Appendix I 175

Appendix II 180

Appendix III 183

Appendix IV 187

Appendix V 191

References 194

LIST OF TABLES

Table 1. Estimated Enthalpies (kJ/mol) for the Formation of $MAsS(HS)(OH)^{(x-1)}$ 4

Table 2. Metal Concentrations Found in the Landfill Leachate, Landfill Influenced Groundwater and Drinkable Groundwater Throughout Switzerland, Italy and France 7

Table 3. Summary of Some Heavy Metal Concentrations Found in Sediments and Overlying Water from Contaminated Harbors 10

Table 4. Summary of Arsenic Speciation for Experiments Involving the Solubility of As_2S_3 18

Table 5. Silver Speciation from Previous Solubility Studies with Silver 29

Table 6. Observed Peaks in the X-Ray Diffraction Pattern of Natural Orpiment Mineral 35

Table 7. Observed Peaks in the X-Ray Diffraction Pattern of the Dolomite Substrate 36

Table 8. Observed Peaks in the X-Ray Diffraction Pattern of the Sphalerite Particles 37

Table 9. Observed Peaks in the X-Ray Diffraction Pattern of Galena 40

Table 10. Observed Peaks in the X-Ray Diffraction Pattern of the $PbS+As_2S_3+S$ Assemblage After 30 days of Equilibration with a Sulfidic Solution 42

Table 11. Observed Peaks in the X-Ray Diffraction Pattern of the HgS 44

Table 12. Observed Peaks in the X-Ray Diffraction Pattern of the $HgS+As_2S_3+S$ Assemblage After 30 days of Equilibration with a Sulfidic Solution 46

Table 13. Observed Peaks in the X-Ray Diffraction Pattern of Ag_2S (acanthite) 48

Table 14. Observed Peaks in the X-Ray Diffraction Pattern of $AgAsS_2$ Starting Material. 50

Table 15. Observed Peaks in the X-Ray Diffraction Pattern of Ag_3AsS_3 Starting Material. 52

Table 16. Observed Peaks in the X-Ray Diffraction Pattern of Ag assemblage A after 30 days in Equilibration with a Sulfide Solution of 0.001 M Starting Total Sulfide, pH 8.10± 0.07. 54

Table 17. EDS Composition Data for Particles in Ag Assemblage A 56

Table 18. Observed Peaks in the X-ray Powder Diffraction Pattern of Ag assemblage B After 40 Days in Equilibration with a Sulfide Solution of 0.001 M Starting Total Sulfide, pH 7.59. 59

Table 19. EDS Composition Data for Particles from Ag assemblage B 61

Table 20. Starting Masses of Solids for Solubility Studies 64

Table 21. Graphite Furnace Program for Lead 66

Table 22. Graphite Furnace Program for Silver 67

Table 23. Reagent Concentrations and Dilution Factors Used to Determine Acid Labile Sulfide 68

Table 24. Comparison between Methods to Measure HS^- 73

Table 25. Dissolution of As_2S_3 in Sulfidic Solutions 80

Table 26. Dissolution of As_2S_3+S in Sulfidic Solutions 81

Table 27. Data from the Dissolution of PbS+As_2S_3+S in Sulfidic Solutions 82

Table 28. Data from the Dissolution of HgS+As_2S_3+S in Sulfidic Solutions 83

Table 29. Data from the Dissolution of Ag_2S in Sulfidic Solutions 83

Table 30. Data from the Dissolution of Ag_2S and S in Sulfidic Solutions 84

Table 31. Data from the Dissolution of Ag Assemblage A in Sulfidic Solutions 85

Table 32. Data from the Dissolution of Ag Assemblage B in Sulfidic Solutions 86

Table 33. Experimental Solution Scheme for the Dissolution of As_2S_3 in Solutions of Varying Degrees of Sulfur Saturation 88

Table 34. Data for the Dissolution of As_2S_3 in Solutions with Varying Degrees of Sulfur Saturation 89

Table 35. Free Energy Data for As(III) and Ag(I) Complexes 107

Table 36. Log β For Individual Species 113

Table 37. Solubility Reactions Used in Chapters II. 141

Table 38. X-Ray Powder Diffraction of Recrystallized As_2O_3..... 146

Table 39. X-Ray Diffraction Pattern of the Reacted Material from the Flask Containing 0.355 m NaCl/0.357 m $NaHCO_3$ in a CO_2 Atmosphere. 147

Table 40. Experimental Conditions for the Equilibration of As_2O_3 for Control, Undersaturated and Oversaturated Solutions. 149

Table 41. Solubility of Undersaturated and Oversaturated Solution to Determine Equilibrium of the Arsenic-carbonate System. 154

Table 42. Exp. Results for Solubility of As_2O_3 in NaCl and $NaHCO_3$ Solutions.... 156

Table 43. Comparison of Filtered and Centrifuged Samples..... 158

Table 44. Comparison of Calculated Equilibrium Constants for $As(OH)_2CO_3^-$, $As(CO_3)_2^-$ and $AsCO_3^+$ 164

Table 45. Experimental Conditions for the Absorbance of a Thioarsenite Species 177

LIST OF FIGURES

Figure 1. Ternary phase diagram for the silver-arsenic-sulfur system. 31

Figure 2. X-ray diffraction pattern for natural orpiment (As_2S_3)..... 35

Figure 3. X-ray pattern of white substrate from natural orpiment.. 36

Figure 4. Black particles on natural orpiment mineral.. 37

Figure 5. X-ray diffraction pattern for galena, PbS.. 40

Figure 6. X-ray powder diffraction pattern of PbS+As_2S_3+S assemblage after 30 days in equilibrium with a sulfidic solution ($1.65x10^{-3}$ M total sulfide, pH=7.5). 41

Figure 7. X-ray diffraction pattern for cinnabar, HgS.. 43

Figure 8. X-ray powder diffraction pattern of HgS+As_2S_3+S assemblage after 30 days in equilibrium with a sulfidic solution ($1.65x10^{-3}$ M total sulfide, pH=7.5). 45

Figure 9. X-ray power diffraction pattern of Ag_2S.. 48

Figure 10. X-ray diffraction pattern for the raw $AgAsS_2$ starting material. 50

Figure 11. X-ray diffraction pattern for the raw Ag_3AsS_3 starting material. 51

Figure 12. X-ray powder diffraction pattern of Ag assemblage A after 30 days in equilibration with a sulfide solution of 0.001 M starting total sulfide, pH 8.10± 0.07..... 54

Figure 13. Electron backscattering image of an Ag assemblage A sample that was reacted with a sulfidic solution for at least 30 days.. 55

Figure 14. X-ray powder diffraction pattern of Ag assemblage B after 40 days in equilibration with a sulfide solution of 0.001 M starting total sulfide, pH 7.59.... 58

Figure 15. Electron backscattering image of Starting Material B that was reacted with a sulfidic solution for at least 30 days..... 60

Figure 16. Schematic of titration curves for potentiometric titrations in the absence and presence of As_2S_3. 71

Figure 17. Equilibration of PbS+As_2S_3+S in replicate ampoules with 20 mL of solution containing 3.5 ± 1.5 mM total sulfide, 0.0071 M MOPS buffer, 0.01M NaCl at pH 7.73.. 77

Figure 18. Equilibration of Ag_2S, S, As_2S_3 in replicate ampoules with 20 mL of a solution containing 0.0071 M MOPS buffer, 1 x 10^{-3} M HS^-, pH approximately 7.42..... 78

Figure 19. Comparison of the solubilities of lead and arsenic in the ternary solubility study..... 87

Figure 20. Fit of the As_2S_3 data in sulfidic solutions..... 91

Figure 21. Fit of the arsenic solubility for As_2S_3, As_2S_3-S, $PbS+As_2S_3+S$ and $HgS+As_2S_3+S$ data in sulfidic solutions..... 95

Figure 22. Fit of Eary (1992) data (As_2S_3 in sulfidic solutions)..... 97

Figure 23. Fit of Webster (1990) data (As_2S_3 in sulfidic solutions)..... 99

Figure 24. Fit of arsenic solubility for the As_2S_3, As_2S_3-S, $PbS+As_2S_3+S$, $HgS+As_2S_3+S$, Ag assemblage A and B data in sulfidic solutions..... 101

Figure 25. Calculated concentration of arsenic species in equilibrium with in orpiment in sulfidic solutions as a function of pH at 0.001 M total sulfide and total sulfide at pH 7.2..... 105

Figure 26. Fit of the silver sulfide data in sulfidic solutions..... 109

Figure 27. Comparison of the equilibrium constant of $Ag(Cl)(HS)^-$ to its theoretical value using the mixed ligand theory..... 113

Figure 28. Absorbance spectrum for a sulfidic solution equilibrated with Ag_2S and S at pH 10.41 and a total sulfide of 3.334 x 10^{-4} M..... 115

Figure 29. Fit of the silver sulfide data in sulfidic solutions..... 117

Figure 30. Comparison of Ag (I) and Hg(II) stability constants for common ligands at 25°C and an ionic strength of 0.05..... 119

Figure 31. Concentration of silver species as a function of pH at 0.001 M total sulfide for the equilibration of AgS_2-S in sulfidic solutions in 0.1 M Cl^- and 0.01 M Cl^-..... 120

Figure 32. Fit of the silver sulfide data in sulfidic solutions with three coordinate species..... 123

Figure 33. UV-Visible Spectra of Ag assemblage A (pH= 7.30, 0.316 mM Total Sulfide, 0.185 μM Ag, 0.161 mM As) and Ag assemblage B (pH=7.25, 0.834 mM Total Sulfide, 0.198 μM Ag, 0.0926 mM As)..... 124

Figure 34. Fit of the Ag assemblage (A and B) data in sulfidic solutions.. 127

Figure 35. Proposed structure of AgAsS(HS)(OH)° from Tossell (2000). 130

Figure 36. Silver speciation diagram for the equilibration of Ag assemblage A and Ag assemblage B in solutions containing 10^{-3} M total sulfide, 10^{-5} M total arsenic, 10^{-7} M total silver and 10^{-1} M Cl^- or Left:10^{-3} M Cl^-. 132

Figure 37. Paquette Base Model and Adjusted Paquette Base Model for Hg Speciation for $HgS+As_2S_3+S$ Experiments in a Sulfidic Solution.. 134

Figure 38. Jay Base Model for Hg Speciation in $HgS+As_2S_3+S$ equilibrated in a sulfidic solution. The pK's refer to the reactions in the text..... 136

Figure 39. X-Ray power diffraction of recrystallized As_2O_3..... 146

Figure 40. X-Ray diffraction pattern of reacted material from flask containing 0.355 m NaCl/0.357 m $NaHCO_3$ in a CO_2 atmosphere.. 147

Figure 41. Experimental Setup for Runs 1 and 2.. 151

Figure 42. Equilibrium from under- and oversaturation at room temperature of arsenic-carbonate system.. 154

Figure 43. Raman spectrum from a solution in which As_2O_3 reacted with a 1.05 m $NaHCO_3$ solution.. 159

Figure 44. Arsenic-Carbonate Models including the species $As(OH)_2(CO_3)^-$, $As(CO_3)_2^-$ and $As(CO_3)^+$. Log (As_{Calc}/As_{Obs}) as a function of pH and HCO_3^- Concentration. 165

Figure 45. UV-Visible spectra of orpiment equilibrated with S^o in a sulfidic solution. pH=7.23, total sulfide = $2.94x10^{-3}$, [As]=$7.88x10^{-4}$.. 176

Figure 46. Formation of As peak followed over time with UV-Visible spectroscopy. Initial As(III) concentration was $3x10^{-4}$ M and the initial HS- concentration was $3x10^{-3}$ M, pH=8.09..... 177

Figure 47. UV-Visible spectra of As(V)-S and As(III)-S species.. 179

Chapter I. Introduction

In this dissertation I will first discuss the complexation of As(III) with Hg, Pb and Ag in sulfidic systems. I will provide experimental evidence that supports quantum mechanical predictions, by Tossell (2000), that Ag forms a stable metal-thioarsenite complex, but Hg does not form a stable metal-thioarsenite complex. A lead-thioarsenite experiment was also conducted but the results were inconclusive. Finally, I will discuss the role bicarbonate plays in complexing As(III).

I.A. The Problem of Metal-Thioarsenite Interactions in Sulfidic Systems

I.A.1. Cu-Thioarsenite Complexing

The first example of metal-thioarsenite interactions was presented by Clarke and Helz (2000), in which the solubility of the three-phase assemblage containing digenite ($Cu_{1.8}S$), a digenite-covellite mixture ($Cu_{1.8}S$-CuS) and Cu_3AsS_4 was studied in sulfidic solutions. They found higher Cu solubility than could be explained by Cu-HS complexing and concluded that the CuH_2AsOS_2 species accounted for the solubility of copper and arsenic. In other words, there was a synergistic solubilization between copper and arsenic that promoted the solubility of each element. In their experiment, the copper solubility was enhanced by several orders of magnitude when the CuH_2AsOS_2 complex was formed compared to solubility studies with just CuS and $Cu_{1.8}S$. They concluded that dithioarsenite ($AsS(HS)(OH)^-$) is a very strong ligand for the copper ion with a log K of +19.82.

Two explanations have been offered for why $AsS(HS)(OH)^-$ is such a strong ligand. The first is that $AsS(HS)(OH)^-$ can function as a soft, multidentate chelating

agent (Clarke and Helz, 2000). Soft bases, like $AsS(HS)(OH)^-$ or HS^-, are highly polarizable and interact with soft acids that are also highly polarizable and have d^8 or d^{10} electron configurations (Pearson, 1963).

Tossell (2000a) offers a different explanation for the enhanced stability of the CuH_2AsOS_2 complex. From quantum mechanical calculations he found evidence that Cu forms a bond to As. The CuH_2AsOS_2 complex has two coordinating S atoms and an electron rich As center. The OH^- group on the As stabilizes a direct bond to copper, producing a very stable complex. It was found that if the OH^- group were replaced by F^-, the complex would become unstable due to the breakage of the Cu-As bond.

The ability of metals to form strong bonds with sulfur containing ligands can be explained by examining their electron configurations. Metals with d^{10} electron configurations, Cu(I), Hg(II) or Ag(I) owe their stability to an ability to back donate electrons from filled d orbitals to unoccupied d orbitals on sulfur, thus forming strong π bonds (Pearson ,1963; Nickless, 1968; Clarke, 1998; Renders and Seward, 1989).

Arsenic can also form strong bonds with sulfur. As(III) (s^2) is very stable because of (s,p^3) hybridization, which lowers the symmetry of the system. Two valence electrons occupy one of the hybrid orbitals, which can be considered nonbonding orbitals. The other three empty orbitals can combine with the filled orbitals of sulfide, so backbonding will stabilize the metal-thioarsenite complexes (Nickless, 1968).

I.A.2. Synergistic Solubilization Involving As, Pb, Hg, or Ag

The stability of CuH_2AsOS_2 could enhance the solubility of copper and arsenic in sulfidic systems, which could have detrimental implications for groundwater contamination. Enhanced solubility could provide the means for Cu and As to become mobile and thus bioavailable. The question then arises, will other d^{10} metals have the same stability with thioarsenites and promote the synergistic solubilization of the metal in question with arsenic?

Tossell (2000) used quantum mechanical calculations to provide enthalpies of formation for bisulfide and thioarsenite complexes with several metals:

$$M(H_2O)_2^{x} + AsS(HS)(OH)^{-} \rightarrow MAsS(HS)(OH)^{(x-1)} + 2H_2O \quad (1)$$

$$M(H_2O)_2^{x} + 2HS^{-} \rightarrow M(HS)_2^{(x-2)} + 2H_2O \quad (2)$$

He proposed that his calculated enthalpies for these reactions are approximations of free energies of reaction. His estimated enthalpies in Table 1 predict which metals would form strong metal-thioarsenite complexes. The ligands, HS^- or $AsS(HS)(OH)^-$, can be thought to be competing for the metal, and the complex with the more negative free energy will predominate if the two ligands are present at equal concentrations. The net enthalpy can be calculated by subtracting Equation 2 from Equation 1. Cu(I), Ag(I) and Au(I) are predicted to form comparatively stable $MAsS(HS)(OH)^{(x-1)}$ complexes (Table 1). It is of interest to note that Tl^+ is also favored to form a Tl-thioarsenite complex.

Table 1. Estimated Enthalpies (kJ/mol) for the Formation of $MAsS(HS)(OH)^{(x-1)}$

Cation	$MAsS(HS)(OH)^{(x-1)}$[1]	$M(HS)_2^{(x-2)}$[2]	Net Enthalpy[3]
Cu^+	-115	-89	-26
Ag^+	-71	-52	-19
Au^+	-189	-173	-16
Zn^{2+}	-13	-1055	+1042
Cd^{2+}	-28	-1003	+975
Hg^{2+}	-89	-1129	+1040
Tl^+	+140	+459	-319
Pb^{2+}	-177	-483	+306

1. $M(H_2O)_2^x + AsS(HS)(OH)^- \rightarrow MAsS(HS)(OH)^{(x-1)} + 2H_2O$
2. $M(H_2O)_2^x + 2HS^- \rightarrow M(HS)_2^{(x-2)} + 2H_2O$
3. $M(HS)_2^{(x-2)} + AsS(HS)(OH)^- \rightarrow MAsS(HS)(OH)^{(x-1)} + 2HS^-$

x are the charges of the metal ions

Tossell (2000)

I.B. Plan for This Dissertation

Solubility experiments will be done to determine if the thioarsenite ligand has the ability to complex other metals forming stable metal-thioarsenite complexes. Chapter II reports on a number of topics. The first is the effect that elemental sulfur has on the solubility and speciation of As_2S_3 in sulfidic solutions. A full discussion on the speciation of arsenic is also presented for all the experiments that have arsenic as a component (As_2S_3, As_2S_3+S, HgS-S-As_2S_3, PbS-S-As_2S_3 and Ag-As-S assemblages). Chapter II then reports on the effect that elemental sulfur has on the solubility of Ag_2S in sulfidic solutions. The solubility of silver in the Ag_2S+S experiment will then be compared to the solubility of silver from two silver assemblages. This will determine if the presence of arsenic increases the solubility of silver in the assemblages in sulfidic solutions, forming a silver-thioarsenite complex. Another goal of Chapter II is to determine the free energy of formation of As_2S_3.

Finally, Chapter II compares the solubility of two other ternary assemblages ($HgS\text{-}S\text{-}As_2S_3$ and $PbS\text{-}S\text{-}As_2S_3$) to HgS and PbS, respectively, to determine if the presence of arsenic increases the solubility of Pb and Hg, forming lead or mercury thioarsenite complexes.

Chapter III deals with the effect bicarbonate has on As_2O_3 solubility. This chapter tests a hypothesis first proposed by Kim et al. (2000) and refined by Tossell (2004) that HCO_3^- can be responsible for elevated As(III) levels in groundwaters. The solubility of As_2O_3 in concentrated bicarbonate solutions is compared to the solubility of As_2O_3 in concentrated NaCl solutions at room temperature, where both solutions had near neutral pH's.

In the remainder of this chapter, some background information is provided on the geochemistry and solution chemistry of As, Pb, Hg and Ag. Specifically, the sources, toxicity and aqueous speciation of the elements are reviewed.

I.C. Metals in the Environment

I.C.1. Some Sulfidic Environments where Metals Could Interact

If thioarsenites are shown to enhance the solubility of d^{10} metals then sulfidic aqueous environments where both As and d^{10} metals are abundant could serve as sources of the elements for the surrounding environment. Examples would be landfills or contaminated sediments in industrial harbors. In these sulfidic environments the hazardous metals may become mobile, enter groundwater systems and thus be bioavailable.

Landfills are constructed to contain waste rather than treat waste. However, there has been evidence that landfills are sources of contamination to their surrounding environments. Mantei and Coonrod (1989) present evidence that a sanitary landfill in Missouri releases silver, zinc and copper into two streams adjacent to the landfill. The stream that drains the landfill directly (stream 1) had a mean sediment metal concentrations of 1.71±0.41 μg/g Ag and 32.88±1.91 μg/g Pb. Stream 2, which is located above stream 1 and does not drain the landfill directly, had a mean sediment metal concentrations of 0.75±0.18 μg/g Ag, 33.32±1.93 μg/g Pb. The Ag is elevated in comparison with the control stream, which is 1.4 km east of the landfill, and had mean sediment metal concentrations of 0.37±0.09 μg/g Ag and 37.60±2.18 μg/g Pb. It was concluded that drainage from the landfill directly enhanced the silver concentration in the sediment of the two streams adjacent to the landfill. Lead was not enhanced in the stream sediment, possibly because it was absorbed or precipitated within the landfill itself.

Looser et al. (1999) sampled 41 leachates from landfills and when possible groundwaters next to landfills throughout Switzerland, Italy and France. Table 2 presents metal concentrations found in the landfill leachate, landfill-influenced groundwater and drinkable groundwater. Silver was undetectable in natural groundwater but was present in landfill-influenced groundwater, indicating that the landfill was discharging Ag to surrounding groundwater. The arsenic concentration is higher in the natural groundwater compared to landfill influenced groundwater and may derive from a natural source. Lead is also elevated in landfill-influenced groundwater, but may come from other anthropogenic origins such as fossil fuels.

Gade et al. (2001) conducted a study on an open landfill in Bavaria. Currently the landfill is under oxidizing conditions and modeling predicts that when the landfill is closed the oxidizing conditions will remain due to the low bacterial activity of the leachate and the presence of waste that has a high oxygen content. Average concentrations of metals in the leachate were 0.0157 ppm (1.5×10^{-7}M) Ag, 2.19 ppm (2.9×10^{-5}M) As, 0.005 ppm (2.5×10^{-8}M) Hg and 0.00651 ppm (3.1×10^{-8}M) Pb. It is important to note that in both cases the As concentration is comparatively larger than the metal concentrations, a necessary but not significant criterion if As is to act as a ligand fir Ag.

Table 2. Metal Concentrations Found in the Landfill Leachate, Landfill Influenced Groundwater and Drinkable Groundwater Throughout Switzerland, Italy and France

	Concentration of Metals (nM)			
	Ag	Pb	As	Hg
Natural groundwater	-	15	130	-
Landfill leachate	93	140	530	15
Landfill influenced groundwater	74	39	40	0.75

Looser et al. (1999)

Pit lakes are another aquatic environment in which metal and arsenic concentrations are high. Pit lakes form when open pit mines are closed. Pit lakes are usually more deep than wide and may contain rock with a high content of sulfide minerals, which could produce anoxic conditions at depth in the lake. Pit lakes intersect and often contaminate groundwater. However, pit lakes have complicated

chemistries and would only be relevant if they are sulfidic at depth. Pit lakes that have high sulfide content have poor water quality and may or may not be acidic, depending upon the amount of limestone in the rocks. Under oxidizing conditions at a basic pH, metal cations (e.g. Cu^{2+}, Pb^{2+} Hg^{2+}) will adsorb to negatively charged mineral surfaces, but elements that form negatively charged oxyanions (e.g. As and Se) will not be strongly adsorbed.

The Getchell gold mine in Nevada is an example of a mine in which a pit lake has formed. The mineral deposit contains arsenopyrite ($AsFeS_2$). When water in the North Pit was sampled, it was found to have the following conditions 0.38 ppm (5100 nM) As, <0.05 ppm (<24 nM) Pb, <0.2 ppm (<990 nM) Hg and <0.005 ppm (<46 nM) Ag, a pH of 7.67 and the bottom portion of the North Pit is believed to be anoxic (Miller et al., 1996). Arsenic is above the EPA's drinking water standard of 0.010 ppm.

Industrial Harbors can also be contaminated with heavy metals as well as arsenic. Silver is often found in harbors due to outputs from wastewater treatment plants. However, literature suggests that elevated silver could also be due to diagenic remobilization from contaminated sediments and could be a source of contamination in aquatic environments with limited hydraulic flushing (Flegal and Sanudo-Wilhelmy, 1993; Smith and Flegal, 1993; Flegal et al., 1997; Sanudo-Wilhelmy and Gill, 1999).

Table 3 summarizes some heavy metal concentrations found in sediments from contaminated harbors. All metal concentrations are compared to biological effect-based guideline values for sediment quality. Below the ERL (effect-range low)

value, adverse biological effects rarely occur; above the ERM (effect range-median) value, adverse biological effects frequently occur; in between the ERM and ERL, biological effects are intermittently observed (Giusti and Zhang, 2002).

Smith and Flegal (1993) demonstrate the importance of silver contamination from sediments in the San Francisco Bay and compare the contamination to the average crustal abundance of silver and to background levels in the Southern California Bight, an uncontaminated site. Pascoe at al. (2002) present sediment metal concentrations in Ostrich Bay, which is an arm of Dyes Inlet on Puget Sound in Washington State. This site was contaminated with nitroaromatic compounds from a naval ordinance facility that washed directly into the bay.

Boston Harbor is one of the oldest harbors in the United States and serious pollution problems began in 1865 (Bothner et al., 1998). The sediments in the harbor have been monitored between 1977 and 1993. Metal concentrations have decreased in the harbor over time, but silver and mercury remain above ERM levels and indicate that Boston Harbor remains toxic to some bethnic organisms.

Hyland et al. (1998) conducted a study in 1994 and 1995 to assess the sediment quality in the Carolinian Providence, which extends from Cape Henry, VA to Indian River Lagoon, FL. They indicated that 49- 60% of the estuaries had good sediment quality. A summary of ranges for sediment metal concentrations was given over the whole study area, but the summary did not present evidence at each individual site. Therefore, it is unclear if a particular estuary was highly contaminated and if elevated metal concentrations occurred at the same site.

Table 3. Summary of Some Heavy Metal Concentrations Found in Sediments and Overlying Water from Contaminated Harbors

	Sediment Metal Concentrations (mg/kg)				Dissolved Concentration Surface Waters (pM)	
	Ag	As	Pb	Hg	Ag	Pb
ERL*	1[a]	8.2[a]	46.7[e]	0.15[g]		
ERM*	3.7[a]	70[a]	218[e]	0.71[g]		
Crustal Abundance	0.08	2.1[f]	100[f]	0.07[f]		
Puget Sound, Ostrich Bay[b]	0.49	9.4	40.6	0.35		
Puget Sound, Dyes Inlet[b]	1.0	18.6	20.2	1.3		
San Francisco Bay[c]	0.4-0.9	nm	nm	nm	49.9±49.2	nm
Baseline- Southern CA Bight[c]					3	18-63[d]
San Diego Bay[d]					66-307	120-184
Burlington Harbor, VT[e]	1.73-5.35	nm	79.1-173.3	nm		
Boston Harbor 1978[i]	5.5	nm	165	0.77		
Boston Harbor 1993[i]	4.1	nm	108	0.69		
Cape Henry, VA – St. Lucie Inlet, FL Estuaries[h]	0.0-0.5	0.0-22.3	0.9-45.6	0.0-0.2		

* ERL is adverse biological effects occasionally occur, ERM is adverse biological effects frequently occur. [a] Giusti and Zhang (2002); [b] Pascoe et al., (2002); [c] Smith and Flegal (1993), nm= not measured; [d] Flegal and Sanudo-Wilhelmy (1993); [e] Lacey et al. (2001); [f] Winter (1993); [g] Kwon and Lee (1998); [h] Hyland et al. (1998) sediment data from 1995; [i] Bothner et al., 1998, depth of sample 0-2 cm

It is clear from the examples cited that arsenic, silver, mercury and lead could be simultaneously present at elevated levels in contaminated environments. It is therefore necessary to know where these metals originate and if they have any harmful effects to aquatic and human life.

I.C.2. Arsenic

I.C.2.1. Sources and Toxicity

Natural and anthropogenic processes play an important role in the distribution and bioavailability of trace metals in the environment. There are over 160 known arsenic-containing minerals in nature (Wagemann, 1978). These minerals constitute natural sources of arsenic through weathering of the earth's crust. Arsenic is found in the earth's crust with an average of 2 mg/kg (Winter, 1993). Anthropogenic sources of arsenic include coal combustion, smelting of copper, runoff from mine tailings, pigment production for paints and dyes and leaching from wood preservatives (Ferguson and Gavis, 1972; Nriaqy and Pacyna, 1988; Rose, 1998; Oremland and Stolz, 2003). Arsenic was also used as a pesticide until 1980; this usage is estimated to have contributed about 10,000 metric tons per year to the environment (Oremland and Stolz, 2003). Arsenic has been replaced by synthetic pigments and pesticides in most cases but is still used in agricultural applications.

Organic arsenicals like roxarsone (3-nitro-4-hydroxyphenylarsonic acid) are added to poultry feed to control coccidiosis, a parasite that can develop in the digestive tract of vertebrates, to stimulate growth and egg production and to improve the pigmentation of the animal (Arai et al., 2003; Oremland and Stolz, 2003). Estimated roxarsone use on the east coast of the United States is between 20 and 50 metric tons annually (Arai et al, 2003; Oremland and Stolz, 2003). The ingested arsenic does not accumulate in the animals but is excreted in their waste, which is applied as manure to agricultural land.

Certain fungi, yeasts and bacteria are known the methylate arsenic. There is also evidence that phytoplankton in the ocean use arsenic methylation as a detoxification mechanism (Cutter, 1992). The detoxification mechanism involves the reduction of As(V) to As(III) and then biomethylation, which produces monomethylarsonic acid (MMA) or dimethylarsonic acid (DMA) (Cullen and Reimer, 1989; Tamas and Wysocki, 2001; Oremland and Stolz, 2003). The methylated arsenic species are less toxic than the inorganic species, as determined by their differing LD_{50}'s for mice (Kaise et al., 1989).

Exposure to arsenic can be detrimental to humans. Blackfoot Disease, found in Taiwan, is attributed to long-term exposure of arsenite in drinking water. Over time, gangrene develops in a person's limb and amputation of the limb is required (Chen et al., 1994). Chronic exposure to moderate levels of arsenic results in arsenic poisoning, where the symptoms are the development of hard nodules on the skin. Long-term exposure will lead to skin cancer, cardiovascular disease and gangrene (Mabuchi et al., 1979; Winder, 1993; Das et al., 1995; Chaterjee et al., 1995; Anawar et al., 2002).

The toxicity of arsenic is highly dependent on its oxidation state. Goldstein and Babich (1989) have shown that arsenite is more toxic to adult flies than arsenate. Arsenite is more toxic than arsenate because arsenite reacts with sulphydryl groups, impairing the functioning of many proteins by inhibiting the catalytic process of enzymes. Arsenite can enter the body through dermal absorption. Inorganic arsenate enters the body through the gut of humans where it can replace phosphorus in metabolic processes. Arsenate is a molecular analog of phosphate and thus can

participate in oxidative phosphorylation (Ferguson and Gavis, 1972; Winder, 1993; Oremland and Stolz, 2003). However, there is new evidence suggesting that the formation of thioarsenite species reduces the toxicity of As(III) when compared to arsenious acid (Rader et al., 2004). To ensure that the public is protected from arsenic related diseases, the United States government has lowered the maximum contaminant level (MCL) for arsenic to 0.010 ppm (10^{-9} M) for drinking water (Environmental Protection Agency, 2001). The World Health Organization (WHO) has also lowered the MCL for arsenic in drinking water to 0.010 ppm (Zheng et al., 2004).

I.C.2.2. The Bangladesh/West Bengal Problem

High arsenic levels in groundwater have been reported all over the world, ranging from Chile to the USA to Bangladesh, but Bangladesh seems to have the worst case of arsenic contamination in groundwater. Bhattacharya et al. (2002) stated that 33 to 75 million people in Bangladesh are at risk due to the high concentration of arsenic found in the groundwater. Bangladesh groundwaters typically exceed arsenic concentrations of 0.200 ppm (Nickson et al., 2000; Bhattacharya et al., 2002; Kinniburgh et al., 2003). The predominant forms of arsenic in drinking water in areas like Bangladesh are the more toxic inorganic arsenic species.

Arsenate has a negative charge at pH's associated with natural waters and is strongly absorbed to minerals, such as ferrihydrite, so its mobility in water is reduced. Arsenite, on the other hand, is neutral at pH's associated with natural water

and is less strongly absorbed to surfaces and is more mobile in groundwater (Oremland and Stolz, 2003). It is estimated that 67 to 99% of the arsenic in Bangladesh groundwater is present as arsenite (Bhattacharya et al., 2002; Ahmed et al., 2004).

There is much debate as to the source of arsenic present in Bangladesh groundwater. The apparent cause of the elevated arsenic concentration is still unknown but is thought to be a natural process rather than an anthropogenic one. The sediments of the Bangladesh region contain <1 to 10 ppm arsenic, which is normal for alluvial sediments (Kinniburgh et al. 2003). Sediments that contain high concentrations of arsenic do not always produce elevated arsenic concentrations in groundwater. This leads to the conclusion that the sediment composition is not directly related to the elevated arsenic levels in the groundwater. However, the younger Holocene alluvial aquifers show elevated levels of arsenic compared to older sediment that have medium grained sand and minimal organic matter. The Holocene sediments are mainly composed of fine to very fine grained sands, silts and clays (Ahmed at al. 2004). The Holocene sediments are also rich in organic matter and reactive minerals leading to water that contains mostly Ca-HCO_3 or Ca-Mg-HCO_3 (Bhattacharya et al., 2002; Ahmed et al., 2004). The pore waters of the sediment are near neutral to slightly alkaline and are often under reducing conditions (Bhattacharya et al., 2002; Ahmed at al., 2004).

There are two main hypotheses to explain the elevated arsenic concentration found in regions like Bangladesh. The first hypothesis is that As rich-pyrite has been oxidized as a result of lowering the water table through irrigation (Nickson et al.,

2000; Kinniburgh et al., 2003; Ahmed et al., 2004; Zheng et al., 2004). This hypothesis is no longer generally accepted. The dissolution of pyrite is not favorable or expected under the reducing conditions found in the groundwater. Another reason the pyrite oxidation hypothesis seems implausible is that the highest arsenic concentrations would be found in shallow aquifers close to the water table. Results show that the highest concentration of arsenic appears in wells that are not shallow and vary between 15 meters and 150 meters (Kinniburgh et al., 2003, Ahmed et al., 2004).

The currently favored hypothesis for arsenic enrichment proposes that arsenic bound to Fe(III)-oxyhydroxide is released as the Fe(III)-oxyhydroxide is reduced (Nickson et al., 2000; Kinniburgh et al., 2003; Ahmed et al., 2004; McArthur et al., 2004 Zheng et al., 2004). This reaction can be represented by the following (where CH_2O represent organic matter in the aquifer):

$$4FeOOH + CH_2O + 7H_2CO_3 \Leftrightarrow 4Fe^{2+} + 8CO_3^- + 6H_2O \quad (3)$$

Microbial processes in these organic rich sediments may help facilitate the reduction of Fe(III) and As(V) to Fe(II) and As(III). In fact, elevated levels of NH_4^+ and PO_4^{3-} usually characterize the groundwater. There is a strong correlation between arsenic and HCO_3^- and a weaker correlation between arsenic and iron (Nickson et al., 2000).

I.C.2.3. Speciation of Arsenic in Seawater and Freshwater Systems

Arsenic is mainly found in aquatic systems in the +5 and +3 oxidation states (Ferguson and Gavis, 1972; Cullen and Reimer, 1989). However, arsenic is stable in

a total of four oxidation states in aquatic systems, +5, +3, 0 and –3 (but elemental arsenic is rare). O'Day et al. (2004) recently presented EXAFS (extended x-ray absorption fine-structure) evidence that AsS (oxidation state of +2) can be found in contaminated shallow aquifer sediments under sulfate reducing conditions.

Freshwater systems typically have a pH range of 5 to 9, while seawater has pH values ranging from 7.5 to 8.3 (Cullen and Reimer, 1989). Under oxidizing conditions As(V) species, H_3AsO_4, $H_2AsO_4^-$, $HAsO_4^{2-}$ and AsO_4^{3-}, are stable. $HAsO_4^{2-}$ and $HAsO_4^{2-}$ are the dominant species in seawater and freshwater, respectively. Under slightly reducing conditions, H_3AsO_3 is the dominant species in natural waters. Under anoxic conditions, in the presence of organic matter and bacteria, sulfate is reduced to hydrogen sulfide. An anoxic marine environment may have a pH of 7.5 and a pE ranging from –2.9 to –4.2 (Cullen and Reimer, 1989). Under these conditions thioarsenite species are dominant.

However arsenic is rarely in equilibrium due to biological redox reactions (Cullen and Reimer, 1989; Aurillo et al., 1994).Arsenite has been reported in the oxic portion of the water column and arsenate has been found in the anoxic portion of the water column in the Black Sea and Oslofjord (Cutter, 1992; Abdullah et al., 1995). In these cases arsenite may be present in oxic waters due to the transport of arsenite from anoxic waters. However, the main reason arsenite is present in oxic waters is due to the uptake of As(V) by plankton, which methylate and release As(III) (Cutter, 1992; Cutter et al, 2001). Arsenite persists in the oxic water column because the oxidation of arsenite by oxygen is slow and its half-life is on the order of days (Cutter, 1992; Kim and Nriagu, 2000). Another oxidizing agent for arsenite is

hydrogen peroxide, present at 0.1 μM in natural waters, but its reaction also has a slow rate constant (~0.33 mol L^{-1} min^{-1} at pH=7) (Pettine et al., 1999). Arsenate is present in the anoxic portion of a water column due to formation of thioarsenates and remobilization of particulate arsenate from sediment coupled with a slow rate of arsenate reduction (Cutter, 1992; Abdullah et al. 1995). The average rate of As(V) reduction in the Black Sea is $1.6x10^{-5}$ day^{-1} (Cutter, 1992).

I.C.2.4. Speciation of As in Sulfidic Solutions

In sulfide-free solutions, H_3AsO_3 is accepted as the dominant As(III) species at near neutral pH (Ivakin et al., 1979; Mironova et al., 1984; Webster, 1990; Eary, 1992). However, when sulfide is present there is disagreement on the stoichiometry of the As(III) sulfide species. Weissberg et al. (1966) suggests that monomers (AsS_2^-, AsS_3^{3-}, $AsS(OH)_2^-$) are the dominant complexes in sulfide solutions at temperatures from 25 to 200°C and pressures from 100 to 1500 bars. The dimer ($As_2S_4^{2-}$) and protonated forms are favored at various sulfide concentrations and temperatures by others (Mironova and Zotov, 1980; Mironova et al., 1990). The trimer ($H_2As_3S_6^-$) also has been reported in mildly acidic, sulfidic solutions (Vorob'eva et al., 1977; Webster, 1990; Eary, 1992). Table 4 summarizes the previous experiments on the solubility of orpiment.

More recently, Helz et al. (1995) utilized ab initio quantum mechanical methods, EXAFS studies and Raman spectra of dissolved thioarsenite to help determine the number of arsenic atoms per thioarsenite molecule. They ruled out the possibility of dimers based on the comparison of calculated stability and abundance

of the dimer to the trimer. It was concluded that in undersaturated solutions the monomer is the predominant thioarsenite species, but that the trimer is the predominant thioarsenite species in saturated solutions. Their conclusions imply that the number of arsenic atoms per thioarsenite molecule is highly dependent on the amount of arsenic present in solution.

Table 4. Summary of Arsenic Speciation for Experiments Involving the Solubility of As_2S_3

Species	Type of Study	Solid	Reference
$AsS(OH)_2^-$ AsS_3^{3-} AsS_2^-	Mineral dissolution	Synthetic, crystalline orpiment	Weissberg et al., 1966
$As_3S_6^{3-}$ $As_2S_5^{4-}$	Spectophotometric	Precipitate	Vorob'eva et al., 1977
$As_3S_6^{3-}$	Mineral dissolution	Precipitate	Ivakin et al., 1979
$H_2As_2S_4^o$ $HAs_2S_4^-$ $As_2S_4^{2-}$	Mineral dissolution	Natural, crystalline orpiment	Mironova and Zotov, 1980
$H_2As_2S_3O^o$ $HAs_2S_4^-$ $As_2S_4^{2-}$	Mineral dissolution	Natural, crystalline orpiment	Mironova et al., 1990
$As(OH)_3$ $H_2As_3S_6^-$	Mineral dissolution	Synthetic, crystalline orpiment	Webster, 1990
$As(OH)_3$ $H_2As_3S_6^-$	Mineral dissolution	Amorphous orpiment	Eary, 1992

Wood et al. (2002) conducted Raman spectroscopic studies on solutions with various ratios of ΣS to ΣAs. They concluded that there are many different thioarsenite species in the As-S-O-H system, but could not resolve the stoichiometry of the thioarsenite species in their experiments. Wilken et al. (2003) also conducted experiments in dilute solutions with various ΣH_2S to ΣAs ratios at pH 7 and 10. They concluded that thioarsenic species with a S/As ratio of 3:1 are the dominant thioarsenite species in sulfidic solution, while species with a S/As ratio of 1:1, 2:1 and 4:1 are still present in solution but to a lesser degree.

I.C.3. Lead

I.C.3.1. Sources and Toxicity

Lead is not abundant in the earth's crust. However, there are high lead concentrations in ore deposits throughout the world. The most important mineral, galena (PbS) is found in fissure veins associated with a host of other metal sulfides (Dudka and Adriano, 1997). The primary uses of lead include the manufacturing of storage batteries, ammunition, cable coverings and pipes (Prosi, 1989; Winder, 1993). Decline in the use of lead in gasoline, paints and plumbing seems to have decreased the amount entering the environment. However, anthropogenic sources of lead still come from smelting, coal combustion and mining (Nriagu and Pacyna, 1988; Dudka and Adriano, 1997).

Exposure to lead results in a number of diseases. Inhalation and ingestion are the main pathways by which lead enters the body. Adults exposed to high levels of lead can experience brain damage, nerve damage, kidney disease, anemia and

damage to the reproductive system. Low levels of lead exposure can lead to the development of lead poisoning, which has flu-like symptoms. Koller et al. (2004) reviewed many epidemiological studies on lead exposure to children. He concluded that lead exposure is extremely damaging and often leaves a child with permanent brain damage, mental retardation and severe behavior problems (McMichael et al., 1988; Factor-Litvak et al., 1999).

Due to the extremely toxic effects of lead, the United States government regulates the amount of lead allowed in air and drinking water. Lead is on the primary drinking water regulation list, where it has a maximum contaminant level goal of zero and action level of 15 ppb in drinking water (Environmental Protection Agency, 2001). The action level means that if more than 10% of the drinking water tested at a treatment plant exceeds the action level further treatment of the drinking water is necessary.

I.C.3.2. Lead in Aquatic Systems

Lead is known to bioaccumulate in microorganisms and plants (Jaworski et al., 1987; Sundelin and Eriksson, 2001). Filter feeding animals, such a mussels, are particularly susceptible to accumulating large amounts of lead from contaminated sediment (Prosi, 1989; Sundelin and Eriksson, 2001). Sediments act as a sink for lead through the precipitation of insoluble lead species. Concentrations of lead in the pore water of sediment in Lake Geneva ranged from 0.030 to 0.200 ppm, whereas uncontaminated levels range from 0.001 to 0.003 ppm (Prosi, 1989). However, there is no evidence that lead undergoes biomagnification throughout the food chain.

Lead is also known to undergo methylation (Ridley et al., 1977; Pelletier, 1995; Sundelin and Eriksson, 2001). However, there is debate on whether the methylation is a biological process or an abiotic reaction, and there are insufficient data to draw conclusions about the fate of methlyated lead species in aquatic systems (Pelletier, 1995).

I.C.3.3. Speciation of Pb in Sulfidic Solutions

There are a few studies on the solubility of PbS (galena). Giordano and Barnes (1979) measured the solubility of galena in sulfidic solutions ranging from 0 to 2.85 m NaHS, at 30 to 300°C and pressures between 0.8 and 75 atm. They favored a neutral lead complex, $Pb(HS)_2^o$, as the dominant species at 30°C under neutral to acidic conditions. They also concluded that $Pb(HS)_3^-$ will be the dominant lead species in basic solutions under highly reducing conditions.

The solubility product of PbS has also been studied. Anderson (1962) reviewed the literature on the solubility product of PbS. Uhler and Helz (1984) measured the stoichiometric solubility product of galena at 298K. Galena was shown to be more than two orders of magnitude more soluble when compared to previous thermodynamic data. Using their solubility product of galena they recalculated the equilibrium constants for the formation of $Pb(HS)_2^o$ and $Pb(HS)_3^-$.

I.C.4. Mercury

I.C.4.1. Sources and Toxicity

Mercury is widely distributed in nature but occurs at low concentrations. The average crustal abundance of mercury is 67 ppb by weight. The most common mercury mineral is cinnabar (HgS), which is found in mineral veins, hot springs or areas around volcanoes. Natural sources of mercury are attributed to volatilization of gaseous mercury from oceans, soils and biota and volcano emissions (Pacyna, 1987; USGS, 1995). Anthropogenic sources are a result of mining, burning fossil fuels, metal smelting, paint, agricultural uses and chloro alkali processes (Pacyna, 1987; Nriagu and Pacyna, 1988; USGS, 1995; EPA, 1997; Dreher and Follmer, 2004).

The toxicity of mercury to humans depends on its chemical form and length of exposure. Mercury is known to biomagnify and bioaccumulate in the body and constant exposure to mercury enhances the toxicity. Humans can be exposed to mercury primarily in two ways; the first is breathing mercury vapor (Hg^{o}), which can be absorbed through the human lung and oxidized to Hg^{2+}. Short-term exposure to mercury vapor results in flu like symptoms. Long-term exposure to mercury vapor results in severe neurological effects (Bakir et al., 1973; Grandjean et al., 1998).

The second exposure route is by ingesting methlymercury (CH_3Hg^{+}) from fish (USGS, 1995; Akagi and Naganuma, 2000). Methylmercury is thought to be more toxic than inorganic forms of mercury. Minamata Bay, Japan and rural Iraq are two well-known examples, where hundreds of people developed central nervous system diseases and some even died as a result of methylmercury exposure (Bakir et al., 1973; Eto et al., 2002).

I.C.4.2. Mercury in Aquatic Systems

Mercury can occur in three valence states, 0, +1 and +2. Hg^o, complexes of Hg(II) with inorganic or organic ligands and organic mercury are the main dissolved species (Ullrich et al., 2001). Hg(I) is stable as a dimer, Hg_2^{2+}, in aqueous solution and will produce Hg^o and Hg(II) in water. According to a review article by Ullrich et al. (2001), mercury is found in oxic freshwaters as $Hg(OH)_2$, HgOHCl and $HgCl_2$. In sulfidic solution mercury forms bisulfide and polysulfide complexes (Paquette and Helz, 1997; Jay et al., 2000).

Sulfate reducing bacteria are responsible for methylating mercury. Mercury is not available to cells as a cation; instead the mercury must be in a neutral, small and hydrophobic form. Soluble mercury species like Hg^{2+}, $HgCl^+$ and $HgCl_2^o$ are charged or have too low a concentration in natural waters to explain the methylation of mercury by sulfate reducing bacteria. There is new evidence that HgS^o could be responsible species for the methylation of mercury by sulfate reducing bacteria in anoxic waters (Compeau and Bartha, 1985; Benoit et al., 1999; Benoit et al., 2001).

I.C.4.3. Speciation of Hg in Sulfidic Solutions

Schwarzenbach and Widmer (1963) conducted the first studies on Hg-sulfide complexes. However, there is a debate on the type of solid HgS used in their solubility experiments. HgS exists in two polymorphs, cinnabar or α-HgS (red) and mettacinnabar or β-HgS (black), with the red form being the most stable (Paquette, 1994). Paquette and Helz (1997) used red cinnabar in their solubility studies and found excellent agreement with Schwarzenbach and Widmer's black cinnabar

solubility data. Paquette and Helz conducted experiments on cinnabar (red) only and cinnabar plus elemental sulfur in 0.7 M KCl at 298 K in sulfidic solutions ranging from 10^{-3} M to 0.1 M and pH ranging from 1 to 12. In the absence of elemental sulfur, mercury solubility could be explained by $Hg(SH)_2$, $HgS(HS)^-$ and HgS_2^{2-}. The addition of elemental sulfur promoted the solubility of mercury. The additional mercury solubility was attributed to the $Hg(S_x)HS^-$ species. Jay et al. (2000) also conducted solubility experiments on cinnabar in the presence of elemental sulfur in sulfidic solutions ranging from 2 μM to 5 mM and pH ranging from 6 to 10. They propose that $Hg(S_x)_2^{2-}$ is the dominant species at high pH, whereas HgS_xOH^- is the dominant species at low sulfide concentrations and high pH.

Benoit et al. (1999) present a chemical equilibrium model for mercury speciation in sulfidic pore waters. They observed that methylmercury (MeHg) decreases as the concentration of sulfide increases in two sediment pore water areas. They propose a model that includes, HgS^o and $Hg(HS)_2$ to explain the observed solubility of Hg and MeHg, where HgS^o is dominant at low sulfide and $Hg(HS)_2$ is dominant at higher sulfide concentrations. Their findings may explain the inverse relationship between sulfide and the formation of MeHg, implying that HgS^o is the dominant neutral species used in the passive uptake across the cell membrane. As the concentration of sulfide increases, the concentration of HgS^o declines as does methylation of mercury.

Tossell (2001a) has done further studies on various mercury (II) species in aqueous solutions. He used quantum mechanical methods to investigate the stability

of HgS^o and found that is was unstable in water with respect to $Hg(HS)(OH)^o$. He further concluded that at neutral pH $Hg(HS)(OH)^o$ would also be uncharged.

I.C.5. Silver

I.C.5.1. Sources and Toxicity

Silver is a minor component in the earth's crust, with an average concentration of 0.1 mg/kg (Purcell and Peters, 1998). However, concentrations of silver can be much greater than 0.1 mg/kg as a result of human activities. Mine tailings can produce elevated concentrations of silver up to 1000 mg/kg (Purcell and Peters, 1998). Today, operating silver mines are mainly located in South America, southern Mexico and the western United States.

Industrial uses of silver account for most of the silver released into the environment. It has been shown that the photographic industry contributes 30-60% of the total silver released into wastewater treatment plants (WWTP) (Schildkrautet et al., 1998). The majority of silver (approximately 90%) released to the environment will be removed at the WWTP (Schildkrautet et al., 1998). However, silver released into the environment will remain in wastewater sludge, soils or sediments as silver sulfide (Hirsch, 1998; Berry et al., 1999; Ratte, 1999; Rozan and Luther, 2002). This is because silver sulfide is the decomposition product of silver thiosulfate, which is the primary species released after the silver waste has been through the wastewater treatment process (Hirsch, 1998; Ratte, 1999). Other industrial uses of silver come from the production of electronic components, brazing alloys and batteries (Purcell and Peters, 1998).

Silver is not particularly harmful to humans. Thus, the Environmental Protection Agency (EPA) has placed silver on the National Secondary Maximum Drinking Water Contaminant Level (SMCL) list. The contaminants on the list mainly cause cosmetic effects in humans. The secondary drinking water standard for silver is 0.1 ppm (Environmental Protection Agency, 2001). Humans exposed to large doses of silver develop argyria, which is a condition that turns certain areas of the skin permanently blue or a blue/gray color.

Today, people are exposed to low levels of silver metal daily in the form of eating utensils and teapots. Silver is also being used for its germicidal properties in the medical field. Dilute solutions of silver nitrate are put into newborn's eyes to prevent infection. Silver based salves are also being used to treat burn victims, and the FDA recently approved a few new drugs for this purpose (Lister, 2001). Silver colloid supplements are promoted by health companies to cure a number of diseases, but the Federal Drug Administration (FDA) issued a final ruling on silver colloids proclaiming them unsafe.

Silver is commonly found in the environment in the 0 and +1 oxidation states; the other two known oxidation states of silver, +2 and +3 are seldom encountered in nature (Purcell and Peters, 1998). Ag(I) is more toxic than Ag(0). Silver's high affinity for sulfur ligands leads to its ability to interfere with protein metabolism in aquatic organisms, resulting in its toxicity at nanomolar levels (Fisher and Wang, 1998; Bell and Kramer, 1999). However, silver is normally found in natural waters at picomolar levels (Bell and Kramer, 1999). Bivalve species and freshwater and marine algae bioaccumulate silver. Silver will kill bacteria at levels as

low as 1 micromolar (Ratte, 1999). Some fish are sensitive to silver; it binds to anions in the gills, preventing the uptake of Cl^- and Na^+. However, in the environment silver is not expected to be highly toxic because it can be transformed to a non-reactive and less toxic species such as Ag_2S (Ratte, 1999). Bianchini et al. (2002) present evidence that the mortality of *Daphnai magna* neonates (crustacean/water flea) was reduced when silver was present with sulfide, in the form of zinc sulfide clusters, compared to conditions when no sulfide was present. Silver can displace iron or zinc from metal sulfide clusters because of its high affinity for sulfur ligands. Rozan and Luther (2002) further demonstrated that silver replaced zinc in a 1:1 ratio when zinc sulfide solutions were titrated with silver.

I.C.5.2. Silver in Aquatic Systems

Adams and Kramer (1999) argue that silver is found as a sulfide in most natural water systems and that silver (I) forms very strong complexes with sulfides such as AgHS. Other organic sulfide species, like thiols (RS^-), have formation constants that are similar to silver sulfide complexes. Adams and Kramer (1999) performed a study on silver speciation in wastewater effluent, receiving waters and pore waters from an anoxic lake sediment. Sulfide and silver were present at an average of 100 nM and less than 1 nM, respectively. It was concluded that as long as sulfide is in excess of silver in the pore water, silver sulfide complexes would be the dominant species because silver forms one of the strongest sulfide complexes (Adams and Kramer, 1999; Rozan and Luther, 2002). Even though thiols were present at low nanomolar levels, they did not contribute to silver speciation.

However, the presence of thiols must also be considered as another potential species that would bind silver. Al-Farawati and Van den Berg (2001) found thiol concentrations ranging from 0.70 to 3.6 nM in the North Sea and English Channel and did not find evidence of sulfides. However, the nature of thiols in water is not well understood and sulfide is the major reduced sulfur species in fresh waters compared to thiols, whereas thiols may be important in estuarine and marine waters (Adams and Kramer, 1999).

I.C.5.3. Speciation of Ag in Sulfidic Solutions

There have been numerous studies on the stability of silver complexes. The aqueous silver complexes proposed to account for silver (I) solubility in equilibrium with AgCl and Ag_2O with no added sulfide include: $AgCl_x^{1-x}$ (Zotov et al., 1982), Ag(OH) (Kozlev et al., 1983) and $AgClOH^-$ complexes (Zotov et al., 1982). The mixed hydroxychloride species is interesting.

There have also been many studies conducted on the solubility of silver sulfide in sulfidic solutions, which are summarized in Table 5. Gammons and Barnes (1989) conducted solubility studies on Ag_2S (acanthite/argentite) in sulfidic solutions ranging from 0.2 to 1.4 molal, at 25-300°C with a pH between 5.8 and 7.3. They concluded that $Ag(HS)_2^-$ was the predominant species. Stefansson and Seward (2003) conducted a solubility study on silver sulfide in sulfidic solutions between 0.007 and 0.176 mol kg^{-1}, at 25-400°C, with a pH range of 3.7 to 12.7. Stefansson and Seward (2003) concluded that AgHS was the dominant species in acidic solution

conditions, $Ag(HS)_2^-$ under neutral pH conditions and $Ag_2S(HS)_2^{-2}$ under basic conditions.

Table 5. Silver Speciation from Previous Solubility Studies with Silver

Silver Complex	Solid	pK	Reference
Chloride Complexes[a]			
AgCl	Silver chloride	6.64±.04	Zotov et al. (1986)
$AgCl_2^-$		4.81±.04	
$AgCl_3^{2-}$		4.75±.1	
Hydroxychlorido Complexes[b]			
$AgClOH^-$	-	5.3±.2	Zotov et al. (1982)
Sulfide Complexes[c]			
$Ag(HS)_2^-$	acanthite/argentite	3.82±.1	Gammons and Barnes (1989)
$Ag_2S(H_2S)$	acanthite/argentite	6.4±.2	Sugaki et al. (1987)
$Ag_2S(H_2S)(HS)^-$		3.9±.2	
$Ag_2S(H_2S)(HS)_2^-$		4.3±.4	
$Ag_2S(HS)_2^{2-}$		5.2±.2	
Ag(HS)	acanthite/argentite	5.62±.04	Stefansson and Seward (2003)
$Ag(HS)_2^-$		3.97±.04	
$Ag_2S(HS)_2^{2-}$		4.78±.04	
Polysulfide Species[c]			
$Ag(S_4)_2^{3-}$	acanthite	7.66	Cloke (1963)
$AgS_4S_5^{3-}$		8.76	
$Ag(HS)S_4^{2-}$		-4.47	

[a] Temperature 18°C, [b] Temperature is an extrapolation to 25°C,
[c] Temperature 25°C

Sugaki et al. (1987) measured the solubility of silver sulfide in solutions containing 0.00 to 4.51molal H_2S/HS^-, at 25 to 250°C, with a pH range from 2.6 to 10.6. Sugaki et al. (1987) found that $Ag_2S(H_2S)$, $Ag_2S(H_2S)(HS)^-$, $Ag_2S(H_2S)(HS)_2^{-2}$

and $Ag_2S(HS)_2^{-2}$ dominated with increasing significance as solution pH increased. However, Sugaki et al. (1987) only considered dinuclear species and did not consider mononuclear silver complexes to account for silver speciation in their experiments.

Cloke (1963) measured the solubility of acanthite at 25°C from pH 7.72 to 12.98 in differing concentrations of sodium polysulfide solutions. Cloke (1963) described the silver solubility with silver polysulfide species, which include $Ag(S_4)_2^{-3}$, $AgS_5S_4^{-3}$, and $Ag(HS)(S_4)^{-2}$.

I.C.5.4. The Ag-As-S System

This dissertation reports on the Ag-As-S system by studying two assemblages that contained the following starting materials $AgAsS_2/Ag_3AsS_3$ (trechmannite /proustite), $Ag_3AsS_3+Ag_2S$. Figure 1 presents a phase diagram for the Ag-As-S system and the temperatures of transition between phases. The minerals presented in Figure 1 are all known to occur in nature in ore veins or hydrothermal deposits. There are three polymorphs of silver sulfide. Acanthite (monoclinic) is the low temperature phase of Ag_2S and occurs in low temperature sulfide veins. Acanthite inverts to argentite at 176.3°C, which is body-centered cubic. Between 586°C and 622°C the body-centered form of Ag_2S inverts to a face-centered cubic form of Ag_2S (Stefansson and Seward, 2003).

Roland (1970) has described two phases of $AgAsS_2$, smithite and trechmannite. The temperature inversion between smithite and trechmannite, the low temperature phase, is 320°C (Hall, 1966; Roland, 1970). $AgAsS_2$ minerals are relatively rare in nature.

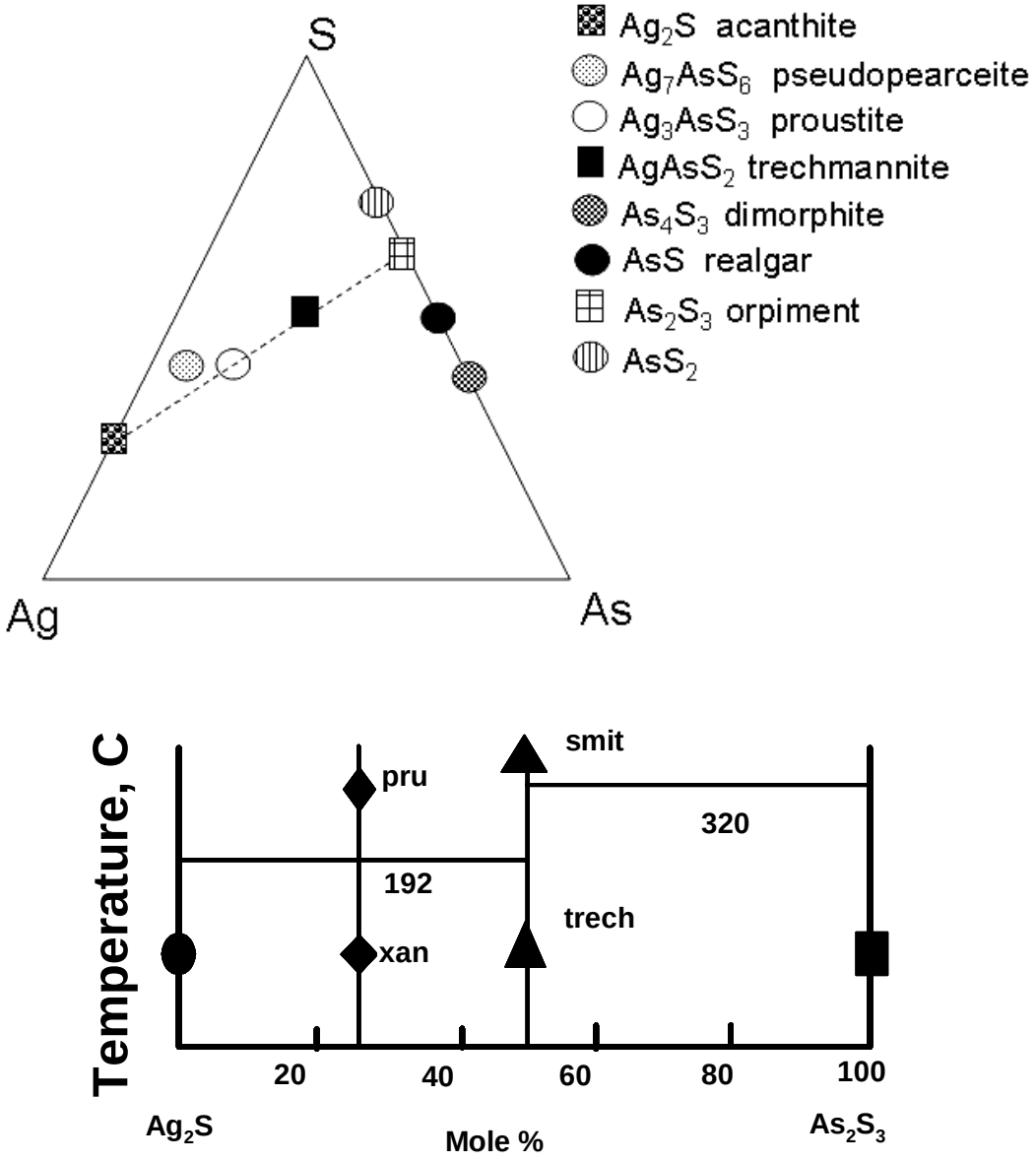

Figure 1. Top: Ternary phase diagram for the silver-arsenic-sulfur system Roland (1970). Low temperature phase is presented first in key. Bottom: Phase relations along Ag_2S-As_2S_3 join, pru=proustie, xan=xanthoconite, smit=smithite and trech=trechmannite.

Ag_3AsS_3 exists in two forms, xanthoconite and proustite, where xanthoconite is always reported to occur with proustite. Xanthoconite is the low temperature phase of Ag_3AsS_3 and will invert to proustite above 192^o C. Proustite and its antimony analog Ag_3SbS_3 (pyrargyrite) and smithite and its antimony analog $AgSbS_2$ (miargyrite) form a complete solid solution series (Ghosal and Sack, 1995; Schonau and Redfern, 2002). Proustite is the most abundant form of the silver sulfosalts in nature and is commonly found with other sulfosalts (Bryndzia and Kleppa, 1989; Schonau and Redfern, 2002).

Ag_7AsS_6 is believed to occur in silver ore deposits and is named billingsleyite. Hall (1966) and Roland (1970) have classified this phase.

Nordstrom and Archer (2003) have reviewed the stability of As_2S_3. As_2S_3 is commonly found in epithermal ore deposits, as a precipitate in hot springs and is commonly formed from the weathering of realgar (AsS). Realgar is also found in the same environments as orpiment, but does not form a precipitate from a solution under 100^{o}C. Hall (1966) reported the synthesis of AsS_2. He also states that the compound was reported as a yellow precipitate in an acid spring in Nasu, Japan.

Chapter II. As, Ag, Pb and Hg Solubility in Sulfidic Solutions

II.A. Introduction

II.A.1. Aim of Study

In this chapter, I will first explore As speciation in equilibrium with orpiment in the absence and presence of elemental sulfur in sulfidic solutions. The data sets considered are from published sources (Webster, 1990; Eary, 1992) as well as from my own experiments involving As_2S_3 alone, and As_2S_3 in combination with either S^o, HgS, PbS or various phases in the Ag-As-S system. In the case of the Hg-, Pb- and Ag-containing assemblages the solubilities of the metals were so small (~10^{-7} M) in relation to the arsenic concentration (~10^{-4}) that no metal complex can contribute significantly to the arsenic speciation. (The only way a metal could affect the arsenic solubility in this situation would be by combining with solid As_2S_3 to form a new phase, a process for which there is no evidence.) After As speciation has been discussed, the effect of the arsenic species on the solubility on each of the metals will be considered in turn.

It is important to note that the experimental conditions used throughout this work are similar to conditions that would be found in nature where thioarsenite would be stable. Natural anoxic sediments normally have a pH of 6 to 8 and a sulfide range of $1x10^{-6}$ to $1x10^{-3}$ M. In my experiments, pH ranged from approximately 6.5 to 8.2 and total sulfide ranged from $1x10^{-4}$ to $1x10^{-3}$ M. It would be interesting to extend these ranges, but by covering a smaller range of conditions, I could investigate more solid phase assemblages in a given amount of time.

II.B. Methodology

II.B.1. Characterization of Materials

II.B.1.1. Characterization of Starting and Reacted Materials Containing As_2S_3, PbS and HgS

Orpiment mineral was obtained from Excalibur Minerals (1000 North Division Street, Peekskill, NY 10566) and originally came from Elbrussky Mine, Caucasus, Russia. The orpiment was removed from a dolomite substrate ($CaMg(CO_3)_2$) and was broken into small pieces. There were small spots of sphalerite (ZnS) at the base of the material, which were also carefully removed.

The solids were characterized by X-ray Diffraction using a Bruker D8 Advance Powder Diffractometer with an area detector and CuKα radiation. The goniometer was aligned with a quartz standard. The X-ray diffraction patterns for orpiment, dolomite and sphalerite are shown in Figures 2-4, respectively. Table 6-8 identifies the peaks from the diffraction patterns.

The diffraction pattern in Figure 2 has prominent peaks at 37.4^o and 38.4^o. Peaks at 37.4^o and 38.4^o in the reference pattern are substantially smaller. Orpiment is a very soft material, and grinding can produce an oriented sample which would enhance certain x-ray reflections and could explain the intensity mismatch between my sample and the standard sample.

The orpiment was further characterized by Energy Dispersive X-Ray Microanalysis (EDAX) with an AMRAY 1820D Scanning Electron Microscope. The material was primarily As_2S_3, although a small peak appeared at approximately 0.6 Kev, which could correspond to chromium. Tim Maugel (Biophysics, UMCP)

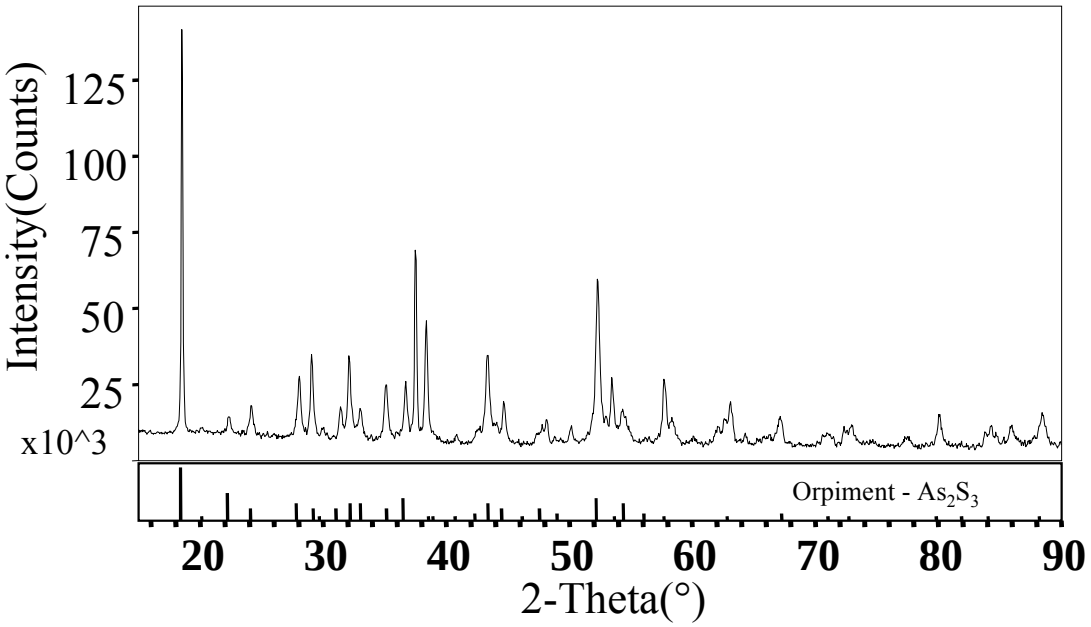

Figure 2. X-ray diffraction pattern for natural orpiment (As_2S_3). Reference is shown below spectra as solid lines. CuKα radiation=1.54 Å.

Table 6. Observed Peaks in the X-Ray Diffraction Pattern of Natural Orpiment Mineral

Peak (2θ), *Intensity x10^3* (measured by hand)	Known Orpiment Peak (2θ), *Intensity x10^3* (measured by hand)
18.8, *141.1*	18.8, *127.0*
28.0, *27.8*	28.1, *30.5*
29.0, *35.0*	29.2, *16.8*
32.1, *35.0*	32.1, *23.0*
35.1, *25.9*	35.2, *21.9*
36.6, *25.9*	36.6, *15.4*
37.4, *69.1*	37.4, *5.8*
38.4, *45.4*	38.4, *7.7*
43.1, *35.0*	43.3, *15.4*
52.4, *63.0*	52.6, *21.9*

Diffraction pattern shown in Figure 2. Peaks given as 2-theta. The known peaks are from the JCPDS database

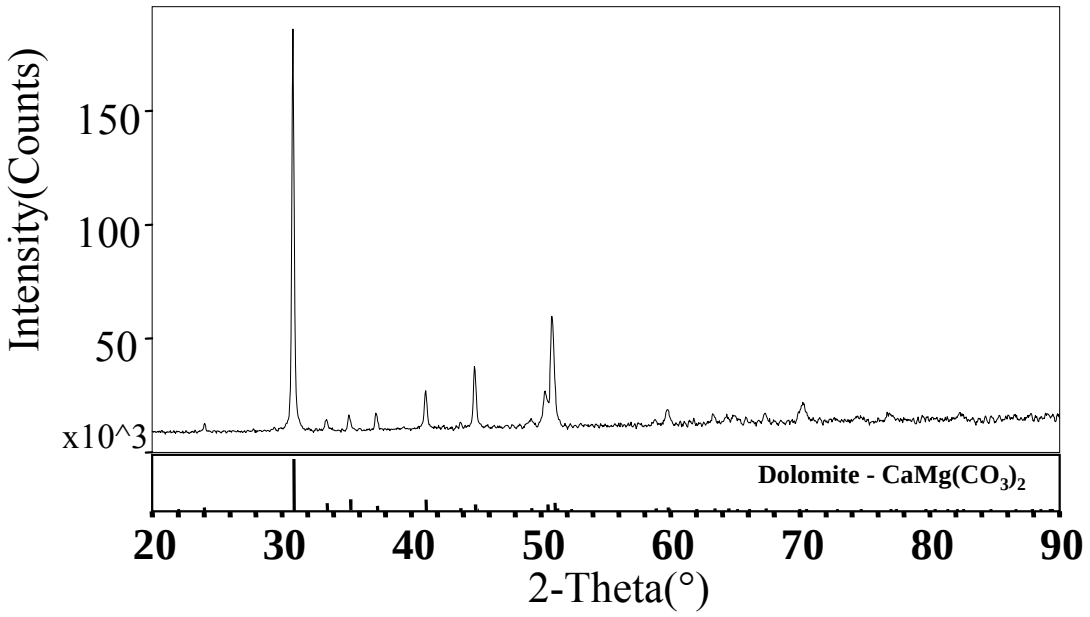

Figure 3. X-ray pattern of white substrate from natural orpiment. A reference spectrum is shown below as solid lines. CuKα radiation=1.54 Å.

Table 7. Observed Peaks in the X-Ray Diffraction Pattern of the Dolomite Substrate

Peak (2θ), *Intensity x10^3* (measured by hand)	Known Dolomite Peak (2θ), *Intensity x10^3* (measured by hand)
30.8, *186.0*	30.8, *156.3*
41.0, *25.6*	41.0, *37.5*
44.8, *36.5*	44.8, *21.5*
50.2, *25.6*	50.2, *28.8*
50.7, *62.5*	50.8, *31.9*

Diffraction pattern shown in Figure 3. Peaks given as 2-theta. The known peaks are from the JCPDS database

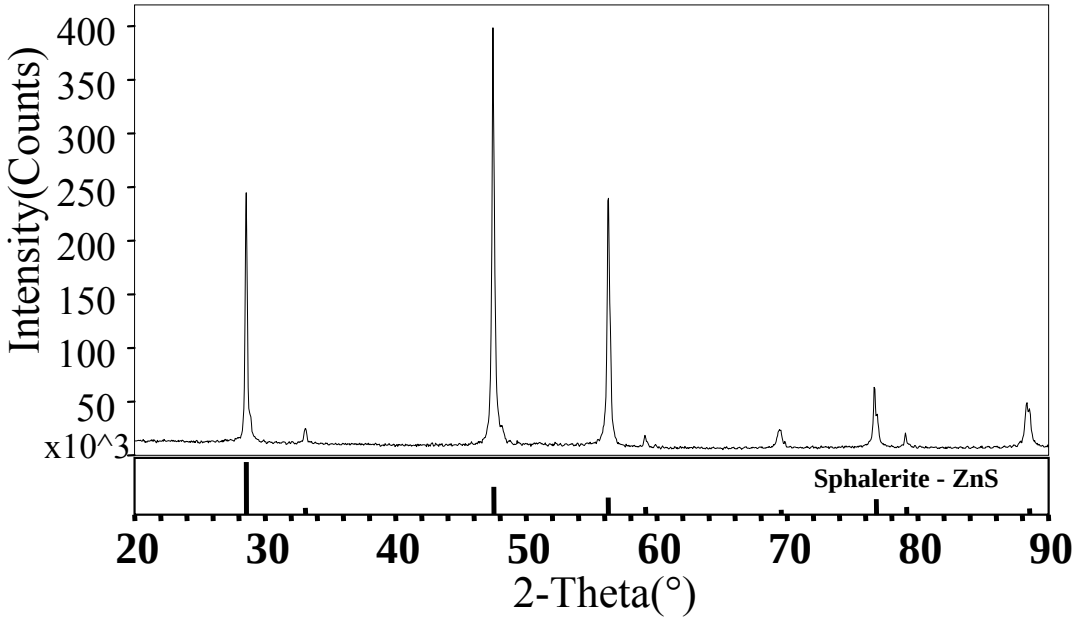

Figure 4. Black particles on natural orpiment mineral. Reference is shown below spectra as solid lines. CuKα radiation=1.54 Å.

Table 8. Observed Peaks in the X-Ray Diffraction Pattern of the Sphalerite Particles

Peak (2θ), *Intensity x10*^{3} (measured by hand)	Known Sphalerite Peak (2θ), *Intensity x10*^{3} (measured by hand)
28.4, *240.0*	28.4, *232.2*
33.0, *24.0*	33.0, *24.0*
47.4, *400.0*	47.4, *124.2*
56.7, *237.5*	56.7, *75.6*
59.0, *13.0*	59.0, *5.4*
69.2, *242.0*	69.2, *14.9*
76.4, *63.0*	76.8, *24.3*
79.0, *24.1*	79.0, *5.4*
88.2, *56.2*	88.4, *27.0*

Diffraction pattern shown in Figure 4. Peaks given as 2-theta. The known peaks are from the JCPDS database

concluded that chromium was absent, because a second chromium peak at approximately 5 Kev was missing from the scan. The sample was relatively large and the 0.6 Kev peak could have come from sample charging. Silicon also appeared in the scan, although it was present in a small quantity.

An effort to synthesize crystalline orpiment by annealing amorphous glassy As_2S_3 (Cerac Inc.) yielded a few crystalline pieces and more of a glassy material; the annealing process is described in Cernosek et al. (1999). Amorphous As_2S_3 was also synthesized by combining sodium arsenite with potassium hydrogen phthalate, as described in Eary (1992). The bright yellow-orange solid that was produced was very soluble. Its high solubility was problematic because the resulting thioarsenite species interfered with the determination of total sulfide. Therefore, natural, crystalline orpiment was used in these experiments.

Galena (PbS) (Alfa Aesar, naturally occurring mineral, 0.06- 0.019 inches in particle size) and sulfur (Aldrich, 99.98% pure) were also characterized. The X-ray diffraction pattern for galena, as received, is shown in Figure 5. The X-ray diffraction pattern for the assemblage, $PbS+S+As_2S_3$, after 30 days equilibrium with a sulfidic solution ($1.65x10^{-3}$ M total sulfide, pH=7.5) is shown in Figure 6. Tables 9 and 10 identify the peaks from these patterns. Major orpiment peaks appear in the reacted material at approximately 18.8^o, 29.0^o and 32.1^o, which are the same positions of the peaks in orpiment prior to equilibration with galena. Prominent peaks for orpiment at 27.4^o and 38.4^o are absent from the reacted diffraction pattern, but present in the original orpiment diffraction pattern (Figure 2). Probably galena in

the sample is preventing the orientation which caused these peaks to appear at exaggerated intensities in Figure 2.

The solids were further characterized by Energy Dispersive X-Ray Analysis (EDS) using a JOEL 8900 Superprobe. A PbS+As_2S_3+S sample that was reacted with a sulfidic solution was first imbedded in epoxy and was then ground with SiC impregnated papers (800 and 500 grit) and polished with 15, 6 and 3 micron diamond paste. The reacted PbS+As_2S_3+S assemblage was inspected by EDS. There was no evidence of any reaction rims on the surfaces of the orpiment or galena. This assemblage was also inspected with a Leitz Orthoplan reflected-light microscope with a Xe light source at 10x magnification in air. The orpiment had rounded edges, indicating leaching of arsenic into solution. The galena had square edges, which indicated minimal dissolution.

An X-ray diffraction pattern for the HgS starting material (99% pure EM Science) is shown in Figure 7, and the peaks are identified in Table 11. A x-ray diffraction pattern was taken (Figure 8) of the HgS+As_2S_3+S assemblage after equilibration for at least 30 days in a sulfidic solution (7.77×10^{-4} M total sulfide, pH=7.22). Table 12 identifies the peaks from the pattern. No peaks were lost and no new peaks appeared in the equilibrated assemblage when compared to the unreacted starting materials. The reacted ternary assemblage was inspected by EDS, and there was no evidence of any reaction rims on the surfaces of the orpiment, which further confirms that the starting and reacted material are the same composition.

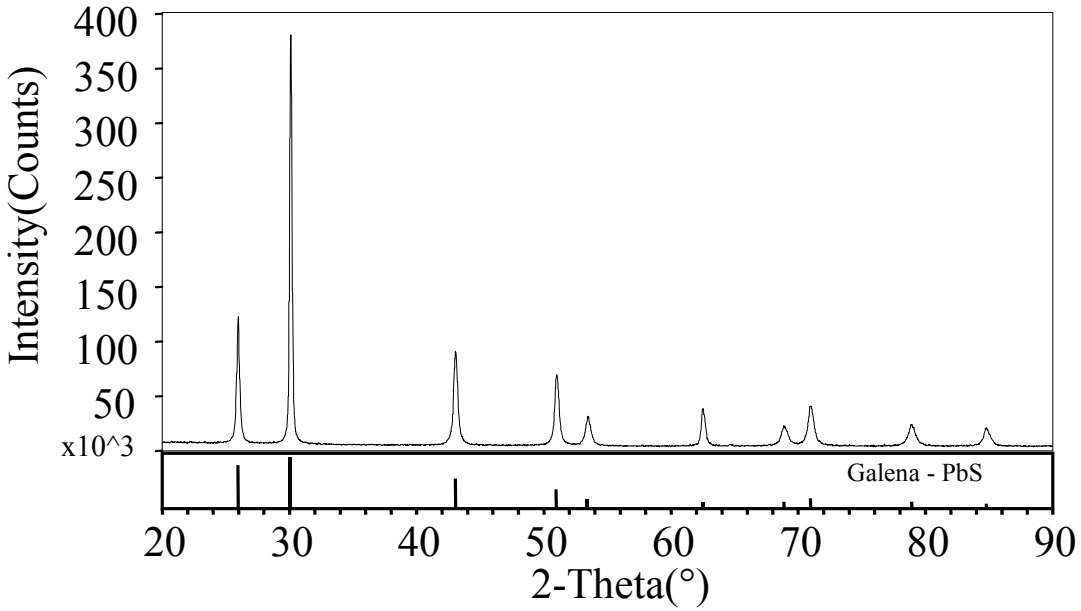

Figure 5. X-ray diffraction pattern for galena, PbS. Reference is shown below spectra as solid lines. CuKα radiation=1.54 Å.

Table 9. Observed Peaks in the X-Ray Diffraction Pattern of Galena

Peak (2*θ*), *Intensity x10*^{3} (measured by hand)	Known Galena Peak (2θ), *Intensity x10*^{3} (measured by hand)
26.0, *120.4*	26.0, *35.5*
29.0, *374.0*	30.1, *44.5*
43.0, *61.0*	43.0, *25.8*
50.8, *71.5*	51.0, *15.8*
53.6, *33.0*	53.6, *7.5*
62.6, *39.6*	62.6, *4.6*
68.5, *27.5*	68.8, *4.5*
71.0, *41.3*	71.0, *8.5*
78.8, *27.7*	78.8, *4.2*
84.6, *27.5*	84.8, *3.0*

Diffraction pattern shown in Figure 5. Peaks given as 2-theta. The known peaks are from the JCPDS database

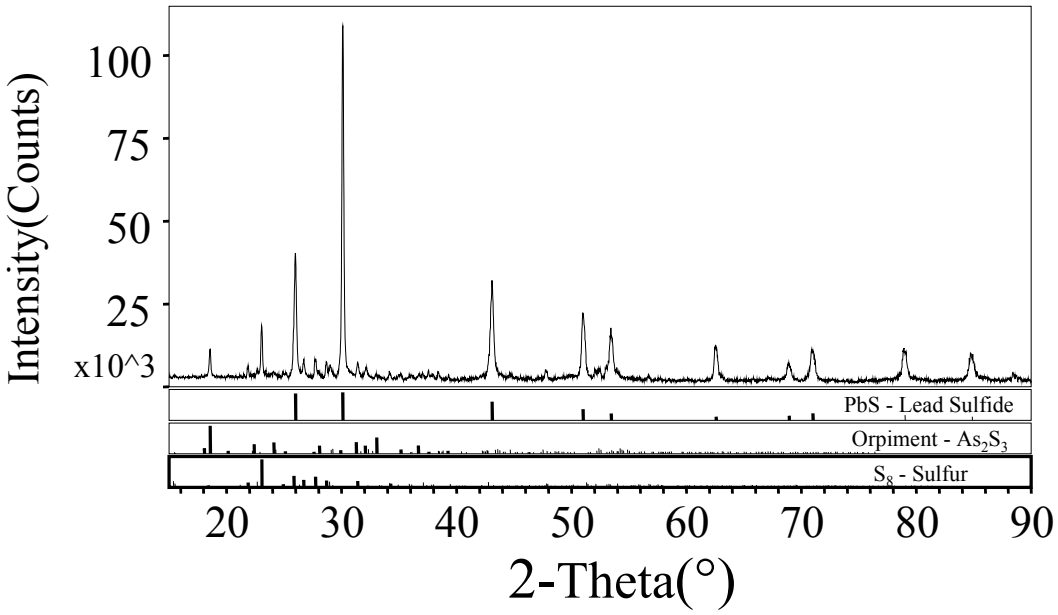

Figure 6. X-ray powder diffraction pattern of $PbS+As_2S_3+S$ assemblage after 30 days in equilibrium with a sulfidic solution ($1.65x10^{-3}$ M total sulfide, pH=7.5). References are shown below spectra as solid lines. CuKα radiation=1.54 Å.

Table 10. Observed Peaks in the X-Ray Diffraction Pattern of the $PbS+As_2S_3+S$ Assemblage After 30 days of Equilibration with a Sulfidic Solution

Peak (2θ), *Intensity x10^3* (measured by hand)	Known Peak (2θ), *Intensity x10^3* (measured by hand)
18.6, *8.5*	orp 18.5, *8.9*
21.9, *3.4*	s 21.9, *1.9*
23.1, *14.9*	s 23.4, *15.5*
26.0, *38.4*	ga 26.0, *104.1*
26.7, *4.5*	s 26.7, *3.4*
27.8, 5.7	s 27.7, *5.4*
29.0, 5.7	orp 29.0, *0.8*. s 29.0, *2.3*
30.1, *110.0*	ga 30.1, *110.0*
31.4, *3.7*	orp 31.5, *0.4*, s 31.4, *2.8*
32.1, *3.1*	orp 32.0, *2.2*
43.0, *26.8*	ga 43.0, *70.3*
47.8, *3.2*	orp 47.8, *0.4*. s 47.8, *0.3*
50.8, *18.3*	ga 51.0, *38.1*
53.6, *14.1*	ga 53.6, *21.8*. orp 53.4, *0.6*. s 53.4, *0.7*
62.6, *10.8*	ga 62.6, *8.9*
68.9, *4.7*	ga 68.5, *12.9*
71.0, *8.5*	ga 71.0, *22.1*
78.9, *9.0*	ga 78.8, *14.3*
84.8, *7.6*	ga 84.6, *7.5*

Diffraction pattern shown in Figure 6. Peaks given as 2-theta. The known peaks are from the JCPDS database. Abbreviations are: orp=orpiment, s=sulfur and ga=galena

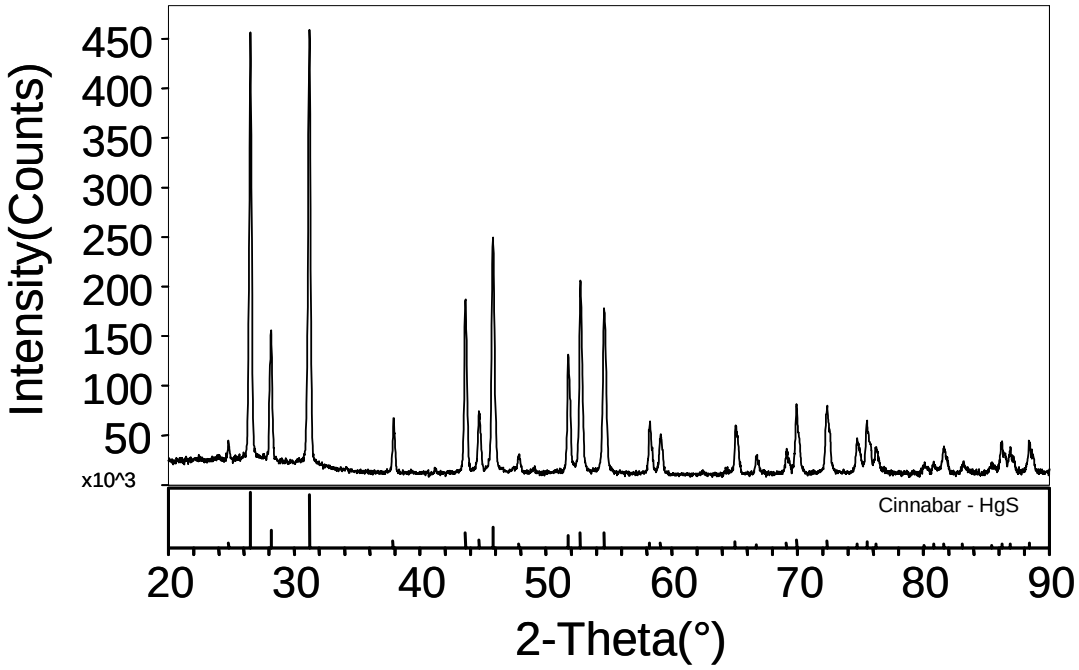

Figure 7. X-ray diffraction pattern for cinnabar, HgS. Reference is shown below spectra as solid lines. CuKα radiation=1.54 Å.

Table 11. Observed Peaks in the X-Ray Diffraction Pattern of the HgS

Peak (2θ), *Intensity x10^3* (measured by hand)	Known HgS Peak (2θ), *Intensity x10^3* (measured by hand)
24.8, *20.2*	24.8, *8.9*
26.5, *452.4*	26.5, *148.0*
28.2, *137.6*	28.2, *44.4*
31.2, *460.2*	31.2, *140.0*
37.9, *58.0*	37.9, *14.8*
43.6, *182.7*	43.6, *37.0*
44.68, *62.12*	44.7, *17.8*
45.8, *247.6*	45.8, *51.8*
47.9, *18.9*	47.8, *5.9*
51.8, *120.6*	51.8, *29.6*
52.7, *198.3*	52.7, *37.0*
54.6, *174.4*	54.6, *37.0*
58.3, *53.4*	58.2, *8.9*
59.1, *40.0*	59.1, *8.9*
65.1, *52.0*	65.0, *8.9*
66.8, *21.2*	66.7, *3.0*
69.1, *22.1*	69.1, *8.9*
69.9, *69.9*	69.9, *17.8*
72.3, *71.8*	72.4, *14.8*
74.8, *30.8*	74.8, *5.9*
75.5, *47.4*	75.5, *11.8*
76.3, *19.3*	76.3, 5.9
80.1, *11.0*	80.7, *3.0*
80.8, *10.1*	80.2, *5.9*
81.6, *28.1*	81.6, *5.9*
83.2, *12.9*	83.1, *5.9*
85.4, *9.7*	85.4, *3.0*
86.2, *27.2*	86.2, *5.9*
86.9, *24.9*	86.9, *5.9*
88.4, *33.1*	88.4, *8.9*

Diffraction pattern shown in Figure 7. Peaks given as 2-theta. The known peaks are from the JCPDS database

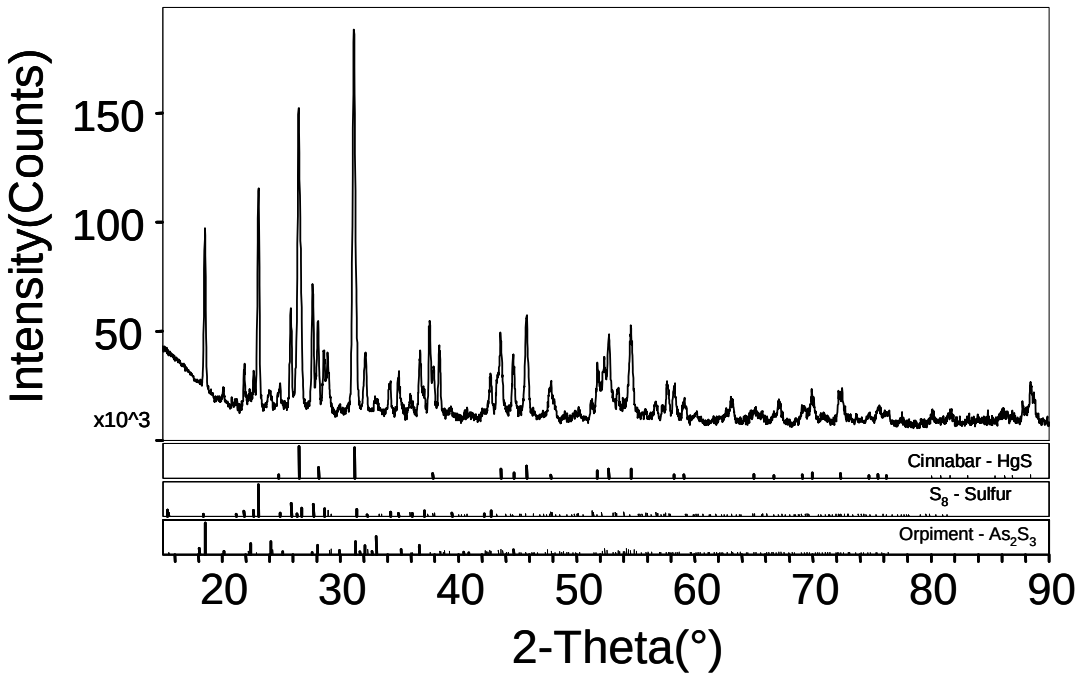

Figure 8. X-ray powder diffraction pattern of $HgS+As_2S_3+S$ assemblage after 30 days in equilibrium with a sulfidic solution ($1.65x10^{-3}$ M total sulfide, pH=7.5). References are shown below spectra as solid lines. CuKα radiation=1.54 Å.

Table 12. Observed Peaks in the X-Ray Diffraction Pattern of the $HgS+As_2S_3+S$ Assemblage After 30 days of Equilibration with a Sulfidic Solution

Peak (2θ), *Intensity x10^3* (measured by hand)	Known Peak (2θ), *Intensity x10^3* (measured by hand)
18.6, *79.3*	s 18.5, *2.0*. orp 18.5, *95.0*
20.2, *7.1*	orp 20.1, *5.7*
21.9, *19.6*	s 21.9, *13.5*
22.7, *17.4*	s 22.7, *16.2*. orp 22.9, *0.7*
23.1, *108.2*	s 23.1, *110.5*
24.9, *10.6*	cin 24.8, *8.9*. s 25.0, *7.3*. orp 25.1, *3.4*
25.8, *44.8*	s 25.9, *41.6*
26.5, *148.0*	cin 26.5, *148.0*. s 26.4, *3.43*
27.7, *39.5*	s 27.8, *38.2*. orp 25.6, *1.62*
28.1, *59.1*	cin 28.2, *44.4*
28.9, *26.6*	s 29.0, *16.4*. orp 290, *8.27*
31.2, *188.8*	cin 31.2, *140.1*. orp 31.2, *36.1*
32.2, *28.1*	s 32.4, *0.3*. orp 32.3, *11.3*
33.0, 7.2	orp 33.0, *53.3*
36.8, *29.5*	orp 36.6, *24.3*
37.6, *42.3*	s 37.5, *2.8*. orp 37.5, *2.4*
38.4, *32.3*	orp 38.4, *4.8*
42.7, *18.9*	s 42.9, *14.2*. orp 42.7, *5.3*
43.6, *38.9*	cin 43.6, *37.0*
44.7, *29.3*	cin 44.7, *17.8*. s 44.7, *0.9*. orp 44.6, *9.0*
45.8, *50.0*	cin 45.8, *51.8*. s 45.8, *3.9*. orp 45.7, *1.4*
47.8, *17.0*	cin 47.8, *5.9*. s 47.9, *8.8*. orp 47.8, *4.8*
51.8, *28.7*	cin 51.8, *29.6*. s 51.8, *1.0*. orp 51.6, *1.0*
52.4, *25.11*	s 52.2, *8.2*. orp 52.3, *14.2*
52.7, *28.7*	cin 52.7, *37.0*. orp 52.5, *8.8*
54.6, *42.3*	cin 54.6, *37.0*. s 54.6, *0.3*. orp 54.5, *6.2*
58.3, *15.1*	cin 58.2, *8.9*. orp 58.3, *1.05*
59.1, *8.3*	cin 59.1, *8.9*. s 59.3, *2.1*
69.1, *6.6*	cin 69.1, *8.9*. s 89.1, *1.9*
72.5, *16.2*	cin 72.4, *14.8*. s 72.5, *2.5*. orp 72.5, *1.0*
88.4, *19.6*	cin 88.4, *8.9*

Diffraction pattern shown in Figure 8. Peaks given as 2-theta. The known peaks are from the JCPDS database. Abbreviations are: orp=orpiment, s=sulfur and cin=cinnabar

II.B.1.2. Synthesis and Characterization of Ag_2S, Ag_3AsS_3 and $AgAsS_2$

II.B.1.2.1. Characterization of Ag_2S

Silver sulfide, Ag_2S (Alfa Aesar, 99.9% metals basis) was characterized as acanthite using Powder X-Ray Diffraction. The solids were characterized using a Bruker D8 Advanced Powder Diffractometer with an area detector. The goniometer was aligned against a quartz standard. The x-ray diffraction pattern for Ag_2S is shown in Figure 9 and listed in Table 13.

X-Ray photoelectron spectroscopy (XPS) was done (Bindu Varughese, UMCP Chemistry Department) on an unreacted sample of Ag_2S, and an Ag_2S+S assemblage that had been equilibrated with a sulfidic solution for at least 40 days. The XPS measurements were done using a Kratos Axis 165 spectrometer at a vacuum of 4 $x10^{-10}$ torr with nonmonochromatic Mg Kα radiation. The powdered sample was introduced into the chamber by dusting the sample directly onto carbon tape. The carbon served as a calibration point for C 1s, which has a characteristic eV of 285.0. A wide scan survey was done and various regions were analyzed. Spectra were recorded in the FAT (fixed analyzer transmission) analyzer mode with a pass energy of 20 eV and with an average of 10 scans with a 60 second duration.

In both cases, XPS revealed that small amounts of oxygen were present in the starting and reacted sample, but the reacted sample had half as much of the oxygen impurity as the starting material. XPS is a surface technique and measures approximately 15 angstroms into the surface, so the bulk material is not necessarily the same as the surface. The binding energies for O 1s in these samples does not closely correspond to the silver oxide species, but could correspond to Ag_2SO_4.

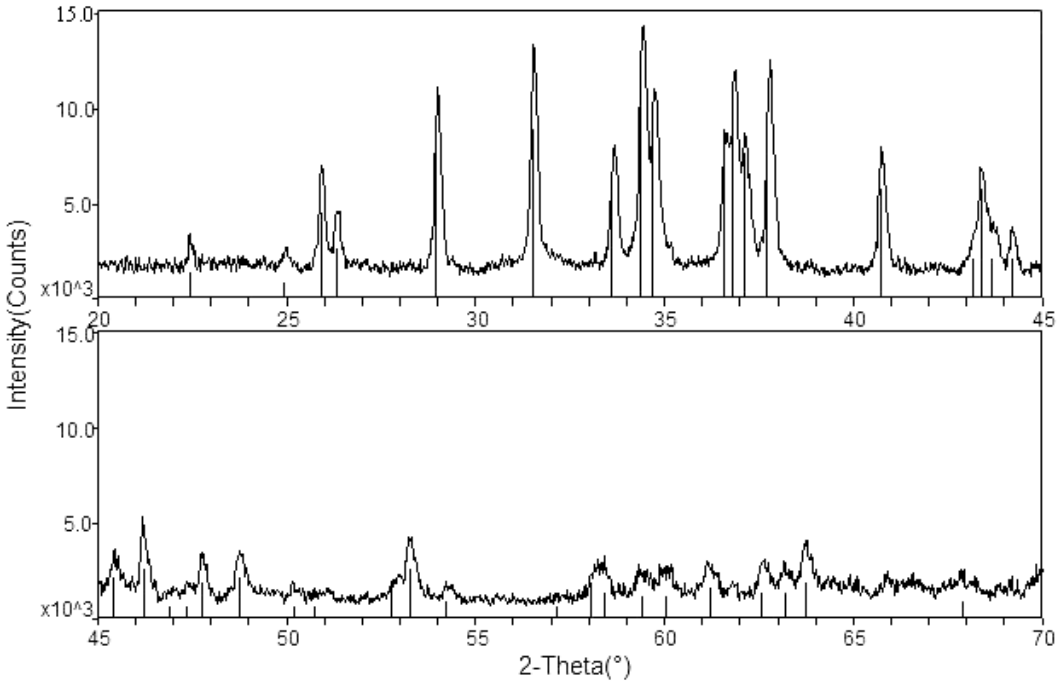

Figure 9. X-ray power diffraction pattern of Ag_2S. Reference is acanthite and is shown as solid lines. CuKα radiation 1.54 Å.

Table 13. Observed Peaks in the X-Ray Diffraction Pattern of Ag_2S (acanthite). The data are 2 theta followed by the estimated intensity.

My Peak (2θ), *Intensity (x10^3)* (measured by hand)	Acanthite Peak (2θ), *Intensity (x10^3)* (measured by hand)
25.81, *7.1*	25.81, *4.8*
26.37, *4.4*	26.30, *2.7*
29.00, *11.3*	28.98, *7.7*
31.52, *13.5*	31.52, *10.7*
33.75, *8.3*	33.62, *5.2*
34.40, *13.5*	34.38, *12.5*
34.68, *11.3*	34.75, *10.6*
36.88, *12.2*	36.75, *10.8*
37.75, *12.7*	37.70, *10.6*
40.73, *8.1*	40.73, *7.5*

Diffraction pattern shown in Figure 9. Peaks given as 2-theta. The known peaks are from the JCPDS database

Because the samples were not etched to remove the top layer, the surface probably had an oxygen layer from contact with air.

II.B.1.2.2. Synthesis and Characterization of $AgAsS_2$ and Ag_3AsS_3

$AgAsS_2$ and Ag_3AsS_3 were synthesized from Ag_2S (Alfa Aesar, 99.9% metals basis) and As_2S_3 (Cerac, 1-6 mm pieces, 99.9% pure). The As_2S_3 was composed of slightly amorphous red glass pieces, and was washed with 0.01M NaOH and water to remove any oxide impurities. To synthesize $AgAsS_2$, 5.5074 grams of Ag_2S and 5.4655 grams of As_2S_3 were combined. To synthesize Ag_3AsS_3, 5.9950 grams of Ag_2S and 1.9907 grams As_2S_3 were combined. The mixtures were placed in the glovebox, ground together and transferred to quartz tubes. The tubes were evacuated for 30 minutes and then heat-sealed while still under vacuum. The tubes were then placed in a furnace where the temperature was increased 15°C per hour over two days until a temperature of 150°C was reached; this temperature was held for 2 weeks. After the first 2 weeks of the reaction the materials were analyzed with x-ray diffraction. The peaks of the diffraction pattern were not very sharp, which led to the conclusion that the reaction did not reach equilibrium. The materials were then reground under acetone in the glovebox, resealed, heated to 195°C and held at this temperature for another 3 weeks. After 3 weeks the temperature was lowered slowly so any high temperature phase would invert to a low temperature phase.

The x-ray diffraction patterns of the starting materials, $AgAsS_2$ and Ag_3AsS_3 are shown in Figures 10 and 11, respectively. Table 14 and 15 identify the peaks

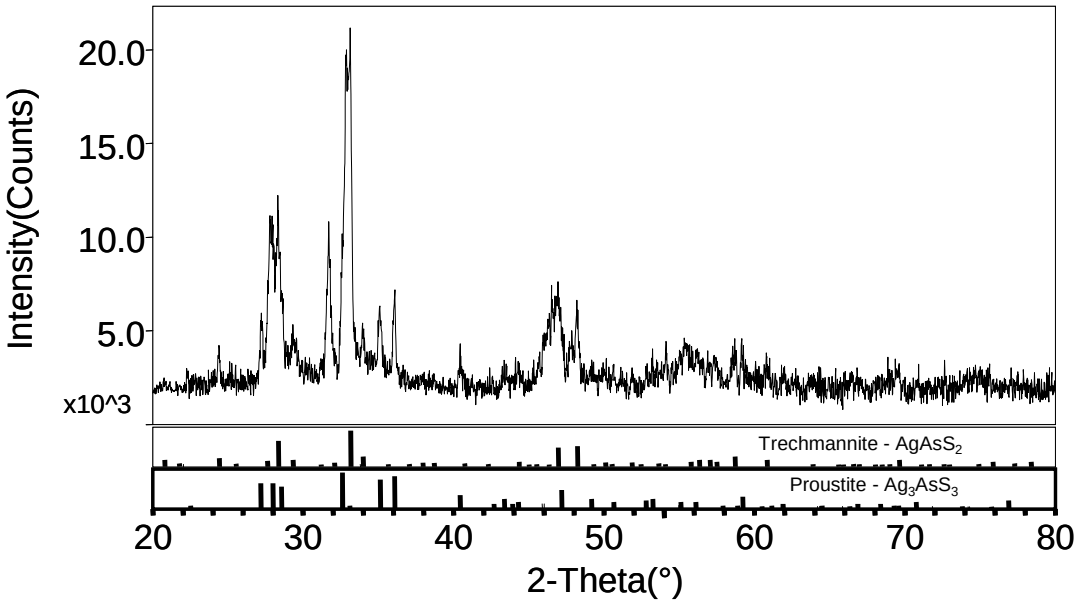

Figure 10. X-ray diffraction pattern for the raw $AgAsS_2$ starting material, trechmannite/proustite ($AgAsS_2/Ag_3AsS_3$). References, trechmannite and proustite, are shown below spectra as solid lines. CuKα radiation 1.54 Å.

Table 14. Observed Peaks in the X-Ray Diffraction Pattern of $AgAsS_2$ Starting Material. The data are 2 theta followed by the estimated intensity.

My Peaks (2θ), *Intensity (x10^3)* (measured by hand)	Known Peaks (2θ), *Intensity (x10^3)* (measured by hand)
24.38, *4.2*	tr 24.38, *4.2*
27.80, *11.3*	tr 27.75, *2.5*, pr 27.10, *11.1*
28.38, *12.5*	tr 28.38, *13.8*, pr 28.05, *11.0*, pr 28.66, *11.0*
31.75, *11.0*	tr 32.06, *2.5*, pr 31.00, *11.3*
33.12, *21.3*	tr 33.22, *17.8*
35.00, *5.3*	tr 35.10, *5.1*
35.48, *7.0*	pr 35.32, *11.0*
40.99, *4.2*	pr 40.56, *3.8*
46.15, *7.5*	pr 46.30, *11.0*
46.90, *7.5*	tr 46.98, *8.8*, pr 47.48, *5.5*
48.25, *7.0*	tr 48.25, *9.8*

Diffraction pattern shown in Figure 10. Peaks given as 2-theta. The known peaks are from the JCPDS database. Abbreviations are: tr = trechmannite and pr=proustite

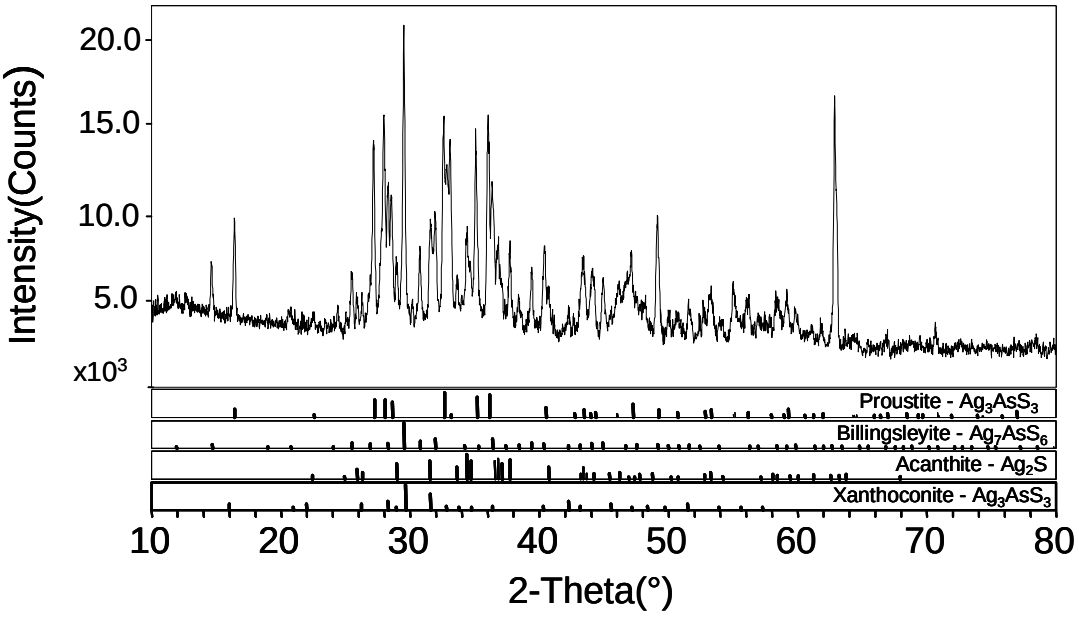

Figure 11. X-ray diffraction pattern for the raw Ag_3AsS_3 starting material (proustite). References, proustite, acanthite and xanthoconite (low temperature phase) are shown below spectra as solid lines. CuKα radiation 1.54 Å.

Table 15. Observed Peaks in the X-Ray Diffraction Pattern of Ag_3AsS_3 Starting Material. The data are 2 theta followed by the estimated intensity.

My Peaks (2θ), *Intensity (x10^3)* (measured by hand)	Known Peaks (2θ), *Intensity (x10^3)* (measured by hand)
14.50, *7.2*	bi 14.75, *1.0*
16.42, *10.0*	xan 16.00, *2.9*
25.40, *6.8*	bi 25.40, *3.2*
25.90, *5.6*	ac 25.99, *3.2*
26.28, *5.6*	xan 26.26, *2.8*, ac 26.30, *2.1*
27.20, *14.5*	pr 27.22, *10.0*, bi 26.91, *3.2*
28.00, *16.1*	pr 28.07, *10.0*
28.28, *12.4*	xan 28.30, *4.3*, bi 28.29, *1.85*
28.56, *11.8*	pr 28.59, *8.6*
29.50, *21.2*	xan 29.58, *13.6*, bi 29.53, *13.2*
31.00, *8.26*	bi 30.75, *3.8*
31.56, *9.7*	xan 31.56, *4.3*
31.92, *7.3*	bi 31.94, *6.9*
32.57, *16.1*	pr 32.59, *14.4*
33.11, *14.5*	pr 33.14, *0.6*
33.59, *6.7*	ac 33.61, *4.3*. xan 33.77, *0.6*
34.46, *9.1*	ac 34.46, *8.99*
35.03, *15.0*	pr 35.15, *11.8*, bi 35.31, *0.6*
36.03, *16.1*	pr 36.15, *13.3*
36.35, *12.1*	xan 36.37, *1.8*
36.42, *8.9*	ac 36.42, *7.4*
37.68, *8.9*	ac 37.71, *7.1*
40.38, *8.5*	xan 40.29, *1.4*, pr 40.44, *4.7*
42.28, *19.3*	xan 42.28, *4.8*
43.35, *7.2*	xan 43.17, *1.4*
44.00, *6.7*	bi 44.00, *2.7*
45.00, *6.5*	bi 44.90, *3.2*
49.15, *10.0*	pr 49.25, *3.8*
62.84, *17.1*	ac 62.63, *1.0*

Diffraction pattern shown in Figure 11. Peaks given as 2-theta. The known peaks are from the JCPDS database. Abbreviations are: ac=acanthite, bi= billingsleyite, xan=xanthoconite and pr=proustite

from the diffraction pattern. The x-ray diffraction pattern for $AgAsS_2$ shows that proustite is also present in the material. The x-ray diffraction pattern of Ag_3AsS_3 shows that the low and high temperature phases of Ag_3AsS_3 (xanthoconite and proustite, respectively) are present as well as Ag_2S and Ag_7AsS_6.

The x-ray diffraction pattern of $AgAsS_2$ after 30 days of equilibration with a sulfidic solution (pH ~8, 0.001 M HS^-) is shown in Figure 12. Table 16 identifies the peaks. In Figure 12 the formation of an orpiment like phase is seen at approximately 18.8 and 23.1^o (slight peak shift by ~0.6^o). The peak at 30.5° is unidentified. These peaks could be the result of the exsolution of As_2S_3 from trechmannite, indicating that the trechmannite may not have been stable. Samples from this data set will be termed Ag assemblage A throughout the dissertation.

A nominally $AgAsS_2$ sample that was reacted with a sulfidic solution was inspected by a JOEL 8900 Superprobe using Energy Dispersive X-Ray Analysis (EDS). The sample was first imbedded in epoxy and was then ground with SiC impregnated papers (800 grit) and polished with 6 micron diamond paste. When the sample was viewed under a microscope there appeared to be two distinct phases, which appeared as either an orange or a honey brown color. Upon further inspection with EDS, sample particles were observed that had cores and reaction rims, as shown in Figure 13. Table 17 identifies the composition of a number of particles in two reacted samples (Ag assemblage A). The bright region, which is the reaction rim, contained Ag_3AsS_3. The darker core region was expected to contain $AgAsS_2$ because it is less rich in Ag. However, the core region contained Ag_3AsS_3 in some instances. $AgAsS_2$ was found in other portions of the sample but not in the core.

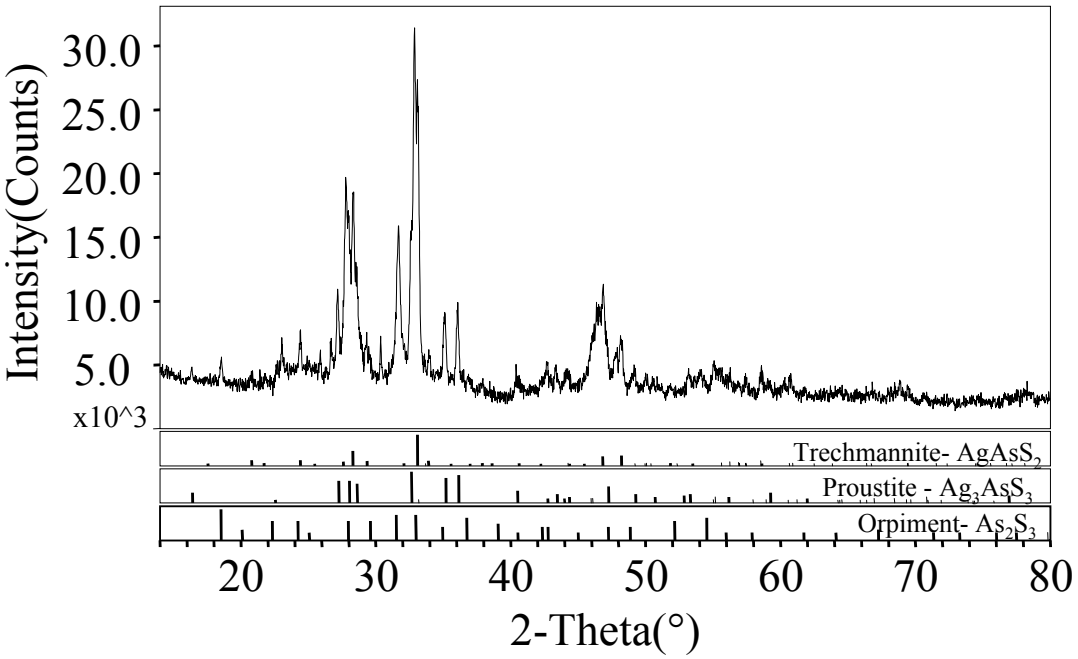

Figure 12. X-ray powder diffraction pattern of Ag assemblage A after 30 days in equilibration with a sulfide solution of 0.001 M starting total sulfide, pH 8.10± 0.07. References, trechmannite, proustite and orpiment, shown below spectra as solid lines. CuKα radiation 1.54 Å.

Table 16. Observed Peaks in the X-Ray Diffraction Pattern of Ag assemblage A after 30 days in Equilibration with a Sulfide Solution of 0.001 M Starting Total Sulfide, pH 8.10± 0.07. The data are 2 theta followed by the estimated intensity.

My Peak (2θ), *Intensity (x10^3)* (measured by hand)	Known Peaks (2θ), *Intensity (x10^3)* (measured by hand)
18.8, *5.1*	orp 18.2, *4.0*
23.10, *7.50*	orp 22.2, *2.0*
24.38, *19.0*	tr 24.38, *4.2*
27.70, *19.0*	tr 27.75, *2.5*, pr 27.10, *11.1*
28.38, *17.6*	tr 28.38, *13.8*, pr 28.66, *11. 0*
30.50, *7.5*	orp 29.6, *1.8*, pr 31.00, *11.3*
31.75, *11.0*	tr 32.06, *2.5*
33.12, *21.3*	tr 33.20, *17.8*, orp 33.15, *2.0*
35.00, *6.0*	tr 35.50, *5.1*, pr 35.10, *11.0*
35.48, *7.0*	pr 35.32, *11.0*
46.98, *7.5*	tr 46.98, *8.8*, pr 47.48, *5.5*
48.25, *7.0*	tr 48.25, *9.8*

Diffraction pattern shown in Figure 12. Peaks given as 2-theta. The known peaks are from the JCPDS database. Abbreviations are: orp = orpiment, tr = trechmannite, s= sulfur, pr=proustite

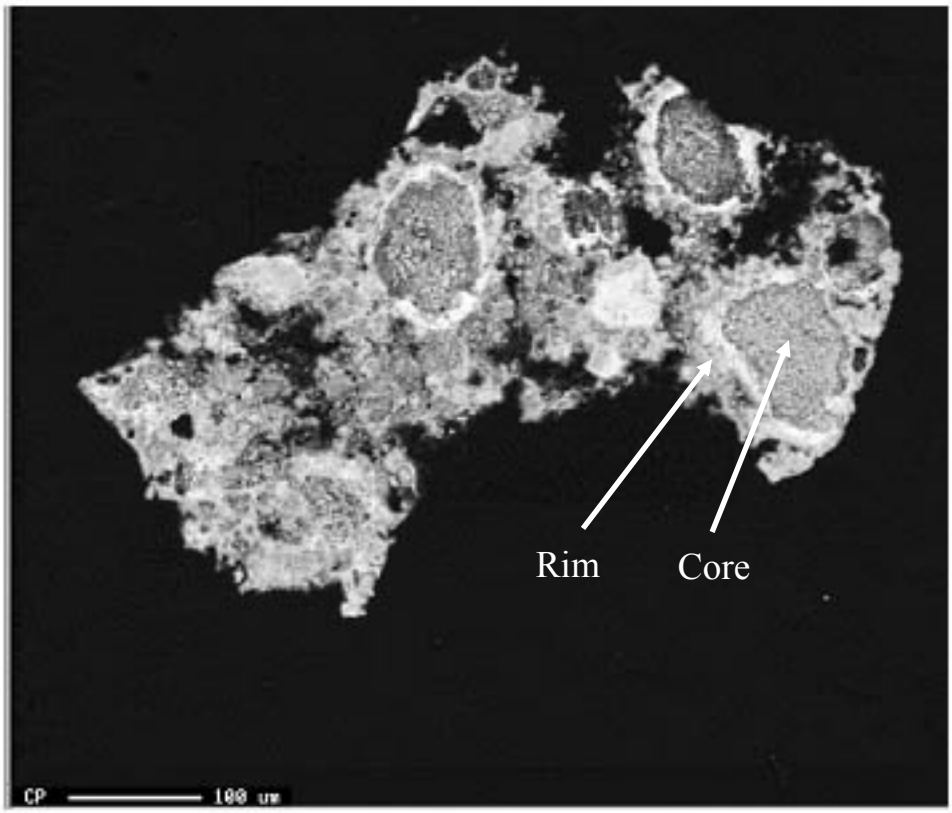

Figure 13. Electron backscattering image of an Ag assemblage A sample that was reacted with a sulfidic solution for at least 30 days. $AgAsS_2$ and Ag_3AsS_3 (rim, bright region) identified as Ag phases.

Table 17. EDS Composition Data for Particles in Ag Assemblage A

Conditions				Weight %				
Grain #	pH	Log ΣS	Sample Spot Description	Ag	As	S	Total	Mole Ratio*
Ag Assemblage A Sample 1- log ΣAs =--3.99, log ΣAg=-7.15, Equilibration=49 d.								
1	7.15	-4.20	bright area	60.7	19.1	20.1	100.0	$Ag_{0.90}As_{0.41}S$
			dark area	46.7	27.9	25.4	100.0	$Ag_{0.55}As_{0.47}S$
2			bright particle (orange)	0.2	62.9	36.8	100.0	$As_{1.28}S$
Ag Assemblage A Sample 2 - log ΣAs =-4.02, log ΣAg=-7.17, Equilibration 44 d.								
1	8.13	-3.42	bright area	67.6	13.9	18.5	100.0	$Ag_{1.08}As_{0.32}S$
			bright rim	65.2	15.7	19.1	100.0	$Ag_{1.02}As_{0.35}S$
			dark core	68.9	13.1	17.9	100.0	$Ag_{1.14}As_{0.31}S$
2			bright particle (orange)	-	61.3	0.61	100.0	$As_{0.69}S$
3			bright particle	48.7	30.7	20.6	100.0	$Ag_{0.70}As_{0.72}S$
4			bright particle	63.4	17.7	18.8	100.0	$Ag_{0.99}As_{0.40}S$
5			dark particle	67.2	14.4	18.3	100.0	$Ag_{1.09}As_{0.34}S$
			Known phase			Ag_2S		Ag_2S
			Known phase			Ag_3AsS_3		$AgAs_{0.3}S$
			Known phase			$AgAsS_2$		$Ag_{0.5}As_{0.5}S$
			Known phase			Ag_5AsS_4		$Ag_{1.25}As_{0.25}S$
			Known phase			Ag_7AsS_6		$Ag_{1.17}As_{0.17}S$

* mole ratio have been normalized with respect to sulfur.

The sample also contained an orange phase that was identified as As_2S_3. Glassy (amorphous) As_2S_3 was used to synthesize the starting material. The transformation to $AgAsS_2$ may not have been quantitative and some glassy As_2S_3 could have been annealed to crystalline As_2S_3. Since there are three phases in this experiment the system may not be at equilibrium.

The x-ray diffraction pattern of Ag_3AsS_3+Ag_2S after 40 days of equilibration with a sulfidic solution (pH=7.59, 8.83 x 10^{-4} M HS^-) is shown in Figure 14. Table 18 identifies the peaks from the diffraction pattern in Figure 14. Figure 14 shows very strong Ag_2S peaks and some weak Ag_3AsS_3 peaks at approximately 27.3 and

28°. It therefore must be concluded that the amount of proustite in the sample was small when compared to Ag_2S. Samples from this data set will be termed Ag assemblage B throughout the dissertation.

Samples containing Ag assemblage B that were reacted with a sulfidic solution were also inspected by EDS. A particle displaying three distinct areas is shown in Figure 15. Table 19 identifies the components in Ag assemblage B from an analysis of three representative samples. The darker region contained Ag_2S, while the brighter region inside the particle contained Ag_3AsS_3 (see labels in Figure 15). The brightness on the rims of the material is misleading because it was also identified as Ag_2S. The contrast in brightness is a result of the sample itself where the rims of the particles were flat, while the interior was slightly pitted. The pitting resulted in decreased weight percents in the interior of the samples, however they were still identified as Ag_2S due to the absence of any As. Ag_7AsS_6 was identified in the tiny particles that circled the Ag_2S particles. Ag_7AsS_6 likely precipitated when Ag_3AsS_3 and Ag_2S were dissolving, which formed a silver rich phase. More Ag_7AsS_6 was identified as small particles in the sample when compared to Ag_3AsS_3. This leads to the conclusion that most of the Ag_3AsS_3 dissolved during equilibration.

The Ag-As-S minerals did not take a very good polish, because they are soft. This affected the quality of the EDS measurement in some cases, by lowering the total weight percent of elements determined. A total weight percent of ~70 was obtained in some cases. However, in most cases the sum of components totaled ~95%, which provided quantitative ratios of the elements. The mole ratio of Ag to S was ~1.6 in areas defined as Ag_2S. The mole ratio of Ag to As to S was 3 to 1 to 3 in

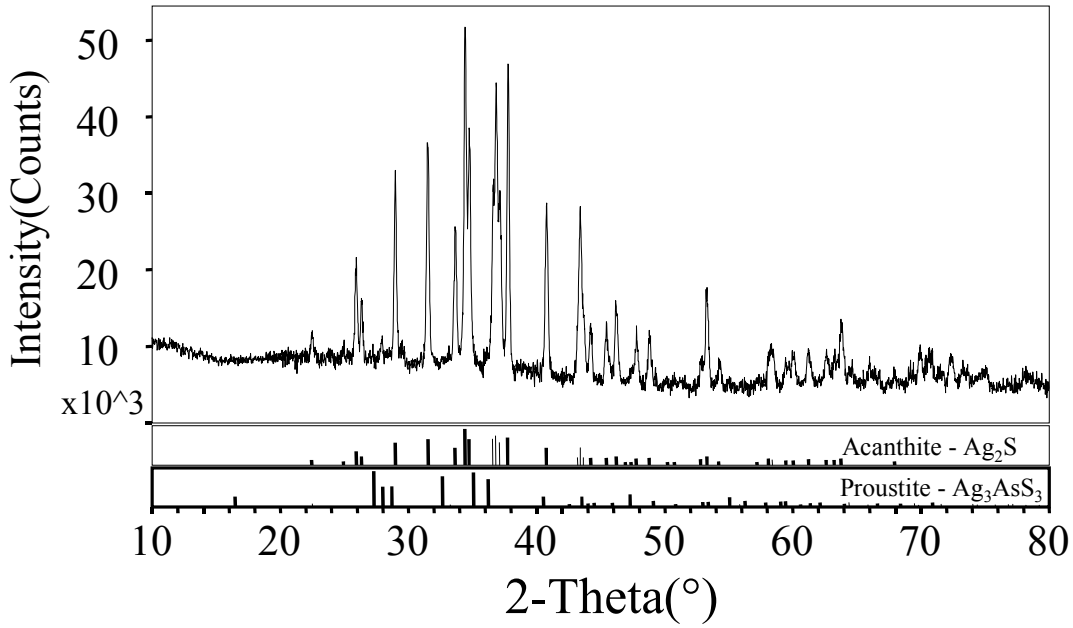

Figure 14. X-ray powder diffraction pattern of Ag assemblage B after 40 days in equilibration with a sulfide solution of 0.001 M starting total sulfide, pH 7.59. References shown below spectra as solid lines. CuKα radiation 1.54 Å.

Table 18. Observed Peaks in the X-ray Powder Diffraction Pattern of Ag assemblage B After 40 Days in Equilibration with a Sulfide Solution of 0.001 M Starting Total Sulfide, pH 7.59. The data are 2 theta followed by the estimated intensity

My Peaks (2θ), *Intensity ($x10^3$)* (measured by hand)	Known Peaks (2θ), *Intensity ($x10^3$)* (measured by hand)
22.50, *4.7*	ac 22.42, *2.0*. pr 22.49, *0.4*
25.94, *15.9*	ac 25.90, *7.0*
26.36, *9.5*	ac 26.32, *4.0*
29.0, *30.3*	ac 28.97, *12.0*
31.48, *35.7*	ac 31.52, *14.0*
33.64, *20.2*	ac 33.61, *9.0*
34.42, *51.2*	ac 34.38, *20.0*
34.74, *36.8*	ac 34.70, *14.0*
36.84, *43.4*	ac 36.8, *16.0*
37.16, *27.1*	ac 37.1, 12.0
37.78, *46.6*	ac 37.72, 15.0
40.80, *27.7*	ac 40.74, *9.0*
43.40, *26.6*	ac 43.40, *9.0*. pr 43.50, *2.5*
44.22, *7.6*	ac 42.20, *3.2*
45.46, *8.9*	ac 45.49, *3.2*
46.18, *12.8*	ac 46.20, *4.0*
47.80, *9.2*	ac 47.70, *2.8*
48.80, *8.7*	ac 48.80, *3.2*
53.30, *15.7*	ac 53.30, *4.0*. pr 53.39, *1.0*
63.76, *8.9*	ac 63.73, *2.8*

Diffraction pattern shown in Figure 14. Peaks given as 2-theta. The known peaks are from the JCPDS database. Abbreviations are: ac=acanthite, pr=proustite

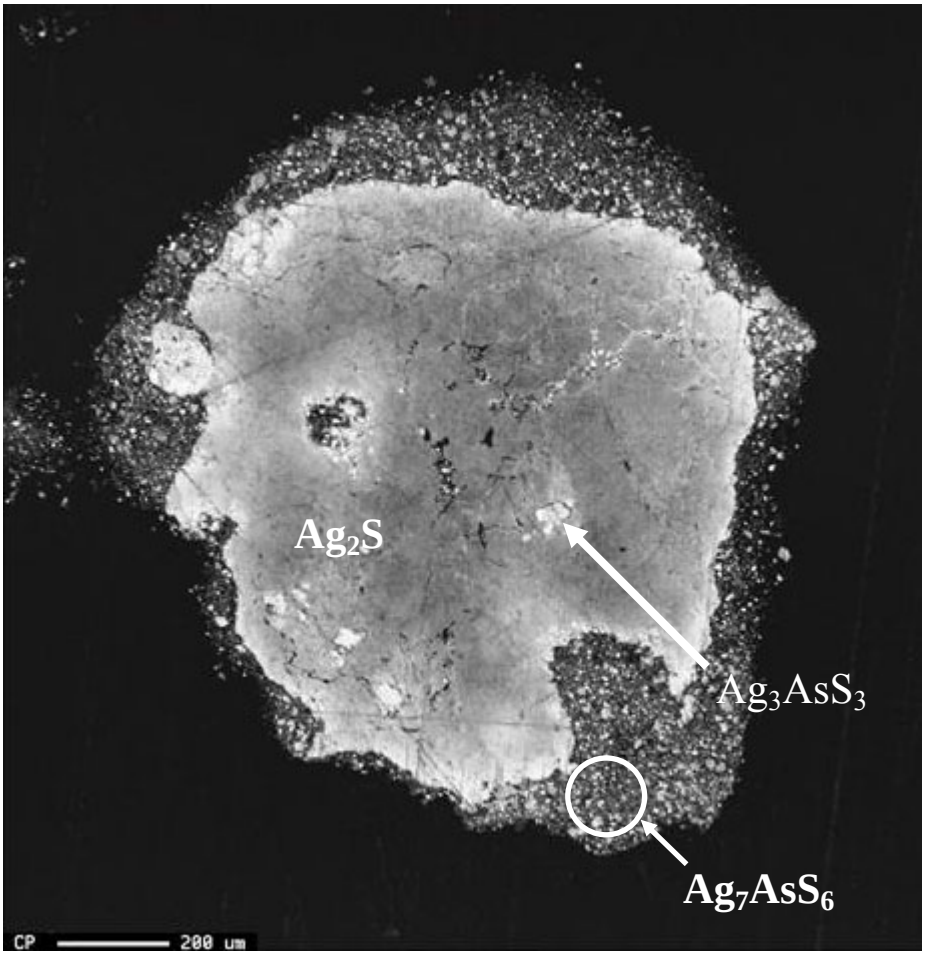

Figure 15. Electron backscattering image of Starting Material B that was reacted with a sulfidic solution for at least 30 days. Ag_2S, Ag_7AsS_6 and Ag_3AsS_3 (dark and bright region) identified as Ag phases.

Table 19. EDS Composition Data for Particles from Ag assemblage B

Conditions				Weight %				
Grain #	pH	Log ΣS	Sample Spot Description	Ag	As	S	Total	Mole Ratio*
Ag Assemblage B Sample 1- log Σ As =-4.11, log Σ Ag=-6.45, Equilibration Time=54 d.								
1	7.66	-3.37	bright rim left side particle	76.3	0	14.3	90.7	$Ag_{1.58}S$
			dark core	58.6	0.32	11.5	70.4	$Ag_{1.51}S$
			dark core	65.0	0	12.0	77.0	$Ag_{1.61}S$
			bright rim right side particle	67.4	0.08	12.1	79.5	$Ag_{1.66}S$
			small bright grains off particle	79.9	4.3	17.0	101.1	$Ag_{1.39}As_{0.11}S$
			small bright grains off particle	77.6	5.1	16.6	99.3	$Ag_{1.39}As_{0.13}S$
			small bright grains off particle	75.3	5.7	16.8	97.9	$Ag_{1.33}As_{0.14}S$
			bright particle in core	57.2	15.4	17.1	89.7	$Ag_{0.99}As_{0.38}S$
2			small bright grains off particle	81.6	3.8	16.8	102.2	$Ag_{1.45}As_{0.10}S$
			small bright grains off particle	78.9	4.0	16.4	99.3	$Ag_{1.43}As_{0.11}S$
Ag Assemblage B Sample 2 - log Σ As =-4.26, log Σ Ag=-6.58, Equilibration Time=52 d.								
1	7.87	-4.26	bright area of particle off rim	71.1	8.9	18.2	98.4	$Ag_{1.16}As_{0.21}S$
			dark area of particle off rim	63.5	0.42	12.1	76.1	$Ag_{1.56}As_{0.01}S$
2			bright area	66.0	9.8	18.6	94.5	$Ag_{1.05}As_{0.22}S$
			bright rim	78.9	0.0	14.1	93.1	$Ag_{1.66}S$
3			slightly darker core	76.8	5.9	18.5	101.2	$Ag_{1.23}As_{0.14}S$
			bright rim	84.5	0.91	15.2	100.5	$Ag_{1.66}As_{0.02}S$
Ag Assemblage B Sample 3 - log Σ As =-4.03, log Σ Ag=-6.70, Equilibration Time, 53 d.								
1	7.25	-3.08	bright rim	82.5	0.19	14.1	96.8	$Ag_{1.74}As_{0.01}S$
2			bright rim	83.8	0.3	14	98.0	$Ag_{1.78}As_{0.01}S$
			dark core	76.7	0.63	13.6	90.9	$As_{1.68}As_{0.02}S$
			dark core	56.3	0.1	10.6	67.0	$Ag_{1.58}As_{0.004}S$
3			bright rim	81.1	0.05	14.5	95.7	$Ag_{1.66}As_{0.001}S$
			dark core	56.1	0.59	10.9	67.7	$Ag_{1.52}As_{0.02}S$
			bright particle off rim	83.5	2.2	14.8	100.5	$Ag_{1.67}As_{0.06}S$
			bright particle off rim	82.0	1.6	15.9	99.5	$Ag_{1.53}As_{0.04}S$
			bright particle off rim	82.3	1.1	15.7	99.2	$Ag_{1.55}As_{0.03}S$
			Known phase			Ag_2S		Ag_2S
			Known phase			Ag_3AsS_3		$AgAs_{0.3}S$
			Known phase			$AgAsS_2$		$Ag_{0.5}As_{0.5}S$
			Known phase			Ag_5AsS_4		$Ag_{1.25}As_{0.25}S$
			Known phase			Ag_7AsS_6		$Ag_{1.17}As_{0.17}S$

* mole ratio have been normalized with respect to sulfur.

most areas defined as proustite. The mole ratio of Ag to As to S was ~7 to ~1 to ~6 in most areas defined as billingsleyite.

The reacted assemblages will therefore be described as follows: orpiment (crystalline) only experiments will be represented as As_2S_3 and orpiment plus elemental sulfur experiments will be represented as As_2S_3+S. Experiments dealing with galena, orpiment and elemental sulfur will be represented as PbS+As_2S_3+S. Experiments dealing with cinnabar, orpiment and elemental sulfur will be represented as HgS+As_2S_3+S. Experiments containing acanthite and elemental sulfur will be defined as Ag_2S+S. Experiments involving the proustite starting material and acanthite will be defined as Ag assemblage B and experiments containing the trechmannite starting material (also contains proustite and unstable orpiment like phase) will be represented as Ag assemblage A.

II.B.2. Mineral Dissolution

II.B.2.1. As_2S_3, As_2S_3+S, HgS+As_2S_3+S, PbS+As_2S_3+S, Ag Assemblage A and B in Sulfidic Solutions

All solutions were prepared with deionized water from an ion exchange/organic adsorption filtration system (Barnstead/Thermolyne). All sample preparations and manipulations were performed in a N_2 glove box unless otherwise specified. Bisulfide solutions were prepared by bubbling high purity H_2S gas (Matheson) through deoxygenated 1.0 M sodium hydroxide solutions for 45 minutes. The bisulfide solution was then bubbled with nitrogen for five minutes to remove

any excess H_2S gas. The reaction vessel was immediately closed and transferred to an N_2 filled glove box. MOPS buffer, 3-(N-morpholino)propane suphonic acid, was used for the pH range of 7.26 to 8.25. All solutions were purged with N_2 for 30 minutes before being placed in the glove box prior to use.

The masses of the solids for the solubility studies are shown in Table 20. The solids were placed in glass ampoules. 20 milliliters of solution with varying pH, MOPS buffer concentrations (0.004M, 0.0071M and 0.014M) and bisulfide concentrations (0.001 M, 0.0005 M, and 0.0001 M) were added to the ampoules. To fix ionic strength sodium chloride (0.010 M) was added to ampoules containing As_2S_3 only, As_2S_3+S, PbS+As_2S_3+S, HgS+As_2S_3+S and Ag_2S+S. Sodium sulfate (J.T. Baker), 3.33 x 10^{-3} M, was used to control the ionic strength in the Ag-As-S systems because chloride was interfering with elemental analysis.

The ampoules were then removed from the glove box after being capped by a balloon attached to a piece of rubber. The balloons prevented the sulfide solutions from coming into contact with air. The ampoules were fusion sealed using an oxygen/propane flame within 10 minutes after removal from the glove box. Ampoules were equilibrated on a tumbler at room temperature for at least 4 weeks. Ampoules containing Ag were covered with aluminum foil during the equilibration period, to prevent the photoreduction of silver sulfide to elemental silver.

After the desired reaction time, ampoules were opened and syringe filtered with a 0.02 μm Whatman Anatop 25 Filter. Approximately 10 milliliters of sample was extracted into a syringe and the first 2 milliliters were discarded. The remaining solution was filtered into a 15 mL polystyrene centrifuge tube.

Table 20. Starting Masses of Solids for Solubility Studies

	Mass Solid (g, ± 0.001 g)						
Experiment	As_2S_3	S	PbS	HgS	Ag_2S	Ag_3AsS_3	$AgAsS_2$
As_2S_3 only	0.130						
As_2S_3+S	0.130	0.130					
PbS+As_2S_3+S	0.130	0.130	0.130				
HgS+As_2S_3+S	0.130	0.130		0.300			
Ag_2S					0.130		
Ag_2S+S		0.130			0.130		
Ag Assemblage B					0.0500	0.0100	
Ag Assemblage A							0.0050

Orpiment (natural material), S (99.98% pure), PbS (99.98% pure), HgS (99% pure), Ag_2S (99.9% pure), $AgAsS_2$ and Ag_3AsS_3 (synthesized material). 20 ml solutions of varying [MOPS] (0.004M, 0.0071M and 0.014M), [HS^-] (0.001, 0.0005, and 0.0001) added to ampoules (50 ml HgS exp.). pH adjusted with NaOH. 0.010 M NaCl and $3.33x10^{-3}$ M Na_2SO_4 used to control ionic strength.

To determine silver using graphite furnace the sample needed to be preserved to prevent the loss of silver. Loss of silver can be due to sorption onto the storage material, formation of colloids and precipitation. To prevent sorption Welz and Sperling (1999) recommend that solutions be acidified to 0.3 M with nitric acid and stored in glass. Two ml of the filtered sample was placed in a glass centrifuge tube to which NaOH was added followed by 30% H_2O_2. This ensured that any reduced sulfur species were converted to sulfate and prevented the precipitation of elemental sulfur. The solution was then acidified with Ultrex nitric acid (J.T. Baker) and stored in a refrigerator until analysis. This procedure was modeled after Sugaki et al. (1987). The remaining solution was left in the polystyrene centrifuge tubes for arsenic analysis.

II.B.3. Sample Analysis

Final pH measurements were obtained using an Orion 420A meter equipped with an Orion 8130 Ross Combination electrode calibrated at pH 7 and 10 with VWR commercial buffers.

Total arsenic was obtained by flame (air-acetylene) atomic absorption spectrometry using a Perkin Elmer 5000 spectrophotometer at a wavelength of 193.7 nm using a hollow cathode lamp. Calibration curves were produced from $6.7x10^{-5}$ M to $6.0x10^{-4}$ M using a commercial arsenic standard (Fisher Scientific) (detection limit of As was $2x10^{-5}$M). Samples and standards were treated with 0.9 M BrCl to oxidize any HS^- to sulfate, which is needed to prevent the formation of metal sulfides. Erickson (1998) provides a procedure to synthesize BrCl, which includes adding 25 grams of KBr to 100 mL of concentrated HCl with stirring. Gradually, 37.5 grams of $KBrO_3$ are added to the mixture with stirring. The mixture is then transferred to a 250 mL volumetric flask and brought to volume with concentrated HCl.

Total lead was obtained with a Perkin Elmer 5100 ZL atomic absorption spectrophotometer equipped with a Perkin Elmer AS-71 auto sampler. Table 21 gives the instrumental program used for graphite furnace analysis. Lead analysis was performed at 283.3 nm using a hollow cathode lamp. A matrix modifier consisting of 3000 mg/L Pd (Alfa Aesar) and 2000 mg/L $Mg(NO_3)_2$ (Fisher Scientific) per 20 µL sample was injected into the furnace. Calibration curves were made over the concentration range of $9.6x10^{-9}$ to $1.4x10^{-7}$ M with a commercial lead standard (VWR Scientific) (detection limit of Pb was $9.6x10^{-9}$ M).

Total mercury was analyzed utilizing dual amalgam cold vapor atomic fluorescence spectroscopy (CVAFS) by Frontier Geosciences, Seattle, WA. The mercury samples were oxidized with 0.1N BrCl prior to analysis by Frontier Geosciences. The detection limit of Hg was $3.0x10^{-12}$ M.

Total silver was measured with a Perkin Elmer 5100 ZL atomic absorption spectrophotometer equipped with a Perkin Elmer AS-71 auto sampler. Table 22 gives the instrumental program used for graphite furnace analysis. Silver analysis was performed at 283.3 nm using a hollow cathode lamp. A matrix modifier consisting of 3000 mg/L Pd (Alfa Aesar) and 2000 mg/L $Mg(NO_3)_2$ (Fisher Scientific) per 20 μL of sample was injected into the furnace. Calibration curves were made over the range of $1.8x10^{-8}$ M to $2.8x10^{-7}$ M with a commercial silver standard (VWR Scientific) (detection limit of Ag was $1.8x10^{-8}$ M). The Ag_2S+S and Ag assemblage B samples were treated with 0.002 M sodium thiosulfate 5 hydrate (J.T Baker). This was to ensure that there would be no interference from the chloride ion and that all the silver was in solution.

Table 21. Graphite Furnace Program for Lead

Step	Temp. (°)	Ramp Time (s)	Hold Time (s)
Dry	120	1	40
Ash	900	1	30
Pre-Cooldown	20	1	10
Atomize	2000	0	5
Cleanout	2400	1	3

Table 22. Graphite Furnace Program for Silver

Step	Temp.(°)	Ramp Time (s)	Hold Time (s)
Dry	110	1	30
Pre-Cooldown	130	15	30
Ash	800	10	20
Atomize	1700	0	5
Cleanout	2400	1	2

In the Ag-As-S experiments there were three methods used to determine sulfide concentrations. These include potentiometric titrations, methylene blue and UV-Visible measurements. In the As_2S_3, As_2S_3+S, PbS+As_2S_3+S and HgS+As_2S_3+S experiments potentiometric titrations and UV-Visible measurements were utilized to obtain sulfide concentrations.

For total sulfide determinations using the potentiometric titration method, an aliquot was pipetted into a titration jar filled with 60 mL of a deoxygenated NaOH solution, which had a pH of approximately 13. At high pH, H_2S is converted to HS^-, which retards any loss of H_2S by degassing. Teflon lined caps were then screwed on the titration jars. After being removed from the glove box, the solutions were potentiometrically titrated with $HgCl_2$ for total sulfide using a Brinkman 760DMS Titrino automatic titrator with an Orion silver sulfide ion selective electrode and an Orion Ag/AgCl double junction reference electrode. The indicating electrode responds to decreasing free sulfide as HgS precipitates. The titration determines ΣS^{2-} or the sum of H_2S, HS^-, polysulfides and thioarsenic species.

UV-Visible spectra were obtained with a Hewlett-Packard 8452A diode array spectrophotometer. When HS^- was present, dilution of the sample was usually needed to obtain spectra that were not offscale. The samples were measured in either 1 cm or 0.1 cm quartz cells. A value of 7800 L mol^{-1} cm^{-1} was used for the molar absorptivity of HS^- at 230 nm (Giggenbach, 1974). However, UV-Visible spectrometry was not a useful technique for samples containing As_2S_3, for reasons discussed in Appendix I.

The methylene blue method, described by Cline (1969), measures acid-labile sulfide throughout a range of sulfide concentrations. Stock solutions of a mixed diamine reagent were prepared according to Table 23. N,N-dimethyl-p-phenylenediamine sulfate (Eastman Kodak) and ferric chloride (J.T. Baker) were dissolved in 250 mL of cooled 50% (v/v) HCl (VWR). Five mL of sample was placed in a centrifuge tube, and then 400 µL of the mixed diamine reagent was added to the sample. The blue color developed in twenty minutes and the absorbance was recorded at 668 nm.

Table 23. Reagent Concentrations and Dilution Factors Used to Determine Acid Labile Sulfide

Sulfide Concentration, (M)	Diamine Concentration, g/250 mL	Ferric Concentration, g/250mL	Dilution Factor (mL:mL)	Path Length (cm)
$3x10^{-6} – 4x10^{-5}$	1.0	1.5	1:1	1
$4x10^{-5}$- $2.5x10^{-4}$	4.0	6.0	2:25	1
$2x10^{-4} – 1x10^{-3}$	10.0	15.0	1:50	1

Method modified from Cline (1969). Diamine concentration was prepared from N,N-dimethyl-p-phenylenediamine sulfate and the ferric concentration was prepared from ferric chloride. The solids were dissolved in 250 mL cooled 50% (v/v) HCl.

The potentiometric titrations yielded the most consistent results; therefore these measurements will be used to determine the speciation of each metal in the modeling program, except in As_2S_3+S and PbS+As_2S_3+S experiments. In experiments relating to the dissolution of As_2S_3 (As_2S_3, As_2S_3+S, PbS+As_2S_3+S and HgS+ As_2S_3+S) the total sulfide as observed by potentiometric titrations often increased by 30-75% during the course of the experiment. The increase in total sulfide by ~30% could be explained by the dissolution of As_2S_3, which results in the formation of one or more dissolved arsenic sulfide complexes as well as the possible release of some free HS^-. The sulfurs bound to the arsenic in the complexes can contribute to the formation of HgS during the titration of the sample with $HgCl_2$. Helz et al. (2002) found that when thioantimonate species were titrated with $HgCl_2$, the S^{2-} bound to the thioantimonite contributed to the total sulfide value. This was the case in As_2S_3 only and HgS+As_2S_3+S experiments. In samples containing As_2S_3+S and PbS+As_2S_3+S the total sulfide concentration, obtained from $HgCl_2$ potentiometric titrations, was over an order of magnitude higher (~70%) when compared to the starting sulfide concentration. Orders of this magnitude can not be attributed to the dissolution of As_2S_3 and must have to do with an analytical artifact.

A possible cause for the extremely elevated total sulfide results, obtained from potentiometric titrations for the As_2S_3+S and PbS+As_2S_3+S samples, could be due to a reaction taking place involving Hg^{2+}. Saxena and Bhatnagar (1960) show that potentiometric titrations of $HgCl_2$ with arsenite solutions form $Hg(AsO_2)_2$, $Hg_2As_2O_5$ and $Hg_3(AsO_3)_2$. Clever et al. (1985) reviewed various solubility products of mercury salts and found that $Hg(AsO_2)_2$ had a K_s=~10^{-35} whereas HgS had a K_s of

$1x10^{-39}$. The potentiometric titration method detects free HS^- in solution, but if Hg^{2+} is reacting with As(III) instead of HS^- the endpoint will be drawn out. Illustrations of titration curves in the absence and presence of As_2S_3 are shown in Figure 16.

An experiment was conducted where a sulfide stock solution (10^{-3} M) was titrated with standard additions of $As(OH)_3$ up to 10^{-2} M to follow the electrode response. The electrode response decreased as the arsenic concentration was increased, but the endpoint did not shift in a manner that would give erroneous total sulfide values. Specifically, after the endpoint the Hg^{2+} was being complexed by As and did not provide a point where free Hg^{2+} was detected.

Total sulfide measured from these titration curves for two of my data sets, As_2S_3+S and PbS+As_2S_3+S, was greater than a theoretical upper limit, which is defined as the sulfide initially added to the sample plus 1.5 times the As dissolved from As_2S_3. Therefore, potentiometric titration data were not used in these two data sets. Instead, the theoretical total sulfide concentration was used. This calculation might overestimate the HS^- in solution, but probably not by more than ~20-50%. This estimate is based on comparing the titration sulfide measurements to the theoretical upper limit in the remaining data sets.

A 10-30% loss of sulfide was experienced during the course of the Ag_2S+S, Ag assemblage A and Ag assemblage B experiments. There could be several reasons for the occurrence. There could have been some solid Ag_2O that consumed sulfide. Some H_2S may have degassed between the time required to fill and seal the ampoules. Sulfide could have been lost as a sulfur rich solid. Or sulfide could have been lost could due to oxidation in the ampoule during the experiment, from the

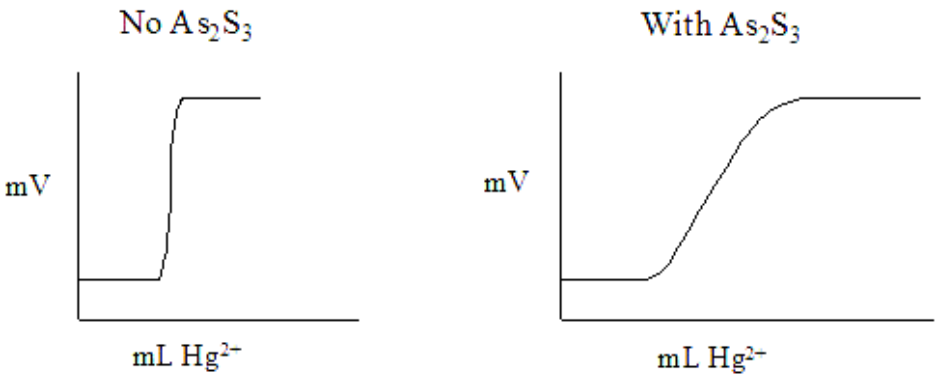

Figure 16. Schematic of titration curves for potentiometric titrations in the absence and presence of As_2S_3.

presence of colloids or the presence of an oxidized material. Most likely sulfide was lost to the volatilization of H_2S during sample handling.

Potentiometric titration, methylene blue and UV-Visible methods tended to agree, but the methylene blue and UV-Visible methods did not provide sulfide values for Ag- and As-containing samples that had total starting HS^- values of 10^{-4} M and in some cases 5 x 10^{-4} M. The blue color did not develop when the ratio of the concentration of HS^- to $AsS(HS)(OH)^-$ was less than 1. Blanks, that did not contain arsenic and silver, were measured for total sulfide with all three methods and reproducible results were obtained. It therefore seems that arsenic or silver is interfering with the development of the blue color at HS^- concentrations around 10^{-4} M. Methylene blue measures reactive sulfide species, which include H_2S, HS^-, S^{2-} and terminal polysulfides (S_xS^{2-}) (Mylon and Benoit, 2001). The methylene blue procedure begins by acidifying the sample to produce H_2S. N,N-dimethyl-p-phenylenediamine sulfate gets oxidized by ferric chloride, and the product reacts

with H_2S producing a blue color. The color development could have been inhibited by a reaction between H_2S and silver or arsenic. Or there could be competition between $AsS(HS)(OH)^-$ and H_2S for the reaction product, at the lowest sulfide concentration (~5 x 10^{-5}M) arsenic is in excess of the sulfide. The data that had reliable concentration of HS^-, obtained from methylene blue, were used to confirm HS^- concentrations obtained from potentiometric titration curves.

Comparison between the three sulfide methods are made in Table 24 for the Ag assemblage A and B experiments; the samples with a starting total sulfide value of 10^{-4} are not in the table because their HS^- concentrations were in disagreement. However, the blank sample that had a starting total sulfide concentration of 10^{-4} M are included in Table 24.

The total sulfide values obtained from potentiometric titration will be used to determine the silver speciation.

II.B.4. Fitting/Modeling Strategy

II.B.4.1. Dissolution of As_2S_3, As_2S_3+S, HgS+As_2S_3+S and PbS+As_2S_3+S in Sulfidic Solutions

The goal of the modeling is to find aqueous As, Ag or Hg species that can account for the observed solubilities and to obtain formation constants for these species assuming chemical equilibrium has been achieved. To accomplish this, the solubility data were modeled using SCIENTIST (Micromath, Inc.), which uses a nonlinear least squares fitting routine. The solubility of As, Ag and Hg species are

calculated from posited sets of reactions and the set which best predicts observed solubilities is adopted.

Table 24. Comparison between Methods to Measure HS^-

Sample	pH	Log ΣAs	$Titration_{Total\ Sulfide}$	Log Concentration HS^- (M)		
				Calc. from Titration	Methylene Blue	UV-Visible Spect.
Ag Assemblage A Experiment						
1	7.78	-3.68	-3.06	-3.13	-3.28	-3.14
2	7.30	-3.79	-3.50	-3.68	-4.00	-3.61
3	8.18	-3.74	-3.26	-3.29	-3.38	-3.31
4	7.73	-3.80	-3.21	-3.29	-3.44	-3.37
5	7.21	-3.97	-3.18	-3.40	-3.54	-3.28
6	8.09	-3.76	-3.32	-3.36	-3.42	-3.39
7	7.98	-3.85	-3.08	-3.13	-3.25	-3.18
8	7.33	-3.88	-3.15	-3.32	-3.30	-3.28
9	8.04	-3.89	-3.11	-3.14	-3.21	-3.18
10	7.89	-4.02	-3.80	-3.86	-3.97	-4.40
11	7.19	-3.89	-3.63	-3.85	-3.82	-3.74
12	8.07	-3.94	-3.46	-3.50	-3.66	-3.59
13	7.33	-4.06	-3.76	-3.93	-3.86	-3.86
14	8.13	-4.02	-3.42	-3.45	-3.51	-3.50
Ag Assemblage B Experiment						
1	7.71	-3.98	-2.93	-2.99	-3.30	-3.18
2	8.16	-4.18	-2.93	-3.01	-3.37	-3.21
3	7.59	-4.18	-3.05	-3.16	-3.55	-3.21
4	7.25	-4.03	-3.08	-3.28	-3.58	-3.38
5	7.02	-4.25	-3.11	-3.40	-3.60	-3.35
6	8.05	-3.88	-3.45	-3.48	-3.58	-3.46
7	7.66	-4.11	-3.37	-3.46	-3.59	-3.41
8	7.65	-4.20	-3.74	-3.83	-3.76	-3.75
9	7.21	-4.29	-3.79	-4.00	-3.81	-3.66
10	6.94	-4.32	-3.49	-3.82	-3.81	-3.61
Blank	8.00	-	-3.20	-3.24	-3.51	-3.24
Blank	7.18	-	-4.25	-4.48	-4.31	-4.19

In all the models, activity coefficients were calculated for each sample using the Davies equation, thus producing equilibrium constants that are corrected to conditions of infinite dilution. Arsenic and the metals (Ag, Hg and Pb) are fit separately in each data set. Arsenic data are modeled first and the As speciation is determined at this stage is used in the analysis of metal speciation. In all cases, metal concentrations were negligible compared to As concentrations so metal-thioarsenite complexes had to be insignificant in the As speciation.

The plots throughout this chapter are presented as the log ($As_{Calculated}/As_{Observed}$) or ($Hg_{Calculated}/Hg_{Observed}$) versus pH or total sulfide. Logarithms of the observed solubilities rather than the solubilities themselves were fit to avoid having deviations at the highest solubilities control the fit. If a model fits the experimental data the points will lie along the zero line. The standard deviation of each plot will also be provided (the equation used to determine the standard deviation is in Appendix II). This is one way to measure the goodness-of-fit of the model. A good model is one in which the observed and calculated solubilities are close to the same value, minimizing the standard deviation. A good model also should have no trend in deviations versus the independent variables, pH and HS^-.

II.B.4.2. Modeling of the Activity of Sulfur in Experiments Containing As_2S_3 in Various Solutions of Polysulfides

In samples that contained zero-valent sulfur, the activity of sulfur and the concentration of total zero valent sulfur were calculated by fitting the UV-Vis absorbances over the 300 to 500 nm range. Polysulfide molar absorbances as a

function of wavelength can be calculated from Gaussian functions determined by Giggenbach (1974). The fitting program varies the activity of sulfur until the absorbances from the resulting polysulfide concentration match the absorbance of the sample between 300 and 500 nm. This wavelength range was chosen because this is where polysulfides dominate the spectrum with minimal interference from HS^- and As(III) species.

II.B.5. Equilibration Rates and General Observations for Lead, Arsenic, Silver and Mercury

Jay et al. (2000) state that equilibration of cinnabar and elemental sulfur takes place within a few days. However, Paquette (1994) presents evidence that the equilibration of cinnabar took six weeks. Ampoules containing cinnabar, orpiment and elemental sulfur in this work were equilibrated for at least 30 days.

Giordano and Barnes (1979) determined that equilibration of lead sulfide (galena) in sulfidic solutions is reached within minutes at 25°C. Anderson (1962) established that equilibrium took place within 6 hours at 30°C in the PbS-H_2S-H_2O system. However, the time needed to equilibrate orpiment is slower than the time needed to equilibrate lead sulfide.

Webster (1990) observed that crystalline orpiment in sulfidic solutions at 25°C reached equilibrium within 30 – 40 days. Eary (1992) states that equilibrium of amorphous orpiment will take place in 10 - 14 days in solutions at pH 4 and 25°C. Figure 17 shows the equilibration of the $PbS+As_2S_3+S$ ternary assemblage in 3.5 ± 1.5 mM total sulfide, 0.0071 M MOPS buffer, 0.0100 M NaCl at pH 7.73. Arsenic

solubilities appear to level at 20 days, whereas lead solubilities level at 14 days. The last three arsenic points have a log arsenic mean value of –3.28 and a standard deviation of 0.03. These values could be closer, but analytical error is probably responsible for the slight deviation in arsenic concentration. Under these conditions the lead concentration is below the detection limit and does not provide equilibrium data. Subsequent to this experiment, all solutions containing As_2S_3, S, PbS or HgS were equilibrated for at least 4 weeks.

Gammons and Barnes (1989) found that equilibrium of Ag_2S (acanthite/ argentite) at 25 to 300°C, with total sulfide of 0.2 to 1.4 m and a pH ranging from 5.8 to 7.3 occurred within 24 hours. Stefansson and Seward (2003) used a flow through system to determine the equilibrium of Ag_2S in sulfidic solution between 25 and 400°C, equilibrium seemed to be reached within hours. The time required for arsenic sulfide minerals to reach equilibrium is longer than silver sulfide minerals.

Figure 18 shows the equilibration of Ag_2S-As_2S_3-S in a sulfidic solution with 7.7±0.019 mM total sulfide at pH 7.42. Silver and arsenic reach equilibrium within 15 days. The last five arsenic points have a log arsenic mean value of –3.31 and a standard deviation of 0.16. These values could be closer, but analytical error is probably responsible for the slight deviation in arsenic concentration. The last five silver points have a log silver mean value of –7.51 and a standard deviation of 0.47. The high error is attributed to the silver solubility on Day 36 in Figure 18. This value is erroneous; possible causes of the elevated silver concentration could be sample contamination or a filtering failure. Subsequent to these experiments, all solutions containing Ag_2S, $AgAsS_2$ or Ag_3AsS_3 were equilibrated for at least 4 weeks.

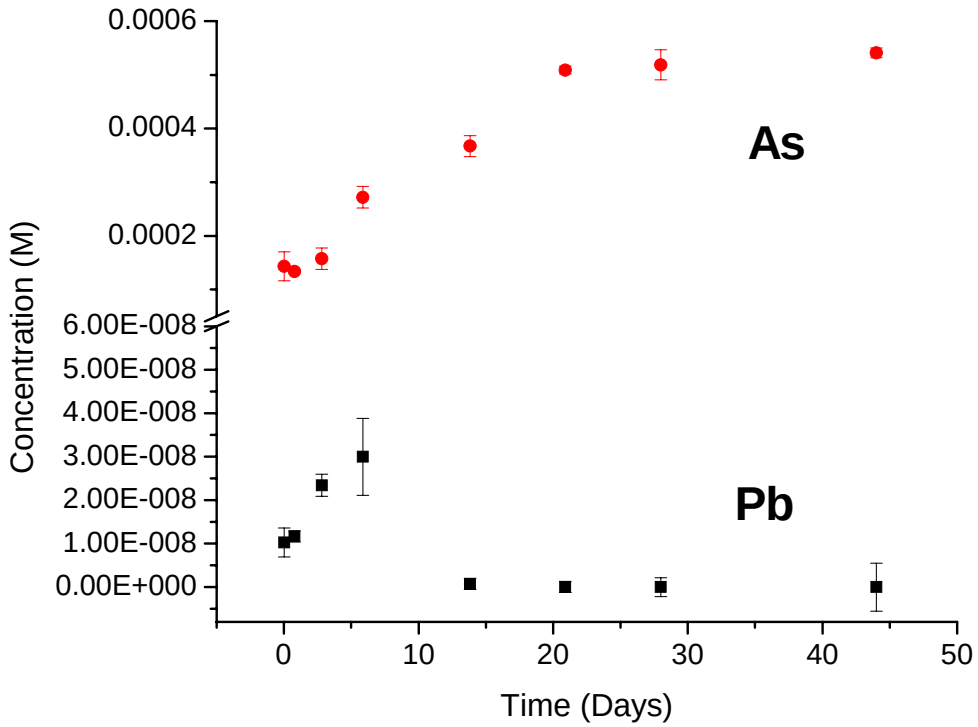

Figure 17. Equilibration of PbS+As_2S_3+S in replicate ampoules with 20 mL of solution containing 3.5 ± 1.5 mM total sulfide, 0.0071 M MOPS buffer, 0.01M NaCl at pH 7.73. Ampoules equilibrated at room temperate in an electronic rocker. Filled circles represent arsenic data and filled squares represent lead data. Error bars represent standard deviation of three replicate readings on each sample. Pb detection limit was 9.6×10^{-9} M.

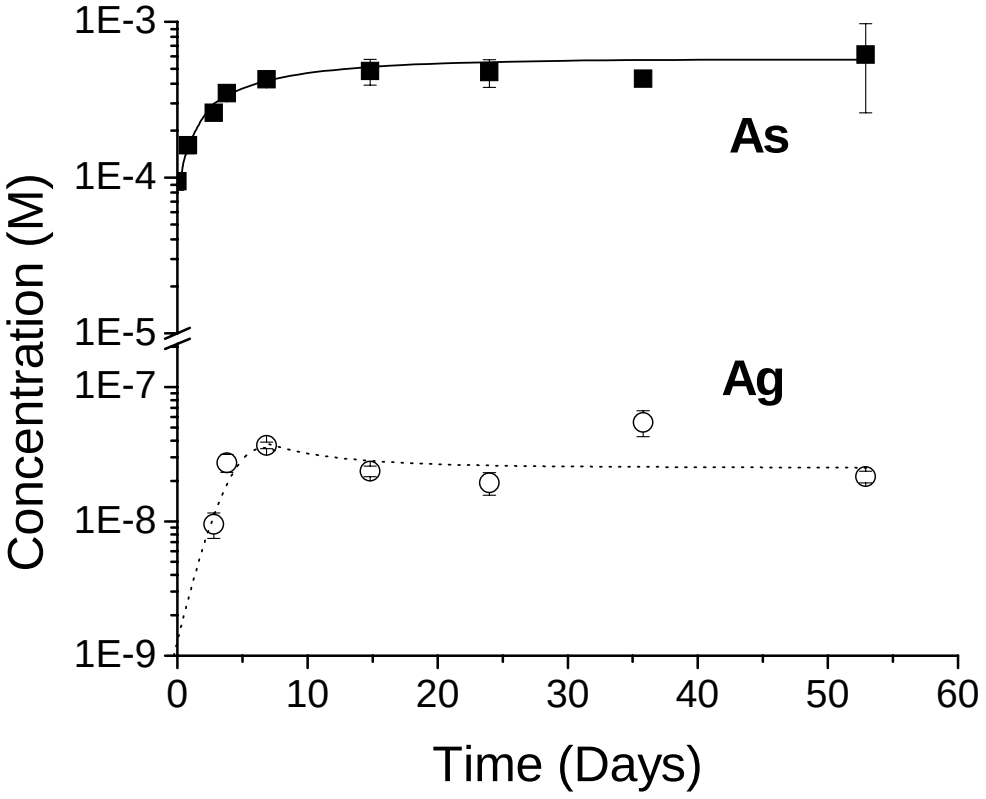

Figure 18. Equilibration of Ag_2S, S, As_2S_3 in replicate ampoules with 20 mL of a solution containing 0.0071 M MOPS buffer, 1 x 10^{-3} M HS^-, pH approximately 7.42. 0.13 g of solid was used in each ampoule. Solid squares represent As data and open circles represent Ag data. Ampoules equilibrated at room temperature. Error represents the standard deviation of three replicate measurements taken on each sample.

II.C. Results

II.C.1. Dissolution of Mineral Assemblages in Sulfidic Solutions

II.C.1.1. Dissolution of As_2S_3, As_2S_3+S, HgS+As_2S_3+S, PbS+As_2S_3+S, Ag Assemblage A and Ag Assemblage B

Data for the dissolution of As_2S_3 and As_2S_3+S in sulfidic solutions are shown in Table 25 and Table 26, respectively. The data for the dissolution of PbS+As_2S_3+S, HgS+As_2S_3+S, assemblages in sulfidic solutions are given in Table 27 and 28, respectively.

Lead concentrations are below the detection limit of 9.6×10^{-9} M. Figure 19 shows that there is a measurable amount of arsenic solubility in Pb solubility experiments but there is undetectable lead solubility. The calculated solubility of $Pb(HS)_2$ is shown in Figure 19 and is well below the detection limit. There was no effect on the solubility of As, Pb, Hg or Ag due to MOPS buffer. This conclusion was reached by making solutions with varying concentrations of MOPS and measuring the elements solubility; the concentrations of those four elements did not depend on the MOPS concentration. This fact can be ascertained by comparing the MOPS concentration to the metals concentration in Tables 25-32.

Data for the dissolution of Ag_2S, Ag_2S+S, Ag assemblage A and Ag assemblage B in sulfidic solutions are given in Tables 29, 30, 31 and 32, respectively. Silver concentrations increase with increasing pH and total sulfide during Ag_2S+S experiments. During Ag assemblage A and B experiments, silver concentrations decreased with decreasing total sulfide, but show no trend with pH.

Solution conditions often changed during the equilibrium period. A gain of sulfide around 1.5 to 3 times usually occurred due to the dissolution of As_2S_3, which can produce some free HS^-. A buffer was needed throughout the experiments, otherwise the pH would shift in the acidic direction. The shift in pH is due to the arsenic equilibria in solution in which As_2S_3 reacts with sulfide producing H^+. The following reactions can be used to describe As_2S_3 dissolution:

$$0.5As_2S_3 + 3H_2O \Leftrightarrow As(OH)_3 + 1.5H_2S \quad (1)$$

$$1.5As_2S_3 + 1.5H_2S \Leftrightarrow H_2As_3S_6^- + H^+ \quad (2)$$

Both products in equation 1 release protons in mildly alkaline solution, yielding HS^-, $AsO(OH)_2^-$ and H^+.

Table 25. Dissolution of As_2S_3 in Sulfidic Solutions

pH_F	[MOPS] (M)	Ionic Strength	$-\log (\Sigma S^{-2})_F$	$-\log (As)_F$
6.88	0.00400	1.10E-02	2.94	3.47
6.90	0.00710	1.01E-02	3.56	3.64
6.91	0.00400	1.01E-02	3.68	3.78
6.98	0.0140	1.01E-02	2.99	3.70
7.00	0.0140	1.05E-02	3.09	3.49
7.07	0.00710	1.10E-02	3.08	3.71
7.74	0.00400	1.01E-02	3.03	3.72
7.75	0.00710	1.01E-02	2.67	3.42
7.76	0.0140	1.10E-02	2.88	3.37
7.78	0.00400	1.05E-02	2.79	3.60
7.83	0.00710	1.05E-02	3.03	3.39
7.84	0.00710	1.10E-02	2.71	3.38
7.89	0.0140	1.05E-02	2.99	3.31
7.91	0.0140	1.05E-02	3.24	3.35
7.30	0.00400	1.01E-02	1.34	3.55

0.010 M NaCl added to ampoules. Equilibration time was 43±3 days. All values were obtained at the end of the experiment. ΣS represents total sulfide determined by potentiometric titration and includes H_2S, HS^-, S_x^{2-} and labile sulfide bound in complexes. Experiments contained 0.130 g As_2S_3 in 20 mL solution.

Table 26. Dissolution of As_2S_3+S in Sulfidic Solutions

pH_F	[MOPS] (M)	Ionic Strength	$-\log (\Sigma S^{-2})_{Calc}$	$-\log (As)_F$
6.92	0.0140	1.10E-02	2.78	3.39
6.99	0.00710	1.10E-02	2.76	3.32
7.22	0.00710	1.05E-02	2.85	3.23
7.23	0.00710	1.10E-02	2.65	3.10
7.23	0.00400	1.05E-02	2.84	3.21
7.27	0.00400	1.10E-02	2.64	3.12
7.34	0.00710	1.01E-02	3.11	3.35
7.34	0.00710	1.10E-02	2.63	3.07
7.52	0.00710	1.01E-02	2.85	3.08
7.52	0.0140	1.01E-02	2.84	3.05
7.95	0.0140	1.05E-02	2.99	3.46
6.67	0.00400	1.01E-02	3.19	3.45
6.83	0.00710	1.01E-02	3.26	3.56
6.83	0.00400	1.10E-02	2.77	3.35
6.94	0.0140	1.01E-02	3.46	3.90
6.99	0.0140	1.05E-02	2.62	3.49
6.99	0.00710	1.05E-02	2.92	3.46
7.00	0.00400	1.05E-02	2.95	3.55
7.35	0.00400	1.01E-02	2.97	3.25
7.37	0.00400	1.05E-02	2.83	3.29
7.39	0.0140	1.01E-02	3.22	3.35
7.41	0.00710	1.05E-02	1.72	3.05
7.43	0.0140	1.05E-02	2.89	3.33
7.48	0.0140	1.10E-02	2.67	3.28
7.62	0.0140	1.10E-02	2.46	3.00

0.010 M NaCl added to ampoules. Equilibration time was 43±3 days. All values were obtained at the end of the experiment. ΣS^{-2} represents total sulfide through calculation where $\Sigma S = HS^-_{intiial} + 1.5As$. Experiments contained 0.130 g As_2S_3 and S^o. Experiments contained 0.130 g As_2S_3 and S in 20 mL solution.

Table 27. Data from the Dissolution of $PbS+As_2S_3+S$ in Sulfidic Solutions

pH_F	[MOPS] (M)	Ionic Strength	$-\log (\Sigma S^{-2})_{Calc}$	$-\log (Pb)_F$	$-\log (As)_F$
7.12	0.00710	1.01E-02	3.07	<8.02	3.34
7.26	0.00400	1.10E-02	2.78	<8.02	3.36
7.32	0.00400	1.05E-02	2.98	<8.02	3.46
7.36	0.00400	1.01E-02	3.04	<8.02	3.27
7.40	0.00400	1.10E-02	2.69	<8.02	3.19
7.44	0.00400	1.05E-02	2.73	<8.02	3.10
7.53	0.0140	1.01E-02	2.98	<8.02	3.21
7.55	0.0140	1.01E-02	2.91	<8.02	3.13
7.57	0.00710	1.01E-02	2.87	<8.02	3.10
7.59	0.0140	1.05E-02	2.77	<8.02	3.10
7.60	0.00400	1.10E-02	2.70	<8.02	3.24
7.63	0.00710	1.05E-02	2.69	<8.02	3.01
7.65	0.00710	1.05E-02	3.04	<8.02	3.58
7.67	0.0140	1.10E-02	2.67	<8.02	3.17
7.74	0.00710	1.10E-02	2.66	<8.02	3.12
7.74	0.0140	1.01E-02	2.86	<8.02	3.09
7.77	0.0140	1.05E-02	2.69	<8.02	3.00
7.12	0.00400	1.01E-02	3.07	<8.02	3.20
7.19	0.0140	1.10E-02	2.72	<8.02	3.28
7.33	0.00710	1.05E-02	3.09	<8.02	3.81
7.42	0.00400	1.01E-02	2.73	<8.02	3.31
7.42	0.00400	1.10E-02	2.81	<8.02	3.11
7.61	0.00400	1.05E-02	2.93	<8.02	3.40
7.68	0.00710	1.01E-02	3.36	<8.02	3.67
7.85	0.0140	1.10E-02	2.59	<8.02	3.03

0.010 M NaCl added to ampoules. Equilibration time was 32±4 days. ΣS^{-2} represents total sulfide through calculation where $\Sigma S=HS_{intiial}+1.5As$. Experiments contained 0.130 g PbS, As_2S_3 and S^o in 20 mL solution. Pb detection limit was $9.6x10^{-9}$ M.

Table 28. Data from the Dissolution of $HgS+As_2S_3+S$ in Sulfidic Solutions

pH_F	[MOPS] (M)	Ionic Strength	$-\log (\Sigma S^{-2})_F$	$-\log (Hg)_F$	$-\log (As)_F$
7.12	0.00710	1.01E-02	4.25	9.366	3.81
7.22	0.00710	1.01E-02	4.01	8.234	3.94
7.22	0.00710	1.03E-02	3.11	7.907	3.64
7.24	0.00710	1.05E-02	2.89	8.210	3.54
7.53	0.00710	1.05E-02	2.61	7.662	3.31
7.66	0.00710	1.03E-02	3.17	8.142	3.61
7.78	0.00400	1.05E-02	2.61	7.439	3.50
7.87	0.0140	1.05E-02	2.71	7.379	3.10
8.20	0.00710	1.05E-02	2.87	7.257	3.47
7.63	0.00710	1.01E-02	4.11	9.208	3.83
7.97	0.00400	1.01E-02	3.55	8.207	3.73
0.010 M NaCl added to ampoules. Equilibration time was 46±1 days. ΣS^{2-} represents total sulfide determined by potentiometric titration and includes H_2S, HS^-, S_5^{2-} and S_4^{2-} and any labile sulfide bound in complexes. Experiments contained 0.130 g HgS and As_2S_3 and 0.300 g S^o in 50 mL solution.					

Table 29. Data from the Dissolution of Ag_2S in Sulfidic Solutions

pH_F	[MOPS](M)	Ionic Strength	Cl^- (M)	$-\log(\sum S^{2-})_{Final}$	$-\log(Ag)_{Final}$
7.83	0.00710	1.10E-02	0.00999	-3.08	-6.69
7.74	0.00710	1.01E-02	0.00999	-4.62	-6.52
7.78	0.0140	1.10E-02	0.00999	-2.82	-6.63
7.70	0.0140	1.05E-02	0.00999	-4.07	-6.34
7.52	0.00400	1.01E-02	0.00999	-3.38	-6.78
0.010 M NaCl added to ampoules. Equilibration time was 59±4 days. ΣS^{2-} represents total sulfide determined by potentiometric titration and includes H_2S, HS^-, S_5^{2-} and S_4^{2-}. Experiments contained 0.130 g Ag_2S in 20 mL solution.					

Table 30. Data from the Dissolution of Ag_2S and S in Sulfidic Solutions

pH_F	Ionic Strength	a_S	Buffer, (M)	Cl^- Total (M)	$-\log(\Sigma S^{2-})_F$	$-\log(Ag)_F$
6.00	3.31E-01	1	KH_2PO_4, 0.0999	0.0300	-3.42	-6.36
6.03	3.11E-01	1	KH_2PO_4, 0.0999	0.0100	-3.34	-6.11
6.10	3.04E-01	1	KH_2PO_4, 0.0999	0.00300	-3.40	-6.72
7.28	1.01E-02	1	MOPS, 0.00710	0.00999	-3.66	-6.33
7.29	1.01E-02	1	MOPS, 0.0140	0.00999	-4.63	-6.22
7.30	1.10E-02	1	MOPS, 0.00710	0.00999	-3.29	-6.32
7.30	1.05E-02	1	MOPS, 0.00710	0.00999	-3.65	-6.20
7.30	1.05E-02	1	MOPS, 0.00400	0.00999	-3.51	-6.30
7.32	1.01E-02	1	MOPS, 0.00400	0.00999	-4.21	-6.12
7.36	1.01E-02	1	MOPS, 0.00710	0.00999	-3.61	-6.28
7.59	1.01E-02	1	MOPS, 0.00400	0.00999	-3.34	-6.31
7.60	1.10E-02	1	MOPS, 0.00710	0.00999	-3.51	-6.09
7.65	1.05E-02	1	MOPS, 0.00400	0.00999	-3.82	-6.38
7.66	1.01E-02	1	MOPS, 0.0140	0.00999	-4.15	-6.36
7.70	1.05E-02	1	MOPS, 0.0140	0.00999	-3.54	-6.18
7.74	1.01E-02	1	MOPS, 0.00710	0.00999	-3.52	-6.14
7.74	1.10E-02	1	MOPS, 0.0140	0.00999	-3.16	-5.83
7.75	1.05E-02	1	MOPS, 0.00400	0.00999	-3.45	-6.20
7.82	1.10E-02	1	MOPS, 0.00400	0.00999	-3.04	-6.01
7.92	1.01E-02	1	MOPS, 0.00400	0.00999	-4.50	-6.14
8.04	1.10E-02	1	MOPS, 0.00710	0.00999	-3.20	-6.19
8.04	1.05E-02	1	MOPS, 0.00710	0.00999	-3.59	-6.04
8.18	1.01E-02	1	MOPS, 0.0140	0.00999	-3.12	-6.02
8.25	1.10E-02	1	MOPS, 0.00400	0.00999	-3.08	-6.09
9.73	1.07E-01	.46	Borate, 0.00801	0.0100	-2.60	-6.40
9.77	1.07E-01	.45	Borate, 0.00801	0.0100	3.00	-6.60
9.88	1.04E-01	.56	Borate, 0.00801	0.0100	-3.62	-6.53
10.38	1.61E-01	.29	Na_2HPO_4, 0.0501	0.0100	-2.70	-6.77
10.41	1.61E-01	.30	Na_2HPO_4, 0.0501	0.0100	-3.48	-6.92
5.99	3.30E-01	1	KH_2PO_4, 0.0999	0.0300	-4.76	-6.48
6.02	3.03E-01	1	KH_2PO_4, 0.0999	0.00300	-4.60	-6.24
7.25	1.05E-02	1	MOPS, 0.0140	0.00999	-2.64	-6.30
7.37	1.10E-02	1	MOPS, 0.00400	0.00999	-1.51	-6.50
7.66	1.05E-02	1	MOPS, 0.00710	0.00999	-2.12	-5.75
8.18	1.01E-02	1	MOPS, 0.00400	0.00999	-4.32	-5.34

0.010 M NaCl added to control ionic strength. Equilibration time was 59±4 days. ΣS^{2-} represents total sulfide determined by potentiometric titration and includes H_2S, HS^-, S_5^{2-} and S_4^{2-}. Experiments contained 0.130 g Ag_2S and S^o in 20 mL solution.

Table 31. Data from the Dissolution of Ag Assemblage A in Sulfidic Solutions

pH_F	[MOPS] (M)	Ionic Strength	SO_4^{2-} (M)	$-\log(\Sigma S^{2-})_F$	$-\log(Ag)_F$	$-\log(As)_F$
7.08	0.0140	1.01E-02	0.00333	-4.63	-6.71	-3.98
7.11	0.00710	1.01E-02	0.00333	-4.18	-6.86	-4.05
7.15	0.00400	1.01E-02	0.00333	-4.20	-7.15	-3.99
7.19	0.00710	1.05E-02	0.00333	-3.63	-6.50	-3.89
7.21	0.0140	1.10E-02	0.00333	-3.18	-7.00	-3.97
7.30	0.00710	1.10E-02	0.00333	-3.50	-6.73	-3.79
7.33	0.00400	1.10E-02	0.00333	-3.15	-7.05	-3.88
7.33	0.00400	1.05E-02	0.00333	-3.76	-6.58	-4.06
7.63	0.0140	1.01E-02	0.00333	-4.19	-6.55	-4.00
7.69	0.0140	1.05E-02	0.00333	-3.84	-6.54	-3.88
7.70	0.00710	1.01E-02	0.00333	-4.12	-6.71	-3.97
7.73	0.0140	1.10E-02	0.00333	-3.21	-6.60	-3.80
7.75	0.00400	1.01E-02	0.00333	-4.02	-7.16	-4.10
7.78	0.00710	1.10E-02	0.00333	-3.06	-7.18	-3.68
7.81	0.00400	1.05E-02	0.00333	-3.99	-6.81	-3.88
7.89	0.00710	1.05E-02	0.00333	-3.80	-6.93	-4.02
7.90	0.00400	1.01E-02	0.00333	-4.27	-7.42	-3.97
7.98	0.00400	1.10E-02	0.00333	-3.08	-7.02	-3.85
8.04	0.00400	1.10E-02	0.00333	-3.11	-7.26	-3.89
8.07	0.00710	1.05E-02	0.00333	-3.46	-6.63	-3.94
8.09	0.0140	1.10E-02	0.00333	-3.32	-6.64	-3.76
8.13	0.00400	1.05E-02	0.00333	-3.42	-7.17	-4.02
8.18	0.00710	1.10E-02	0.00333	-3.26	-6.55	-3.74
7.81	0.00400	1.05E-02	0.0100[a]	-3.37	-6.24	-4.16
8.23	0.00710	2.00E-02	0.0100[a]	-1.96	-6.47	-3.91
8.02	0.00710	1.01E-02	0.00333	-4.37	-6.81	-4.06
8.07	0.0140	1.01E-02	0.00333	-4.16	-7.08	-4.02
8.37	0.0140	1.05E-02	0.00333	-3.98	-6.58	-3.95

[a] Samples had 0.0100 M Cl^- instead of SO_4^{2-}. Equilibration time was 44±4 days. ΣS^{2-} represents total sulfide determined by potentiometric titration and includes H_2S, HS^-, S_5^{2-} and S_4^{2-}. Experiments contained 0.00500 g $AgAsS_2$ in 20 mL solution.

Table 32. Data from the Dissolution of Ag Assemblage B in Sulfidic Solutions

pH_F	[MOPS] (M)	Ionic Strength	SO_4^{2-} (M)	$-\log(\Sigma S^{2-})_F$	$-\log(Ag)_F$	$-\log(As)_F$
6.86	0.00710	1.01E-02	0.00333	-4.23	-6.45	-3.79
6.94	0.00710	1.05E-02	0.00333	-3.49	-6.72	-4.32
7.02	0.00710	1.10E-02	0.00333	-3.11	-6.80	-4.25
7.11	0.00710	1.01E-02	0.00333	-4.22	-6.61	-4.13
7.21	0.00710	1.05E-02	0.00333	-3.79	-6.59	-4.29
7.25	0.00710	1.10E-02	0.00333	-3.08	-6.70	-4.03
7.43	0.00400	1.01E-02	0.00333	-4.26	-6.69	-3.87
7.50	0.00710	1.01E-02	0.00333	-4.26	-6.62	-3.94
7.59	0.00710	1.10E-02	0.00333	-3.05	-6.37	-4.18
7.59	0.00710	1.01E-02	0.00333	-4.07	-6.68	-3.92
7.65	0.00710	1.05E-02	0.00333	-3.74	-6.71	-4.20
7.66	0.00400	1.05E-02	0.00333	-3.37	-6.45	-4.11
7.71	0.00400	1.10E-02	0.00333	-2.93	-6.70	-3.98
7.87	0.00710	1.01E-02	0.00333	-4.26	-6.58	-3.92
8.05	0.00710	1.05E-02	0.00333	-3.45	-6.74	-3.88
8.16	0.00710	1.10E-02	0.00333	-2.93	-6.58	-4.18
Equilibration time was 53±4 days. ΣS^{2-} represents total sulfide determined by potentiometric titration and includes H_2S, HS^-, S_5^{2-} and S_4^{2-}. Experiments contained 0.050 g Ag_2S and 0.010 g Ag_3AsS_3 in 20 mL solution.						

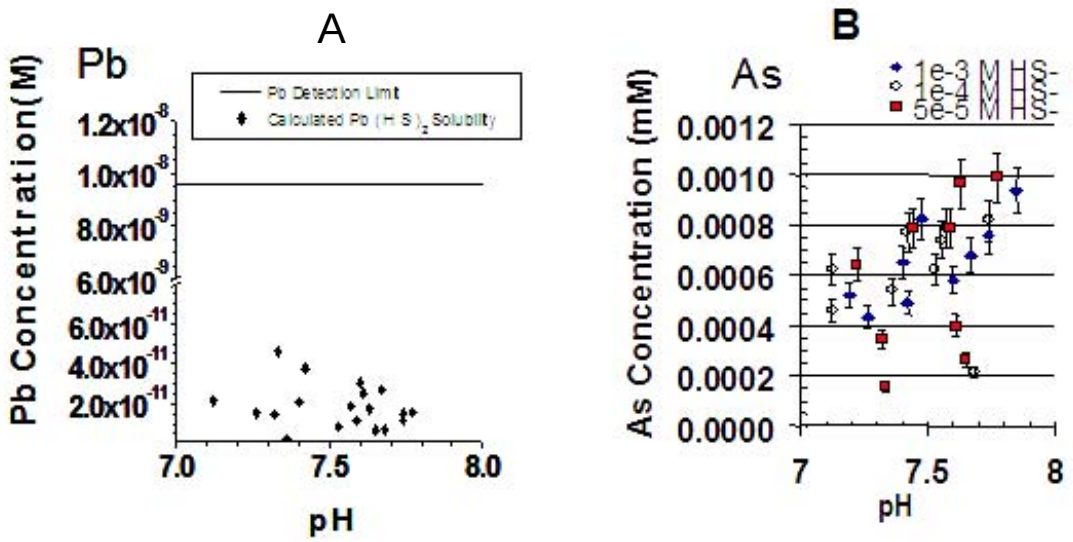

Figure 19. Comparison of the solubilities of lead and arsenic in the ternary solubility study. A. The predicted solubility of $Pb(HS)_2$ is shown with filled diamonds. The detection limit of lead is shown with the solid line. B. Solubility of arsenic is shown as a function of total starting sulfide concentrations. Predicted solubility of $Pb(HS)_2$ calculated using equilibrium constants from Giordano and Barnes (1979)

II.C.1.2. Dissolution of As_2S_3 in Various Polysulfide Solutions

This section will help determine if As-polysulfides are present in experiments involving As_2S_3+S. Approximately, 0.13 grams of As_2S_3 was placed in glass ampoules. Two stock solutions were prepared. The first solution contained 0.0100 M HS^-, 0.0200 M $Na_2B_4O_7 \bullet 10H_2O$, 0.0100 M NaCl and had a pH of 8.96. Approximately, 0.65 grams of elemental sulfur (Aldrich, 99.98% pure) was placed in a round bottom flask and the first solution was added to the flask. The flask was stirred in the glovebox for 1 week to allow polysulfide formation (this solution is designated to be 100% S_x^{2-}). The second solution contained 0.0100 M HS^-, 0.0200 M $Na_2B_4O_7 \bullet 10H_2O$, 0.0100 M NaCl and had a pH of 9.00 (this solution is designated to be 100% HS^-). A series of ampoules was made that had a mixture of the solutions and is displayed in Table 33. After the two solutions were added to the ampoules in their respective ratios, the As_2S_3-bearing ampoules were removed from the glovebox, fusion sealed and equilibrated for 30 days. Data for the dissolution of As_2S_3 in various polysulfide solutions are given in Table 34. The arsenic concentration is nearly constant with solutions of varying polysulfide concentrations. These data will be discussed further in Section II.D.1.2.

Table 33. Experimental Solution Scheme for the Dissolution of As_2S_3 in Solutions of Varying Degrees of Sulfur Saturation

Sample ID	1	2	3	4	5	6
Percent of Solution 1 (polysulfide)	100	75	50	25	10	0
Percent of Solution 2 (HS^-)	0	25	50	75	90	100

Table 34. Data for the Dissolution of As_2S_3 in Solutions with Varying Degrees of Sulfur Saturation

Sample ID	pH_F	$-\log (\Sigma S^{-2})_F$	$-\log (As)_F$
1 (100% S_x^{2-})	8.65	1.52	1.94
2 (75% S_x^{2-}/25% HS^-)	8.66	1.63	1.99
3 (50% S_x^{2-}/50% HS^-)	8.68	1.72	2.02
4 (25% S_x^{2-}/75% HS^-)	8.60	1.66	2.04
5 (10% S_x^{2-}/90% HS^-)	8.54	1.88	2.13
6 (100% HS^-)	8.48	1.78	2.09

II.D. Discussion

II.D.1 Speciation of Arsenic in Experiments with As_2S_3, As_2S_3+S, PbS+As_2S_3+S, HgS+As_2S_3+S, Ag Assemblage A and Ag Assemblage B in Sulfidic Solutions

II.D.1.1. Speciation of Arsenic in Experiments Containing As_2S_3 in Sulfidic Solution

For arsenic modeling, complexes of the form $H_hAs_xO_yS_z^{(h+3x-2y-2z)}$, were tried to fit the data. The activity of orpiment was defined to be one in these experiments. The Scientist fitting program used to model the arsenic data and discussion of the standard deviation calculation is in Appendix II. The procedure for modeling the data was discussed in Section II.B.4.1.

The last sample in Table 25 was not used in the fitting procedure because the total sulfide appeared to be erroneous (potentiometric titration yielded a concentration that was an order of magnitude over starting sulfide concentrations); the reasons for this determination was discussed in II.B.3. The ionic strength of the samples varied between 0.0101 - 0.0110 M.

Solubility-based studies on As_2S_3 have defined two dominant species. The reactions can be represented by:

$$0.5As_2S_3 + 3H_2O \Leftrightarrow As(OH)_3 + 1.5H_2S \quad (1)$$

$$1.5As_2S_3 + 1.5H_2S \Leftrightarrow H_2As_3S_6^- + H^+ \quad (2)$$

The previous solubility-based determinations of pK_1 were 11.9±0.3 (Eary, 1992), 12.60±0.11 (Webster, 1990) and 13.07 (Spycher and Reed, 1898). The previous solubility-based determinations of pK_2 were 5.0±0.3 (Eary, 1992), 6.91±0.09 (Webster, 1990) and 8.19±0.3 (Spycher and Reed, 1898). The previous authors obtained very similar equilibrium constants for $As(OH)_3$ when compared to a calculated pK_1 of 12.58, using ΔG values from Nordstrom and Archer, 2003.

Clarke and Helz (2000) studied the solubility of CuS-$Cu_{1.8}S$-Cu_3AsS_4. The arsenic solubility was dominated by $AsS(HS)(OH)^-$, $As(OH)_3$ and $H_2As_3S_6^-$, where $AsS(HS)(OH)^-$ can be represented by:

$$0.5As_2S_3 + H_2O + 0.5H_2S \Leftrightarrow AsS(HS)(OH)^- + H^+ \quad (3)$$

The corresponding equilibrium constants are pK_3=8.23±0.32, pK_1=12.28±0.18 and pK_3=5.38±0.21, respectively.

The complexes proposed by Webster (1990) and Eary (1999), $H_2As_3S_6^-$ and $As(OH)_3$, for the equilibration of As_2S_3 in sulfidic and non-sulfidic solutions were first tested as a base model for the As_2S_3 data. Using equilibrium constants from Webster (1990) produced the Webster Base Model in Figure 20. The log ($As_{calculated}/As_{observed}$) as a function of pH and total sulfide is shown in Figure 20. There was an underprediction of arsenic solubility over the whole pH and total sulfide range, implying that there is more observed arsenic solubility than calculated. The standard deviation of the model, shown in Figure 20, was calculated for the

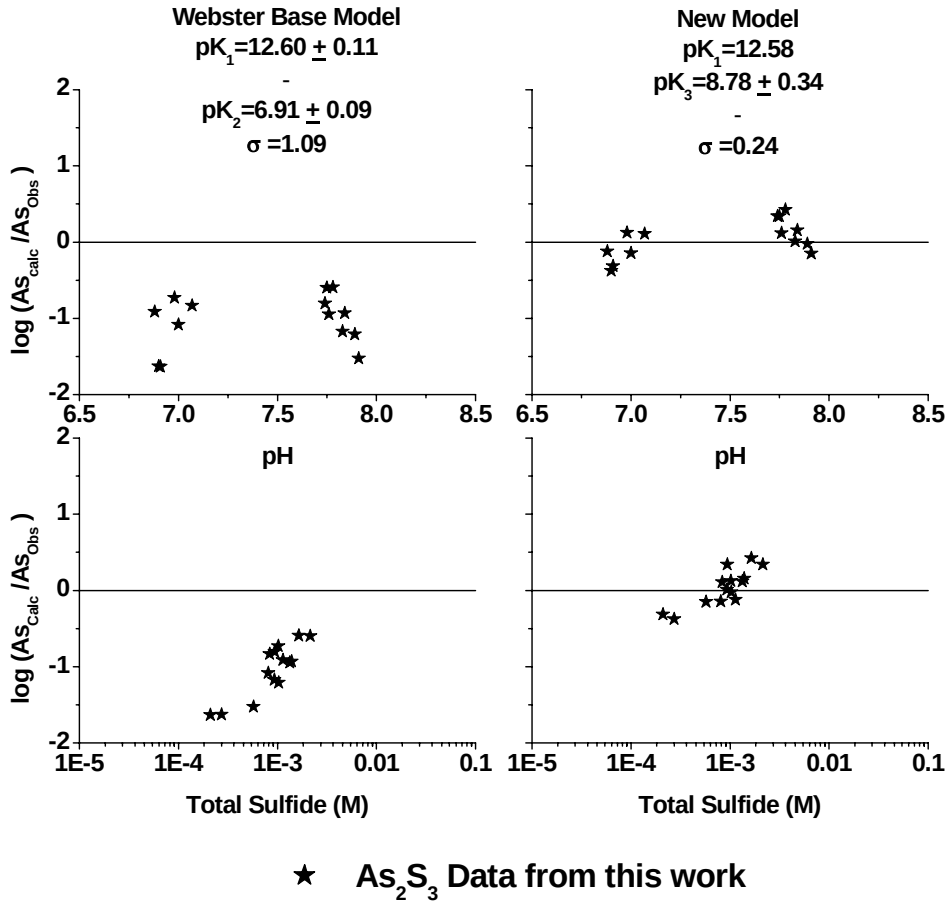

Figure 20. Fit of the As_2S_3 data in sulfidic solutions. The pK's refer to the reactions in the text. If any pK is not listed in the figure, the reaction corresponding to the pK was not included in the model.

As_2S_3 data set and implies that the fit is not satisfactory.

To improve the fit of the data the equilibrium constant of reaction 1 was held constant at $2.66x10^{-13}$. The equilibrium constant of reaction 1 was calculated using ΔG_R^o values taken from Nordstrom and Archer (2003), because my data set does not contain enough points to fit an equilibrium constant accurately. A new species, $AsS(HS)(OH)^-$, was added to the model to account for the extra arsenic solubility. The $H_2As_3S_6^-$ species was excluded from the model because it was negligible. The New Model therefore contains two species, $As(OH)_3$ and $AsS(HS)(OH)^-$. The New Model is a better fit to the data, and has a better standard deviation when compared to the Webster Base Model.

II.D.1.2. Speciation of Arsenic in Experiments Containing As_2S_3, As_2S_3+S, PbS+As_2S_3+S, HgS+As_2S_3+S, Ag Assemblage A and Ag Assemblage B in Sulfidic Solutions

The first evidence that polysulfides do not play any role in the speciation of arsenic can be obtained from experiments where As_2S_3 was equilibrated with solutions of different ratios of polysulfides (experimental method and results located in Section II.C.1.2.). Some possible reactions that occur in this experiment include:

$$0.5\ As_2S_3 + H_2O + 0.5HS^- \Leftrightarrow AsS(HS)(OH)^- + 0.5H^+ \qquad (3)$$

$$HS^- + (x\text{-}1)S^o \Leftrightarrow S_x^{2-} + H^+ \qquad (4)$$

If the solubility were controlled by S_x^{2-} complexes then the samples with large concentration of S_x^{2-} should have a higher concentration of arsenic. The arsenic concentrations did not increase with increasing polysulfide but instead followed the

opposite trend. The activity of sulfur could not be determined from the UV-Visible spectra (refer to Appendix I for discussion of spectral problems associated with As(III) solutions) of samples that contained a polysulfide solution.

The experiments that contain As_2S_3+S will now be added to the As_2S_3-only data to determine if the new model developed for the As_2S_3 only system is an adequate fit for all the data or if As-S_x^{2-} species are needed to account for As solubility. The Scientist fitting program used to model the arsenic data is in Appendix II. In experiments containing S^o, some dissolved sulfide is associated with S_x^{2-}. The potentiometric titration determines ΣS, which includes H_2S, HS^-, S_x^{2-} and any labile sulfide bound in As(III) complexes (potentiometric titration data used for As_2S_3 only and HgS+As_2S_3+S experiments). Therefore, the Scientist model includes corrections for S_x^{2-} species, allowing H_2S to be calculated (derivation shown after Scientist model in Appendix II).

The arsenic solubility data from the PbS+As_2S_3+S and HgS+As_2S_3+S experiments are also used because the dissolved Pb and Hg concentrations were negligible compared to the total As concentration. As a consequence, no Hg- or Pb-containing species could contribute significantly to the As solubility.

The samples in Table 26 (As_2S_3+S experiments), Table 27 (PbS+As_2S_3+S) and Table 28 (HgS+As_2S_3+S) were used in the fitting. The last two samples in Table 28 were not used in the modeling process because the arsenic concentrations were low, which could be due to some sample precipitation during elemental analysis. ΣS values in Table 26 and 27 have been calculated and discussed in Section II.B.3. The ionic strength of the samples varied between 0.0101-0.0110 M.

The New Model, developed from the As_2S_3 only experiments, contains two species, $As(OH)_3$ and $AsS(HS)(OH)^-$. The New Model was used as the base model for arsenic data from As_2S_3, As_2S_3+S, PbS+As_2S_3+S and HgS+As_2S_3+S experiments and is shown in Figure 21 as the New Model. The New Model shows a slight trend with sulfide, where there is an overprediction at high total sulfide.

The New Model was first adjusted in the Scientist program by allowing pK_3 to vary, to account for the trend in total sulfide and is shown as the Adjusted Model in Figure 21. There is still a slight overprediction in solubility at high total sulfide. However, a slight adjustment in pK_3 improved the standard deviation of the New Model.

Other species were added to the model to account for the overprediction at high total sulfide. In solutions that are saturated with elemental sulfur, arsenic polysulfides would increase in concentration as sulfide increases, so they would not lower the arsenic solubility at high total sulfide. $As(HS)(OH)_2$ is one species that might account for the overprediction of arsenic at high total sulfide. $As(HS)(OH)_2$ can be formed through the following reactions:

$As(OH)_3 + H_2S \Leftrightarrow As(HS)(OH)_2 + H_2O$	pK_4=-9.5±1.3	(5)
$0.5\ As_2S_3 + 3H_2O \Leftrightarrow As(OH)_3 + 1.5H_2S$	pK_1 =12.58	(1)
$0.5\ As_2S_3 + 2H_2O \Leftrightarrow As(HS)(OH)_2 + 0.5H_2S$	pK_5 =3.08	(6)

Values for pK_5 and pK_1 were taken from Clarke (1998) and Nordstrom and Archer (2003), respectively. Overall, this species was insignificant in the model and was not considered further. No other arsenic species could account for the observed trend in the arsenic data. Thus, with only a small adjustment in pK_3, the model used

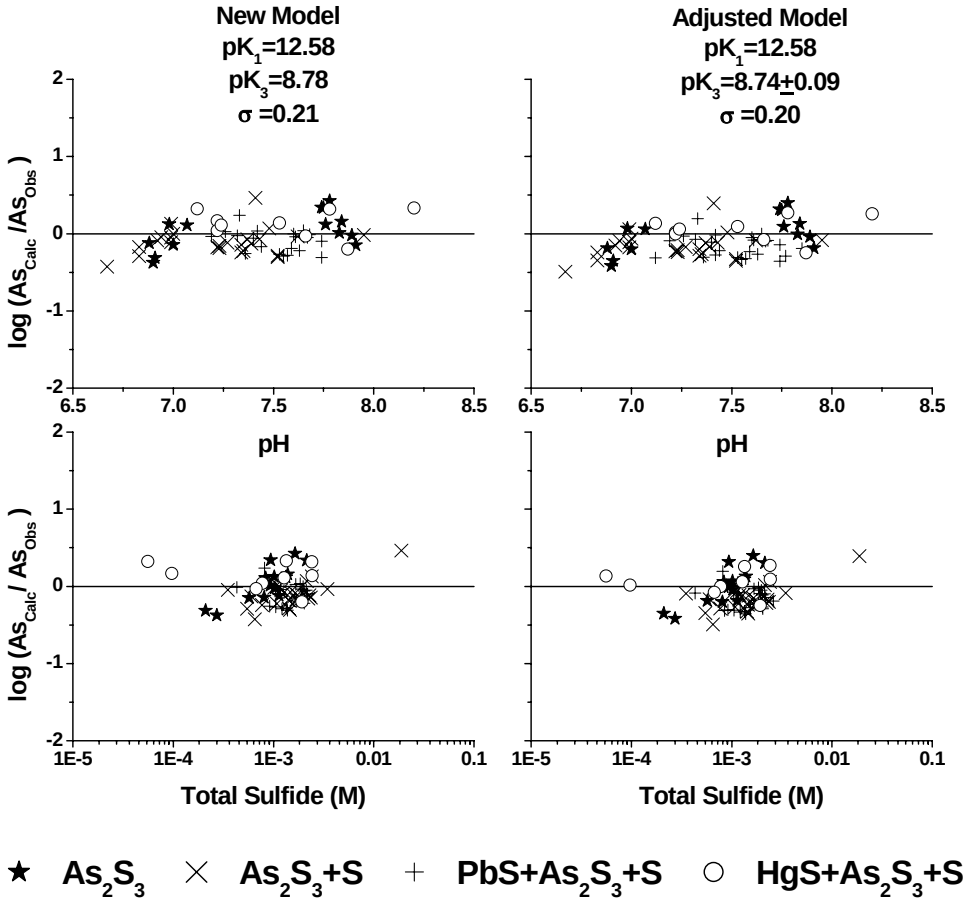

Figure 21. Fit of the arsenic solubility for As_2S_3, As_2S_3-S, PbS+As_2S_3+S and HgS+As_2S_3+S data in sulfidic solutions. The pK's refer to the reactions in the text. If any pK is not listed in the figure, the reaction corresponding to the pK was not included in the model.

to explain the solubility of As_2S_3 alone can be used to explain the solubilities of assemblages containing sulfur.

The means of the log (As_{obs}/As_{Calc}) of the As_2S_3 only data and means of the log (As_{obs}/As_{Calc}) of the As_2S_3+S, PbS+As_2S_3+S, HgS+As_2S_3+S data were compared, using a t-test, to determine if there is any statistical difference between the data that contain S^o and data that did not contain S^o. Samples with no S^o had a mean=0.198± 0.62 (uncertainty is σ^2) and samples containing S^o had a mean=0.00184±.029 (uncertainty is σ^2). The t-test indicates that these are not significantly different (95% confidence level). This result supports the conclusion from modeling that no new As species is required to describe solubilities when elemental sulfur is added to systems containing orpiment. Since the Adjusted Model in Figure 21 is different from previously proposed arsenic speciation models, it is important to test whether this model is consistent with previous data.

Eary's data (located in Appendix II) as fit with his proposed speciation model is shown as the Eary Model in Figure 22. The New Model containing $As(OH)_3$ and $AsS(HS)(OH)^-$ is shown as the New Adjusted Model in Figure 22. Since Eary used amorphous As_2S_3 in his experiments and natural crystalline orpiment was used throughout my work, the activity of the As_2S_3 component will be different in our experiments. Therefore, the activity of As_2S_3 for Eary's data was allowed to vary in the New Adjusted Model and my activity was set at 1. The equilibrium constants of the New Adjusted Model are the same as in Figure 21 and the activity of Eary's orpiment was calculated to be 8.61±3.12. There is a noticeable trend with total sulfide in the New Adjusted Model with an overprediction at low sulfide and an

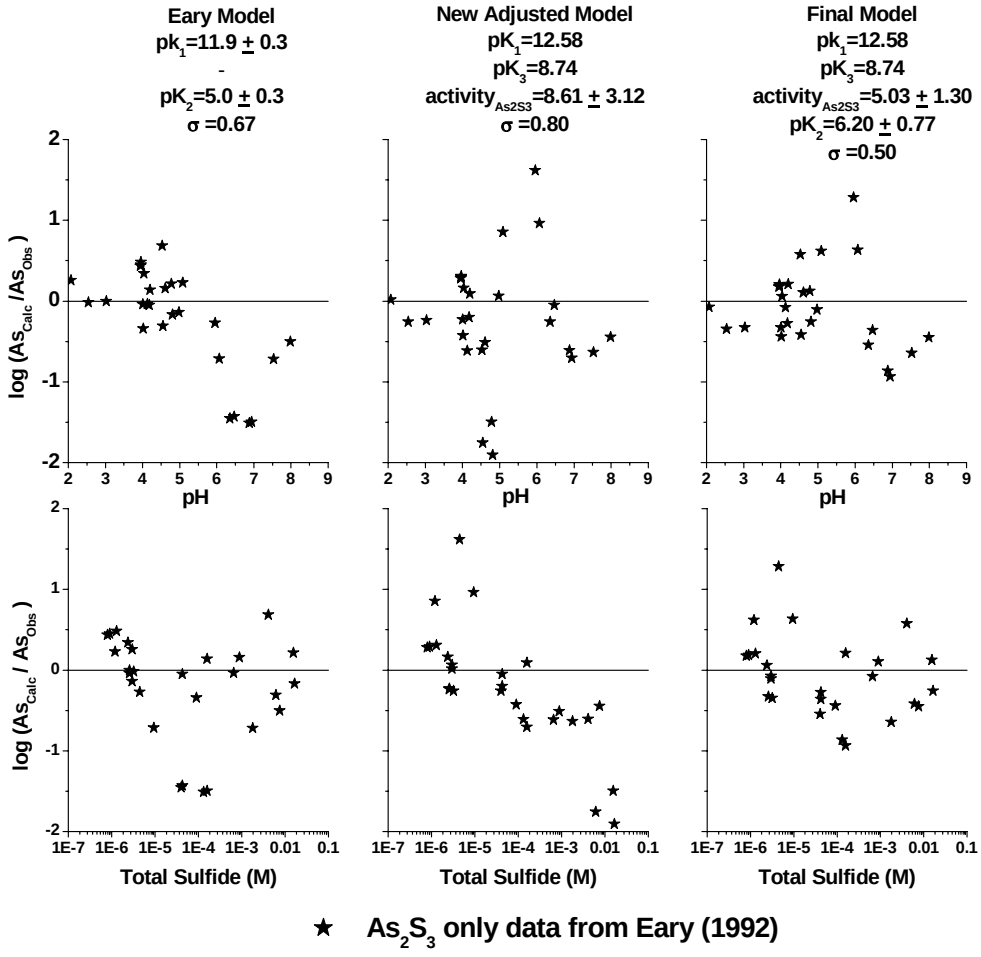

Figure 22. Fit of Eary (1992) data (As_2S_3 in sulfidic solutions). The pK's refer to the reactions in the text. If any pK is not listed in the figure, the reaction corresponding to the pK was not included in the model. The data are listed in Appendix II.

underprediction at high sulfide. The underprediction means there is not enough calculated arsenic solubility at high total sulfide and the overprediction means there is too much calculated arsenic solubility at low sulfide. Also the standard deviation is greater than in the Eary Model.

Eary's proposed trimer, $H_2As_3S_6^-$, was added to the New Adjusted Model to account for the trend with total sulfide and is shown in Figure 22 as the Final Model. The activity of As_2S_3 for Eary's data and the equilibrium constant of $H_2As_3S_6^-$ were allowed to vary. The activity of orpiment was calculated to be 5.03±1.30, which is a more reasonable value than the previously calculated value. The physical meaning of this number is that in solutions of identical pH and HS^- concentration, Eary's amorphous As_2S_3 would be 5.03 times more soluble than my As_2S_3. The standard deviation of the Final Model was better than Eary's original model and there are no significant trends in the data. The Final Model is consistent with the Eary data and now this model needs to be checked with the other literature data from Webster (1990).

Figure 23 shows Webster's (1990) As_2S_3 in sulfidic solutions data. These data are located in Appendix II, with her model (Webster Model). The equilibrium constants for the $As(OH)_3$ and $H_2As_3S_6^-$ species were taken from Webster (1990). There is an underprediction in solubility over the entire pH and total sulfide range. The Final Model in Figure 23 is the same as the Final Model that was fit to Eary's data in Figure 22, except that the activity of As_2S_3 has been adjusted. The activity of Webster's synthetic orpiment was calculated to be 0.35±0.09, compared to an activity defined as 1 for my natural orpiment.

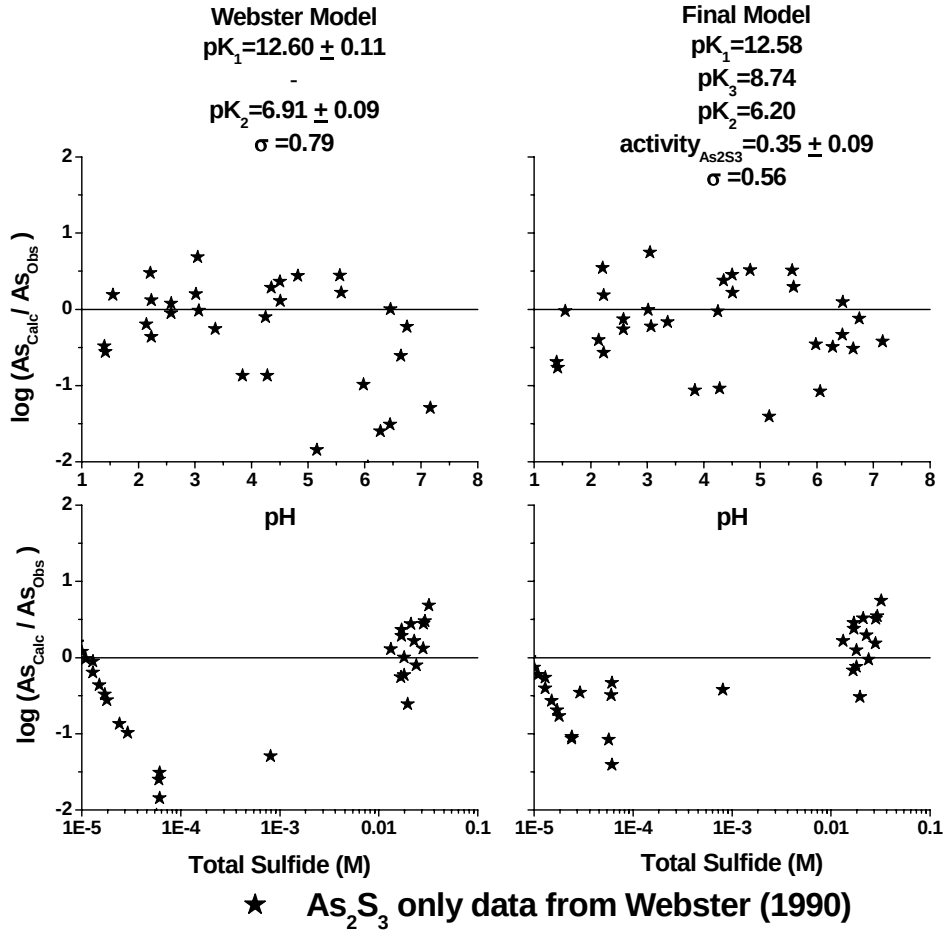

Figure 23. Fit of Webster (1990) data (As_2S_3 in sulfidic solutions). The pK's refer to the reactions in the text. If any pK is not listed in the figure, the reaction corresponding to the pK was not included in the model. The data are listed in Appendix II.

Now the Final Model that was fit to Eary's and Webster's data needs to be retested to ensure that it is still consistent to my data. In Figure 24, Final Model A fits the arsenic data from As_2S_3, As_2S_3-S, PbS+As_2S_3+S and Hg+As_2S_3+S experiments reasonably well without adjustments to the constants used to fit the Eary and Webster data (determination made by comparing Adjusted Model to Final Model A). It should also be noted that the model containing $As(OH)_3$, $AsS(HS)(OH)^-$ and $H_2As_3S_6^-$ is a better fit to the Eary and Webster data, than their proposed models which only contained the $As(OH)_3$ and $H_2As_3S_6^-$ species.

All of the data discussed so far in this section were obtained from samples that were saturated with orpiment. Now I consider extending Final Model A to samples that were undersaturated with orpiment. The arsenic solubility from Ag assemblage A and B experiments can be added to the previous data sets to determine if their solubility is consistent with Final Model A.

The last 5 samples in Table 31 (Ag assemblage A experiments) were not used in the model. A reliable value for H_2S could not be calculated for these five samples. Specifically, if the total sulfide concentration for a sample was calculated to equal TS, the highest limit allowed for the H_2S calculation, (refer to Appendix II under lines with *// Calculate HS^- given current estimates of K values and activity of orpiment* heading) an equilibrium constant could not be attained because the K value went above the set range in the Scientist Programming. For example, an approximate [As] is 10^{-4}, if the TS was calculated as 10^{-3} then K3 (refer to Appendix II, line in bold type) would equal ~0.1; which is above the set range (0<1.3e-9<1e-3) allowed

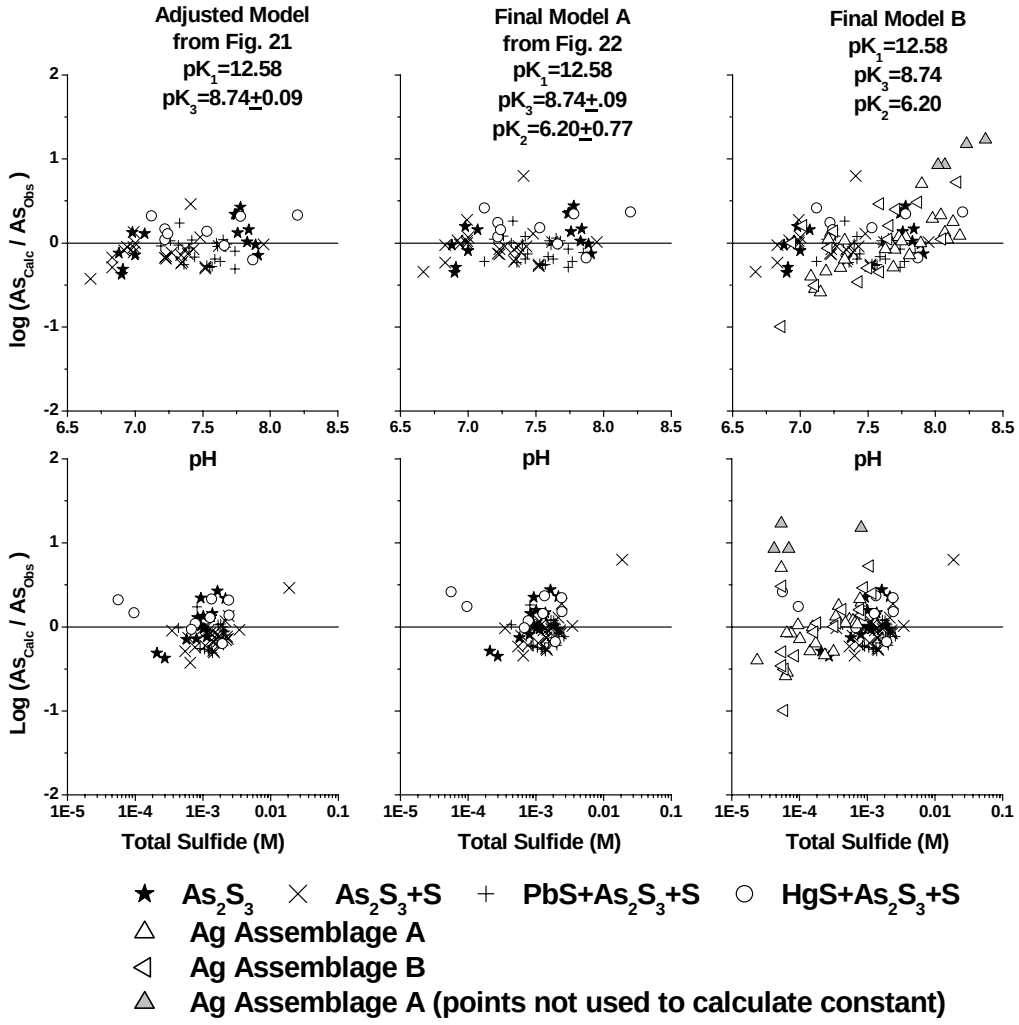

Figure 24. Fit of arsenic solubility for the As_2S_3, As_2S_3-S, $PbS+As_2S_3+S$, $HgS+As_2S_3+S$, Ag assemblage A and B data in sulfidic solutions. The pK's refer to the reactions in the text. If any pK is not listed in the figure, the reaction corresponding to the pK was not included in the model. Activity of As_2S_3 is 1, except in Ag assemblage A (0.09±0.02) and Ag assemblage B (0.07±0.03) experiments. Final Model B includes the Ag-bearing phase assemblages, where the activity of orpiment was adjusted to produce a fit.

for a reasonable estimation of K3. A K3 value above 0.1 would be unreasonable if it was needed for just five points and did not improve the fit of the data. It is unclear why these five samples went outside the acceptable range. Therefore they are shown in Figure 24, but not used to calculate any equilibrium constants. All the data from the Ag assemblage B experiment were used in the model.

The activity of As_2S_3 was treated as a fittable parameter for each assemblage, Ag assemblage A and B, where the activity must be less than one because the system is undersaturated with respect to a pure As_2S_3 phase. To illustrate this point the mass action law for reaction 3 can be written as:

$$0.5As_2S_3 + H_2O + 0.5H_2S \Leftrightarrow AsS(HS)(OH)^- + H^+$$

$$K_3 = \frac{\gamma^-[AsS(HS)(OH)^-][H^+]}{[H_2S]^{0.5} a_{As2S3}^{0.5}} \qquad (3)$$

The activity of orpiment in the denominator was set to 1 in systems saturated with orpiment; this allowed K_3 (and the other K's) to be adjusted by the least-squares method to obtain a model that optimally predicted observed solubilities. In the Ag assemblage A and B experiments the K's will be set equal to the values obtained in the orpiment-saturated system and $a_{As2S3(orp)}$ will be fit to obtain the optimum prediction of solubilities in orpiment-undersaturated systems. The activity of orpiment must be a constant in solutions equilibrated with two phases in the Ag_2S-As_2S_3 binary system at a given temperature and pressure. This can be shown by the following reaction, in which $a_{As2S3(orp)}$ is equal to the square of the equilibrium constant:

$$Ag_3AsS_{3(proust)} \Leftrightarrow 1.5Ag_2S_{(acant)} + 0.5As_2S_{3(orp)} \quad K = e^{\frac{-\Delta G_R^\circ}{RT}} = \frac{a_{Ag2S}^{1.5} \; a_{As2S3}^{0.5}}{a_{Ag3AsS3}} = a_{As2S3}^{0.5} \quad (7)$$

In this equation the activities of acanthite and proustite cancel each other, because they are present in the system. The activity of the As_2S_3 component must be less than one because the system is undersaturated in respect to this phase.

When the activity of As_2S_3 in Ag assemblage A has an activity of 0.09±0.02 and the activity of As_2S_3 in Ag assemblage B has an activity of 0.07±0.03, then the data can be compared to the pure As_2S_3+S system where the activity of As_2S_3 is 1. The Final Model B contains $As(OH)_3$, $AsS(HS)(OH)^-$ and $H_2As_3S_6^-$ and Figure 24 shows the log (As_{Calc}/As_{Obs}) vs. pH or total sulfide for all the data (As_2S_3, As_2S_3+S, HgS+As_2S_3+S, PbS+As_2S_3+S, Ag assemblage A and Ag assemblage B in sulfidic solutions), that includes all the samples in Table 31. The Final Model A and the Final Model B can be compared in Figure 24. The addition of the Ag-As-S data points does not degrade the original model, when the erroneous Ag assemblage A data are not considered. Final Model A and B, which contains $As(OH)_3$, $AsS(HS)(OH)^-$ and $H_2As_3S_6^-$, shows a slight trend in the data with pH with the erroneous Ag assemblage A points. However, this model has an overall good fit to all the data.

Although the model is a satisfactory fit to the above data, it is necessary to examine the arsenic concentration range in the data. One consideration for elevated arsenic concentrations in these experiments can be filtration failure. Another possible cause of errant concentrations could be sample contamination. Although, great efforts were made to maintain trace metal free conditions during the analysis. Low concentrations of arsenic could have resulted in sample absorption to the walls of the storage container. However, this does not seem possible because concentrations of arsenic did not vary with length of sample storage. Duplicate samples were opened

and stored in the refrigerator for various amounts of time and there was no significant change in their arsenic concentration at the time of measurement.

To conclude the arsenic speciation discussion Figure 25 shows the calculated concentration of arsenic as a function of pH and total sulfide. The major arsenic species in As_2S_3, As_2S_3-S, PbS+As_2S_3+S, HgS+As_2S_3+S, Ag assemblage A and B experiments in sulfidic solutions are $As(OH)_3$, $AsS(HS)(OH)^-$ and $H_2As_3S_6^-$. $AsS(HS)(OH)^-$ is dominant under conditions found in the environment, with ΣS=0.001 and a pH range of 7 to 8.

II.D.1.3. Free Energy of Formation for As_2S_3

Using the activities calculated in this study for Eary's (5.03±1.30) and Webster's (0.35±0.09) As_2S_3 and the ΔG_f^o of amorphous orpiment from Nordstrom and Archer (-76.8 kJ/mol), the ΔG_f^o of the As_2S_3 component of my natural orpiment can be calculated. The reaction used to calculate the activity of my natural orpiment was obtained from the following derivation using Eary's data:

$$As_2S_{3\ (This\ Work)} \Leftrightarrow As_2S_{3\ (Eary)} \quad K = e^{\frac{-\Delta G_r^\circ}{RT}} = \frac{a_{As2S3(Eary)}}{a_{As2S3(ThisWork)}} = \frac{1}{5.03 \pm 1.30} \qquad (8)$$

From this, ΔG_R^o is calculated to be +3.6 kJ/mol. Assigning ΔG_f^o =-76.8 kJ/mol for Eary's As_2S_3 results in a $\Delta G_{f\ (As2S3\ This\ Work)}^o$ of -80.8±1.6 kJ/mol ($\Delta G_{f\ (As2S3\ This\ Work)}^o = \Delta G_{f\ (Eary)}^o - \Delta G_R^o$). The activity of orpiment from Webster's data led to a ΔG_f^o of -83.4±2.7 kJ/mol for her synthetic orpiment. Nordstrom and Archer (2003) state that natural orpiment and amorphous orpiment should have a ΔG of –84.9 kJ/mol and -76.8 kJ/mol, respectively. The difference in the ΔG values of the natural material

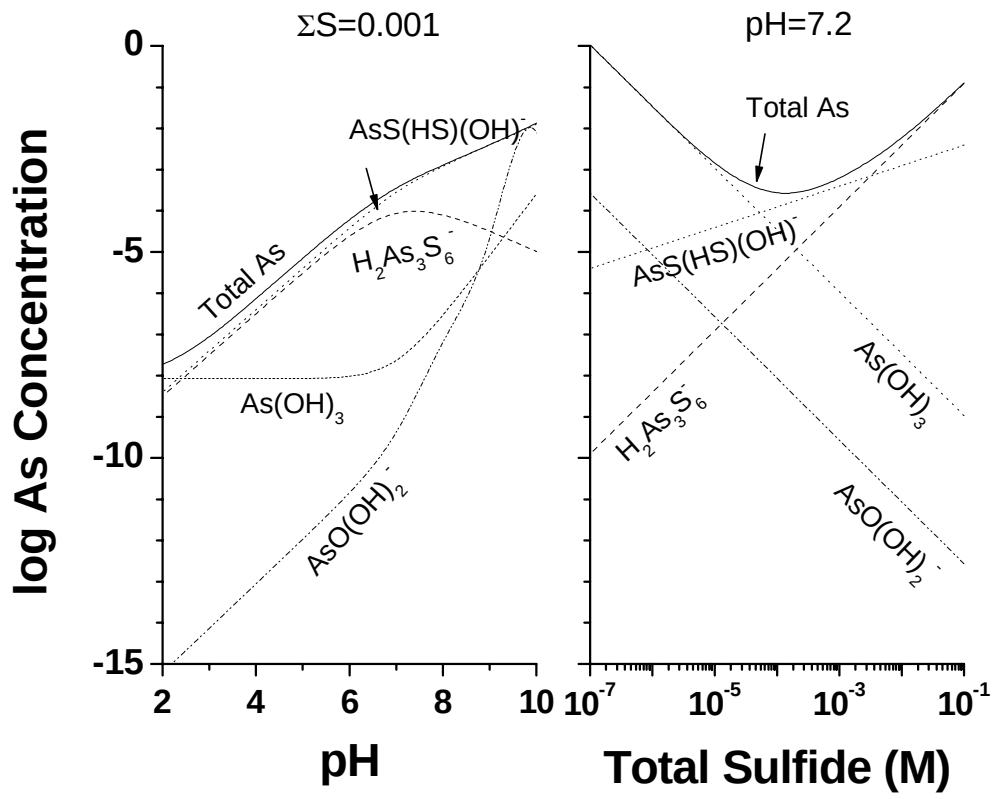

Figure 25. Calculated concentration of arsenic species in equilibrium with in orpiment in sulfidic solutions as a function of (left) pH at 0.001 M total sulfide and (right) total sulfide at pH 7.2

from this experiment and Nordstrom and Archer's value may come from using different starting materials.

The ΔG_f^o of $AgAsS_2$, Ag_7AsS_6 and Ag_3AsS_3 are not well defined. Hall (1966) calculated the ΔG_f^o values of $AgAsS_2$ and Ag_3AsS_3 at high temperatures. At 25°C the ΔG_f^o values of $AgAsS_2$, Ag_7AsS_6 and Ag_3AsS_3 are estimated as –75 kJ/mol, -150 kJ/mol and –110 kJ/mol, respectively. Bryndzia and Kleppa (1989) calculated the ΔH_f of $AgAsS_2$ and Ag_3AsS_3 at 298K. The ΔH_f values of $AgAsS_2$ and Ag_3AsS_3 are –74.77±2.9 kJ/mol and -111.3±3.4 kJ/mol, respectively. The ΔG_f^o of Ag_7AsS_6 could not be calculated in this work because this component is ternary. The calculation would require that the activity of S^o be known in addition to the ΔG_f^o of As_2S_3 and Ag_2S. Experiments in this work did not contain elemental sulfur so the activity could not be reliably determined. The ΔG_f^o of $AgAsS_2$ could have been calculated through the following reaction if a reversible equilibrium had been reached in these experiments:

$$As_2S_3 + Ag_3AsS_3 \Leftrightarrow 3AgAsS_2 \qquad (9)$$

However, the experiments dealing with $AgAsS_2$ appear to be unstable and therefore a ΔG_f^o could not be calculated. The known and calculated ΔG_f^o's are in Table 35.

II.D.2. Speciation of d^{10} Metals in Sulfidic Solutions Equilibrated with Silver, Lead, Mercury, Sulfur and Arsenic

Now that the solubility of arsenic has been established, the solubility of silver, mercury and lead in the presence of dissolved As(III) will be investigated. The issue to be determined is whether the solubilities of the metals are greater when

Table 35. Free Energy Data for As(III) and Ag(I) Complexes

Species or Compound	ΔG_f^o (kJ/mol)	Source
$As_2S_{3\ (crystalline)}$	-84.9	1
$As_2S_{3\ (amorphous)}$	-76.8	1
$As_2S_{3\ (natural\ crystalline)}$	-80.8±1.6	3
Ag_2S	-39.7	2
$AgAsS_2$	-75	5
Ag_7AsS_6	-150	5
Ag_3AsS_3	-110	5
HS^-	12.05±0.08	1
H_2S (aq)	-27.87±0.08	1
H_2O	-237.178±0.008	1
$As(OH)_3$	-640.03±0.08	1
$AsS(HS)(OH)^-$	-244.60±0.6	4
1. Nordstrom and Archer (2003), 2. Robie and Hemingway (1995), 3. This work, 4. Helz et al. (1995), 5. Hall (1966)		

thioarsenite ligands are present compared to when they are absent. This section will first compare the solubility of Ag from Ag-As-S assemblages to the solubility of Ag from Ag_2S and Ag_2S+S experiments. Then the Hg-As-S and Pb-As-S systems will be discussed.

II.D.2.1. Speciation of Silver in Sulfidic Solutions Equilibrated with Ag_2S, Ag_2S+S

For silver modeling, complexes of $Ag_xS_yH_z^{x+z-2y}$, $AgCl_x^{1-x}$, $AgCl_xHS^{1-x}$ and AgS_x^{1-} were tested in fits of the data. The Scientist program used to model the Ag_2S+S solubility is given in Appendix III. The procedure for modeling the data was discussed in Section II.B.4.1. The last sample in Table 29 (Ag_2S only experiment) and the last six samples in Table 30 (Ag_2S+S experiment) were not used in the fitting procedure. The samples were disqualified because the starting voltage of these

samples during the potentiometric titration for total sulfide was less than 180 mV, which implied that no sulfide was present. The loss of HS^- could have resulted in the volitilazation of HS^- in the time before the potentiometric titration. The ionic strength of the samples varied between 0.01 and 0.31 M. A few of the samples had an ionic strength above 0.1 M, and the Davies equation will not produce an accurate activity for these samples.

The fitted data set includes Stefansson and Sewards's (2003) solubility data, which are shown in Appendix III, for silver sulfide (acanthite/ argentite) in sulfide solutions at 25°C. A small set of experiments shown in Table 29, which include Ag_2S reacted with sulfide solutions in the absence of zero-valent sulfur, were also included in the model. The main set of experiments included in the model is shown in Table 30, which include Ag_2S and S reacted with various sulfide solutions.

The complexes proposed by Stefansson and Seward (2003), AgHS, $Ag(HS)_2^-$ and $Ag_2S(HS)_2^{2-}$, for the equilibration of silver sulfide (acanthite/argentite) in solutions with a total reduced sulfur ranging from 7 mM to 0.176 M and a pH of 3.7 to 12.7 were tested in the Stefansson and Seward Base Model (Figure 26). The formation of these silver species can be represented by the following reactions:

$$0.5Ag_2S_{(s)} + 1.5\ HS^- + 0.5\ H^+ \Leftrightarrow Ag(HS)_2^- \quad (10)$$

$$Ag_2S_{(s)} + 2\ HS^- \Leftrightarrow Ag_2S(HS)_2^{2-} \quad (11)$$

$$0.5Ag_2S_{(s)} + 0.5\ HS^- + 0.5\ H^+ \Leftrightarrow Ag(HS) \quad (12)$$

Using the equilibrium constants from Stefansson and Seward (2003) produced the Stefansson and Seward Base Model in Figure 26. The Stefansson and Seward data

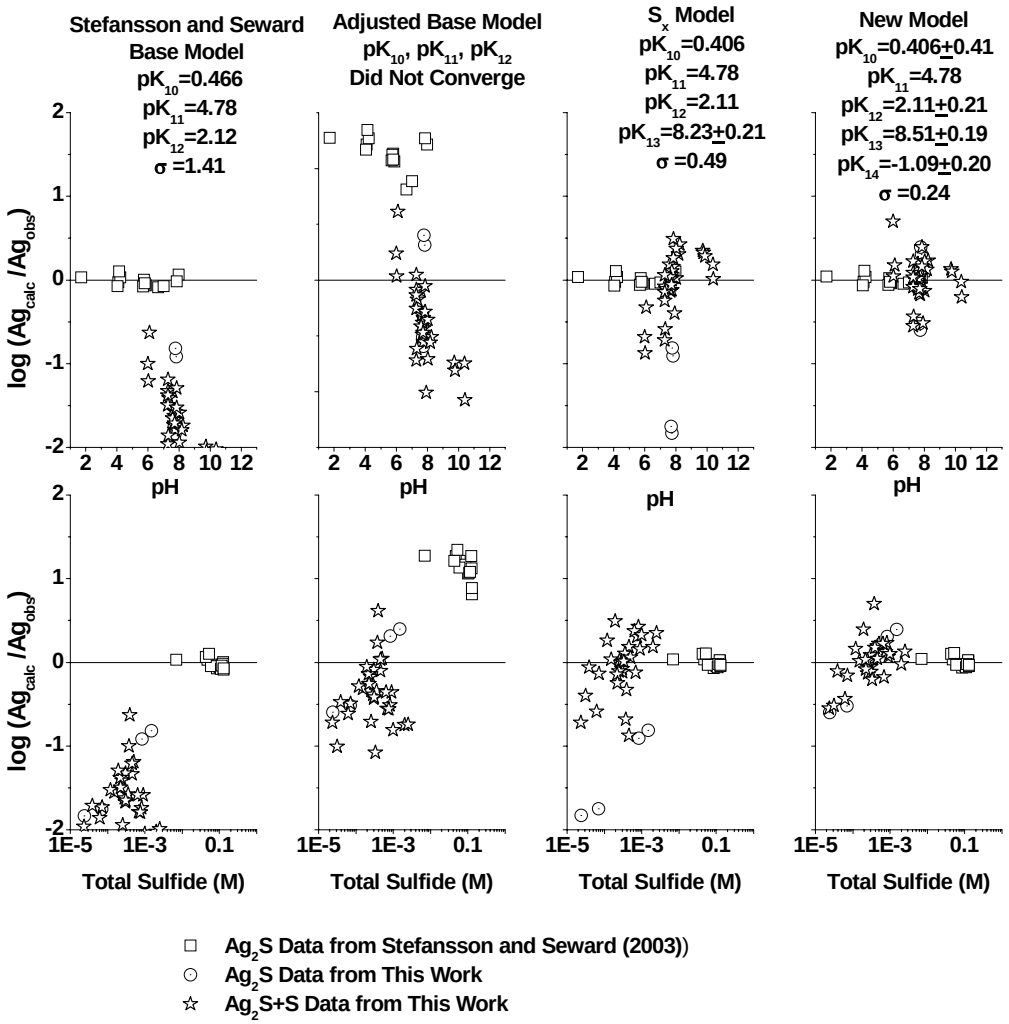

Figure 26. Fit of the silver sulfide data in sulfidic solutions. The pK's refer to the reactions in the text. If any pK is not listed in the figure, the reaction corresponding to the pK was not included in the model.

are well-fit by their model. However, my solubilities are greatly under-predicted at a pH greater than 6 and at total sulfide below 0.001 by approximately fifty-fold. This implies that there is more observed silver solubility when elemental sulfur is present in the system.

Next, the Stefansson and Seward Base Model was adjusted by allowing the equilibrium constants to vary, as shown in the second column from the left in Figure 26. The model did not converge to give meaningful equilibrium constants, and the derived equilibrium constants deviated substantially from Stefansson and Seward's original constants. Therefore, this adjustment was unsatisfactory. Clearly additional silver species are needed to account for the extra solubility observed in the Ag_2S+S experiments.

The first species added to the model to account for the extra silver solubility was AgS_x^-. When this species was added to the Stefansson and Seward Base Model (shown in Figure 26 as the S_x Model) there were still trends in the data and another species is needed to account for the extra solubility.

The species that resulted in the best fit to the data are AgHS, $Ag(HS)_2^-$, $Ag_2S(HS)_2^{2-}$, $Ag(Cl)(HS)^-$, and AgS_x^-. The additional species can be represented by the following reactions:

$$0.5Ag_2S_{(s)} + (x-1)S^\circ + 0.5\ HS^- \Leftrightarrow AgS_x^- + 0.5\ H^+ \qquad (13)$$

$$0.5Ag_2S_{(s)} + Cl^- + 0.5\ HS^- + 0.5\ H^+ \Leftrightarrow Ag(Cl)(HS)^- \qquad (14)$$

The fit that includes these species is shown in Figure 26 as the New Model. It should be noted that pK_{11} is the equilibrium constant from Stefansson and Seward (2003). pK_{11} was held constant because this work does not provide any data at pH's above

~9, where $Ag_2S(HS)_2^{2-}$ is dominant. Figure 26 shows the fit of the silver data using the New Model, which produced the best fit to the data and the fit is good over the whole pH range. It appears as though the $Ag(Cl)(HS)^-$ species is essential to the model; otherwise a satisfactory fit could not be obtained. The fit to total sulfide has a slight trend at low total sulfide data, but no other species could account for the under prediction at low sulfide concentrations.

Other species were added to the New Model, but were eliminated by the fitting procedure. The first species added to the model were $AgCl_x^{1-x}$ (AgCl, $AgCl_2^-$ and $AgCl_3^{2-}$) species. However, the calculated equilibrium constants deviated from known constants and provided an unsatisfactory fit. $Ag(OH)(HS)^-$ and $Ag(S_x)(OH)^-$ were added separately to the New Model to try to account for the under prediction of silver at low total sulfide values. The formation of these species can be represented by the following reactions:

$$0.5Ag_2S_{(s)} + H_2O + 0.5\ HS^- \Leftrightarrow Ag(OH)(HS)^- + 0.5\ H^+ \qquad (15)$$

$$0.5Ag_2S_{(s)} + (x\text{-}1)S^\circ + 0.5\ HS^- + H_2O \Leftrightarrow Ag(OH)S_x^{2-} + 1.5\ H^+ \qquad (16)$$

The addition of these species to the New Model each produced a standard deviation of 0.24, the same value obtained without them.

The best-fit model to the Ag_2S+S data includes the following silver species: AgHS, $Ag(HS)_2^-$, $Ag_2S(HS)_2^{2-}$, $Ag(Cl)(HS)^-$, and AgS_x^-. These species will be used as a comparison for the solubility of silver in the silver assembages. However, it would first be helpful to justify the two additional species that were needed to get a good fit to the data.

II.D.2.1.1 Evidence for the $Ag(Cl)(HS)^-$ Species

When a metal is in the presence of more than one strong covalent ligand, such as Cl^-, HS^-, OH^- or Br^-, mixed ligand species are observed sometimes (Zotov et al., 1982; Cosden and Byrne, 2003). $Ag(Cl)(OH)^-$ is known to exist and was added to the model, but this species did not produce an improved fit. However, the addition of $Ag(Cl)(HS)^-$ improved the fit of the data in the New Model.

The calculated equilibrium constant in Figure 27 for $Ag(Cl)(HS)^-$ was compared to a theoretical value calculated from mixed ligand theory, as represented by the following equation:

$$\log \beta_{MAmBn} = \frac{m}{n+m} \log \beta_{MAm+n} + \frac{n}{n+m} \log \beta_{MBm+n} + \log S \qquad (17)$$

where, $\beta_{MAmBn=} MA_mB_n / [M][A]^m * [B]^n$ and $S=(m+n)!/m!n!$. The β values are shown in Table 36. The experimental equilibrium constant for $Ag(Cl)(HS)^-$ does not agree with the calculated constant using mixed equilibrium theory.

Zotov et al. (1982) has shown that the species $Ag(Cl)(OH)^-$ exists in solutions that are alkaline and contain chloride. The calculated equilibrium constant for $Ag(Cl)(OH)^-$ using mixed ligand theory and the experimental work of Zotov et al. (1982) are in excellent agreement. Even though the calculated equilibrium constant for $Ag(Cl)(HS)^-$ does not agree with mixed ligand theory, the presence of the $Ag(Cl)(HS)^-$ species in this work can be justified by the improvement in the fit of the data when this is species is included. It may be concluded that the $Ag(Cl)(HS)^-$ species is essential to the model, but is probably not always the dominant species.

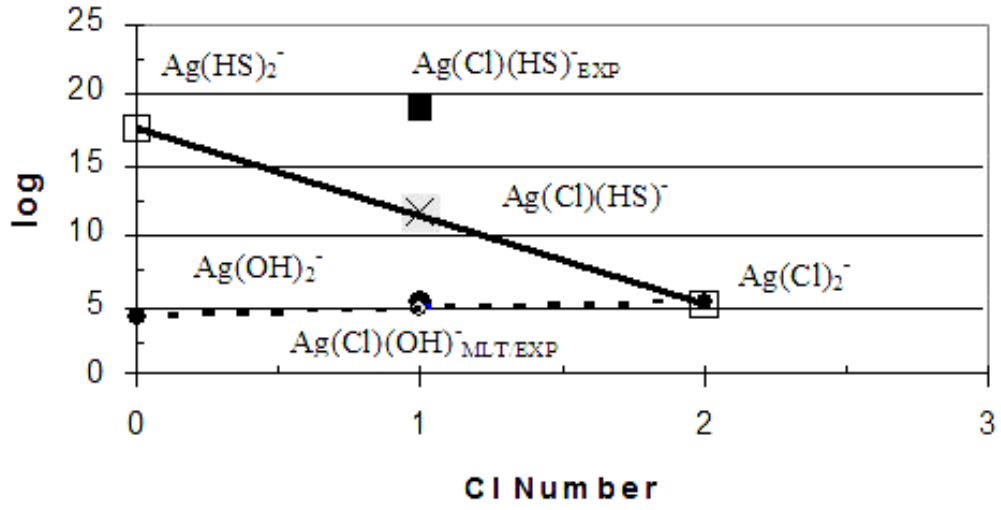

Figure 27. Comparison of the equilibrium constant of $Ag(Cl)(HS)^-$ to its theoretical value using the mixed ligand theory. Open squares represent equilibrium constants of $Ag(HS)_2^-$ and $Ag(Cl)_2^-$. The gray square with a x on the solid line is the theoretical equilibrium constant for $Ag(Cl)(HS)^-$ using mixed ligand theory (MLT). The filled square is the experimental equilibrium constant for $Ag(Cl)(HS)^-$calculated from this work (EXP). The closed circles represent equilibrium constants for $Ag(OH)_2^-$ and $Ag(Cl)_2^-$. The gray and filled circle in the middle of the dotted line represent the theoretical equilibrium constant of $Ag(Cl)(OH)^-$ from mixed ligand theory and an experimental value from Zotov et al. (1982), respectively.

Table 36. Log β For Individual Species

Species	Log β	Source
Known Values		
$AgCl_2^-$	5.18	1
$Ag(OH)_2^-$	4.22	1
$Ag(HS)_2$	17.54	1
Experimental Values		
$Ag(Cl)(OH)^-$	5.30	2
$Ag(Cl)(HS)^-$	19.12	3
Calculated from Mixed Ligand Theory		
$Ag(Cl)(OH)^-$	5.00	4
$Ag(Cl)(HS)^-$	11.70	4

1. Martell and Smith (1974); 2. Zotov et al. (1982), experimental value; 3. This Work, experimental value; 4. Calculated form mixed ligand theory

II.D.2.1.2. Evidence for Polysulfide Species

Polysulfide complexes of silver have been proven to exist through experimental work done by Cloke (1963). According to the model developed by Cloke involving acanthite and elemental sulfur in sodium polysulfide solutions, polysulfide will become the dominant sulfur species in solutions that have a pH between ~9 and 11. To test the proposed model samples were made with pH's ranging from 9.7 to 10.4. When these samples were analyzed there was a yellowish coloration visible in the sample, which is an indication that polysulfides (S_x^{2-}) had formed. In the kinds of solutions studied here polysulfides, S_5^{2-} and S_4^{2-}, are the dominant optical absorbers between 500 nm and approximately 300 nm. Below 300 nm, absorption is dominated by a yet uncharacterized thioarsenite species and by HS^- (at 230 nm) (Chen and Morris, 1972; Giggenbach, 1974). Figure 28 clearly shows there is absorption in those two areas that is related to polysulfide formation.

Spectra that displayed polysulfide absorption and had the characteristic yellow color were then fit using SCIENTIST (Micromath, Inc) to determine their a_S value. The modeling process was discussed in Section II.B.4.2. The activity of sulfur was 1 if polysulfides formed in solution and there was excess solid sulfur present. There were some instances where the activity of sulfur was calculated to be ~0.5, because S^o was reacting with HS^-, and was depleted in solution. There were only four samples that had an $a_S<1$ and they are shown in Table 30. The other samples had an a_S of approximately 1, because there was excess S present in the experiments. Once the activity of sulfur was determined it was placed into the final model to determine if polysulfide species were significant to the model.

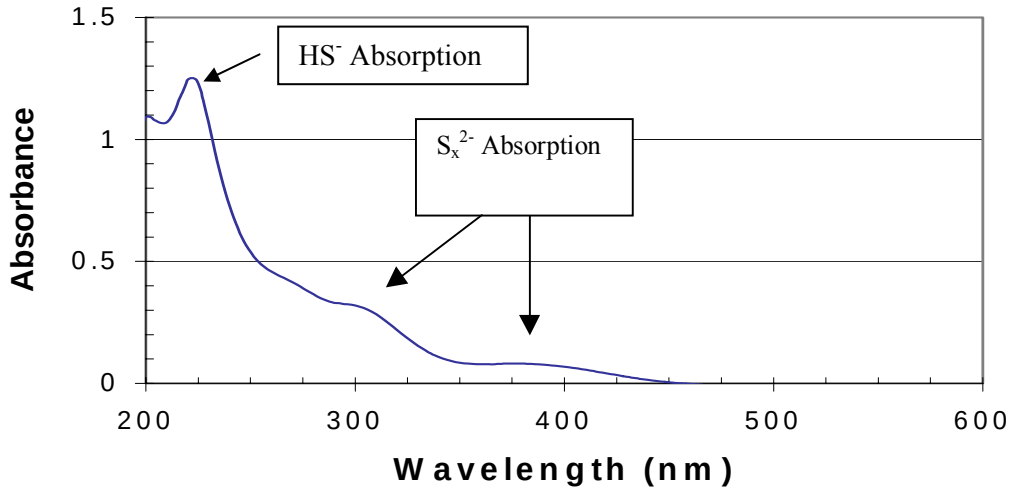

Figure 28. Absorbance spectrum for a sulfidic solution equilibrated with Ag_2S and S at pH 10.41 and a total sulfide of 3.334×10^{-4} M. (Ag) = 1.19×10^{-7} M. Spectrum was taken with a 1cm pathlength quartz cuvette.

When Cloke (1963) conducted experiments on acanthite in solutions with varying concentrations of sodium polysulfide, he concluded that $Ag(S_4)_2^{3-}$, $AgS_5S_4^{3-}$ and $Ag(HS)S_4^{2-}$ were responsible for the silver solubility. These species were tried in the modeling program, instead of $AgS_{x,}^-$ but did not converge meaning that one or more of the species was insignificant in the model and an equilibrium constant could not be calculated. It is known that silver likes to have a coordination of two, but Cloke's $Ag(S_4)_2^{3-}$ species was chosen in a last effort to fit the data (Gammons and Barnes, 1989). So $Ag(S_4)_2^{3-}$ was tried with the $Ag(Cl)(HS)^-$ species in the modeling program, instead of AgS_x^-, to do a final test on $Ag(S_4)_2^3$. $Ag(S_4)_2^{3-}$ is represented by:

$$Ag_2S + 12S° + 3HS^- \Leftrightarrow 2Ag(S_4)_2^{3-} + 3H^+ \qquad (18)$$

Figure 29 compares the Cloke Model to the New Model to show that the addition Cloke's polysulfide species does not increase the goodness of fit. The fit of the data with pH is worse with the $Ag(S_4)_2^{3-}$ species when compared to the model containing AgS_x^-. Thus all of the silver polysulfide species from Cloke (1963) were eliminated from the fitting procedure.

AgS_x^- was added to the model as an alternative polysulfide species and produced a satisfactory fit. It can be assumed that the single polysulfide species in AgS_x^- can form two bonds with silver and have a coordination of two. Since the majority of my experiments were saturated with sulfur, the activity of sulfur is assumed to be one. At a constant activity the number of sulfur atoms, x, in AgS_x^- cannot be determined and modeling would produce a satisfactory fit for every AgS_x^- species.

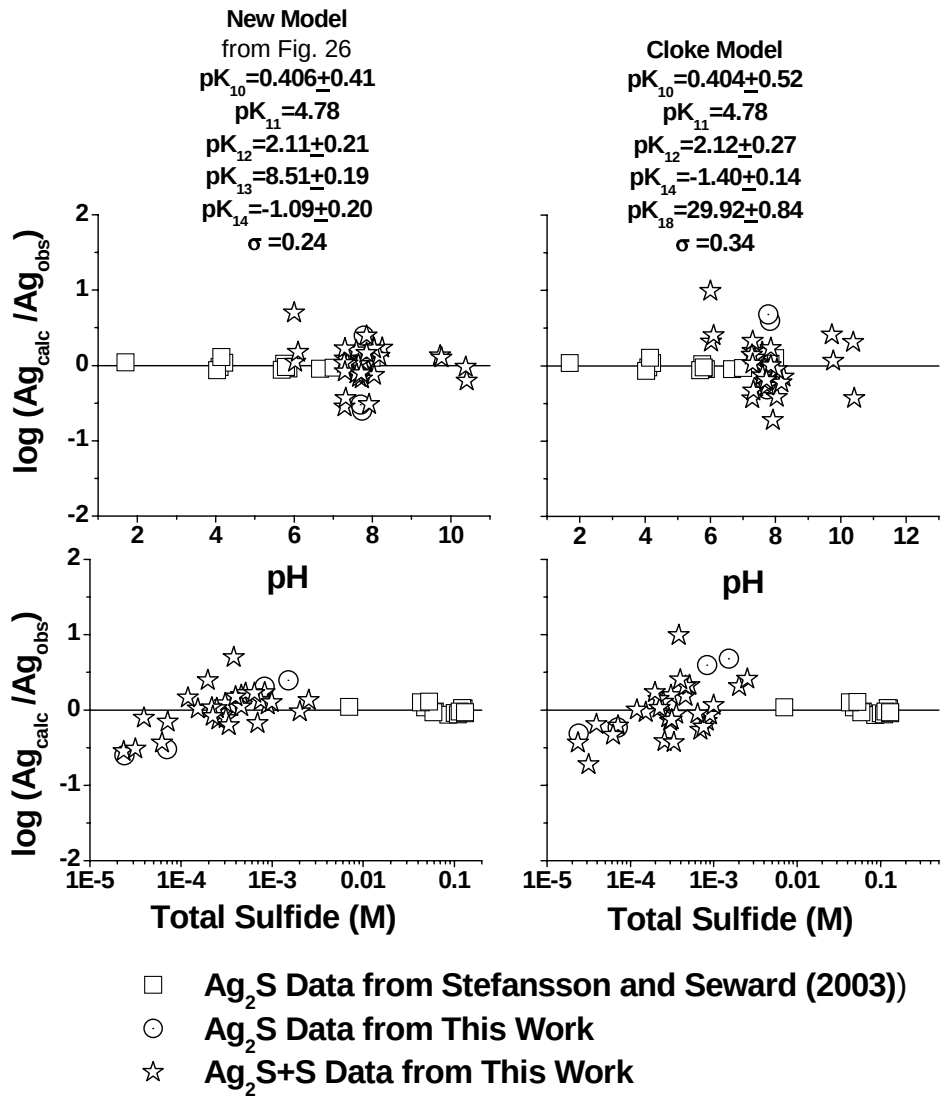

Figure 29. Fit of the silver sulfide data in sulfidic solutions. The pK's refer to the reactions in the text. If any pK is not listed in the figure, the reaction corresponding to the pK was not included in the model.

To test if the equilibrium constant calculated for the AgS_x^- is reasonable it can be compared to HgS_x. Stability constants for d^{10} metals like Ag (I) and Hg (II) produce a linear relationship with one another (Hancock et al., 1973; Stefansson and Seward,2003). It is not possible to determine the correct polysulfide species involved in AgS_x^-, but to compare the two polysulfide species S_x^{2-} was used as the polysulfide ligand attached to either Ag(I) or Hg(II). Jay et al. (2000) does not define the x in HgS_x. Figure 30 shows that there is a linear relationship between the Ag(I) and Hg(II) polysulfide species indicating that the calculated equilibrium constant for AgS_x^- agrees with the experimental equilibrium constant for HgS_x that was calculated by Jay et al. (2000).

II.D.2.1.3. Speciation Diagram for Ag_2S-S System

Using the best-fit model a speciation diagram for the equilibration of Ag_2S+S in a sulfide solution with 0.001M total sulfide can be made and is shown in Figure 31. AgS_x^- is the dominant silver complex above pH 5 in solutions with ΣCl=0.01M. $Ag(Cl)(HS)^-$ is dominant below pH 5 under these conditions. $Ag(Cl)(HS)^-$ may become important at neutral pH's when there are higher sulfide and sodium chloride concentrations. When the ΣCl was raised by ten times the $Ag(Cl)(HS)^-$ species became dominant until a pH of 5.5. The speciation model includes AgS_x^- as a dominant species, and implies that there is a dependence on a_s. In solutions where sulfur is not in excess, the AgS_x^- species may become insignificant.

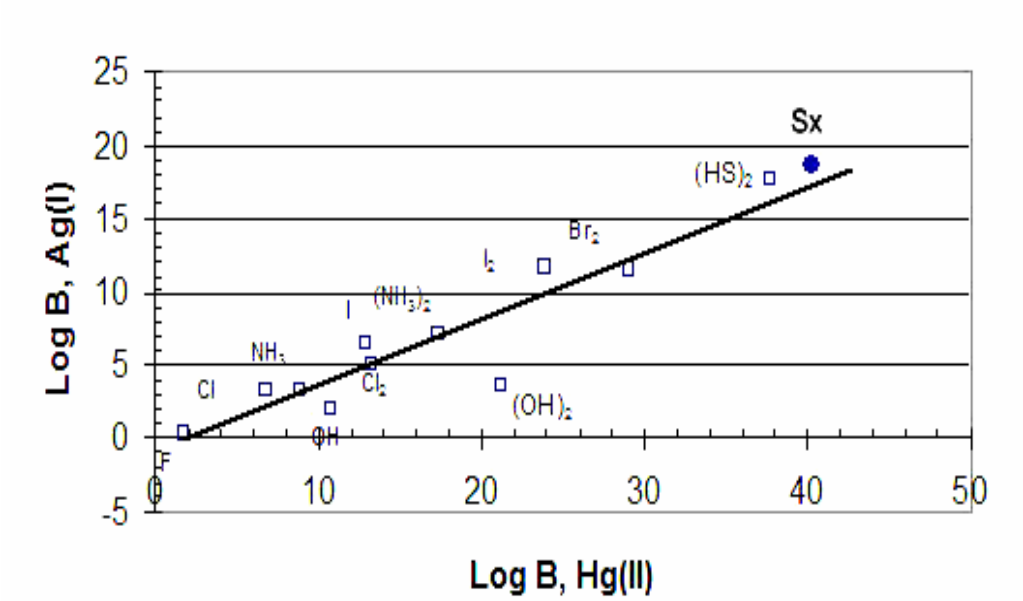

Figure 30. Comparison of Ag (I) and Hg(II) stability constants for common ligands at 25°C and an ionic strength of 0.05. Data from Martell and Smith (1973). HgS_x value from Jay et al. (2000). AgS_x^- value from this work. Polysulfide species is represented by filled circle.

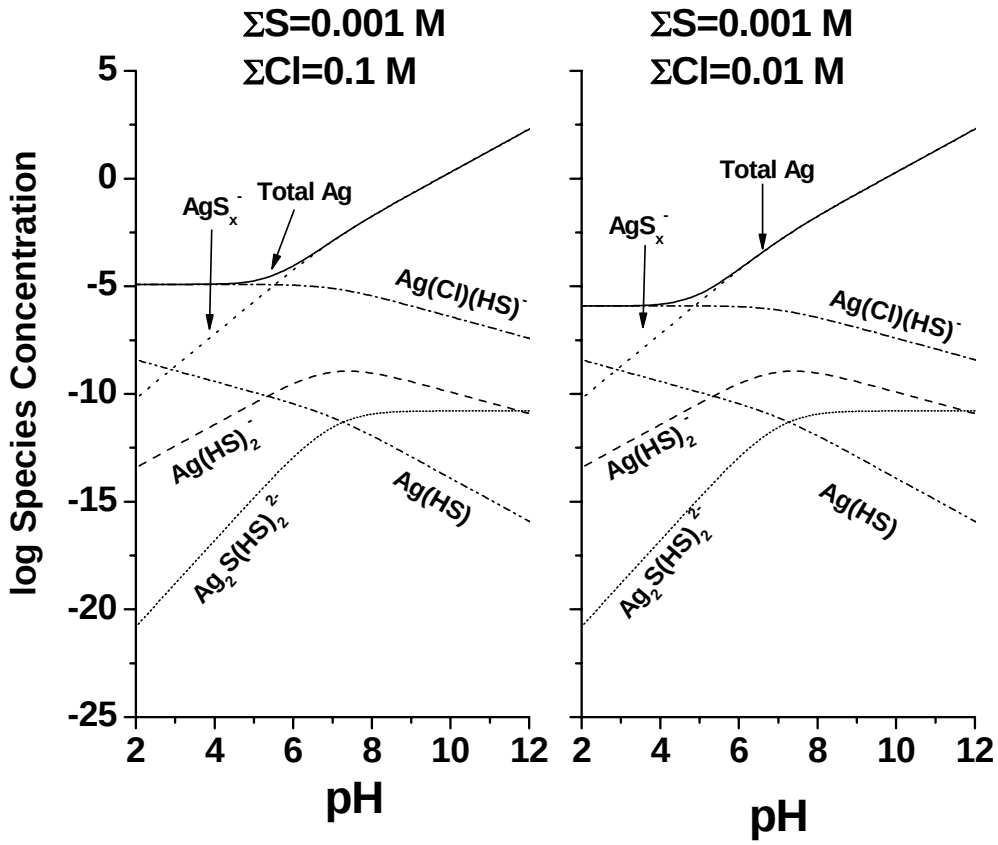

Figure 31. Concentration of silver species as a function of pH at 0.001 M total sulfide for the equilibration of Ag_2S-S in sulfidic solutions in Left: 0.1 M Cl^- and Right: 0.01 M Cl^-. Represents system saturated with sulfur.

II.D.2.1.4. Two versus Three Coordination for Ag

Sugaki et al. (1987) explained the solubility of Ag_2S in solutions of 0.0 to 4.1 m NaHS solutions with a temperature range of 25°C to 250°C with dinuclear silver sulfide complexes, i.e. $Ag_2S(H_2S)(HS)_2^-$. A review by Bell and Kramer (1999) presents evidence that polynuclear silver complexes would result in a zigzag chain, with the coordination of silver being two. This configuration is supported by Fijolek et al. (1997) who present evidence that the structure of $Ag_2[S(CH)_2)_5S]$ has a layered geometry. However, Habibi et al. (1999) and Fujisawa et al. (2000) have identified three coordinate silver (I) thiolate complexes. Silver is in a ring formation and contains S ligands that bridge two Ag atoms. If this structure is valid then the complex proposed in reaction 21 by Sugaki (1987) in concentrated sulfide solutions could be three coordinate where silver is in a ring formation and bridged by S atoms.

The solubility of Ag_2S in less concentrated sulfide solutions is usually explained with two coordinate silver sulfide complexes, i.e. $Ag(HS)_2^-$. The difference in coordination seems to be related to the sulfide concentration in the system. This phenomenon is also seen with copper. Mountain and Seward (1999) predict that a two coordinate copper sulfide complex dominates at low sulfide concentrations, while a three coordinate species becomes the dominant species at high sulfide concentrations.

The Ag_2S and Ag_2S+S data were used to determine if a three coordinate Ag species could explain the silver solubility in this study, which had starting total sulfide concentrations ranging from 0.1 mM to 1 mM. Sugaki's Ag_2S solubility data at 25°C and the data from this study were modeled together using the Scientist

program. The model is shown in Appendix III. The Sugaki Base Model consisted of Sugaki's dinuclear silver species, which can be written as:

$$Ag_2S + HS^- + H^+ \Leftrightarrow Ag_2S(H_2S) \quad (19)$$

$$Ag_2S + 2HS^- + H^+ \Leftrightarrow Ag_2S(H_2S)(HS)^- \quad (20)$$

$$Ag_2S + 3HS^- + H^+ \Leftrightarrow Ag_2S(H_2S)(HS)_2^{2-} \quad (21)$$

$$Ag_2S + 2HS^- \Leftrightarrow Ag_2S(HS)_2^{2-} \quad (22)$$

Figure 32 shows the Sugaki Base Model and the Sugaki Adjusted Model. The Sugaki Adjusted Model only adjusted the equilibrium constants for the $Ag_2S(H_2S)$ and $Ag_2S(HS)_2^{2-}$ species, the other two species were insignificant and were held at a constant value. The three coordinate species did not fit the silver solubility in these experiments. This evidence does not exclude the possibility that at higher concentrations of total sulfide three coordinate species may become important, but at lower concentrations of total sulfide two coordinate species are dominant.

II.D.2.2. Speciation of Silver in Sulfidic Solutions Equilibrated with Arsenic

II.D.2.2.1. Role of Sulfur in Ag Assemblage A and B Experiments

The role of elemental sulfur will be discussed first because this species greatly enhances silver solubility. There was no excess zero valent sulfur added to the solutions used in the study of the Ag-As-S phases. There was also no evidence that zero valent sulfur was formed throughout Ag assemblage A and B experiments. Evidence is provided by the UV-Visible spectra that were taken of each sample. An example of a common spectrum of an Ag assemblage A and an Ag assemblage B sample is displayed in Figure 33. Polysulfides form if zero valent sulfur and HS^-

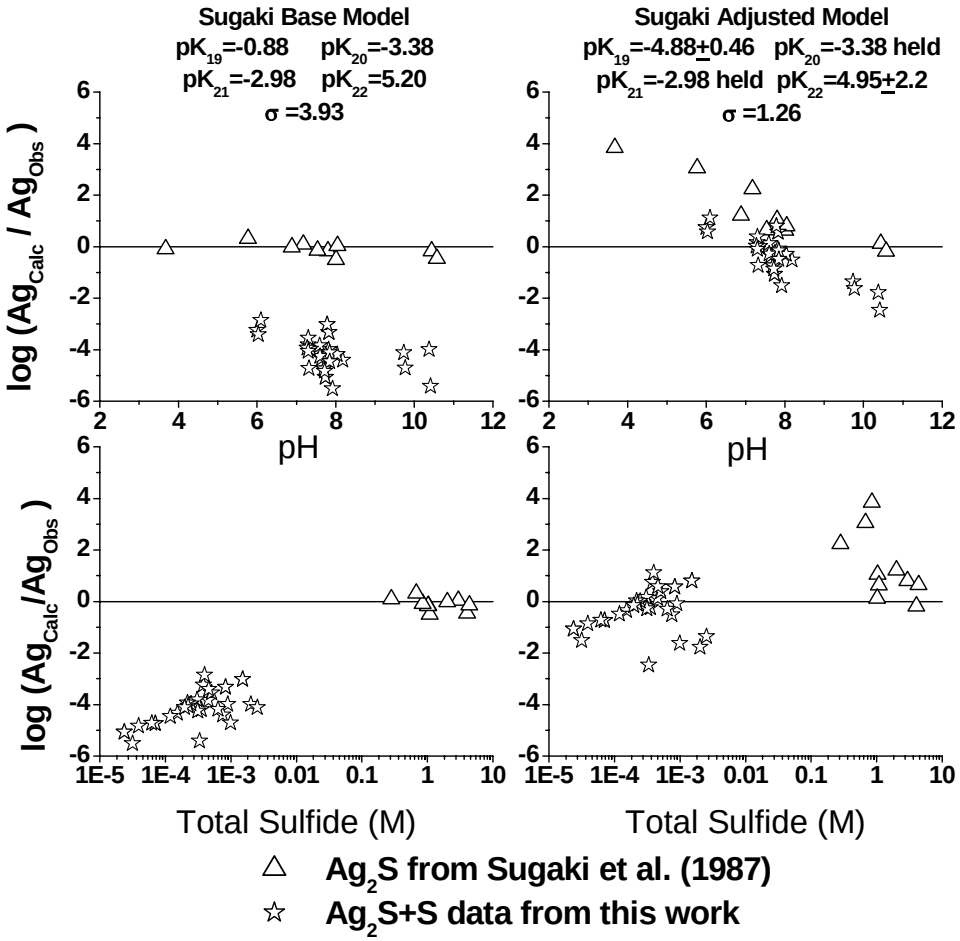

Figure 32. Fit of the silver sulfide data in sulfidic solutions with three coordinate species. The pK's refer to the reactions in the text. If any pK is not listed in the figure, the reaction corresponding to the pK was not included in the model.

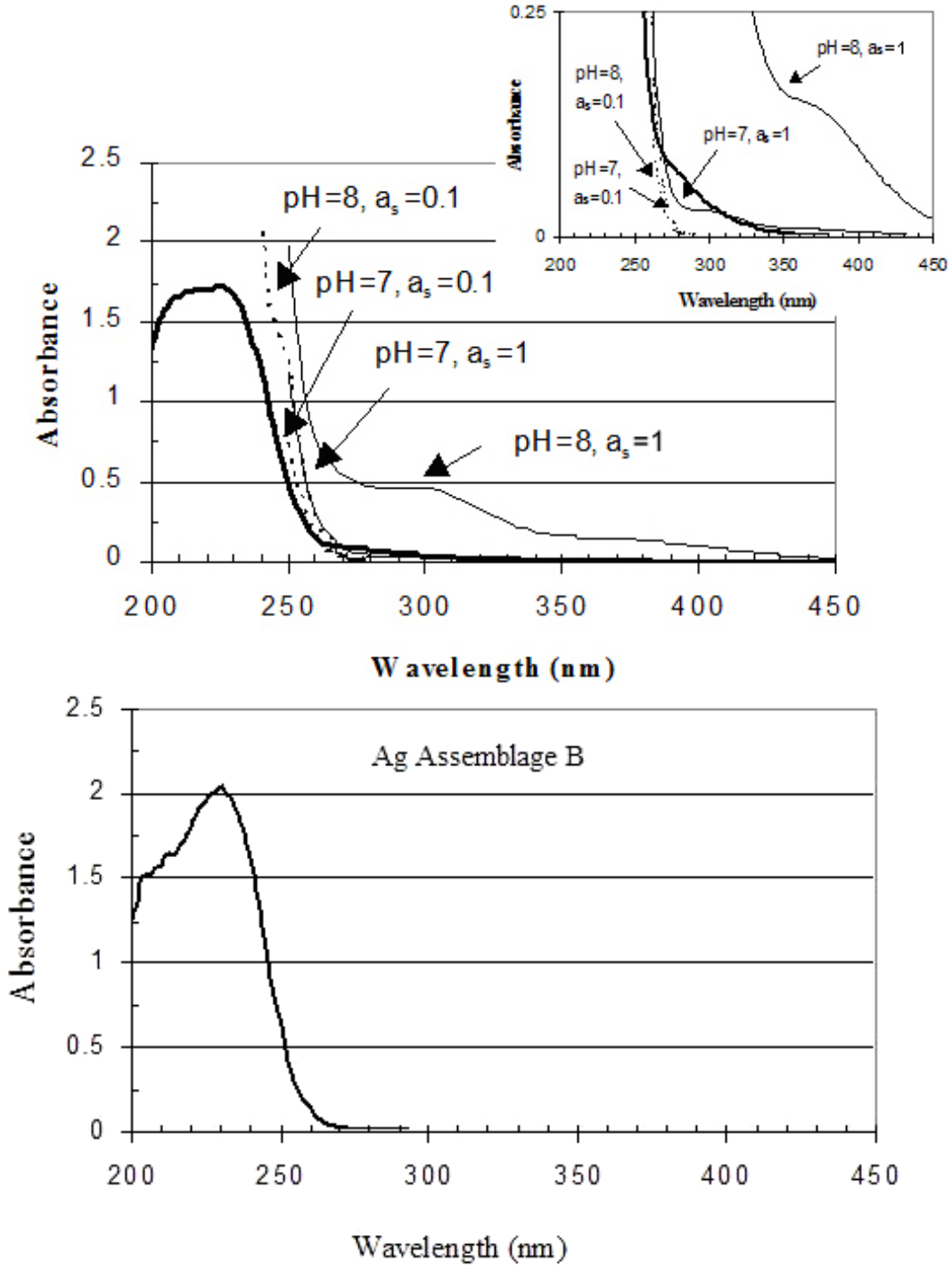

Figure 33. UV-Visible Spectra of Top: Ag assemblage A (pH= 7.30, 0.316 mM Total Sulfide, 0.185 μM Ag, 0.161 mM As); Thin solid and dotted lines represent calculated polysulfide spectra Bottom: Ag assemblage B (pH=7.25, 0.834 mM Total Sulfide, 0.198 μM Ag, 0.0926 mM As).

are present in solution. Polysulfides, S_5^{2-} and S_4^{2-}, are the dominant optical absorbers between 500 nm and approximately 300 nm. (Chen and Morris, 1972; Giggenbach, 1974). Calculated spectra of polysulfide absorption is shown in Figure 33 at two pH's (dotted (a_S=0.1) and thin solid (a_S=1) lines). Spectra were calculated assuming an a_S=0.1. A spectra was also calculated assuming an a_S=1, this value represents a system saturated with sulfur. There is no evidence of polysulfide formation in the Ag assemblage B spectrum, because there is no sample absorbance where the polysulfides were calculated to absorb. There is also no evidence of polysulfide formation in the Ag assemblage A spectrum because the calculated polysulfide absorbancies do not match the sample absorbance (thick black line) in Figure 33. The small amount of absorbance at 300 nm in the Ag assemblage A spectra could be from As species; See Appendix I).

II.D.2.2.2. Silver Speciation in Sulfidic Solutions Equilibrated with Ag Assemblage A and Ag Assemblage B

The data from experiments containing Ag assemblage A and B equilibrated with sulfidic solutions were added to the model that explained the solubility of Ag_2S and S. A list of the Ag assemblage B and Ag assemblage A samples used in the modeling are given in Table 32 and Table 31. The ionic strength of the samples varied between 0.0101 and 0.011 M.

Because elemental sulfur was absent in Ag assemblage A and B experiments, any enhancement in Ag solubility can not be attributed to Ag-polysulfide species. Also sodium sulfate was used to control ionic strength in Ag assemblage B and Ag

assemblage A experiments, so there should be no Ag enhancement due to $Ag(Cl)(HS)^-$ species. However, these two species were included in the models to confirm the assumptions using the following models.

The first model tried on this set of data was the best-fit model from the Ag_2S+S data, which included AgHS, $Ag(HS)_2^-$, $Ag_2S(HS)_2^{2-}$, $Ag(Cl)(HS)^-$, and AgS_x^-. This model is shown as the Base Model in Figure 34. The observed silver concentrations of Ag assemblage A and B samples were at least an order of magnitude more soluble than the Ag_2S+S samples, which is shown in Figure 34. This implies that the silver solubility is enhanced in the presence of arsenic. The difference between the calculated and observed values is greatest at low total sulfide.

Next, the base model was adjusted by letting the SCIENTIST program vary the equilibrium constants for Ag(HS), AgS_x^- and $Ag(Cl)(HS)^-$. The equilibrium constants for $Ag(HS)_2^-$ and $Ag_2S(HS)_2^{2-}$ were not varied because they became insignificant in the model. The fit of the Adjusted Base Model shown in Figure 34, shows a trend with pH and total sulfide, so additional species are needed to account for the extra solubility of silver when arsenic is present in the sample.

Clearly the first species to try to fit this model is the silver thioarsenite species, AgAsS(HS)(OH)°. The New Ag-As-S Model includes the addition of $AgAsS(HS)(OH)^o$ to $Ag(HS)_2^-$, $Ag_2S(HS)_2^-$, Ag(HS), $Ag(Cl)(HS)^-$ and AgS_x^- and is shown in Figure 34. The new species can be expressed by the following reaction:

$$0.5Ag_2S + AsS(HS)(OH)^- + 0.5H^+ \Leftrightarrow AgAsS(HS)(OH)^o + 0.5HS^- \quad (23)$$

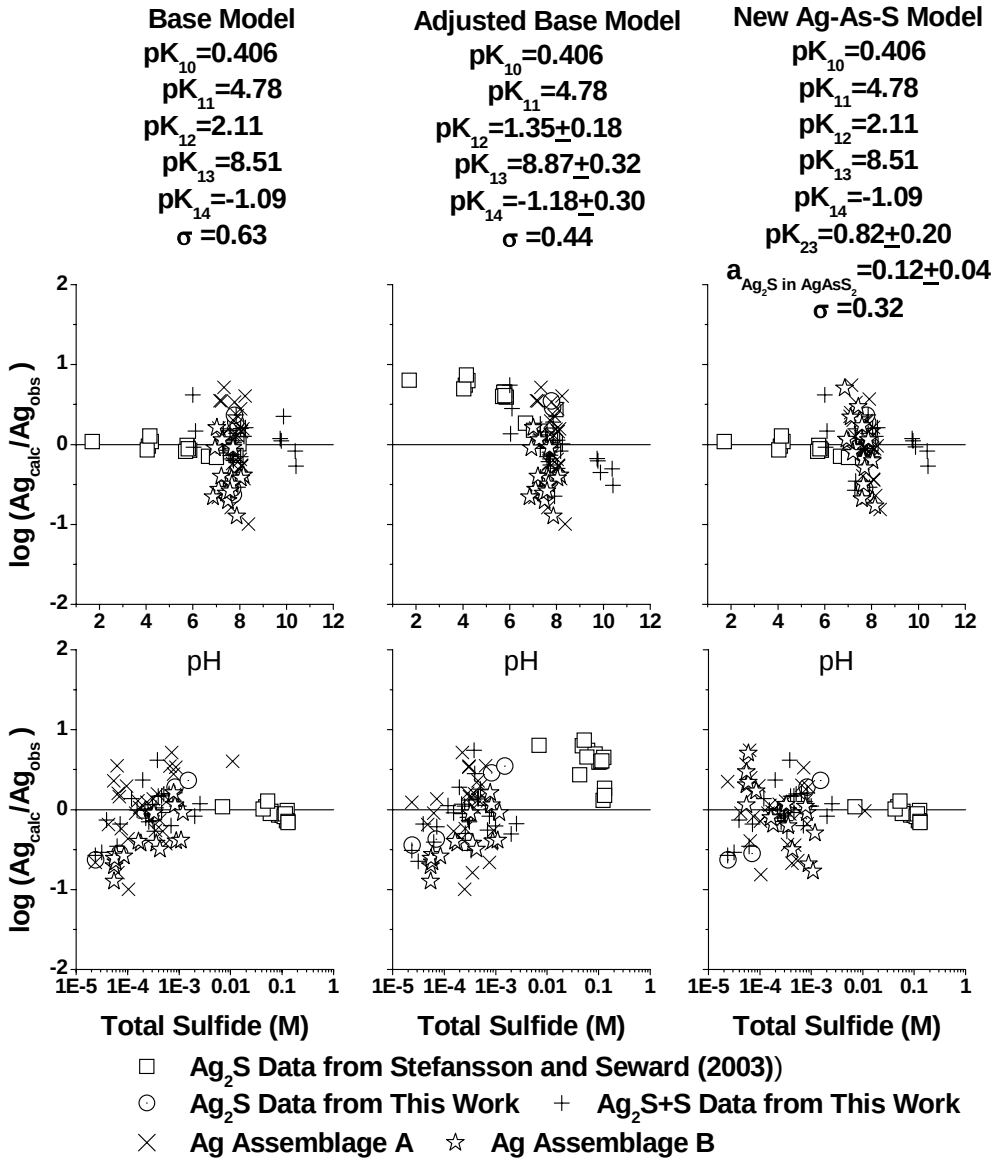

Figure 34. Fit of the Ag assemblage (A and B) data in sulfidic solutions. The pK's refer to the reactions in the text. If any pK is not listed in the figure, the reaction corresponding to the pK was not included in the model. Assume a_S is negligible and $[Cl^-]$ is zero in Ag assemblage experiments (pK_{13} and pk_{14} to low to have any effect in New Ag-As-S Model).

In Ag assemblage B experiments acanthite is present in the reaction and its activity is equal to 1. In Ag assemblage A experiments the initial reaction can be expressed as:

$$0.5Ag_3AsS_3 + AsS(HS)(OH)^- + 0.5H^+ \Leftrightarrow$$

$$AgAsS(HS)(OH)^o + 0.5HS^- + 0.5AgAsS_2 \quad (24)$$

Proustite decomposes to acanthite and trechmannite, so the final reaction would be the same reaction for Ag assemblage B experiments, which is Reaction 23. But, the activity of Ag_2S in Ag assemblage A experiments would be less than one because the system is undersaturated with respect to acanthite. Figure 34 shows the New As-Ag-S Model, where the calculated equilibrium constant is $pK_{23}=0.82\pm0.20$ and the activity of Ag_2S in Ag assemblage A experiments was calculated to be 0.12 ± 0.04. The other equilibrium constants were held constant. The model has a good fit to the data and no trends are observed. A comparison can be made between the calculated activity of Ag_2S from modeling and the activity of Ag_2S using the free energies of formation of acanthite, trechmannite (Hall, 1966) and proustite (Hall, 1966, located in Table 35). The activity of acanthite calculated from the free energy of formation values is 0.01 ± 0.04. There is a difference between the calculated activity of Ag_2S from the New As-Ag-S Model and the derived activity from the free energies. This may be one instance were there is an inconsistency in Hall's estimation of the free energy of formation of trechmannite and proustite that would produce a lower activity of acanthite than observed in experiments.

There is strong evidence that the solubility of silver is increased in the presence of arsenic in Ag assemblage A and B experiments and the extra solubility can be attributed to one species, $AgAsS(HS)(OH)^o$.

A reaction between Ag^+ and $AsS(HS)(OH)^-$ can be obtained by combining Reaction 23 with the solubility product of silver sulfide which can be represented by:

$$Ag^+ + 0.5HS^- \Leftrightarrow 0.5Ag_2S + 0.5H^+ \qquad pK_{25}=-17.99 \quad (25)$$

$$0.5Ag_2S + AsS(HS)(OH)^- + 0.5H^+ \Leftrightarrow AgAsS(HS)(OH)^o + 0.5HS^- \quad pK=0.82 \quad (23)$$

$$Ag^+ + AsS(HS)(OH)^- \Leftrightarrow AgAsS(HS)(OH)^o \quad pK=-17.17\pm0.20 \quad (26)$$

Stefansson and Seward (2003) provide a value for pK_{25}. Using the calculated pK for reaction 23 provides the equilibrium constant for Reaction 26, where pK_{26} is calculated to be –17.17±0.20. This indicates that the Ag-thioarsenite reaction is very strong and is comparable to the analogous reaction with Cu^+, where the pK was calculated to be -19.82±0.17 (Clarke and Helz, 2000). In fact, the calculated stability (Cu>Ag) is in agreement with the predictions from Tossell (2000).

II.D.2.2.3. Proposed Structure for $AgAsS(HS)(OH)^o$ and Silver Speciation Diagram

A potential structure of the AgAsS(HS)(OH)° complex is shown in Figure 35 (Tossell, 2000). The structure is preliminary, but it appears as though the arsenic is bound to a hydroxide molecule, which seems unusual for a sulfidic solution. The hydroxide molecule was taken out of the AgAsS(HS)(OH)° complex and the new species was modeled. The standard deviation of the fit was unsatisfactory, so it appears as though the hydroxide molecule is needed in the complex. In this structure

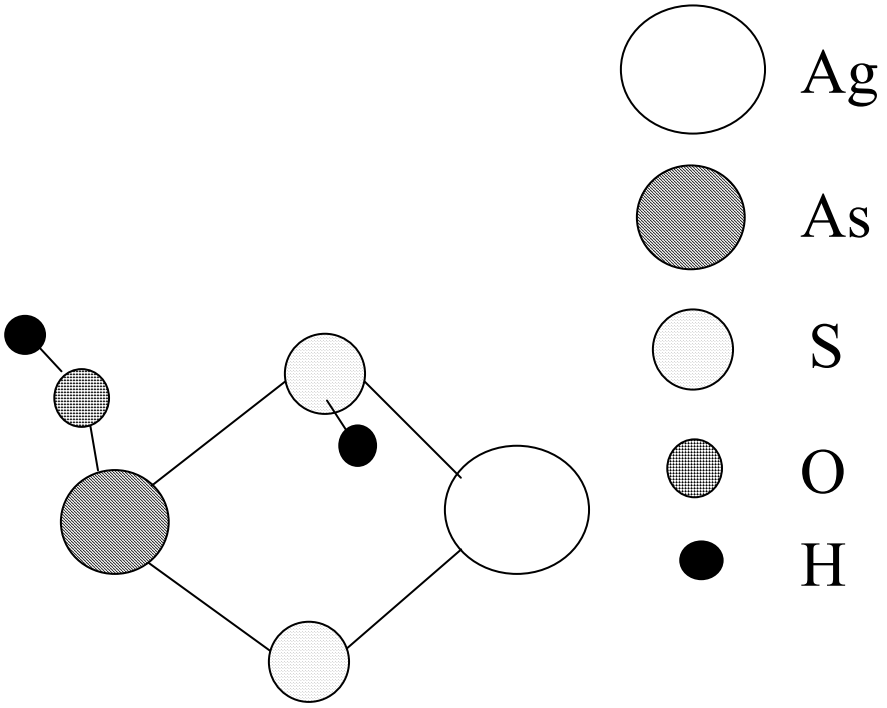

Figure 35. Proposed structure of AgAsS(HS)(OH)° from Tossell (2000).

Ag is bound to two atoms and As is bound to three atoms, which are their preferred number of bonds.

Using the best-fit model a speciation diagram of the Ag-As-S system is shown in Figure 36. Under seawater conditions for Cl^-, $\Sigma Cl^-=10^{-1}$, $\Sigma HS^-=10^{-3}$ $\Sigma As^{3+}=10^{-5}$ and $\Sigma Ag^+=10^{-7}$, Figure 36 shows that $AgAsS(HS)(OH)^o$ is negligible and the dominant species is $Ag(Cl)(HS)^-$. However, under natural groundwater conditions for Cl^-, $\Sigma Cl^-=10^{-3}$, $\Sigma HS^-=10^{-3}$ $\Sigma As^{3+}=10^{-5}$ and $\Sigma Ag^+=10^{-7}$, the $AgAsS(HS)(OH)^o$ complex becomes dominant between a pH of 5 to 7.5. These conditions could be found in landfills or contaminated sediment and the model predicts that the $AgAsS(HS)(OH)^o$ complex is dominant and thus become mobile.

II.D.2.3. Speciation of Lead and Mercury in Sulfidic Solutions Equilibrated with $PbS+As_2S_3+S$ or $Hg+As_2S_3+S$

II.D.2.3.1. Speciation of Mercury in Sulfidic Solutions Equilibrated with $HgS+As_2S_3+S$

The mercury data from the $HgS+As_2S_3+S$ experiment were modeled using Scientist (Micromath, Inc.). The mercury fitting program are in Appendix IV. The modeling procedure was discussed in Section II B.4.1. The data are in Table 28 and the ionic strength of the samples varied between 0.0101 - 0.0110 M.

The first step in the modeling procedure is to chose a base model, which must contain species that have been proposed in the literature to explain HgS only and

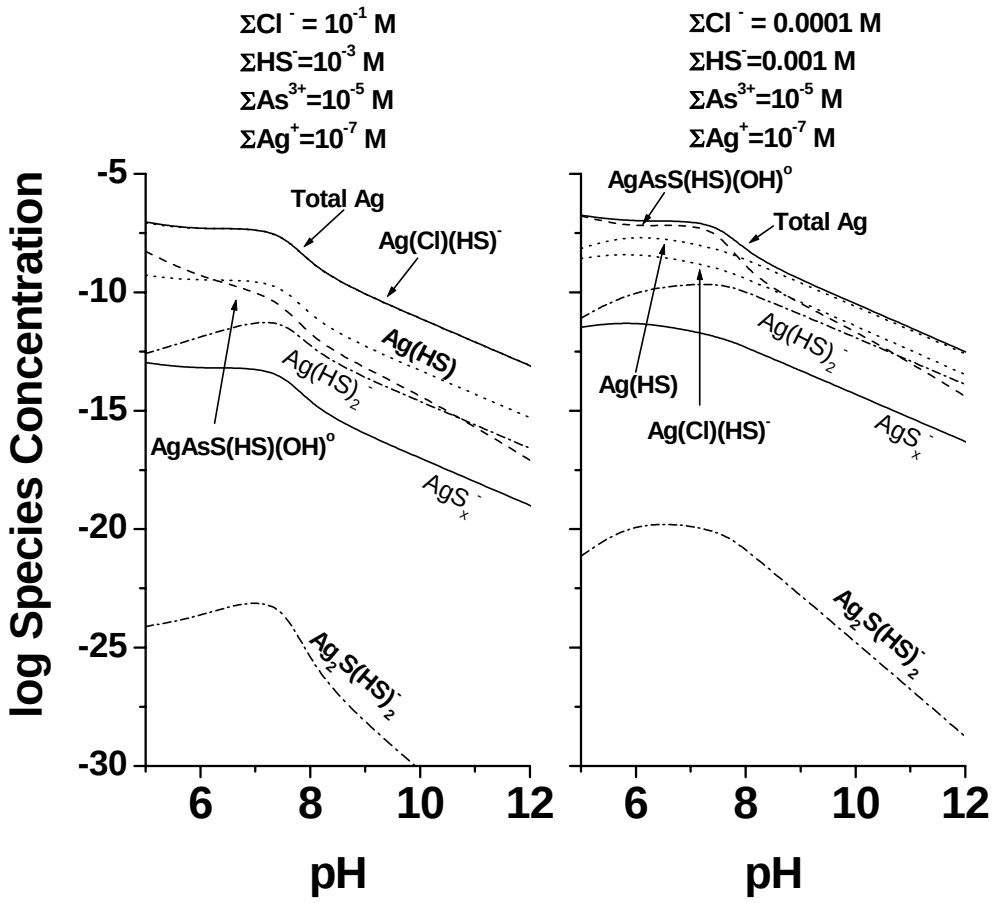

Figure 36. Silver speciation diagram for the equilibration of Ag assemblage A and Ag assemblage B in solutions containing 10^{-3} M total sulfide, 10^{-5} M total arsenic, 10^{-7} M total silver and Right:10^{-1} M Cl^- and Left:10^{-3} M Cl^-. Assumes system is undersaturated in a_S relation to $AgAsS(HS)(OH)^o$.

HgS and elemental sulfur solubility. The Paquette model was chosen as the base model and included the following Hg species:

$$HgS\ (cinn) + H_2S\ (aq) \Leftrightarrow Hg(SH)_2 \quad (27)$$

$$HgS\ (cinn) + HS^- \Leftrightarrow HgS(SH)^- \quad (28)$$

$$HgS\ (cinn) + 2HS^- \Leftrightarrow HgS_2^{2-} + H_2S \quad (29)$$

$$HgS + (x\text{-}1)S^0 + HS^- \Leftrightarrow Hg(S_x)HS^- \quad (30)$$

Equilibrium constants were taken from Paquette and Helz (1997). Figure 37 shows the Paquette Base Model and the Adjusted Paquette Base Model for the mercury solubility in the $HgS+As_2S_3+S$ experiments. The Paquette Base Model shows that there is less observed solubility in this experiment with pH and total sulfide, implying that Paquette's model calculated more mercury solubility than observed in these experiments. To account for the observed solubility the equilibrium constants were allowed to vary using the least squares fitting routine. The Adjusted Paquette Base Model brought the residuals closer to zero without changing the equilibrium constants substantially. Since the two models equilibrium constants lie within uncertainty of each other, the Paquette Model also explains the mercury solubility of the $HgS+As_2S_3+S$ system in this work. This implies that the solubility of mercury is not enhanced when arsenic is present in solution and that the formation of a mercury-thioarsenite complex is negligible.

Jay et al. (2000) conducted experiments with HgS and S^o in sulfidic solutions (data in Appendix IV), but attributed the mercury solubility to the mercury species proposed by Paquette and Helz (1997), $Hg(SH)_2$, $HgS(SH)^-$, HgS_2^{2-} in addition to:

$$HgS + HS^- + 2(x\text{-}1)S^o \Leftrightarrow Hg(S_x)_2^{2-} + H^+ \quad (31)$$

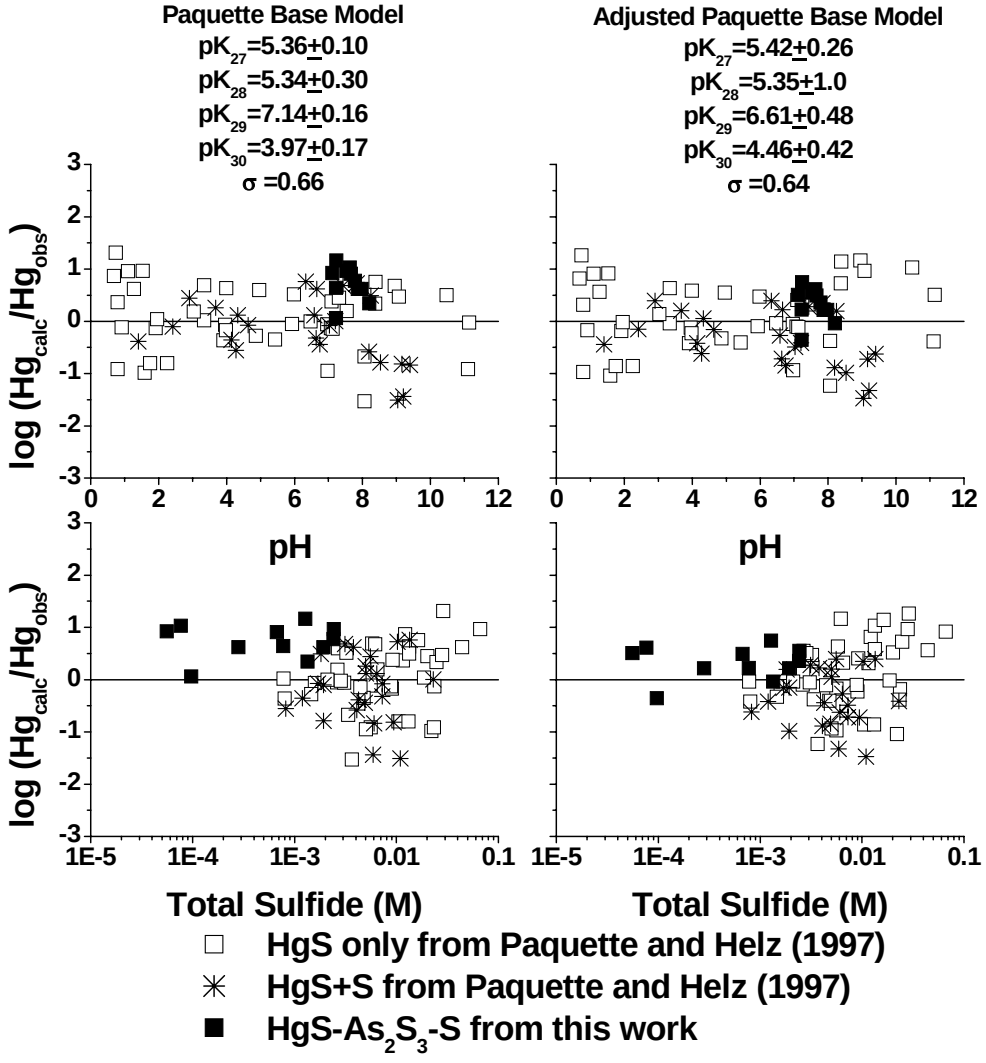

Figure 37. Paquette Base Model and Adjusted Paquette Base Model for Hg Speciation for HgS+As_2S_3+S Experiments in a Sulfidic Solution. The pK's refer to the reactions in the text. If any pK is not listed in the figure, the reaction corresponding to the pK was not included in the model. Paquette Data in Appendix IV.

$$HgS + H_2O + (x-1)S^o \Leftrightarrow Hg(S_x)OH^- + H^+ \quad (32)$$

$$HgS \Leftrightarrow HgS^o \quad (33)$$

Equilibrium constants were taken from Jay et al. (2000). It should be noted that Jay et al. (2000) used data from Paquette and Helz to model their mercury data. Figure 38 shows the Jay Base Model, which includes Reactions 27, 28, 29 31, 32 and 33. Using the Jay Base Model still produced mercury solubilities that were higher than the observed values, but this model has slightly better fit to the data when compared to the Paquette Model. However, the same conclusion is reached using the Jay Base Model, that the formation of a mercury-thioarsenite complex is negligible.

The Paquette model was chosen to estimate an upper limit on K for a Hg-thioarsenite complex. The Paquette model was chosen because there was more data used in the model, which could lead to a more accurate value of the equilibrium constant. The formation of a Hg-thioarsenite complex can be represented by:

$$HgS + AsS(HS)(OH)^- + H^+ \Leftrightarrow HgAsS(HS)(OH)^+ + HS^- \quad (34)$$

It was assumed that a K for the Hg-thioarsenite complex must be smaller than the value that increases the standard deviation of the Adjusted Paquette Base Model by 5%. The upper limit for the equilibrium constant of Hg-thioarsenite was calculated to be $1x10^{-4}$ (pK=4).

Even though the formation of a Hg-thioarsenite complex is negligible there is one concern. If a ternary phase formed in the $HgS+As_2S_3+S$ system, then the solubility of the Hg would be reduced because of the lower solubility of the HgS component in the ternary phase. However, a literature search did not provide any

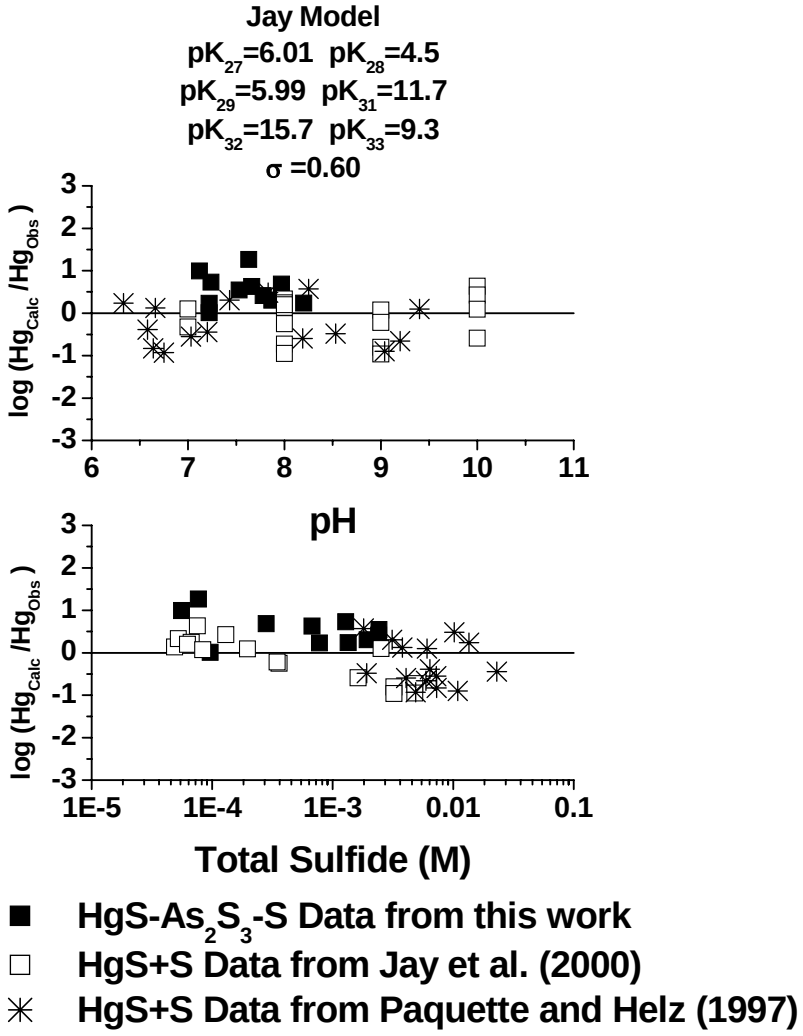

Figure 38. Jay Base Model for Hg Speciation in $HgS+As_2S_3+S$ equilibrated in a sulfidic solution. The pK's refer to the reactions in the text. If any pK is not listed in the figure, the reaction corresponding to the pK was not included in the model. Jay et al. (2000) data in Appendix IV.

references to a ternary phase involving the As-Hg-S system and the x-ray diffraction pattern did not have any peaks that were unaccounted.

II.D.2.3.2. Speciation of Pb in Sulfidic Solutions Equilibrated with $PbS+As_2S_3+S$

The speciation of lead could not be determined in these experiments because the lead concentrations were below the detection limit for graphite furnace analysis (shown in Figure 19). There could be some enhancement in the lead solubility, but no measurement could be obtained. Therefore, thioarsenite complexing of lead may occur but it is too weak to raise the lead solubility above the $9.6x10^{-9}$ M detection limit. This implies that the formation of a lead-thioarsenite complex is negligible.

II.D.3. Critical Evaluation of Work

At this point it is always necessary to offer a critical review of the work. The first concern is that the solid phases have been properly identified and that the solutions were equilibrating with these phases. By inspecting the solids with EDS the proustite experiments contained three phases. Ag_2S and Ag_7AsS_6 were present in the bulk of the material, while Ag_3AsS_3 was present to a lesser extent and was enclosed in Ag_2S particles.

The trechmannite experiments seemed to be equilibrating with a meatastable phase. This is indicated by EDS and X-Ray diffraction measurements that identify three components in the Ag_2S-As_2S_3 binary system. However, the As_2S_3 component seems to be inert in the system, which is indicated by the low activity of As_2S_3 that

was calculated in the As speciation model. Because the system was equilibrated with a metastable phase the ΔG_f^o of trechmannite could not be calculated.

Sulfur is also a critical component and was used to determine if polysulfide species were of any importance in metal speciation. Assemblages equilibrated with sulfur were given an a_S=1, meaning sulfur was in excess. Visual inspection of the samples before filtration revealed that sulfur was indeed present after equilibrium had been reached.

Chloride also turned out to be a critical component in Ag_2S+S experiments. The $Ag(Cl)(HS)^-$ species has never been identified before, so this species must be questioned. However, this species is essential to Ag speciation and is shown to be necessary in Figure 26. However, if this species turned out to be insignificant, the Ag-As-S model would not be affected because no chloride was used in these experiments.

II.E. Conclusions

Experiments provided arsenic speciation information for the As_2S_3-S system. The dominant arsenic species was $AsS(HS)(OH)^-$, other important species included $As(OH)_3$ and $H_2As_3S_6^-$. Arsenic polysulfide species were not found to be important in this system. Natural waters can contain >$1x10^{-4}$ M levels of polysulfides, concentrations in this work ranged from $2x10^{-4}$ M to $1x10^{-5}$ M. Natural waters do not contain a much larger concentration of polysulfides and As-polysulfide species would not likely form in natural waters. Table 37 reviews the reactions and equilibrium constants utilized and calculated for the last two chapters.

The same arsenic speciation model used to explain the solubility of orpiment alone can be used without modification to explain solubilities of orpiment in experiments in equilibrium with sulfur, cinnabar and galena. With modification of a singe parameter, the activity of As_2S_3, this model can also explain As solubilities in equilibrium with amorphous As_2S_3, Ag assemblage A and Ag assemblage B.

In contrast, the model from Stefansson and Seward (2003) that explains the solubility of acanthite had to be enhanced with additional species: $Ag(Cl)(HS)^-$ to explain the effect of Cl^-, AgS_x^- to explain the effect of polysulfide and AgAsS(HS)(OH)° to explain the effect of thioarsenites.

A reaction between Ag^+ and $AsS(HS)(OH)^-$ forming $AgAsS(HS)(OH)^o$ was obtained and the pK is –17.17±0.20. This indicates that the Ag-thioarsenite reaction is very strong and is comparable to the analogous reaction with Cu^+, where the pK was calculated to be -19.82±0.17 (Clarke and Helz, 2000). The calculated stability (Cu>Ag) is in agreement with the predictions from Tossell (2000).

There could have been some enhancement in lead solubility in these experiments, but the lead solubility was below the $9.6x10^{-9}$ M detection limit of the graphite furnace. The solubility of the $HgS+As_2S_3+S$ system was compared to literature data of the HgS-S system. There was no significant difference between the solubility of mercury in the two systems. Therefore, Hg-thioarsenite and Pb-thioarsenite complexes are negligible at thioarsenite concentrations up to 0.1 mM at near-neutral pH's.

The formation of a metal thioarsenite depends on the HS^- and thioarsenite concentration found in the system. Natural freshwaters have a typical arsenic

concentration of $1.9x10^{-8}$M (Cullen and Reimer, 1989; Cutter, 1992). Experiments conducted in this work would represent concentrations of thioarsenite that are above those found in freshwater systems and it is therefore unlikely that Pb and Hg thioarsenite complexes would form in nature. The formation of the metal-thioarsenite complexes is also dependent on $[HS^-]$, where the complex could be enhanced in highly sulfidic systems.

Table 37. Solubility Reactions Used in Chapters II.

Reaction	$pK_{This\ Work}$	$pK_{Literature}$ (Source)
As		
$0.5As_2S_{3(crys)} + H_2O + 0.5H_2S \Leftrightarrow AsS(HS)(OH)^- + H^+$	8.7±0.1	9.12±0.32 (1)
$1.5As_2S_{3(crys)} + 1.5H_2S \Leftrightarrow H_2As_3S_6^- + H^+$	6.2±0.8	6.91±0.09 (3)
$1.5As_2S_{3\ (amorp)} + 1.5H_2S \Leftrightarrow H_2As_3S_6^- + H^+$	-	5.0±0.3 (2)
$0.5As_2S_{3(crys)} + 3H_2O \Leftrightarrow As(OH)_3 + 1.5H_2S$	-	12.60±0.11 (3)
$0.5As_2S_{3(crys)} + 3H_2O \Leftrightarrow As(OH)_3 + 1.5H_2S$	-	12.58 (4)
$0.5As_2S_{3(amorp)} + 3H_2O \Leftrightarrow As(OH)_3 + 1.5H_2S$	-	11.90±0.3 (2)
Hg		
$HgS_{(cinn)} + H_2S\ (aq) \Leftrightarrow Hg(SH)_2$	5.4±0.3	5.35±0.10 (5)
$HgS_{(cinn)} + HS^- \Leftrightarrow HgS(SH)^-$	5±1	5.34±0.30 (5)
$HgS_{(cinn)} + 2HS^- \Leftrightarrow HgS_2^{2-} + H_2S$	6.6±0.5	7.14±0.16 (5)
$HgS_{(cinn)} + (x-1)S^0 + HS^- \Leftrightarrow Hg(S_x)HS^-$	4.5±0.4	3.97±0.17 (5)
Ag		
$0.5Ag_2S_{(acan)} + 1.5\ HS^- + 0.5\ H^+ \Leftrightarrow Ag(HS)_2^-$	0.41±0.41	0.466±0.07 (6)
$0.5Ag_2S_{(acan)} + 0.5\ HS^- + 0.5\ H^+ \Leftrightarrow Ag(HS)$	2.1±0.2	2.12±0.04 (6)
$0.5Ag_2S_{(acan)} + Cl^- + 0.5\ HS^- + 0.5\ H^+ \Leftrightarrow Ag(Cl)(HS)^-$	-1.1±0.2	-
$0.5Ag_2S_{(acan)} + (x-1)S° + 0.5\ HS^- \Leftrightarrow AgS_x^- + 0.5\ H^+$	8.5±0.2	-
$0.5Ag_2S_{(acan)} + AsS(HS)(OH)^- + 0.5H^+ \Leftrightarrow AgAsS(HS)(OH)^o + 0.5HS^-$	0.8±0.2	-
$Ag_2S_{(acan)} + 2\ HS^- \Leftrightarrow Ag_2S(HS)_2^{2-}$	-	4.78±0.04 (6)
$Ag^+ + 0.5HS^- \Leftrightarrow 0.5Ag_2S + 0.5H^+$	-	-17.99 (6)
$Ag^+ + AsS(HS)(OH)^- \Leftrightarrow AgAsS(HS)(OH)^o$	-17.2±0.2	-
Miscellaneous		
$H_2S \Leftrightarrow HS^- + H^+$	-	7.01 (7)

1. Clarke and Helz (2000); pK value corrected to crystalline orpiment value using activity of orpiment from Eary's amorphous material calculated in this work. Original reaction had activity of orpiment with respect to Eary's amorphous material. 2. Eary (1992), 3. Webster (1990), 4. Nordstrom and Archer (2003), 5. Paquette and Helz (1997), 6. Stefansson and Seward (2003), 7. Ellis and Milestone (1967)

Chapter III. The Solubility of As_2O_3 in Carbonate Solutions

III.A. Introduction

The elevated arsenic concentrations in groundwater throughout certain regions of the world, including Bangladesh, Vietnam and India threaten the health of millions of people. In these regions groundwater has low dissolved oxygen concentrations, low redox potentials and is thus under reducing conditions (Kim et al., 2000; Appelo et al., 2002; Battacharya et al., 2002). The groundwater also tends to have a high alkalinity and elevated concentrations of dissolved iron, manganese and As(III) (Kim et al., 2000). The concentration of total arsenic can reach mg/L levels, whereas the maximum contamination level (MCL) for arsenic in drinking water for the United States is 10 μg/L (Environmental Protection Agency, 2001). The elevated arsenic concentrations pose a serious health concern to many individuals who drink the groundwater. Identification of the chemical and geological processes that give rise to the elevated levels might lead to reduction in the risk of arsenic related diseases to many people.

Causes for the elevated arsenic levels have been a source of controversy. Two accepted theories, pyrite oxidation and iron oxide reduction, have been presented in previous chapters of this work. However, some new interpretations of the elevated arsenic concentrations in groundwater have recently emerged. Appelo et al. (2002) attribute the high arsenic concentrations to the displacement of arsenic by dissolved carbonate on ferrihydrite ($Fe(OH)_3$). Kim et al. (2000) attributed the elevated arsenic concentrations in groundwater to the formation of stable arseno-carbonate complexes.

Kim et al. (2000) have shown that the bicarbonate concentration is highly correlated with the release of arsenic from Marshall Sandstone, which contains arsenic-rich pyrite and arsenic sulfides. They proposed that arsenic sulfides interact with bicarbonate and are responsible for elevated arsenic concentrations in groundwater through the production of arsenic carbonate complexes. They further propose large stability constants for the complexes and state that "according to these estimates, which need to be confirmed experimentally, the carbonate complexes may be the most stable inorganic arsenic species in the aquatic environment." Their experiments using ion chromatography produced evidence of arseno-carbonate complexes and likely species include: $As(CO_3)_2^-$, $As(CO_3)(OH)_2^-$ and $As(CO_3)^+$. The reactions can be written as:

$$As(OH)_3 + 2HCO_3^- + H^+ \rightarrow As(CO_3)_2^- + 3H_2O \quad (1)$$

$$As(OH)_3 + HCO_3^- + 2H^+ \rightarrow As(CO_3)^+ + 3H_2O \quad (2)$$

$$As(OH)_3 + HCO_3^- \rightarrow As(OH)_2(CO_3)^- + H_2O \quad (3)$$

Tossell (2004) has conducted quantum mechanical calculations to study the stability of arsenite carbonate complexes. He used Hartree Fock (HF) and Moller-Plessett many body perturbation theory 2nd order (MP2) to calculate the stability of various arsenite carbonate complexes, which included $As(CO_3)^+$, $As(OH)_2(CO_3)^-$ and $As(OH)_2(CO_3)Na$. He found that the $As(OH)_2(CO_3)Na$ complex was the most stable complex through a condensation reaction, but the $As(OH)_2(CO_3)^-$ complex was also found to be stable. These results seem to support the evidence of one of the species predicted by Kim et al. (2000), but challenge the existence of the other two. Tossell favors species in which the arsenic is bound to bicarbonate through one oxygen from

the bicarbonate, rather than being bound maximally with two oxygens from the bicarbonate.

Tossell (2004) also calculated the IR and Raman spectra for the $As(OH)_2(CO_3)Na(OH_2)_2$ complex using the hydrated ion-pair model with HF and MP2. Pokrovski et al. (1996) characterized arsenite bands using Raman Spectroscopy at 700 cm^{-1} and a depolarized shoulder at approximately 650 cm^{-1} associated with the symmetric and asymmetric stretching of $As(OH)_3$. As $As(OH)_3$ is deprotonated there are three strong Raman bands, which are attributed to $AsO(OH)_2^-$ (Loehr and Plane, 1968; Goldberg and Johnston, 2001).

In this chapter, the solubility of As_2O_3 in the presence of HCO_3^- and Cl^- will be determined. Raman Spectroscopy will be also be used to examine the effect bicarbonate has on arsenic solubility.

III.B. Methodology

III.B.1. Materials

III.B.1.1. Recrystallization and Characterization of As_2O_3

Arsenic trioxide powder (As_2O_3) (J. T. Baker, Primary standard) was recrystallized in deionized water through the following procedure: 210 grams of arsenic trioxide powder was placed in deionized water so approximately one third would dissolve at 100°C. The As_2O_3 was cycled four times between room temperature and boiling, water was added to replace any water lost after the solution slowly cooled, which permitted the dissolution of small particles and the precipitation of larger As_2O_3 particles. After the final cooling the solution was

stirred and left to settle overnight. The particles still suspended in the solution were decanted and discarded. The remaining As_2O_3 was filtered and allowed to air dry. The recrystallized As_2O_3 appeared to be a course powder when compared to the very fine starting material. Experiments were conducted with two different compositions of As_2O_3 starting materials, even though the same procedure was followed to synthesize both. The x-ray diffraction pattern of the recrystallized As_2O_3 from runs 3 and 4 is shown in Figure 39, where the starting material is arsenolite.

The recrystallized As_2O_3 used in Runs 1 and 2 was synthesized at a later time than Runs 3 and 4. The same procedure stated above was utilized in the recrystallization of As_2O_3 for Runs 1 and 2. Claudetite was found in Runs 1 and 2, specifically in the reacted material from Run 2. Possible explanations could be that the material had an impurity that could stabilize claudetite over arsenolite. However, an impurity does not seem likely because the As_2O_3 starting material had a purity of 100%±0.05. A more likely cause could have been the formation of a metastable state. Runs 1 and 2 were conducted twice. In the first trial there was rapid evaporation that could have produced sufficient supersaturation to precipitate a metastable solid phase. The reacted material from the first trial was then washed with deionized water, dried and used in the second trial of Runs 1 and 2, where there was much less evaporation. Figure 40 and Table 39 clearly shows arsenolite and claudetite, the monoclinic form of As_2O_3, in the reacted material from Run 2.

The free energies of arsenolite (cubic As_2O_3) and claudetite (monoclinic As_2O_3) are very similar. It is therefore difficult to determine the most stable phase of As_2O_3. Stranski et al. (1958) determined that claudetite is more soluble than

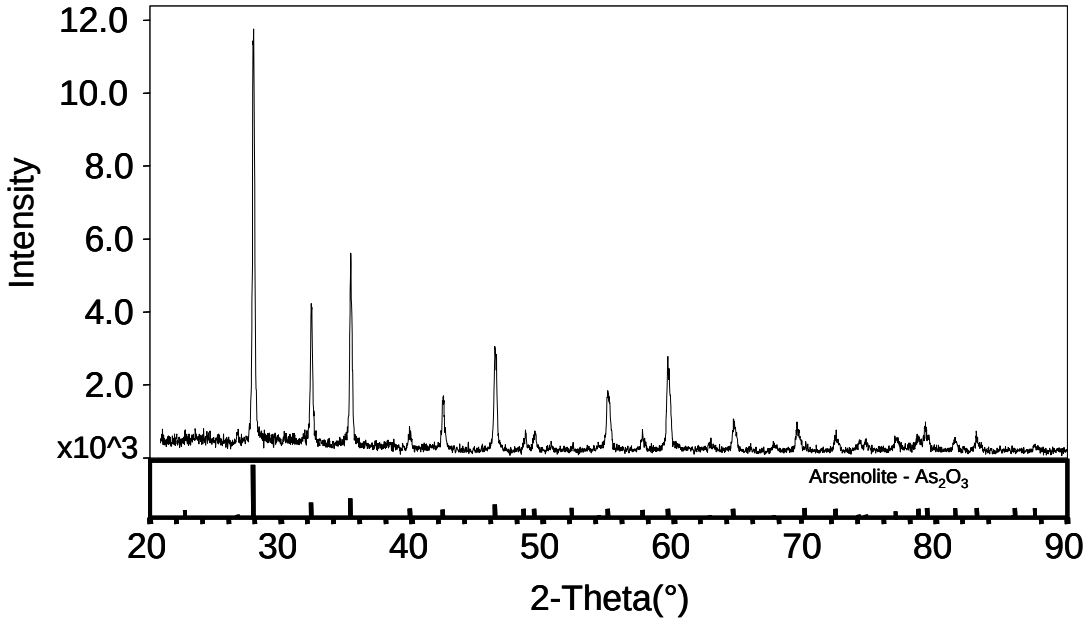

Figure 39. X-Ray power diffraction of recrystallized As_2O_3. Reference is arsenolite and is shown as solid lines under spectra. CuKα radiation, 1.54 Å.

Table 38. X-Ray Powder Diffraction of Recrystallized As_2O_3

Peak (2θ), *Intensity x10^3* (measured by hand)	Known Arsenolite Peak (2θ), *Intensity x10^3* (measured by hand)
28.00, *11.8*	28.00, *400.0*
32.67, *4.0*	32.33, *100.0*
35.19, *4.3*	35.29, *140.4*
42.67, *1.2*	42.67, *54.6*
46.33, 2.9	46.33, *56.6*
54.99, *1.8*	54.93, *62.4*
59.93, *2.7*	59.67, *62.4*

Diffraction pattern shown in Figure 39. Peaks given as 2-theta. The known peaks are from the JCPDS database

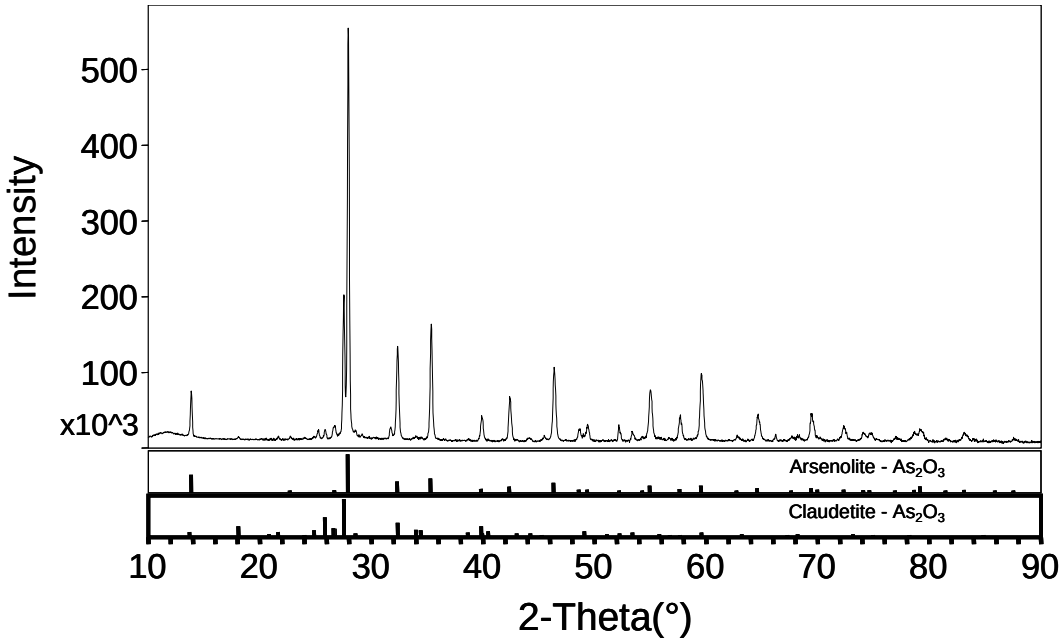

Figure 40. X-Ray diffraction pattern of reacted material from flask containing 0.355 m NaCl/0.357 m $NaHCO_3$ in a CO_2 atmosphere. References, arsenolite and claudetite, are shown below the spectra as solid lines. CuKα radiation, 1.54 Å.

Table 39. X-Ray Diffraction Pattern of the Reacted Material from the Flask Containing 0.355 m NaCl/0.357 m $NaHCO_3$ in a CO_2 Atmosphere.

Peak (2θ), *Intensity x10^3* (measured by hand)	Known Peak (2θ), *Intensity x10^3* (measured by hand)
13.83, *74.1*	ar 13.83, *179.4*; cl 13.67, *1.9*
25.83, *27.3*	cl 25.83, *100.0*
26.57, *37.4*	cl 26.55, *46.0*
27.47, *200.0*	cl 27.47, *200.0*
28.00, *554.6*	ar 28.00, *400.0*
32.67, *140.4*	ar 32.33, *100.0*; cl 32.34, *74.1*
35.19, *163.8*	ar 35.29, *140.4*
40.00, 46.0	cl 39.83, *54.5*; ar 39.83, *54.6*
42.67, *74.1*	ar 42.67, *54.6*
46.33, *109.2*	ar 46.33, *93.6*
53.40, *21.8*	cl 53.40, *21.8*
54.99, *78.0*	ar 54.93, *62.4*
59.93, *100.0*	ar 59.67, *62.4*; cl 59.67, *21.8*

Diffraction pattern shown in Figure 40. ar=arsenolite and cl=claudetite. Peaks given as 2-theta. The known peaks are from the JCPDS database

arsenolite at temperatures below 50°C and is therefore less stable. Pokrovski et al. (1996) found the opposite and postulated that claudetite is the more stable phase at any temperature. Archer and Nordstrom (2003) concluded that claudetite is the more stable phase by –0.19 kJ/mol. The formation of an arsenolite/claudetite phase seems to be dependent on some variable, possibly temperature, humidity or grain size of the material.

III.B.1.2. Gasses and Solutions of Runs

The control solutions (Runs 1 and 3) contained 0.710 m NaCl (J.T. Baker, A.C.S. Reagent) and were bubbled with nitrogen. The undersaturated solution (Run 4) contained 0.715 m $NaHCO_3$ (J.T. Baker, A.C.S. Reagent) and was bubbled under CO_2. Saturation with CO_2 was used to lower the pH of the system making $AsO(OH)_2^-$ negligible while enhancing the total dissolved arsenic-carbonate species. The oversaturated solution started at high pH and contained 0.351 m Na_2CO_3 (Fisher Scientific, A.C.S. Reagent), this solution was bubbled with N_2 for one day to dissolve arsenic into the solution. CO_2 was then bubbled into the solution for the remainder of the experiment forcing the dissolved arsenic to precipitate as it was acidified with CO_2 to a pH of approximately 7.7.

Runs 1 and 2 compared the arsenic solubility between a 0.710 m NaCl solution under a N_2 atmosphere and a 0.355 m NaCl/ 0.357 m $NaHCO_3$ solution saturated with CO_2, where both solutions had approximately the same pH. The pH of Run 1 (0.710 m NaCl) was adjusted with NaOH (J. T. Baker) to match closely the

pH of Run 2. The starting experimental conditions for the experiments are shown in Table 40.

Table 40. Experimental Conditions for the Equilibration of As_2O_3 for Control, Undersaturated and Oversaturated Solutions.

Solution	Solution Composition	$pH_{Initial}$	Gas Used
Control A (Run 1)	0.710 m NaCl	7.00	N_2
Undersaturated A (Run 2)	0.355 m NaCl/ 0.357 m $NaHCO_3$	7.15	CO_2
Control (Run 3)	0.710 m NaCl	5.75	N_2
Undersaturated (Run 4)	0.715 m $NaHCO_3$	8.18	CO_2
Oversaturated	0.351 m Na_2CO_3	11.51	$N_2 \rightarrow CO_2$

III.B.1.3. Analytical Reagents and Standardization

III.B.1.3.1. PAO

0.00564 N (0.00282 M) PAO, phenyl arsine oxide was obtained from Fisher Scientific.

III.B.1.3.2. PAO Standardization

0.7332 grams of $KH(IO_3)_2$, potassium bi-iodate, (Fisher Scientific) was dissolved in 1.00 L of deionized water. The $KH(IO_3)_2$ was diluted by 10, then 5.00 mL of the diluted standard was added to 195.00 mL of deionized water. 1.5 grams of KI was dissolved in the solution and 1.00 mL of pH 4 acetate buffer (0.082 M glacial acetic acid/ 0.018 M sodium acetate) was added to the solution. The solution was left in the dark for 6 minutes and then titrated with PAO. The PAO normality was determined to be 0.0056 ± 0.0002 N (0.0021 M).

III.B.1.3.3. Synthesis and Standardization of 0.05 M I_2

Approximately 40 grams of KI (Fisher Scientific) and approximately 13 grams of resublimed I_2 (Fisher Scientific) was added to a beaker. Then 20 mL of deionized water was added to the beaker and stirred with a magnetic stirrer. The liquid was decanted, using a sintered-glass crucible, into a bottle containing 1 L of deionized water.

The I_2 solution was standardized by adding aliquots to titration jars, which contained 100.00 mL deionized water and 4.00 mL pH 4 acetate buffer, and then titrating with PAO. The I_2 standardization on day 8, in Runs 3 and 4, was determined by fitting the previously measured I_2 concentrations to an exponential decay curve.

III.B.2. Experimental Procedures

III.B.2.1. Experimental Setup

At the outset of each run, 250.00 mL of the appropriate solution was added to an Erlenmeyer flask and bubbled with the appropriate gas for 30 minutes, to remove oxygen, prior to the addition of recrystallized As_2O_3. Approximately 40 – 80 grams of the recrystallized As_2O_3 was then added to a flask, which was then stirred continuously. The mass of the As_2O_3 was determined from the expected solubility of As_2O_3 based on the pH of the run. After addition of the solid, the gas delivery tube was positioned to blow gas over the solution surface for the remainder of the experiment. In Runs 1 and 2 an additional Erlenmeyer flask with the same matrix but no solid was used to prevent evaporation. Figure 41 shows the schematic of the experimental setup for Runs 1 and 2. In Runs 3 and 4 the gas was bubbled directly

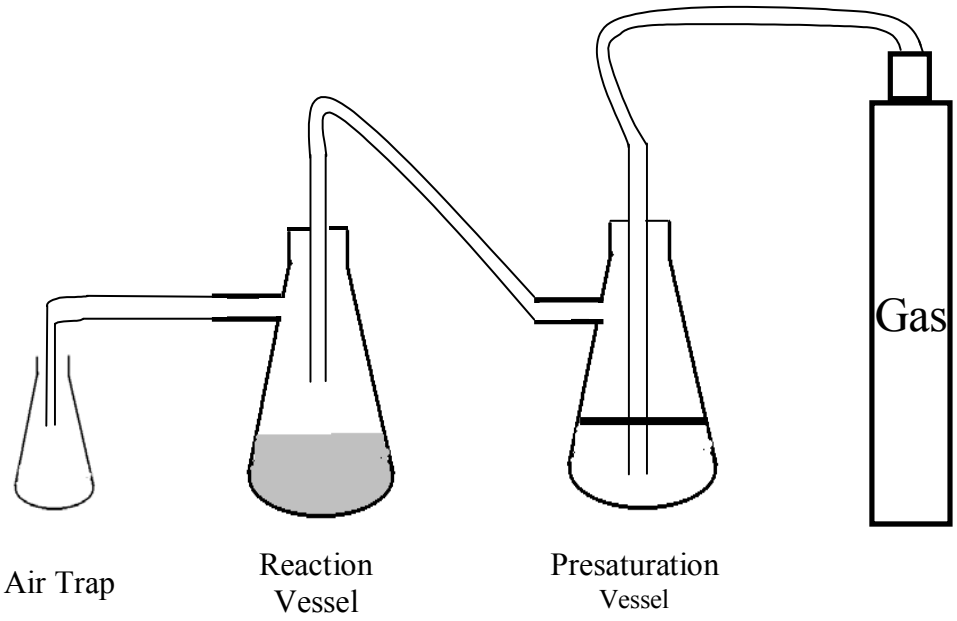

Figure 41. Experimental Setup for Runs 1 and 2. The presaturation vessel contained just solution, while the reaction vessel contained the same solution plus recrystallized As_2O_3.

into the flask containing the solid.

The oversaturated solution was bubbled with nitrogen for one day at pH 11.51 and then bubbled with CO_2 for the remainder of the experiment. The gas was bubbled directly into the solution for the first three days. On day 3, the gas tube with the oversaturated solution became blocked by the precipitation of As_2O_3 and the solution was lost.

III.B.3. Sampling

Stirring was stopped right before sampling to allow the solid to settle. Runs 1 through 4 were sampled over 9 days. In Runs 1 and 2, a 3-5 mL sample was taken from each flask and centrifuged with a bench top centrifuge until the supernatant was visibly clear. In Runs 3 and 4, two 3-5 mL samples from each flask were collected. The first sample was centrifuged. The second sample was syringe filtered with a 0.02 um Whatman Anatop 25 Filter. The first milliliter was discarded to prevent sample contamination. All samples were then diluted 10 times with deionized water and added to a titration jar.

III.B.4. Analysis

Final pH measurements were obtained using an Orion 420A meter equipped with an Orion 8130 Ross Combination electrode calibrated at pH 7 and 10 with VWR commercial buffers.

Total arsenic was obtained using an amperometric method involving titrations with PAO. Titration jars were filled with 100.00 mL of deionized water

and 4.00 mL of pH 4 acetic acid/ sodium acetate buffer. A 282.0 μL sample aliquot was added to each jar followed by aliquots (100.0 μL or 1.00 mL) of approximately 0.05 or 0.005 M I_2, until the color of the solution became yellow/brown. Arsenite was oxidized by the following reaction:

$$As(OH)_3 + I_2 + H_2O \rightarrow 2I^- + AsO(OH)_3 + 2H^+ \quad (4)$$

The excess I_2 was back titrated with a Brinkman 760DMS Titrino automatic titrator with a rotating platinum electrode and a stationary platinum cathode using phenyl arsine oxide (PAO) as the titrant. The reaction can be represented by:

$$C_6H_5AsO\ (PAO) + I_2 + 2H_2O \rightarrow C_6H_5AsO(OH)_2 + 2H^+ + 2I^- \quad (5)$$

The moles of As(III) in the sample is the difference between the I_2 not used in Reaction 5, which is related to the moles of titrant needed to titrate the sample, and the moles of the original I_2 added to the sample.

Raman spectra were then taken of selected solutions with a Thermo Nicolet Nexus 870 FT-IR attached to a FT-Raman module. The spectrometer was controlled using OMNIC software.

III.C. Results

III.C.1. Measurement of Reversibility of Recrystallized As_2O_3

Equilibration time was determined by examining the change in arsenic solubility over time for initially undersaturated and oversaturated solutions. Figure 42 and Table 41 show the data for the determination of equilibrium in the arsenic-carbonate system. Arsenic equilibrates within one to two days. The oversaturation curve approaches the undersaturation curve within one day, which implies that

Table 41. Solubility of Undersaturated and Oversaturated Solution to Determine Equilibrium of the Arsenic-carbonate System.

Total Arsenic (m)	Average Total Arsenic (m)	pH	Reaction Time (Hours)
Undersaturated Solution			
0.227, 0.229	0.228	7.78	24
0.201, 0.201, 0.190	0.197	7.74	48
0.199, 0.204, 0.211	0.205	8.03	73
Oversaturated Solution			
0.228, 0.226, 0.225	0.226	7.61	23
0.190, 0.182, 0.195	0.189	7.72	47
0.208, 0.189, 0.206	0.201	7.98	75
Undersaturated Solution – 0.715 m $NaHCO_3$ (arsenolite), (Run 4) Oversaturated Solution- 0.351 m Na_2CO_3 (arsenolite)			

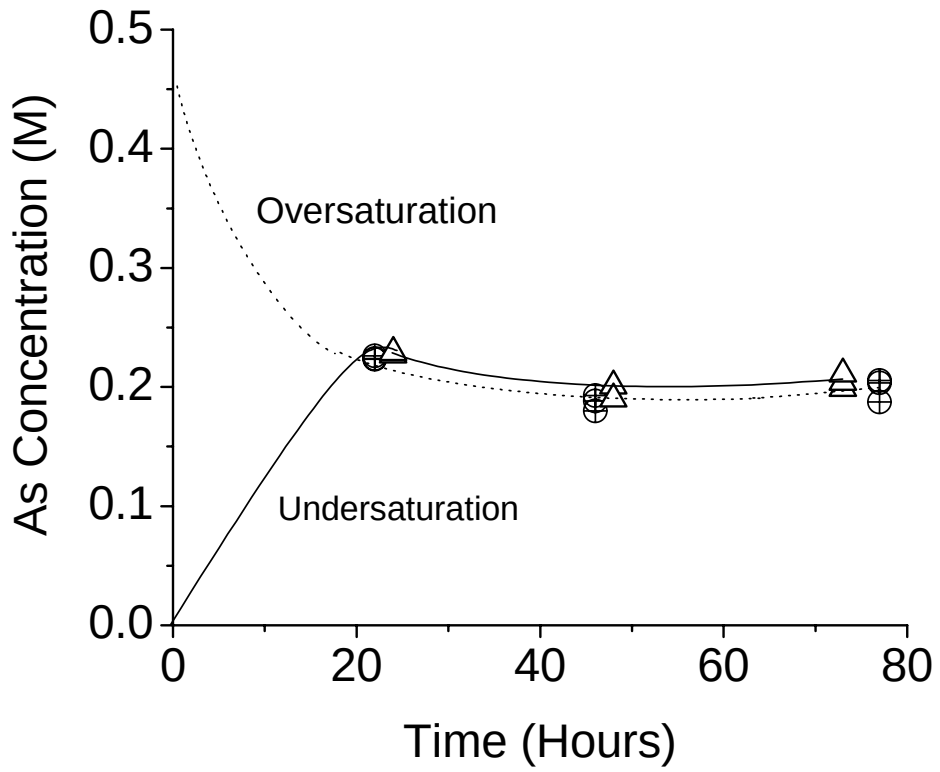

Figure 42. Equilibrium from under- and oversaturation at room temperature of arsenic-carbonate system. Triangles represent undersaturation (0.715 m $NaHCO_3$) and hashed circles represent oversaturation (0.351 m Na_2CO_3).

equilibrium was reached in one day. However, on day one the undersaturation curve is slightly above the oversaturation curve, implying that a few particles had excess free energy and that the recrystallized arsenic trioxide was converting to a more stable form. By day two the solubility was no longer changing.

III.C.2. Solubility of Recrystallized As_2O_3

The solubility of As_2O_3 (arsenolite only or arsenolite/claudetite) was measured in NaCl and $NaHCO_3$ solutions at room temperature under a N_2 or CO_2 atmosphere. The results of these experiments are given in Table 42 and show that the arsenic solubility is greater in solutions that contain bicarbonate when compared to solutions that contain chloride. As an example in Run 3 (0.710 m NaCl) the average As(III) concentration was 0.159±0.016 m, while in Run 4 (0.715 m $NaHCO_3$) the average concentration was 0.207±0.018 m. The average arsenic concentration difference between the NaCl solution (Run 1, 0.710 m NaCl) and the HCO_3^- solution (Run 2, 0.355 m NaCl/ 0.357 m $NaHCO_3$) was less substantial when the HCO_3^- concentration was halved. The average arsenic concentrations were 0.246±0.011 m for Run 1 and 0.257±0.012 m for Run 2.

The other important feature of the data is the difference in the starting materials between Runs 1 and 2 and Runs 3 and 4. The starting material in Run 1 (0.710 m NaCl) was an arsenolite/claudetite mixture and had an average arsenic solubility of 0.243±0.11 m. Run 3 (0.710 m NaCl) contained arsenolite only and had an average arsenic of 0.159±0.16 m. The claudetite/arsenolite mixture was more soluble and thus considered to be less stable than arsenolite alone.

Table 42. Exp. Results for Solubility of As_2O_3 in NaCl and $NaHCO_3$ Solutions.

Total As (m)	pH	Reaction time (h)
Run 1. 0.710 m NaCl, ar+cl, N_2 atm.		
0.250	6.97	49
0.239	6.97	49
0.254	6.97	49
0.243	6.94	74
0.236	6.94	74
0.247	6.94	74
0.247	6.96	97
0.257	6.96	97
0.255	6.96	97
0.246	6.96	97
0.253	6.96	97
0.242	6.96	97
0.231	7.02	167
0.230	7.02	167
0.231	7.02	167
0.237	7.02	167
0.220	7.02	167
0.226	7.02	167
0.252	6.90	215
0.231	6.90	215
0.237	6.90	215
0.260	6.90	215
0.262	6.90	215
0.260	6.90	215
Run 2. 0.355 m NaCl, 0.357 m $NaHCO_3$, ar+cl, CO_2 atm		
0.253	7.09	49
0.239	7.09	49
0.254	7.09	49
0.251	7.11	74
0.260	7.11	74
0.253	7.11	74
0.264	7.11	97
0.267	7.11	97
0.269	7.11	97
0.269	7.11	97
0.272	7.11	97
0.276	7.11	97
0.249	7.12	167
0.254	7.12	167
0.249	7.12	167
0.247	7.12	167
0.245	7.12	167
0.219	7.12	167
0.266	7.15	215
0.264	7.15	215
0.261	7.15	215
0.269	7.15	215
0.260	7.15	215
0.270	7.15	215
Run 3. 0.710 m NaCl, ar only, N_2 atm.		
0.181	5.54	48
0.160	5.54	48
0.169	5.54	48
0.186	5.64	73
0.188	5.64	73
0.173	5.64	73
0.139	5.54	144
0.152	5.54	144
0.152	5.54	144
0.147	5.67	218
0.147	5.67	218
0.143	5.67	218
0.154	5.67	218
0.152	5.67	218
0.151	5.67	218
Run 4. 0.715 m $NaHCO_3$, ar only, CO_2 atm.		
0.201	7.74	48
0.201	7.74	48
0.190	7.74	48
0.199	8.03	73
0.204	8.03	73
0.211	8.03	73
0.188	7.97	144
0.176	7.97	144
0.184	7.97	144
0.221	7.71	218
0.211	7.71	218
0.240	7.71	218
0.232	7.71	218
0.231	7.71	218
0.220	7.71	218

ar= arsenolite, cl = claudetite

The solubility of arsenic was tested on centrifuged and filtered samples to see if the method of removing particles had any effect on the amount of arsenic measured in the samples. The filtered data are compared to the centrifuged data in Table 43. In most cases the measured arsenic concentration from centrifugation was in close agreement with the filtered samples. It is known that Anatop filters contain an alumina membrane and can adsorb cations (Baumgarten and Kirschausen-Dusing, 1997). However, the species present in this work should be neutral or anionic.

III.C.3. Identification of As-carbonate species from Raman Spectra

After equilibrium was reached in the flasks containing arsenic trioxide and either sodium chloride or bicarbonate, the samples were filtered and a Raman spectrum was taken of each sample. An example is shown in Figure 43. The most intense peaks for the $As(OH)_2(CO_3)Na(OH_2)_2$ complex are predicted to occur at 669, 696 and 729 cm^{-1} (Tossell, 2004). There are no distinguishable peaks related to an arsenic-carbonate complex in the Raman spectrum in Figure 43. Also, the intensities of the peaks do not agree with calculated values for the $As(OH)_2(CO_3)Na(OH_2)_2$ species from Tossell (2004). This could be due to the fact that when the samples were placed in the spectrometer the signal declined, indicating that the complex is a weak Raman absorber. Thus, Raman spectroscopy does not appear to be a useful technique in characterizing arsenic-carbonate complexes.

Table 43. Comparison of Filtered and Centrifuged Samples

	Total As (m)		Average As (m)	
Reaction Time (Hrs)	Filtered Sample	Centrifuged Sample	Filtered Sample	Centrifuged Sample
	Run 3: 0.710 m NaCl, arsenolite only, N_2 atm.			
48	0.172	0.181		
48	0.179	0.160	0.174	0.170
48	0.172	0.169		
74	0.183	0.186		
74	0.199	0.188	0.188	0.182
74	0.183	0.173		
144	0.143	0.139		
144	0.169	0.152	0.156	0.148
144		0.152		
218	0.156	0.147		
218	0.146	0.147		
218	0.153	0.144	0.151	0.150
218	0.153	0.155		
218	0.153	0.153		
218	0.145	0.152		
	Run 4: 0.715 m $NaHCO_3$, arsenolite only, CO_2 atm.			
48	0.207	0.201		
48	0.209	0.201	0.207	0.197
48	0.206	0.190		
73	0.197	0.199		
73	0.192	0.204	0.194	0.204
73	0.194	0.211		
144	0.206	0.188		
144	0.215	0.176	0.210	0.183
144		0.184		
218	0.161	0.221		
218	0.182	0.211		
218	0.189	0.240	0.180	0.226
218	0.174	0.232		
218	0.186	0.231		
218	0.186	0.220		

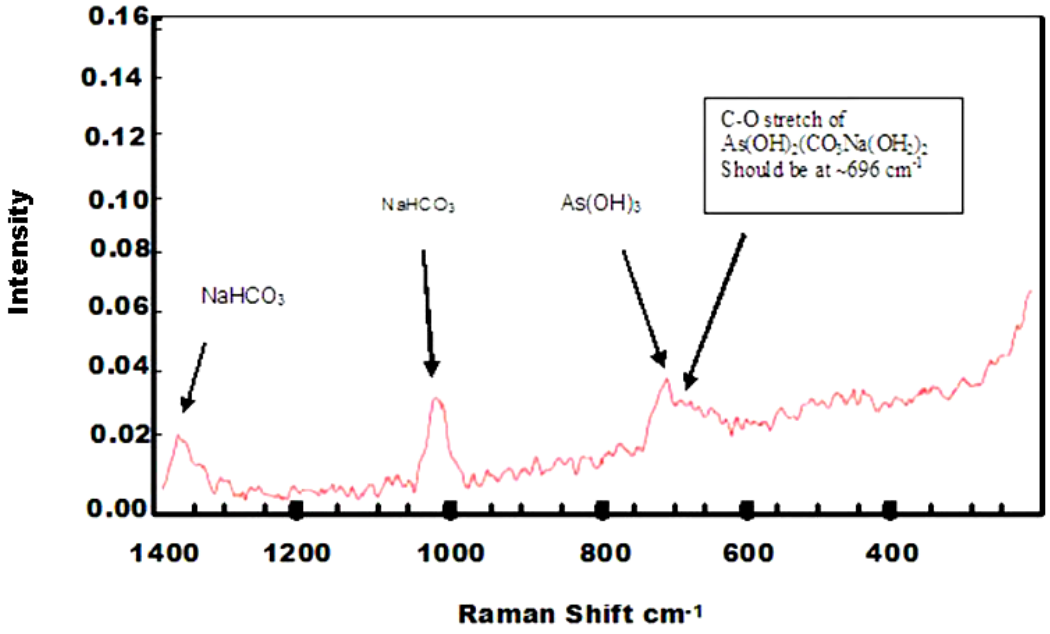

Figure 43. Raman spectrum from a solution in which As_2O_3 reacted with a 1.05 m $NaHCO_3$ solution. [As]=0.186 M, pH 8.15. Scan number = 3600, resolution of 8 and gain of 64.

III.D. Discussion

III.D.1. Solubility Measurements

The data clearly show that the solubility of arsenic is enhanced in the presence of bicarbonate. There are a few reasons why the arsenic concentration would be higher in the presence of bicarbonate. The first possible reason is the pH difference between NaCl (5.61±.06, Run 3) and $NaHCO_3$ (7.85±.14, Run 4). This possibility was excluded by Run 1 and 2 when the control and undersaturated solution had approximately the same pH, and enhanced solubility was still observed. A second possible reason could be formation of arsenic hydroxo chloro species (i.e. $As(OH)_2Cl$), which are known to increase the solubility of arsenic in acidic solutions. Using an equilibrium constant for the formation of $As(OH)_2Cl$ from Arcand (1957) provides evidence that even if there were 1M Cl present in the bicarbonate runs the concentration of an arsenic hydroxo chloro species would be negligible compared to the $As(OH)_3$ concentration. Another possible reason for increased arsenic solubility could come from the formation of an arsenic dimer ($HAs_2O_4^-$). From Garrett et al. (1940):

$$As_2O_3\ (s) + H_2O \Leftrightarrow HAs_2O_4^- + H^+ \qquad K=3.1x\ 10^{-11} \qquad (6)$$

The concentration of the dimer is approximately 0.001 M at a pH of 7 and is negligible relative to a total solubility of 0.2 M. The more plausible reason for the increased arsenic concentration in bicarbonate experiments comes from $As(OH)_3$-HCO_3 condensation, which would produce an arsenic-carbonate species.

III.D.2. Determination of As-Carbonate Equilibrium Constant Expressions

Each one of the three previously proposed species, $As(CO_3)^+$, $As(CO_3)_2^-$ and $As(OH)_2(CO_3)^-$, were separately tested to see which could best account for the enhanced As solubility in the presence of HCO_3^-. The Scientist programs used to calculate the equilibrium constants for the data set can be found in Appendix V. The Scientist program for calculating the equilibrium constant of $As(OH)_2(CO_3)^-$ was made with two basic assumptions. The first assumption was that the concentration of the arsenic dimer was negligible. A calculation for the dimer concentration, using the K from Garrett et al. (1940) implies that the species is negligible under these experimental conditions. The second assumption was that:

$$Total_{As} = [As(OH)_3] + [AsO(OH)_2^-] + [As(OH)_2(CO_3)^-] \quad (7)$$

The following equations are needed to solve for $Total_{As}$ in the second assumption:

$$0.5As_2O_3\ (Arsenolite) + 1.5H_2O \Leftrightarrow As(OH)_3 \qquad K_{SO} = \frac{[As(OH)_3]\ \gamma_{As(OH)3}}{a_a^{0.5}} \quad (8)$$

$$0.5As_2O_3\ (Claudetite) \Leftrightarrow 0.5As_2O_3\ (Arsenolite) \qquad K_p = \frac{a_a^{0.5}}{a_c^{0.5}} \quad (9)$$

and then through the addition of Reaction 8 and 9,

$$0.5As_2O_{3(Claudetite/Arsenolite)} + 1.5H_2O \Leftrightarrow As(OH)_3$$

$$K_{SO}\ K_p = [As(OH)_3]\ \gamma_{As(OH)3} \quad (10)$$

Two additional equations are needed to solve for $Total_{As}$. Reaction 10 will substituted into the additional equations for $As(OH)_3$. The additional equations are:

$$As(OH)_3 \Leftrightarrow AsO(OH)_2^- + H^+ \quad K=10^{-9.17} \text{ (Nordstrom and Archer, 2003)} \quad (11)$$

$$\text{So, } 10^{-9.17}\ K_{SO}\ K_p = [AsO(OH)_2^-]\ \gamma_{AsO(OH)2}\ [H^+]$$

$As(OH)_3 + HCO_3^- \rightarrow As(OH)_2(CO_3)^- + H_2O$ (3)

$$\text{So, } K_{ACO}\ K_{SO}\ K_p = \frac{[As(OH)_2(CO_3)^-]}{[HCO_3^-]}$$

Where γ are activity coefficients. The activity coefficient for $AsO(OH)_2^-$ was assumed to be equivalent to the activity coefficient of HCO_3^-, 0.68 (from Stumm and Morgan, 1996). The activity coefficients of HCO_3^- and $As(OH)_2(CO_3)^-$ were also considered to be equal. The activity coefficient for $As(OH)_3$ was calculated using the Garrett et al. (1940) arsenic solubility data in 0-1 m HCl experiments. This calculation assumed that:

$$\log \gamma_{As(OH)3} = \log (S_o/S_{HCl}) = \sigma I, \quad (12)$$

where S_0 is the solubility of As in water, S_{HCl} is the arsenic solubility in HCl, I is the ionic strength and σ is the Setchenow coefficient (0.051). The Setchenow coefficient was determined from fitting Garrett's data in the 0-1 m HCl range. The activity coefficient of $As(OH)_3$ was calculated to be 1.09. Ion pairs, $NaAs(OH)_2(CO_3)$ and $NaAsO(OH)_2$, were considered to be negligible in relation to the total amount of arsenic present.

The final step in calculating the equilibrium constants involved substituting equations 10, 11 and 3 into equation 7, permitting $Total_{As}$ to be calculated:

$$Total_{As} = \frac{K_{SO}\ K_p}{\gamma_{As(OH)3}} + \frac{K_{SO}\ 10^{-9.17}\ K_p}{\gamma_{AsO(OH)2}\ 10^{-pH}} + K_{ACO}\ K_{SO}\ K_p\ \ [HCO_3^-] \quad (13)$$

This equation computes $Total_{As}$ for the unstable claudetite/arsenolite mixture; K_p is omitted (set=1) to compute $Total_{As}$ for the arsenolite only experiments.

The final derivation of the $Total_{As}$ expressions for $As(CO_3)^+$ and $As(CO_3)_2^-$ are shown in Appendix V, where the same assumptions were made for these species in relation to $As(OH)_2(CO_3)^-$.

The final correction needed before fitting the data with the Scientist program was to calculate the free HCO_3^- concentration, by correcting the total HCO_3^- concentration for ion pairing with Na^+. To correct for ion pairing the stoichiometric association constant of $NaHCO_3$ in seawater was used, which was 0.28 (taken from Johnson and Pytkowicz, 1978). The ion pairing reaction can be represented by:

$$Na^+ + HCO_3^- \Leftrightarrow NaHCO_3 \qquad K^*=0.28 \qquad (14)$$

Knowing the total HCO_3^- concentration and assuming the total Na^+ concentration is 0.7 m, the concentration of the $NaHCO_3$ can be calculated with a quadratic equation. Through subtracting the calculated $NaHCO_3$ concentration from the known total HCO_3^- concentration, the free HCO_3^- was determined to be 0.310 m in Run 2 and 0.640 m in Run 4.

III.D.3. Comparison of Carbonate Species through Computer Modeling

The log ($As_{calculated}/As_{observed}$) as a function of pH and bicarbonate is shown in Figure 44 for each As-carbonate species proposed by Kim et al. (2000). The fitting was done by the least squares method. The results for the three different species are presented in Table 44.

Figure 44 shows that $As(OH)_2(CO_3)^-$ is the best-fit model to describe the solubility of arsenic in the presence of bicarbonate with data from this work. There

are no trends in the data and the corresponding equilibrium constant for the reaction containing $As(OH)_2(CO_3)^-$ has a pK_3=0.57±0.15 and a standard deviation of 0.032.

Table 44. Comparison of Calculated Equilibrium Constants for $As(OH)_2CO_3^-$, $As(CO_3)_2^-$ and $AsCO_3^+$

Species	Log K_{ACO}	Log K_{SO}	Log Kp	Standard deviation of model
$As(OH)_2(CO_3)^-$	-0.57±0.15	0.75±0.02	-0.17±0.03	0.032
$As(CO_3)_2^-$	7.35±0.17	0.74±0.02	-0.15±0.03	0.034
$As(CO_3)^+$	13.70±0.43	0.72±0.02	-0.14±0.03	0.040

$As(CO_3)_2^-$ in Figure 44 shows a slight trend with both pH and bicarbonate and the model has a standard deviation of 0.034. $As(CO_3)^+$ has the worst fit to the data, which is demonstrated by a standard deviation of 0.040. There is also an obvious trend with pH and bicarbonate. These two species have a slightly worse fit to the data when compared to the $As(OH)_2(CO_3)^-$ species and given the uncertainties in the measurements, $As(CO_3)_2^-$ and $As(CO_3)^+$ could possibly explain the As solubility.

Calculations done by Tossell suggest that $As(OH)_2(CO_3)^-$ is one of the most stable species and is formed from a condensation dimerization reaction. This type of reaction occurs in the formation of $HAs_2O_4^-$ and can be represented by (Garrett et al., 1940):

$$2As(OH)_3 + OH^- \Leftrightarrow HAs_2O_4^- + 3H_2O \qquad K= 1.52 \times 10^4 \qquad (15)$$

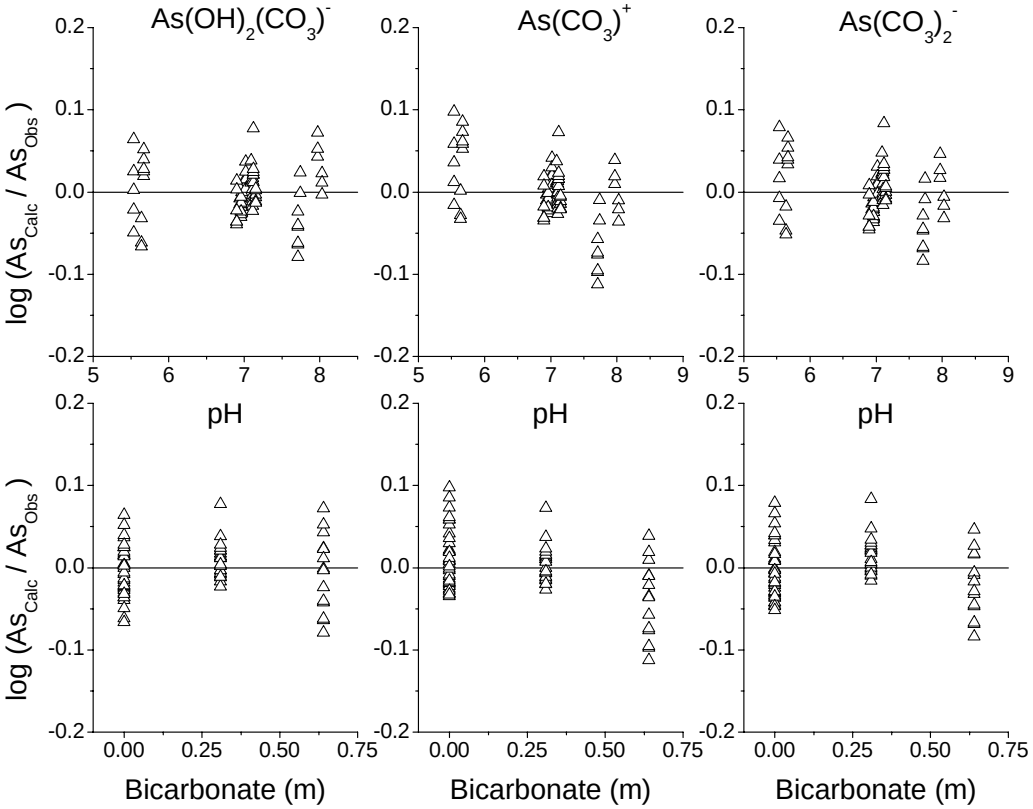

Figure 44. Arsenic-Carbonate Models including the species $As(OH)_2(CO_3)^-$, $As(CO_3)_2^-$ and $As(CO_3)^+$. Log (As_{Calc}/As_{Obs}) as a function of Top: pH and Bottom: HCO_3^- Concentration.

A: $As(OH)_3 + HCO_3^- \Leftrightarrow As(OH)_2CO_3^- + H_2O$ pK=0.57±0.15

B: $As(OH)_3 + 2HCO_3^- + H^+ \Leftrightarrow As(CO_3)_2^- + 3H_2O$ pK=-7.35±0.17

C: $As(OH)_3 + HCO_3^- + 2H^+ \Leftrightarrow As(CO_3)^+ + 3H_2O$ pK=-13.70±0.43

All Data are from this work.

and is analogous to the formation of $As(OH)_2(CO_3)^-$:

$$As(OH)_3 + HCO_3^- \rightarrow As(OH)_2(CO_3)^- + H_2O \qquad K=0.267\pm0.04 \qquad (3)$$

The dimerization of $As(OH)_3$ in reaction 15 can be put into comparable terms with reaction 3 by using the first dissociation constant of $As(OH)_3$ and the water ionization constant, which results in the following:

$$As(OH)_3 + AsO(OH)_3^- \Leftrightarrow HAs_2O_4^- + 2H_2O \qquad K=0.253 \qquad (16)$$

The similar equilibrium constants for reaction 3 and 16 indicate that the stability of $As(OH)_2(CO_3)^-$ predicted by Tossell (2004) is confirmed through these experiments. Therefore, $As(OH)_2(CO_3)^-$ describes the solubility of arsenic in the presence of bicarbonate.

Kim et al. (2000) proposed two alternate species that could be responsible for the slight arsenic enhancement in the presence of bicarbonate. However, if we approach the problem strictly from a coordination standpoint, arsenic prefers a coordination of three and tends to form pyramidal configurations due to three bonding p orbitals and a lone pair (Nickless, 1968). Therefore, $As(OH)_2(CO_3)^-$ would be favored over $As(CO_3)_2^-$ and $As(CO_3)^+$. In this light, quantum mechanical calculations may be useful in determining the stability of complexes in natural waters.

III.D.4. Comparison of $As(OH)_3$ Solubility with Previous Literature Values

There have been numerous studies on the solubility of As_2O_3. Garrett et al. (1940) completed a study on the solubility of As_2O_3 in dilute solutions of hydrochloric acid and sodium hydroxide at 25°C. They determined that the

solubility of As_2O_3 was 0.1035 m, which is equivalent to 0.207 m $As(OH)_3$. Experiments in this work determined that the solubility of $As(OH)_3$ was 0.159±0.016 m (arsenolite) and 0.246±0.012 m (arsenolite and claudetite) in solutions with a pH of approximately 5.6 and 7.0, respectively. Anderson and Story (1923) also conducted a study to determine the solubility of $As(OH)_3$ in water. They determined the solubility of $As(OH)_3$ to be 0.207 m at 25°C. A more recent study conducted by Pokrovski et al. (1996) also studied the solubility of As_2O_3 in water under acidic conditions. They determined that the solubility of arsenolite at 22°C (low temperature form of As_2O_3) to be 0.148 m. They also determined the solubility of claudetite to be 0.135 m. The differences in solubility in these experiments could be due to the variation in the starting material or temperature, experiment in this study were carried out at room temperature, which ranged from 23.8 to 26.8°C.

The equilibrium constant, K_p, for the conversion of arsenolite to the arsenolite-claudetite mixture was determined to be 1.47±0.26. The calculated Gibb's free energy value for arsenolite-claudetite mixture was 0.95 kJ/mol more than arsenolite only runs. This is not consistent with other literature data, which favor claudetite as the more stable phase by -0.19 kJ/mol (Nordstrom and Archer, 2003; Pokrovski et al., 1996).

III.D.5. Significance for As(III) in Natural Waters

The concentration of bicarbonate found in river and ocean water is 9.2×10^{-4} M and 2.3×10^{-3} M, respectively (Stumm and Morgan, 1996). In typical groundwaters the concentration of bicarbonate can range from 1.3 mM to 5.5 mM. It should be

noted that the concentration of bicarbonate used throughout these experiments was much higher than concentrations found in nature. In waters that have a bicarbonate concentration of 5 mM, I would predict that $As(OH)_2(CO_3)^-$ could be present as 0.1% of the total arsenic and would not contribute significantly to the total arsenic concentration in solution. The results indicate that there is not a significant increase in arsenic solubility when bicarbonate is present. This leads to the conclusion that an arsenic carbonate complex may exist but is not environmentally important as to increase arsenic in water systems when bicarbonate is present.

Chapter IV. Conclusions

The primary goal of this work was to identify the heavy metals that form a stable complex with the thioarsenite ligand under sulfidic conditions. Another goal of this dissertation involved exploring the role zero valent sulfur had on the solubility of As(III) and Ag(I). The study also explored if HCO_3^- had the ability to promote the solubility of As(III). A brief synopsis of the results from this work and some ideas for future work are presented in this chapter.

IV.A. Understanding As Chemistry in Sulfidic- and Carbonate-Containing Systems

Solubility experiments were done to determine if the thioarsenite ligand had the ability to complex d^{10} metals forming stable metal-thioarsenite complexes in sulfidic solutions. This study was partially done in response to studies which indicated that copper had a high affinity for the thioarsenite ligand and formed a stable Cu-thioarsenite complex, enhancing the solubility of both metals (Clarke, 1998; Clarke and Helz, 2000). This study also tested the quantum mechanical calculations done by Tossell (2000) who predicted which metals form stable metal-thioarsenite complexes.

The first step in this research was to compare the solubility of arsenic and the metal of interest in the assemblages (HgS+As_2S_3+S, PbS+As_2S_3+S, Ag assemblage A and Ag assemblage B) to the solubility of As_2S_3+S and the other single phase (HgS, PbS or Ag_2S) in sulfidic solutions. It is important to remember that if a metal-thioarsenite species is significant, then the solubility of a metal will be greater in the

presence of As-bearing phases when compared to solubility of the metal-sulfide phases alone.

The first important result was that hydroxide and sulfide species, not polysulfide species, explained the solubility of As in the As_2S_3+S experiments. Elemental sulfur did not promote the solubility of arsenic and it was concluded that elemental sulfur had no effect on the solubility of As_2S_3 in sulfidic solutions. This effect is contradictory to previous experiments involving Sb(III) (Helz et al., 2002). Helz et al. (2000) found that zerovalent sulfur increased the solubility of Sb(III) by three orders of magnitude in sulfidic solutions at near-neutral to alkaline pH's.

The solubility of arsenic in experiments involving As_2S_3+S (As_2S_3, As_2S_3+S, HgS+As_2S_3+S, PbS+As_2S_3+S, Ag assemblage A and Ag assemblage B) was attributed to three species $As(OH)_3$, $AsS(HS)(OH)^-$ and $H_2As_3S_6^-$. These species also agree with previous literature data on the solubility of As_2S_3 in sulfidic solutions. Under conditions found in nature, pH=7-8, $\Sigma S=10^{-6}$ to 10^{-3} M, the $AsS(HS)(OH)^-$ species is dominant. Under conditions were the total sulfide in solution is $>\sim10^{-2}$ the $H_2As_3S_6^-$ species may become dominant.

Elemental sulfur was found to increase the solubility of silver when Ag_2S+S were equilibrated in sulfidic solutions. Research in this dissertation indicated that AgHS, $Ag(HS)_2^-$, $Ag_2S(HS)_2^{2-}$, $Ag(Cl)(HS)^-$, and AgS_x^- are responsible for the increased silver solubility.

The solubility of PbS could not be measured in the presence of elemental sulfur because the lead solubility was below the detection limit of $9.6x10^{-9}$ M.

Therefore, there could have been some solubility enhancement in these experiments due to Pb-polysulfide species but it could not be measured.

Once the effect of elemental sulfur on As_2S_3, HgS, PbS and Ag_2S had been individually defined, the primary aim of the work could be undertaken. To determine if the presence of arsenic increased the solubility of silver, mercury or lead in binary and ternary assemblages in sulfidic solutions.

The solubility of silver was elevated in the presence of arsenic and the extra silver solubility was attributed to one species, AgAsS(HS)(OH)°. The dithioarsenite ligand strongly complexed Ag(I) with a pK of –17.17±0.20. This synergistic interaction between Ag(I) and As(III) could have environmental implications such as mobilization of Ag and As from landfills. The silver thioarsenite complex enhances the solubility of silver at thioarsenite concentrations up to 0.1 mM at near neutral pH's, which are conditions found in the environment.

There was no significant difference between the solubility of mercury in the cinnabar-orpiment-elemental sulfur assemblage when compared to literature data on the solubility of mercury in the cinnabar-elemental sulfur assemblage. There could have been some enhancement in lead solubility in these experiments, but the lead solubility was below the $9.6x10^{-9}$ M detection limit of the graphite furnace and could not be measured.

These findings are in agreement with the quantum mechanical predictions done by Tossell (2000). He correctly predicted that Cu and Ag form stable metal-thioarsenite complexes and that Hg and Pb form stable metal-HS complexes. It therefore seems that Group 11 metals, and possibly Tl^+, are favored to form stable

metal-thioarsenite complexes. Cu^{+}, another Group 11 element, and $AsS(HS)(OH)^{-}$ form a stable Cu-thioarsenite complex, where the pK was calculated to be -19.82 ±0.17 (Clarke and Helz, 2000). The calculated stability (Cu>Ag) is also in agreement with predictions by Tossell (2000).

It is interesting to develop a preliminary theory on why Cu and Ag form stable metal-thioarsenite complexes, while Pb and Hg do not. One possible reason could be due to soft acid-base interactions. Pearson (1988) ranked the absolute hardness of the cations I have studied in order of decreasing hardness: $Hg^{2+}>Pb^{2+}>Ag^{+}>Cu^{+}$. This may explain why Hg^{2+} and Pb^{2+} do not bind to the dithioarsenite ligand, which is a soft base. Another explanation could be that Hg^{2+} and Pb^{2+} have an affinity for HS^{-} over $AsS(HS)(OH)^{-}$ because the HS^{-} ligand is smaller and able to better bind Hg^{2+} and Pb^{2+}.

The free energy of formation of natural As_2S_3 was calculated. as –80.8±1.6 kJ/mol.

The second part of this work also dealt with a system involving As(III), but examined the effect bicarbonate had on As(III) solubility in the absence of sulfide. Groundwaters in Bangladesh contain organic matter, are under reducing conditions and have elevated As(III) concentrations. Kim et al. (2000) estimated large formation constants for As-carbonate complexes, implying that HCO_3^{-} could promote As(III) solubility. To examine this hypothesis, the solubility of As_2O_3 in concentrated bicarbonate solutions was compared to the solubility of As_2O_3 in concentrated NaCl solutions at room temperature, where both solutions had near neutral pH's. The solubility of As(III) was slightly increased in the presence of bicarbonate and an

attempt was made to fit the data with individual carbonate complexes proposed by Kim et al. (2000) and Tossell (2004). $As(OH)_2(CO_3)^-$ provided a slightly better fit to the data. An equilibrium constant was determined which supports that an arsenic carbonate complex may exist but is not environmentally very important.

IV.B. Future Work

There are still areas of this work that leave certain question unanswered. This section will provide some ideas for future work on this project.

The first experiment that needs confirmation is the amount of time needed to reach equilibrium in $AgAsS_2$ and Ag_3AsS_3 systems. Forty days should be enough time to reach equilibrium, but this fact should be confirmed experimentally.

Another area of future research is the effect arsenic has on the solubility of gold. Tossell (2000) predicts that a stable gold-thioarsenite complex is likely to form under sulfidic conditions. However, it should be noted that gold is not particularly important in the environment, but it would be interesting to know if all Group 11 elements form stable metal-thioarsenite complexes. There are no known Au-As ternary minerals, so solubility studies would have to contain Au_2S, As_2S_3, and S.

It would also be interesting to investigate higher sulfide concentrations with the $PbS+As_2S_3+S$ ternary assemblages. This would allow a higher concentration of lead in solution and may facilitate a result that could be quantified.

The currently favored hypothesis for the arsenic enrichment in groundwaters is that arsenic bound to Fe(III)-oxyhydroxide is released as the Fe(III)-oxyhydroxide is reduced (Nickson et al., 2000; Kinniburgh et al., 2003; Ahmed et al., 2004;

McArthur et al., 2004 Zheng et al., 2004). It would be interesting to conduct solubility studies on As(III) in the presence of Fe(II). Another study would have to be done involving As solubility in the presence of Fe(III), under oxidizing conditions so a comparison of the two systems could be made. The experimental conditions would have to include both oxidizing and reducing conditions at near neutral pH's. The reduction of organic matter would favor reducing condition and a N_2 or CO_2 atmosphere may facilitate reducing conditions by eliminating O_2 from the atmosphere and sample solution. This may prove that Fe is responsible for the elevated arsenic levels in groundwater under reducing conditions.

Appendix I

HS^- and As(III) – UV-Visible Absorption Interference

The first reason UV-Visible spectroscopy was not useful was because [HS^-] could not be determined in experiments containing As_2S_3. A typical UV-Visible spectrum of an orpiment sample equilibrated with S^o in a sulfidic solution is shown in Figure 45. A species (most likely an arsenite species) absorbs at 248 nm and overlaps the HS^- absorption at 230 nm.

To determine if As(III) species are absorbing in the UV-Visible range, four experiments with varying concentrations of As(III) and HS^- were studied over time (approximately 1300 minutes). The experimental conditions are shown in Table 45. Sodium chloride was also added to some solutions to minimize colloid formation by promoting flocculation. A Tyndal beam was used to detect colloid formation. Figure 46 shows one experiment where the initial As(III) concentration was $3x10^{-4}$ M and the initial HS^- concentration was $3x10^{-3}$ M (other experiments produced the same trend in absorption over time). Figure 46 shows that an As(III) species forms at 140 minutes (~278 nm) and then transforms to another As (III) species at 1400 minutes (~250 nm). It is possible that HS- is being replaced by OH- groups on the As(III), resulting in a peak shift. Therefore, the results of this experiment do not provide evidence of one particular As-S species that is responsible for the absorbance between 230 nm and 325 nm. In fact, it seems multiple As(III) species absorb over this range because the arsenic peak is shifting in wavelength as time progresses. However, it is important to rule out As(III) oxidation to As(V) as the reason for the peak shift.

Appendix I

HS^- and As(III) – UV-Visible Absorption Interference cont.

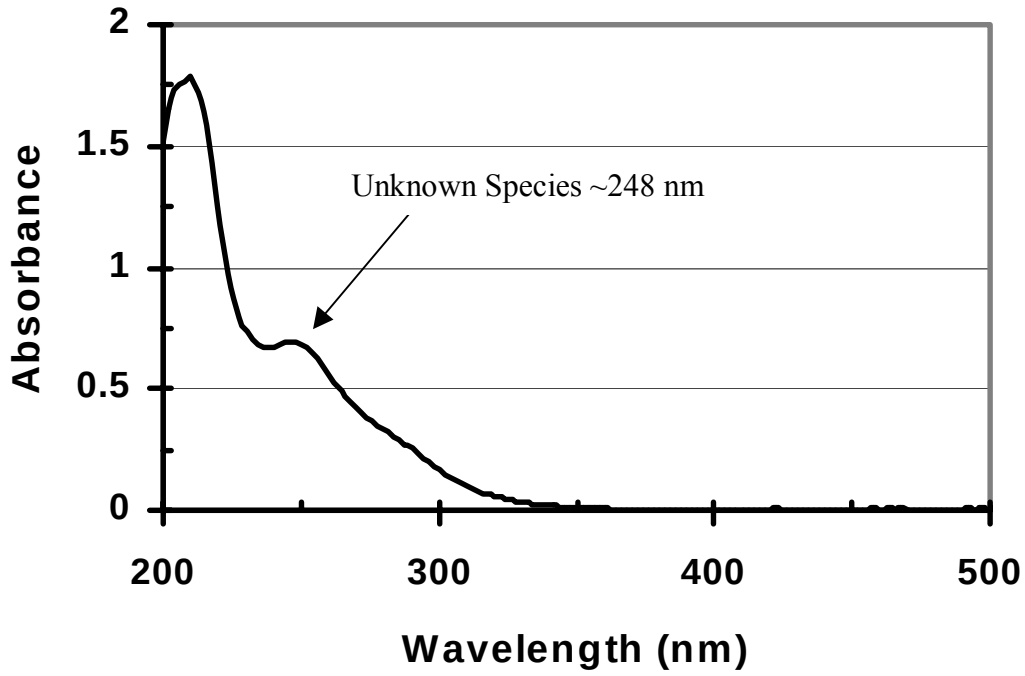

Figure 45. UV-Visible spectra of orpiment equilibrated with S^o in a sulfidic solution. pH=7.23, total sulfide = 2.94×10^{-3}, [As]=7.88×10^{-4}. No sample dilution, 0.1 cm cell.

Appendix I

HS^- and As(III) – UV-Visible Absorption Interference cont.

Table 45. Experimental Conditions for the Absorbance of a Thioarsenite Species

Experiment No.	Initial Concentration $NaAsO_2$ (M)	Initial Concentration NaHS (M)	pH	NaCl (M)
1	3.00×10^{-4}	3.00×10^{-3}	8.09	-
2	5.00×10^{-4}	5.00×10^{-3}	8.36	-
3	3.00×10^{-4}	3.00×10^{-3}	8.09	0.106
4	3.00×10^{-4}	3.00×10^{-3}	13.29	-
All solutions were buffered with 0.00710 M MOPS.				

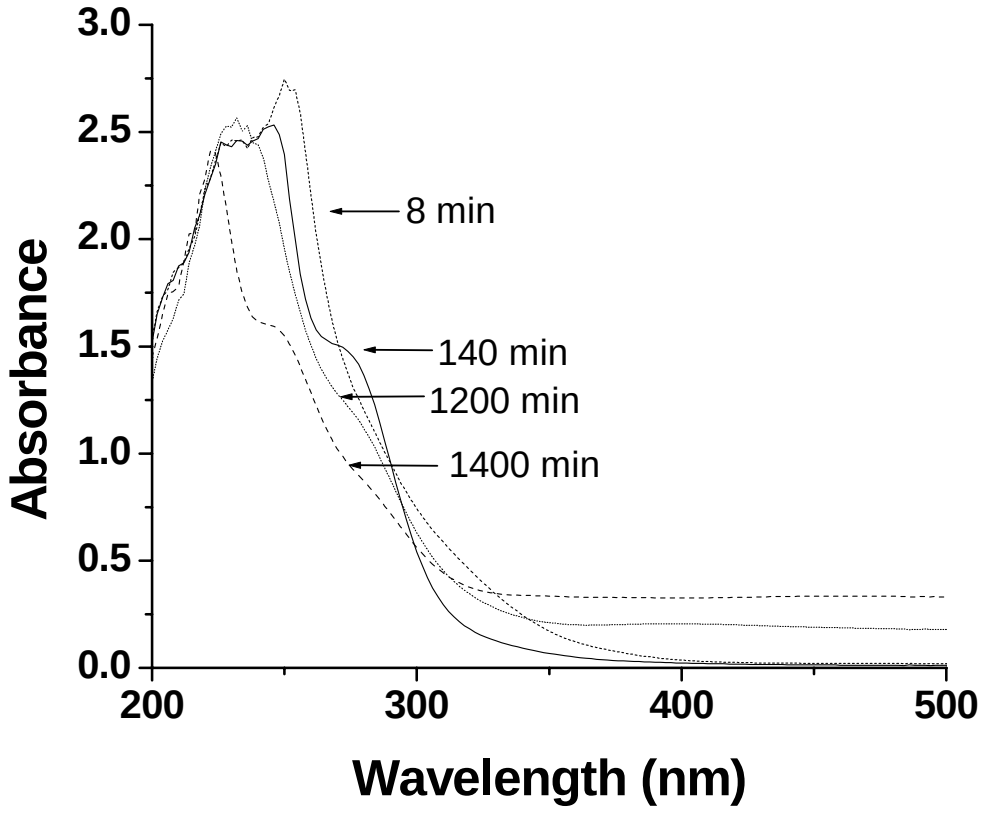

Figure 46. Formation of As peak followed over time with UV-Visible spectroscopy. Initial As(III) concentration was 3×10^{-4} M and the initial HS- concentration was 3×10^{-3} M, pH=8.09. Absorbance measured in 1 cm cell.

Appendix I

HS^- and As(III) – UV-Visible Absorption Interference cont.

An As(V) and an As(III) solution were made to compare their absorbencies. A 0.0107 M $Na_2HAsO_4 \bullet 7H_2O$ solution was bubbled with H_2S gas forming an As(V)-S solution. A 0.0102 M $NaAsO_2$ solution was bubbled with H_2S gas, forming an As(III)-S solution. Figure 47 shows that the As(V) solution does not absorb above 250 nm, whereas the As(III) solution absorbs over the 230 to 325 nm range. This evidence is not conclusive because the pH's of the solutions were not measured and there is no way to tell which species was formed after H_2S was added to the solution.

However, the arsenic absorption can be attributed to a combination of many different As(III) species ranging from $As(OH)_3$ to $AsS(HS)_2^-$. Tossell (2001) used quantum mechanical methods to calculate the UV spectra for $As(SH)(OH)_2$ and $As(HS)_2(OH)$ and found that substitution of OH^- by HS^- formed thioarsenite species that produced spectra that are between the spectra of $As(OH)_3$ and $As(HS)_3$. He calculated transition energies using the TD B3LYP level and found that $As(OH)_3$ should absorb around 187 nm and $As(HS)_3$ around 302 nm, respectively. It is therefore difficult to assign a single thioarsenite species to the observed absorbance in this experiment and monitoring the arsenic speciation optically is impossible.

The second reason that UV-Visible spectroscopy was insufficient in measuring HS^- had to do with samples that had a starting sulfide value of 10^{-4} M.

Appendix I

HS^- and As(III) – UV-Visible Absorption Interference cont.

These samples did not produce any absorption at 230 nm, where HS^- absorbs. This is quite surprising and a possible cause could be that HS^- volatilized from the sample before a measurement could be taken.

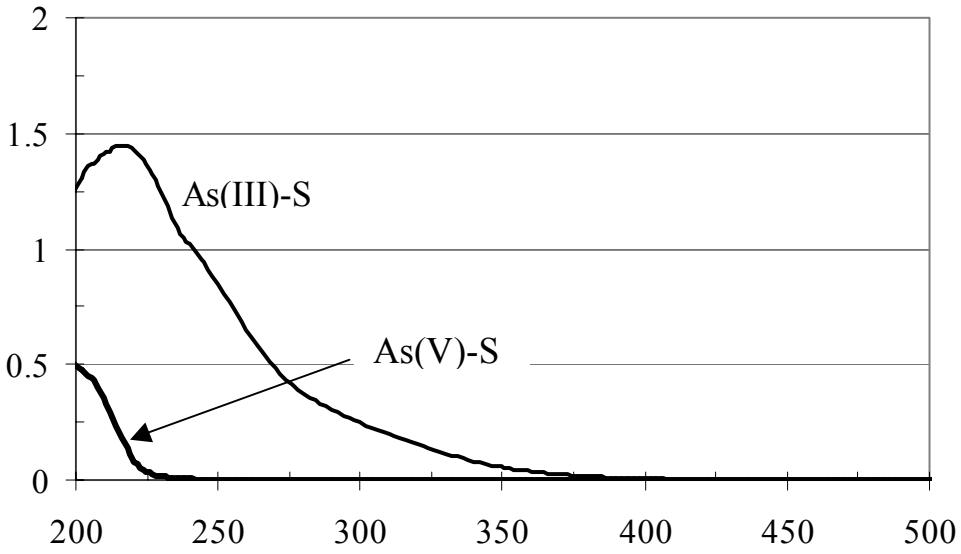

Figure 47. UV-Visible spectra of As(V)-S and As(III)-S species. Samples were $1x10^{-3}$ M and were in 0.1 cm cells.

Appendix II

Arsenic Speciation Models and Data

Scientist Fitting Program Used to Model Arsenic Data

// MicroMath MINSQ Model File

// Independent variables are variables in a set of equations that are not constant and do not depend on any of the other variables. They include: total sulfide (TS), pH (PH), ionic strength (I), index and activity of sulfur (as)*

IndVars: TS, PH, I, index, as

// *Dependent variables are the unknowns, which can be calculated from independent variables, parameters, constants, or other dependent variables. L10AS is the logarithm of the calculated total [As] and will be compared to the logarithm of the observed total [As]*.

DepVars:L10AS, H2S, AsOH3, As2As3S6, AsSHSOH, AsHSOH2, AsOOH2

// Parameters are variables whose values are changed during least squares fitting. K's are equilibrium constants and aas is the activity of As_2S_3 in orpiment.

Params: K1, K2, K3, K4, aas

// Calculate activity coefficients from Davies Eq. and H^+

SQI=I^0.5

H=10^(-PH)

Y=(-0.5*SQI/(1.0+SQI)+0.1*I)

G1=10^Y

G2=10^(4*Y)

// Calculate HS^- given current estimates of K values and activity of orpiment

H2S^0.5*(H2S^0.5+H2S^0.5*1.05E7/(H*G1)+6*K2*(aas^(1.5*index))*(H2S)/(H*G1)+2*K3*(aas^(0.5*index))/(H*G1)+K4*aas^(0.5*index)/(H2S)+(K5*aas^(index)*H2S^0.5/(H*G1))+(2.89e17*as^4/(H^2)*(A2*G1))+(3.78e17*as^3/(H^2)*(A2*G1)))=TS

1E-7<H2S<TS

// Calculate HS^- and polysulfide ion concentrations

HS=1.05e-7*H2S/(H*G1)

S5=(2.75e-10*as^4*HS/H/A2)

S4=(3.63e-10*as^3*HS/H/A2)

SOT=(3*S4)+(4*S5) // Calculate total zero-valent sulfur

// Calculate concentration of As species given current estimate of K values

AsOH3=K1*(aas^(0.5*index))/(H2S^1.5)

As2As3S6=K2*(H2S^1.5)*aas^(1.5*index)/(H*G1)

AsSHSOH=K3*H2S^0.5*aas^(0.5*index)/(H*G1)

AsHSOH2=K4*aas^(0.5*index)/(H2S^(0.5))

AsOOH2=5.01e-10*K1*aas^(0.5*index)/(H2S^1.5*H*G1)

TAS=AS1+(3*AS2)+AS3+AsHSOH2+AsOOH2

L10AS=LOG10(TAS)

** Index value set to 0 for samples containing orpiment. This was the effect of overriding the current value of aas and forcing aas to equal 1 for these samples. Index value is set to 1 for samples that contained no orpiment, so the computer program will apply the current value of aas to fit these samples.*

Appendix II

Arsenic Speciation Models and Data cont.

Derivation used to Calculate H_2S from ΣS

$$\Sigma S = H_2S + HS^- + 2AsS(HS)(OH)^- + 6H_2As_3S_6^- + S_5^{2-} + S_4^{2-} \quad (1)$$

$$H_2S \Leftrightarrow HS^- + H^+ \qquad 1.05\times10^{7} = [HS^-][H^+]/[H_2S] \quad (2)$$

$$0.5As_2S_3 + H_2O + 0.5H_2S \Leftrightarrow AsS(HS)(OH)^- + H^+$$

$$K_3 = ([AsS(HS)(OH)][H^+])/a_{As2s3}^{0.5}[H_2S]^{0.5} \quad (3)$$

$$1.5As_2S_3 + 1.5H_2S \Leftrightarrow H_2As_3S_6^- + H^+ \qquad K_2 = ([H_2As_3S_6^-][H^+])/a_{As2s3}^{1.5}[H_2S]^{1.5} \quad (4)$$

$$H_2S + 4S^o \Leftrightarrow S_5^{2-} + 2H^+ \qquad 2.89\times10^{17} = [S_5^{2-}][H^+]^2/a_S^4[H_2S] \quad (5)$$

$$H_2S + 3S^o \Leftrightarrow S_4^{2-} + 2H^+ \qquad 3.78\times10^{17} = [S_4^{2-}][H^+]^2/a_S^3[H_2S] \quad (6)$$

Polysulfide equilibrium constants taken from Giggenbach (1974)

Equations 2 through 6 were then solved for H_2S substituted into equation 1

Equation used to Calculate the Standard Deviation of the Models (applies to all models used in this work)

$$\sigma = \sqrt{\frac{\Sigma(Y_{calc} - Y_{obs})^2}{n - p}} \quad (7)$$

Where n=number of samples and p=number of parameters. Parameters that are held constant are not included in the calculation since they do not contribute to the improvement of the fit.

Appendix II

Arsenic Speciation Models and Data cont.

Eary (1992) Arsenic Data Used to Model Arsenic Speciation

Experiments with No Added Sulfide			Experiments with Added Sulfide		
pH	As (mg/kg)	mSTot_(mmol/kg)	pH	As (mg/kg)	mSTot_(mmol/kg)
2.07	10.1±7.5	0.0030±0.0004	3.95	48.4±12.5	0.0008±0.0004
2.54	17.2±5.3	0.0032±0.0003	3.96	39.3±3.8	0.0009±0.0001
3.03	22.6±2.8	0.0026±0.0004	3.96	21.1±5.2	0.0013±0.0004
4.01	24.8±9.2	0.0026±0.0006	4.04	11.6±5.2	0.0024±0.0002
4.98	26.1±4.7	0.0030±0.0005	4.18	0.4±0.1	0.0427±0.0136
5.09	44.2±11.6	0.0012±0.0005	4.02	0.3±0.1	0.0912±0.0043
5.96	26.0±4.6	0.0045±0.0006	4.2	0.1±0.3	0.1585±0.0193
6.07	27.8±5.7	0.0095±0.0034	4.13	0.7±0.2	0.6607±0.0979
6.36	47.3±10.9	0.0407±0.0094	4.61	1.9±0.5	0.8913±0.1559
6.47	50.7±4.9	0.0427±0.0063	4.53	4.2±0.2	4.0738±0.7125
6.88	118.7±27.5	0.1318±0.0127	4.55	76.7±17.7	6.1660±0.2906
6.94	136.3±27.8	0.1585±0.0320	4.78	113.4±10.9	15.4882±1.8898
7.53	278.4±64.4	1.7783±0.5126	4.81	312.3±54.6	16.593±3.3567
7.99	749.2±239.5	7.5858±1.3267			

Webster (1990) Arsenic Data Used to Model Arsenic Speciation

Experiments with No Added Sulfide				Experiments with Added Sulfide			
pH	mStot ($x10^5$)	Ipart	As (mg/kg)	pH	mStot ($x10^5$)	Ipart	As (mg/kg)
1.40	1.7	0.444	0.82	1.45*	0.0016	0.392	0.64
1.42	1.8	0.444	0.89	2.21	0.0294	0.036	0.009
1.55	0.9	0.400	0.46	2.23	0.0282	0.036	0.02
2.14	1.3	0.040	0.64	3.05	0.0320	0.005	0.04
2.23	1.5	0.040	0.76	3.36	0.0168	0.011	0.28
2.58	1.0	0.011	0.50	4.25	0.0239	0.000	2.3
2.58	1.3	0.011	0.64	4.35	0.0170	0.000	0.71
3.02	0.9	0.004	0.44	4.50	0.0170	0.000	0.84
3.07	1.1	0.004	0.54	4.51	0.0133	0.001	1.1
3.84	2.4	0.001	1.2	4.82	0.0212	0.001	2.1
4.28	2.4	0.000	1.2	5.56	0.0283	0.002	16
5.16	6.1	0.000	3.0	5.59	0.0228	0.000	20
5.98	2.9	0.000	1.4	6.46	0.0180	0.026	110
6.06	5.7	0.000	2.9	6.64	0.0197	0.079	620
6.28	6.0	0.000	3.0	6.75	0.0180	0.057	280
6.45	6.1	0.050	3.0				
7.16	81	0.000	41				

* Point not used in modeling in this dissertation

Appendix III

Silver Models and Data

Silver Model to Calculate Ag_2S+S Silver Speciation

// MicroMath Scientist Model File AgAsS(SH)(OH)
// Independent variables are variables in a set of equations that are not constant and do not depend on any of the other variables. They include: pH (PH), total sulfide (S), ionic strength (I), activity sulfur (as), activity chloride (acl) & [arsenic]$_{OBS}$ (ARS)
IndVars: PH, S, I, as, acl, ARS
// *Dependent variables are the unknowns, which can be calculated from independent variables, parameters, constants, or other dependent variables. L10AG is the logarithm of the calculated [Ag] and will be compared to logarithm of the observed [Ag].*
DepVars: AGT, AGHS2, AGSHS2, AGHS, AGS42, AGHSS4, AGS4S5, AGCLHS, AGS5OH, AGOHHS, AGS5
// Parameters are variables whose values are changed during least squares fitting. K's are equilibrium constants of Ag species
Params: K1, K2, K3, K4, K5, K6, K9, K10, K11, K12
// Calculate H^+ and activity coefficients from Davies Equation
H=10^(-PH)
A1=10^(-0.5*(I^0.5/(1+I^0.5)-0.2*I))
A2=10^(-2*(I^0.5/(1+I^0.5)-0.2*I))
A3=10^(-4.6*(I^0.5/(1+I^0.5)-0.9*I))
// Calculate HS^-
aHS=S/(H/9.77e-8+1/A1+2.75e-10*aS^4/H/A2+3.63e-10*aS^3/H/A2+2.88e-12*aS^2/H/A2+1.38e-15*aS/H/A2)
HS=aHS/A1
S5=(2.75e-10*aS^4*aHS/H/A2)
S4=(3.63e-10*aS^3*aHS/H/A2)
S3=(2.88e-12*aS^2*aHS/H/A2)
S2=(1.38e-15*aS*aHS/H/A2)
S0T=4*S5+3*S4+2*S3+S2
// Calculate concentrations of Ag species given current estimate of K's
AGHS2=((K1*(HS^1.5)*(H^0.5)*(A1^0.5)))
AGSHS2=(K2*(HS^2)*(A1^2))/(A2^1)
AGHS=((K3*(HS^0.5)*(H^0.5)*(A1^0.5)))
AGS42=(((K4*(HS^3)*(A1^3)*(as^12))/((H^3)*(A3^2)))^0.5)
AGHSS4=(((K5*(HS^3)*(A1^3)*(as^6))/((H)))^0.5)
AGS4S5=(((K6*(HS^3)*(A1^3)*(as^14))/((H^3)))^0.5)
AGCLHS=K9*(acl)*(HS^0.5)*(H^0.5)*(a1^0.5)
AGS5OH=(((K10*(HS^0.5)*(A1^0.5)*(as^4))/((H^1.5)*(A2))))
AGS5=(K11*(as^4)*(HS^0.5))/((H^0.5)*(A1^0.5))
AGOHHS=((K12)*(HS^0.5)*(A1^0.5))/(H^0.5)
AG=AGHS2+AGSHS2+AGHS+AGS42+AGHSS4+AGS4S5+AGCLHS+AGS5OH+AGOHHS+AGS5
AGT=LOG10(AG)

Appendix III

Silver Models and Data cont.

Sugaki Silver Model

// MicroMath Scientist Model File SUGAKI MODEL
// Independent variables are variables in a set of equations that are not constant and do not depend on any of the other variables. They include: pH (PH), total sulfide (S), ionic strength (I), activity sulfur (as) and activity chloride (acl)
IndVars: PH, S, I, as, acl
// *Dependent variables are the unknowns, which can be calculated from independent variables, parameters, constants, or other dependent variables. AGT is the logarithm of the calculated [Ag] and will be compared to logarithm of the observed [Ag]*
DepVars: AGT, AG2SH2S, AG2SH2SHS, AG2SH2SHS2, AG2SHS2, AGCLHS, AGS5, AGOHHS
// Parameters are variables whose values are changed during least squares fitting. K's are equilibrium constants of Ag species
Params: K1, K2, K3, K4, K5, K6
// Calculate H^+ and activity coefficients from Davies Equation
H=10^(-PH)
A1=10^(-0.5*(I^0.5/(1+I^0.5)-0.2*I))
A2=10^(-2*(I^0.5/(1+I^0.5)-0.2*I))
A3=10^(-4.6*(I^0.5/(1+I^0.5)-0.9*I))
// Calculate HS^- and polysulfide concentrations
aHS=S/(H/9.77e-8+1/A1+2.75e-10*aS^4/H/A2+3.63e-10*aS^3/H/A2+2.88e-12*aS^2/H/A2+1.38e-15*aS/H/A2)
HS=aHS/A1
S5=(2.75e-10*aS^4*aHS/H/A2)
S4=(3.63e-10*aS^3*aHS/H/A2)
S3=(2.88e-12*aS^2*aHS/H/A2)
S2=(1.38e-15*aS*aHS/H/A2)
S0T=4*S5+3*S4+2*S3+S2
// Calculate concentration of Ag species given current estimates of K's
AG2SH2S=(K1*(HS)*H*A1)
AG2SH2SHS=K2*(HS^2)*H*A1
AG2SH2SHS2=(K3*(HS^3)*H*(A1^3))/(A2)
AG2SHS2=(K4*(HS^2)*(A1^2))/A2
AGCLHS=K5*acl*(HS^0.5)*(H^0.5)*(A1^0.5)
AGS5=(K6*(as^4)*(HS^0.5))/((H^0.5)*(A1^0.5))
AG=AG2SH2S+AG2SH2SHS+AG2SH2SHS2+AG2SHS2+AGCLHS+AGS5
AGT=LOG10(AG)
***

Appendix III

Silver Models and Data cont.

Stefansson and Seward (2003) Silver Data

P/bar	m S (mol/kg)	m NaOH (mol/kg)	m Ag (mol/kg)
1	0.061	0.000	6.27e-07
1	0.048	0.000	4.90e-07
1	0.086	0.000	8.30e-07
1	0.101	0.008	1.12e-06
1	0.059	0.004	7.20e-07
1	0.110	0.006	1.16e-.06
1	0.115	0.008	1.15e-06
1	0.127	0.008	1.09e-06
1	0.053	0.000	4.97e-07
1	0.007	0.000	1.85e-07
1	0.131	0.053	2.70e-06
1	0.043	0.040	3.75e-07
1	0.131	0.080	3.09e-06
1	0.101	0.113	5.52e-07
1	0.039	0.108	1.02e-07
1	0.122	0.112	2.03e-06
1	0.176	0.210	1.94e-06

The pH of the samples were calculated based on the NaOH and total sulfide concentrations

Appendix III

Silver Models and Data cont.

Model to Calculate AgAsS(HS)(OH)

// MicroMath Scientist Model File AgAsS(SH)(OH)
// Independent variables are variables in a set of equations that are not constant and do not depend on any of the other variables. They include: pH (PH), total sulfide (S), ionic strength (I), activity sulfur (as) and activity chloride (acl)
IndVars: PH, S, I, as, acl, ARS, index*
// *Dependent variables are the unknowns, which can be calculated from independent variables, parameters, constants, or other dependent variables. AGT is the logarithm of the calculated [Ag] and will be compared to the logarithm of the observed [Ag]*
DepVars: AGT, AGHS2, AGSHS2, AGHS, AGCLHS, AGS5, AGASSHSOH
// Parameters are variables whose values are changed during least squares fitting. K's are equilibrium constants of Ag species
Params: K1, K2, K3, K7, K9, K11, aag
// Calculate H^+ and activity coefficients from Davies Equation
H=10^(-PH)
A1=10^(-0.5*(I^0.5/(1+I^0.5)-0.2*I))
A2=10^(-2*(I^0.5/(1+I^0.5)-0.2*I))
A3=10^(-4.6*(I^0.5/(1+I^0.5)-0.9*I))
// Calculate HS^- and polysulfide concentrations
HS=S/(H/9.77e-8+1/A1+2.75E-10*as^4/H/A2+3.63e-10*as^3/H/A2+
2.88e-12*as^2/H/A2+1.38e-15*as/H/A2+2*ARS)
// Calculate concentration of Ag species given current estimates of K's
AGHS2=((K1*(HS^1.5)*(H^0.5)*(aag^(0.5*index))*(A1^0.5)))
AGSHS2=(K2*(HS^2)*(aag^(index))*(A1^2))/(A2^1)
AGHS=((K3*(HS^0.5)*(H^0.5)*(aag^(0.5*index))*(A1^0.5)))
AGCLHS=K9*(acl)*(HS^0.5)*(H^0.5)*(a1^0.5)*(aag^(0.5*index))
AGS5=(K11*(as^4)*(HS^0.5)*(aag^(0.5*index)))/((H^0.5)*(A1^0.5))
AGASSHSOH=(K7*ARS*A1*(aag^(0.5*index))*(H^0.5))/((HS^0.5)*(A1^0.5))
AG=AGHS2+AGSHS2+AGHS+AGCLHS+AGS5+AGASSHSOH
AGT=LOG10(AG)

**Index value set to 0 for samples containing acanthite. This was the effect of overriding the current value of aag and forcing aag to equal 1. Index value set to 1 for trechmannite samples because it did not contain acanthite, so the computer program will apply the current value of aag to fit the samples.*

Appendix IV

Mercury Models and Data

Paquette Model

// MicroMath Scientist Model File
// Independent variables are variables in a set of equations that are not constant and do not depend on any of the other variables. They include: pH (PH), total sulfide (S), ionic strength (I), activity sulfur (as) and activity HgS (aHGS)
IndVars: pH, S, I, aS, aHGS
// *Dependent variables are the unknowns, which can be calculated from independent variables, parameters, constants, or other dependent variables. HGT is the logarithm of the calculated [Hg] and will be compared to the logarithm of the observed [Hg]*
DepVars: HGT, HS, HGSH2, HGSHS, HGS2, HGSnHS
// Parameters are variables whose values are changed during least squares fitting. K's are equilibrium constants of Hg species
Params: K1, K2, K3, K4
// Calculate H^+ and activity coefficient form Davies Equation
H=10^(-pH)
A1=10^(-0.5*(I^0.5/(1+I^0.5)-0.2*I))
A2=10^(-2*(I^0.5/(1+I^0.5)-0.2*I))
A3=10^(-4.6*(I^0.5/(1+I^0.5)-0.9*I))
// Calculate HS^- and polysulfide concentrations
aHS=S/(H/9.77e-8+1/A1+2.75e-10*aS^4/H/A2+3.63e-10*aS^3/H/A2+2.88e-12*aS^2/H/A2+1.38e-15*aS/H/A2)
HS=aHS/A1
S5=(2.75e-10*aS^4*aHS/H/A2)
S4=(3.63e-10*aS^3*aHS/H/A2)
S3=(2.88e-12*aS^2*aHS/H/A2)
S2=(1.38e-15*aS*aHS/H/A2)
S0T=4*S5+3*S4+2*S3+S2 *// Calculate total zero-valent sulfur*
// Calculate concentration of Hg species given current estimate of K's
HGSH2=K1*HS*H*A1*aHGS
HGSHS=K2*HS*aHGS
HGS2=(K3*HS*aHGS)/(H*A2)
HGSnHS=K4*aS*HS
HG=HGSH2+HGSHS+HGS2+HGSnHS
HGT=LOG10(HG)
***

Appendix IV

Mercury Models and Data cont.

Mercury Data from Paquette and Helz (1997)

No S^o Added			S^o Added		
pH	Sulfide (mM)	ΣHg (nm)	pH	Sulfide (mM)	ΣHg (nm)
0.68	12.2	7.23	1.21	0.7	10.3
0.74	28.7	6.13	1.4	4.26	45.5
0.79	11.6	21.8	2.42	1.92	10.6
0.79	5.6	202	2.91	5.57	8.77
0.91	5.6	32.3	3.68	5	12.2
1.1	142	68.4	4.14	1.2	12.5
1.27	44.1	46.5	4.28	0.82	14.5
1.53	66.6	31.4	4.33	5.05	17.9
1.59	22	937	4.63	1.7	9.97
1.75	10.5	292	6.33	13.5	65.6
3.34	0.78	3.29	6.58	6.41	194
3.91	0.8	8.13	6.64	7.29	660
3.96	1.59	8.13	6.66	3.78	40.1
3.98	9.01	58.9	6.75	4.89	663
3.99	13.4	13.6	7.03	7.24	571
4.86	1.46	12.1	7.2	23	1690
4.96	2.67	2.94	7.43	3.12	53.4
5.43	4.79	47.2	7.83	10.2	170
10.48	13.4	3917.42	819	4.07	1290
1.92	23.5	139	8.25	1.81	47.7
1.96	18.6	74.5	8.53	1.92	824
2.25	13.1	365	9.04	10.9	15800
3.04	2.64	7.43	9.16	9.43	2480
3.34	5.82	5.23	9.2	5.92	6230
5.93	2.62	12.9	9.4	6.06	1320
5.98	3.24	4.34			
6.47	2.12	9.52			
6.97	5.03	206.8			
7.07	8.89	56.2			
7.09	9.21	18.1			
7.13	4.43	29.4			
7.31	20.2	35.5			
7.54	6.54	22.6			
8.06	3.36	125.0			
8.06	3.65	968			
8.38	24.7	132			
8.39	16.4	34			
8.95	6.2	40.9			
9.07	28	377			
11.11	23.3	745000			
11.14	2.84	12500			
9.65	2.64	39.7			
9.76	3.27	88.8			
10.48	13.4	13.4			
10.52	29.9	29.9			

Appendix IV

Mercury Models and Data cont.

Jay Model

// MicroMath Scientist Model File
// Independent variables are variables in a set of equations that are not constant and do not depend on any of the other variables. They include: pH (PH), total sulfide (S), ionic strength (I), activity sulfur (as) and activity HgS (aHGS)
IndVars: pH, S, I, aS, aHGS
// *Dependent variables are the unknowns, which can be calculated from independent variables, parameters, constants, or other dependent variables. HGT is the logarithm of the calculated [Hg] and will be compared to the logarithm of the observed [Hg]*
DepVars: HGT, HS, HGSH2, HGSHS, HGS2, HGSH, HG2, HGS, HGSx2, HGSxOH
// Parameters are variables whose values are changed during least squares fitting. K's are equilibrium constants of Hg species
Params: K1, K2, K3, K4, K5, K6, K7, K8
// Calculate H^+ and activity coefficient form Davies Equation
H=10^(-pH)
A1=10^(-0.5*(I^0.5/(1+I^0.5)-0.2*I))
A2=10^(-2*(I^0.5/(1+I^0.5)-0.2*I))
A3=10^(-4.6*(I^0.5/(1+I^0.5)-0.9*I))
// Calculate HS^- and polysulfide concentrations
aHS=S/(H/9.77e-8+1/A1+2.75e-10*aS^4/H/A2+3.63e-10*aS^3/H/A2+
2.88e-12*aS^2/H/A2+1.38e-15*aS/H/A2)
HS=aHS/A1
S5=(2.75e-10*aS^4*aHS/H/A2)
S4=(3.63e-10*aS^3*aHS/H/A2)
S3=(2.88e-12*aS^2*aHS/H/A2)
S2=(1.38e-15*aS*aHS/H/A2)
S0T=4*S5+3*S4+2*S3+S2 *// Calculate total zero-valent sulfur*
// Calculate concentration of Hg species given current estimate of K's
HGSH2=K1*HS*H*A1*aHGS
HGSHS=K2*HS*aHGS
HGS2=(K3*HS*aHGS)/(H*A2)
HGSH=K4*aHGS*H
HG2=(K5*H)/(HS)
HGS=K6
HGSx2=K7*HS*aS
HGSxOH=(K8*aS)/H
HG=HGSH2+HGSHS+HGS2+HGSH+HG2+HGS+HGSx2+HGSxOH
HGT=LOG10(HG)

Appendix IV

Mercury Models and Data cont.

Mercury data from Jay et al., (2000)

Data Set	pH	Sulfide (M)	Soluble Hg (M)
1	6.33	1.35E-02	6.56E-08
1	6.58	6.41E-03	1.94E-07
1	6.64	7.29E-03	6.60E-07
1	6.66	3.78E-03	4.01E-08
1	6.75	4.89E-03	6.63E-07
1	7.03	7.24E-03	5.71E-07
1	7.2	2.30E-02	1.69E-06
1	7.43	3.12E-03	5.34E-08
1	7.83	1.017E-02	1.7E-07
1	8.19	4.07E-03	1.29E-06
1	8.25	1.81E-03	4.77E-08
1	8.53	1.92E-03	8.24E-07
1	9.04	1.089E-02	1.58E-05
1	9.2	5.92E-03	6.23E-06
1	9.4	6.06E-03	1.32E-06
2	8	4.89E-05	1.71E-08
2	8	5.26E-05	1.09E-08
2	8	6.70E-05	1.39E-08
2	7	2.25E-06	5.40E-09
2	8	3.59E-04	7.21E-08
2	8	4.81E-03	1.56E-06
2	9	3.22E-03	4.37E-06
2	8	6.25E-05	1.52E-08
2	8	4.81E-03	2.59E-06
2	9	8.36E-05	1.80E-07
2	9	8.36E-05	1.81E-07
2	9	3.47E-04	4.19E-07
2	9	3.22E-03	6.24E-06
2	10	7.53E-05	4.65E-07
2	10	1.30E-04	7.56E-07
2	10	1.96E-04	1.66E-06
2	10	1.63E-03	9.04E-06
2	7	2.52E-03	4.34E-08
1. Data from Paquette & Helz (1997), 2. Data from Jay et al. (2000)			

Appendix V

Derivation and Programs for As-HCO_3 Complexes

Derivation for $As(CO_3)_2^-$

$As(CO_3)_2^- = K_{Asc} \times K_{SO} \times a^{0.5} \times T_{As\text{-}NaCl} \times (HCO_3^-)^2 \times H^+ \times \gamma_{HCO3} \times \gamma_{AS(OH)3}$

$$Total_{As} = \frac{K_{SO} * K_p^{(index)}}{\gamma_{As(OH)3}} + \frac{K_{SO} * 10^{-9.17} * K_p^{(index)}}{\gamma_{AsO(OH)2} * 10^{-pH}} + K_{ACO} * K_{SO} * K_p^{(index)} * HCO_3^{-2} * H * \gamma_{HCO3}$$

Derivation for $As(CO_3)^+$

$As(CO_3)^+ = K_{Asc} \times K_{SO} \times a^{0.5} \times T_{As\text{-}NaCl} \times HCO_3^- \times (H^+)^2$

$$Total_{As} = \frac{K_{SO} * K_p^{(index)}}{\gamma_{As(OH)3}} + \frac{K_{SO} * 10^{-9.17} * K_p^{(index)}}{\gamma_{AsO(OH)2} * 10^{-pH}} + K_{ACO} * K_{SO} * K_p^{(index)} * HCO_3^{-} * H^2$$

Programs Used to Calculate Equilibrium Constants for Individual Arsenic-Carbonate Complexes

$As(OH)_2(CO_3)^-$

// MicroMath Scientist Model File

*// Independent variables are variables in a set of equations that are not constant & do not depend on any other variables. Include: [bicarbonate] (HCO), pH, & index**

IndVars: HCO, Index, pH

// *Dependent variables are the unknowns, which can be calculated from independent variables, parameters, constants, or other dependent variables. AST is the logarithm of the calculated [As] and will be compared to the logarithm of the observed [As]*

DepVars: AST, ASOOH, ASCARB

// Parameters are variables whose values are changed during least squares fitting. K's are equilibrium constants of As species

Params: Ks, Kc, Kp

// Activity coefficients for $As(OH)_3$ (g0) and HCO_3^- (g1)

g0=1.09

g1=0.68

// Calculate concentration of As species

ASOOH=10^(-9.17)*Ks* K_p^(index)/(g1*pH)

ASCARB=Kc*Ks*Kp^(index)*HCO

AS=Ks*Kp^(Index)/g0+ 10^(-9.17)*Ks* K_p^(index)/g1/10^(-pH) + Kc*Ks* K_p^(index)*HCO

AST=LOG10(AS)

Appendix V

Derivation and Programs for As-HCO_3 Complexes cont.

Programs Used to Calculate Equilibrium Constants for Arsenic-Carbonate Complexes

$As(CO_3)_2^-$

// MicroMath Scientist Model File

*// Independent variables are variables in a set of equations that are not constant & do not depend on any other variables. Include: [bicarboante] (HCO), pH, & index**

IndVars: HCO, Index, pH

// *Dependent variables are the unknowns, which can be calculated from independent variables, parameters, constants, or other dependent variables. AST is the logarithm of the calculated [As] and will be compared to the logarithm of the observed [As]*

DepVars: AST, ASOOH, ASCARB

// Parameters are variables whose values are changed during least squares fitting. K's are equilibrium constants of As species

Params: Ks, Kc, Kp

// Activity coefficients for $As(OH)_3$ (g0) and HCO_3^- (g1)

g0=1.09

g1=0.68

// Calculate concentration of As species

ASOOH=10^(-9.17)*Ks*K_p^index/(g1*10^-pH)

ASCARB=Kc*Ks*a^(0.5)*(HCO^2)*10^(-pH)*g1

AS=Ks*K_p^(Index)/g0+ 10^(-9.17)*Ks*K_p^(Index)/g1/10^(-pH) + Kc*Ks*K_p^(Index)*(HCO^2)*10^(-pH)*g1

AST=LOG10(AS)

***

$As(CO_3)^+$

// MicroMath Scientist Model File

*// Independent variables are variables in equations that are not constant & do not depend on any other variables. Include: [bicarbonate] (HCO), pH, & index**

IndVars: HCO, Index, pH

// *Dependent variables are the unknowns, which can be calculated from independent variables, parameters, constants, or other dependent variables. AST is the logarithm of the calculated [As] and will be compared to the logarithm of the observed [As]*

DepVars: AST, ASOOH, ASCARB

// Parameters are variables whose values are changed during least squares fitting. K's are equilibrium constants of As species

Params: Ks, Kc, Kp

// Activity coefficients for As $(OH)_3$ (g0) and HCO_3^- (g1)

g0=1.09

g1=0.68

// Calculate concentration of As species

ASOOH=10^(-9.17)*Ks*a^.05/(g1*pH)

ASCARB=Kc*Ks*K_p^(index)*(HCO)*(10^(-pH)^2)*g1

Appendix V

Derivation and Programs for As-HCO_3 Complexes cont.

Programs Used to Calculate Equilibrium Constants for Arsenic-Carbonate Complexes

$As(CO_3)^+$ cont.

AS=Ks*Kp^(Index)/g0+ 10^(-9.17)*Ks* K_p^(index)/g1/10^(-pH) + Kc*Ks* K_p^(index)*(HCO)*(10^(-pH)^2)
AST=LOG10(AS)
***

** The index value of K_p was set to 0 in Runs with Arsenolite only, so in any experiment with arsenolite K_p will be given a value of 1. The index value of K_p in the Runs with claudetite and arsenolite will be set to 1, so the computer program will vary the equilibrium constant to calculate the actual equilibrium constant (K_p).*

References

Abdullah M.I., Shiyu Z., and Mosgren K. (1995) Arsenic and selenium species in the oxic and anoxic waters of the Oslofjord, Norway. *Marine Pollution Bulletin* **31**, 116-126.

Adams N. W. H. and Kramer J. R. (1999) Silver speciation in wastewater effluent, surface waters, and pore waters. *Environ. Toxicology and Chemistry* **18**, 2667-2673.

Ahmed K., Bhattacharya P., Hasan M., Akhter S., Alam S.M., Bhuyian M. A., Imam M., Khan A., and Sracek O. (2004) Arsenic enrichment in groundwater of the alluvial aquifers in Bangladesh: an overview. *Applied Geochemistry* **19**, 181-200.

Akagi H.and Naganuma, A. (2000) Human exposure to mercury and the accumulation of methylmercury that is associated with gold mining in the Amazon Basin, Brazil. *J. of Health Science* **46**, 323-328.

Al-Farawati R.and Van Den Berg C.M.G. (2001) Thiols in coastal waters of the Western North Sea and English Channel. *Environ. Sci. Tech.* **35**, 1902-1911.

Anawar H. M., Akai J., Mostofa K. M. G., Safiullah S., and Tareq S. M. (2002) Arsenic poisoning in groundwater health risk and geochemical sources in Bangladesh. *Environment International* **27**, 597-604.

Anderson E. and Story L.G. (1923) Studies on certain physical properties of arsenic trioxide in water solution. *J. American Chemical Society* **45**, 1102-1105.

Anderson G. M. (1962) The solubility of PbS in H_2S water solutions. *Economic Geology* **57**, 809-828.

Appelo C. A. J., van der Weiden M. J. J., Tournassat C., and Charlet L. (2002) Surface Complexation of Ferrous Iron and Carbonate on Ferrihydrite and the Mobilization of Arsenic. *Environ. Sci. Technol.* **36**, 3096-3103.

Arai Y., Lanzirotti A., Sutton S., Davis J. A., and Sparks, D. L. (2003) Arsenic speciation and reactivity in poultry litter. *Environ. Sci. Technol*. **37**, 4083-4090.

Arcand G. M. (1957) Distribution of tripositive arsenic between hydrochloric acid solutions and β,β'-dichlorodiethyl ether. *J. of the American Chemical Society* **79**, 1865-1870.

Aurillo A., Mason R., and Hemond H. (1994) Speciation and fate of arsenic in three lakes of the Aberjona Watershed. *Environ. Sci. Technol*. **28**, 577-585.

Bakir F., Damluji S. F., Amin-Zaki L., Murtadha M., Khalidi A., Al-Rawi N. Y., Tikriti S., Dhahir H. I., Clarkson T. W., Smith J. C., and Doherty R. A. (1973) Methylmercury poisoning in Iraq. *Science* **181**, 230-241.

Baumgarten E. and Kirchhausen-Dusing, U. (1997) Sorption of metal ions on alumina. *J. Coll. Interface Sci.* **194**, 1-9.

Bell R. A. and Kramer J. R. (1999) Structural chemistry and geochemistry of silver-sulfur compounds: critical review. Environ. *Toxicology and Chemistry* **18**, 9-22.

Benoit J. M., Gilmour C. C., Mason R. P., and Heyes A. (1999) Sulfide controls on mercury speciation and bioavailability to methylating bacteria in sediment pore waters. Environ. *Sci. Technol.* **33**, 951-957.

Benoit J.M., Gilmour C.C., and Mason R.P. (2001) The influence of sulfide on solid-phase mercury bioavailability for methylation by pure cultures of desulfobulbus propionicus (1pr3). *Environ. Sci. Technol.* **35**, 127-132.

Berry W., Cantwell M., Edwards P., Serbst J., and Hansen D. (1999) Predicting toxicity of sediments spiked with silver. *Environ. Toxicology and Chemistry* **18**, 40-48.

Bianchini A., Bowles K. C., Brauner C. J., Gorsuch J. W., Kramer J. R.., andWood C. M. (2002) Evaluation of the effect of reactive sulfide on the acute toxicity of silver (I) to Daphnia Magna. Part 2: Toxicity Results. *Environ. Toxicology and Chemistry* **21**, 1294-1300.

Bhattacharya P., Jacks G., Ahmed K.M., Routh J., and Khan A.A. (2002) Arsenic in the groundwater of the Bengal Delta plain aquifers in Bangladesh. *Bull. Environ. Contam. Toxicol.* **69**, 538-545.

Bothner M.H., Buchholtz ten Brink M., and Manheim F. T. (1998) Metal concentrations in surface sediments of Boston harbor-changes with time. *Marine Environ. Research* **45**, 127-155.

Boulegue J., Lord III C. J., and Church T. M. (1982) Sulfur speciation and associated trace metlas (Fe, Cu) in the pore waters of Great Marsh, Delaware. *Geochim. Cosmochim. Acta* **46**, 453-464.

Bryndzia L. T. and Kleppa O. J. (1989) Standard molar enthalpies of formation of sulfosalts in the Ag-As-S system and thermochemistry of the sulfosalts of Ag with As, Sb and Bi. *American Mineralogist* **74**, 243-249.

Cernosek Z., Cernoskova E., and Benes L. (1999) Crystalline arsenic trisulfide: preparation, differential scanning calorimetry and Raman scattering measurements. *Materials Letters* **38**, 336-340.

Chatterjee A., Das D., Mandal B., Chowdury T., Samanta G., and Chakraborti D. (1995) Arsenic in groundwater in six districts of West Bengal, India: The biggest arsenic calamity in the World. Part 1. Arsenic species in drinking water and urine of the affected people. *The Analyst* **120**, 643-650.

Chen K. Y. and Morris J. C. (1972) Kinetics of oxidation of aqueous sulfide by O_2. *Environ. Sci. Technol*. **6**, 529-537.

Chen S., Dzeng S., Yang M., Chiu K., Shieh G., and Wai C. (1994) Arsenic species in groundwaters of the blackfoot disease area, Taiwan. *Environ. Sci. Technol*. **28**, 877-881.

Clarke M. B. (1998) Arsenic, copper and cadmium in sulfidic waters; Thioarsenites as ligands for Cu(I). Doctoral Dissertation, University of Maryland, College Park, MD.

Clarke M. B. and Helz G. R. (2000) Metal-thiometalate transport of biologically active trace elements in sulfidic environments. 1. Experimental evidence for copper thioarsenite complexing. *Environ. Sci. Technol. **34***, 1477-1482.

Clever H. L., Johnson S. A., and Derrick M. E. (1985) The solubility of mercury and some sparingly soluble mercury salts in water and aqueous electrolyte solutions. *J. Phy. Chem. Ref. Data* **14**, 631-680.

Cline J. D. (1969) Spectrophotometric determination of hydrogen sulfide in natural waters. *Limnology and Oceanography* **14**, 454-458.

Cloke P. L. (1963) The geological role of polysulfides-Part II The solubility of acanthite and covellite in sodium polysulfide solutions. *Geochimica et Cosmochimica Acta* **27**, 1299-1319.

Compeau G.C. and Bartha R. (1985) Sulfate-reducing bacteria: Principal methylators of mercury in anoxic estuarine sediments. *Applied and Environ. Microbiology* **50**, 498-502.

Cosden J. M. and Byrne R. H. (2003) Comparative geochemistries of Pd(II) and Pt(II): Formation of mixed hydroxychloro and chlorocarbonato-complexes in seawater. *Geochimica et Cosmochimica Acta* **67**, 1331-1338.

Cullen W. and Reimer K. J. (1989) Arsenic speciation in the environment. *Chem, Rev.* **89**, 713-764.

Cutter G. (1992) Kinetic controls on metalloid speciation in seawater. *Marine Chemistry* **40**, 65-80.

Cutter G., Cutter L., Featherstone A., and Lohrenz S. (2001) Antimony and arsenic biogeochemistry in the western Atlantic Ocean. *Deep-Sea Research* **48**, 2895-2915.

Das D., Chaterjee A., Mandal B. K., Samanta G., and Chakraborti D. (1995) Arsenic in ground water in six districts of west Bengal, India: the biggest arsenic calamity in the world. Part 2. Arsenic concentration in drinking water, hair, nails, urine, skin-scale and liver tissue (biopsy) of the affected people. *Analyst* **120**, 643-650.

Dreher G. B. and Follmer L. R. (2004) Mercury content of Illinois soils. *Water, Air, and Soil Pollution* **156**, 299-315.

Dudka S. andAdriano D. (1997) Environmental impacts of metal ore mining and processing: a review. J. *Environ. Qual.* **26**, 590-602.

Eary L.E. (1992) The solubility of amorphous As_2S_3 from 25 to 90°C. *Geochimica et Cosmochimica Acta* **56**, 2267-2280.

Ellis A. J. and Milestone N. B. (1967) The ionization constants of hydrogen sulfide from 20^o to 90^o. *Geochimica et Cosmochimica Acta* **31**, 615-620.

Environmental Protection Agency. (2001) Federal Register, Part VIII, 40 CFR Parts 9, 141, and 142 national primary drinking water regulations; arsenic and clarifications to compliance and new source contaminants monitoring; final rule. National Archives and Records Administration, Washington, DC.

Erickson B. (1998) The speciation of molybdenum in sulfidic natural waters. Ph.D. Dissertation, University of Maryland, College Park, MD.

Eto K., Tokunga H., Nagashima K., and Takeuchi T. (2002) An autopsy case of Minamata Disease (methylmercury poisoning)-pathological viewpoints of peripheral nerves. *Toxicological Pathology* **30**, 714-722.

Factor-Litvak P., Wasserman G., Kline J. K., and Graziano J. (1999) The Yugoslavia Prospective Study of environmental lead exposure. *Environmental Health Perspectives* **107**, 9-15.

Ferguson J. and Gavis J. (1972) A review of the arsenic cycle in natural waters. *Water Research* **6**, 1259-1274.

Fijolek H. G., Gonzalez-Duarte P., Park S., Suib S. L., and Natan M. J. (1997) Structure-spectroscopy correlations in silver thiolates: application to the structure of silver 1,5-pentanedithiolate. *Inorg. Chem*. **36**, 5299-5305.

Fisher N. S. and Wang W. (1998) Trophic transfer of silver to marine herbivores: a review of recent studies. Environ. *Toxicology and Chemistry* **17**, 562-571.

Flegal A. R. and Sanudo-Wilhelmy S. A. (1993) Comparable levels of trace metal contamination in two semi-enclosed embayments: San Diego Bay and South San Francisco Bay. *Environ. Sci. Technol.* **27**, 1934-1936.

Flegal A. R., Rivera-Duarte I., and Sanudo-Wilhelmy S. A. (1997) Silver contamination in aquatic environments. *Reviews of Environ. Contamination and Toxicology* **148**, 139-160.

Fujusawa K., Imai S., Suzuki S., Yoshihiko M., Miyashita Y., Yamada, Y., and Okamoto K. (2000) M-S vibrational study in the three-coodinate thiolato compounds $(Net_4)_2[M(SC_6H_4\text{-}p\text{-}X)_3]$ and $(Net_4)_2[M_4(\mu\text{-}SC_6H_4\text{-}p\text{-}Cl)_6]$: M=Cu(I) and Ag(I), X=Cl and Br. *J. of Inorg. Biochem*. **82**, 229-238.

Gade B., Pollman H., Heindl A., and Westermann H. (2001) Long-term behavior and mineralogical reactions in hazardous waste landfills: a comparison of observation and geochemical modeling. Env*ironmental Geology* **40**, 248-256.

Gammons C. H. and Barnes H. L. (1989) The solubility of Ag_2S in near-neutral aqueous sulfide solutions at 25 to 300°C. *Geochimica et Cosmochimica Acta* **53**, 279-290.

Garrett A.B., Holmes O., and Laube A. (1940) The Solubility of Arsenious Oxide in Dilute Solutions of Hydrochloric Acod and Sodium Hydroxide. The Character of the Ions of Trivalent Arsenic. Evidence for Polymerization of Arsenious Acid. *J. of the American Chemical Society* **62**, 2024-2028.

Ghosal S. and Sack R. O. (1995) As-Sb energetics in argentian sulfosalts. *Geochimica et Cosmochimica Acta* **59**, 3573-3579.

Giggenbach W. F. (1974) Equilibria involving polysulfide ions in aqueous sulfide solutions up to 240°. *Inorganic Chemistry* **13**, 1724-1730.

Giordano T.H. and Barnes H.L. (1979) Ore solution chemistry VI. PbS solubility in bisulfide solution to 300°C. *Economic Geology* **74**, 1637-1646.

Giusti L. and Zhang H. (2002) Heavy metals and arsenic in sediments, mussels and marine water from Murano (Venice, Italy). *Environ. Geochemistry and Health* **24**, 47-65.

Goldberg S. and Johnston C. T. (2001) Mechanisms if arsenic adsorption on amorphous oxides evaluated using macroscopic measurements, vubrational spectroscopy and surface complexation modeling. *J. of Colloid and Interface Science* **234**, 204-216.

Goldstein S.H. and Babich H. (1989) Differential effects of arsenite and arsenate to Drosophila melanogaster in a combined adult/developmental toxicity assay. *Bulletin of Environ. Contam. and Toxicol*. **42**, 276-282.

Grandjean P., Weihe P., White R. A., and Debes F. (1998) Cognitive performance of children prenatally exposed to "safe" levels of methylmercury. *Environ. Research Section A* **77**, 165-172.

Habibi D., Ghaemi E., Parish R.V., and Pritchard R. G. (1999) A polymeric silver(I) thiolate with diverse co-ordination numbers: $[\{AgSCH_2CH_2NMe_2\}_5 \bullet 0.5H_2O]_n$. *Polyhedron* **18**, 2977-2979.

Hall H. T. (1966) The systems Ag-Sb-S, Ag-As-S and Ag-Bi-S: Phase relations and mineralogical significance. Ph. D. Dissertation, Brown University, Providence, RI.

Hancock R. D., Finkelstein N. P., and Evers A. (1974) Linear free energy relationships in aqueous complex-formation reactions of the d^{10} metal ions. *J. Inorg. Nucl. Chem.* **36**, 2539-2543.

Helz G. R., Tossell J. A., Charnock J. M., Pattrick R. A. D., Vaughan D. J., and Garner C. D. (1995) Oligomerization in As(III) sulfide solutions: Theoretical constraints and spectroscopic evidence. *Geochimica et Cosmochimica Acta* **22**, 4591-4604.

Helz G. R., Valerio M. S., and Capps N. E. (2002) Antimony speciation in alkaline sulfide solutions: Role of zerovalent sulfur. *Environ. Sci. Technol.* **36**, 943-948.

Hirsch M. (1998) Availability of sludge-borne silver to agricultural crops. *Environ. Toxicology and Chemistry* **17**, 610-616.

Hyland J. L., Snoots T. R., and Balthis W. L. (1998) Sediment quality of estuaries in the southeastern U.S. *Environ. Monitoring and Assessment* **51**, 331-343.

Ivakin A. A., Vorob'eva S. V., Golelov, A. M., and Gertman E. M. (1979) Solubility of arsenic (III) sulphide in aqueous NaCl solutions. *Russian J. of Inorganic Chemistry* **24**, 1965-1969.

Jay J. A., Morel F. M. M., and Hemond H. F. (2000) Mercury speciation in the presence of polysulfides. *Environ. Sci Technol.* **34**, 2196-2200.

Jaworski J. (1987) Chapter 1 Lead. *In Lead, Mercury, Cadmium and Arsenic in the Environment* (ed. Hutchinson, T.C. and Meema, K.M.), John Wiley and Sons, New York.

Johnson K.S. and Pytkowicz R.M. (1979) Ion association of chloride and sulphate with sodium, potassium, magnesium and calcium in seawater at 25° C. *Mar. Chem.* **8**, 87-93.

Kaise T., Yamauchi H., Horiguchi Y., Tani T., Watanabe S., Hirayama T., and Fukui S. (1989) A comparative study on acute toxicity of methylarsonic acid, dimethylarsinic acid and trimethylarsine oxide in mice. *Applied Organometallic Chemistry* **3**, 273-7.

Kim M. and Nriagu J. (2000) Oxidation of arsenite in groundwater using ozone and oxygen. *The Science of the Total Environ.* **247**, 71-79.

Kim M., Nriagu J., and Haack S. (2000) Carbonate Ions and Arsenic Dissolution by Groundwater. *Environ. Sci. Technol.* **34**, 3094-3100.

Kinniburgh D., Smedley P., Davies J., Milne C., Gaus I., Tafford J., Burden S., Huq S.M., Ahmad N., and Ahmed K. (2003) The scale and cause of the groundwater arsenic problem in Bangladesh. In *Arsenic in Ground Water* (ed. Welch, Allen and Stollenwerk, Kenneth), Kluwer Academic Publishers, Norwell, MA. pp 211-257.

Koller K., Brown T., Spurgeon A., and Levy L. (2004) Recent developments in low-level lead exposure and intellectual impairment in children. *Environmental Health Perspectives* **112**, 987-994.

Kozlov V. K., Kuznetsov V. N., and Khodakovskiy I. L. (1983) The thermodynamic parameters of Ag_2O (c) and silver (I) hydroxy complexes in aqueous solution at elevated temperatures. *Geokhimiya* **2**, 215-227.

Kwon Y. T. and Lee C. W. (1998) Application of multiple ecological risk indices for the evaluation of heavy metal contamination in a coastal dredging area. *The Science of the Total Environ*. **214**, 303-210.

Lacey E. M., King J. W., Quinn J. G., Mecray E. L., Appleby P. G., and Hunt, A. S. (2001) Sediment quality in Burlington Harbor, Lake Champlain, U.S.A. *Water, Air, and Soil Pollution* **126**, 97-120.

Lister S. (2001) Center Speeds Approvals of Emergency IND. *Center for Drug Evaluation and Research* **7**, 1,8.

Loehr T. M. and Plane R. A. (1968) Raman spectra and structures of arsenious acid and arsenites in aqueous solution. *Inorganic Chemistry* **7**, 1708-1714.

Looser M. O., Parriaux A., and Bensimon M. (1999) Landfill underground pollution detection and characterization using inorganic traces. *Wat. Res*. **33**, 3609-3616.

Luther G. W., Giblin A. E., and Varsolona R. (1985) Polarographic analysis of sulfur species in marine porewaters. *Limnol. Oceanogr*. **30**, 727-749.

Mabuchi K., Lilienfeld A. M., and Snell L. M. (1979) Lung Cancer among pesticide workers exposed to inorganic arsenicals. *Archives of Environm. Health* **34** 312-320.

Mantei E. J. and Coonrod D. D. (1989) Heavy metal content in the stream sediments adjacent to a sanitary landfill. Environ. *Geol. Water Sci.* **13**, 51-58.

Martell A. E. and Smith R. M. (1974) *Critical Stability Constants* Plenum Publishing Corp., New York.

McArthur J. M., Banerjee D. M., Hudson-Edwards K. A., Mishra R., Purohit R., Ravenscroft P., Cronin A., Howarth R. J., Chaterjee A., Talukder T., Lowry D., Houghton S., Chadha D. K. (2004) Natural organic matter in sedimentary basins and its relation to arsenic in anoxic ground water: the example of West Bengal and its worldwide implications. *Applied Geochemistry* **19**, 1255-1293.

McMichael A. J., Baghurst P. A., Wigg N. R., Vimpani G. V., Robertson E. F., and Roberts R. J. (1988) Port Pirie Cohort Study: environmental exposure to lead and children's abilities at the age of four years. *New England Journal of Medicine* **319**, 468-475.

Miller G. C., Lyons W. B., and Davis A. (1996) Understanding the water quality of pit lakes. *Environ. Sci. Technol.* **30**, 119A-123A.

Mironova G. D. and Zotov A. V. (1980) Solubility studies of the stability of As(III) sulfide complexes at 90°C. *Geochem. Intl.* **17**, 46-54.

Mironova G. D., Zotov A. V., and Gul'ko N. I. (1984) Determination of the solubility of orpiment in acid solutions at 25-150°C. *Geochem. Intl.* **21**, 53-59.

Mironova G. D., Zotov A. V., and Gul'ko N. I. (1990) The solubility of orpiment in sulfide solutions at 25-150°C and the stability of arsenic sulfide complexes. *Geochem. Intl*. **27**, 61-73.

Mountain B. W. and Seward T. M. (1999) The hydrosulphide/sulphide complexes of copper(I): Experimental determination of stoichiometry and stability at 22^{o}C and reassessment of high temperature data. *Geochimica et Cosmochimica Acta* **63**, 11-29.

Mylon S. E. and Benoit G. (2001) Subnanomolar detection of acid-labile sulfides by the classical methylne blur method coupled to HPLC. *Environ. Sci. Technol.* **35**, 4544-4548.

Nickless G. (ed.) (1968) *Inorganic Sulfur Chemistry*. Elsevier Publishing Co, Amsterdam pp 672-657.

Nickson R. T., McArthur J. M., Ravenscroft P., Burgess W. G., and Ahmed K. M. (2000) Mechanism of arsenic release to groundwater, Bangladesh and West Bengal. *Applied Geochemistry* **15**, 403-413.

Nordstrom K.D. and Archer D.G. (2003) Arsenic thermodynamic data and environmental geochemistry. In *Arsenic in Ground Water* (eds. Welch A.H, and Stollenwerk K.G.), Kluwer Academic Publishers, Boston, pp. 1-25.

Nriagu J. and Pacyna J. (1988) Quantitative assessment of worldwide contamination of air, water and soil by trace metals. *Applied Geochemistry* **15**, 403-413.

O'Day P. A., Vlassopoulos D., Root R., and Rivera N. (2004) The influence of sulfur and iron on dissolved arsenic concentrations in the shallow subsurface under changing redox conditions. *Proceedings of the National Academy of Sciences of the United States of America* **101**, 13703-13708.

Oremland R. and Stolz J. (2003) The ecology of arsenic. *Science* **300**, 939-944.

Paquette K.E. (1994) Solubility of cinnabar (Red HgS) and implications for mercury speciation in sulfidic waters. Ph.D. Dissertation, University of Maryland, College Park, MD.

Paquette K. E. and Helz G. R. (1997) Inorganic speciation of mercury in sulfidic waters: The importance of zero-valent sulfur. *Environ. Sci. Technol*. **31**, 2148-2153.

Pacyna J. (1987) Chapter 7 Atmospheric emissions of arsenic, cadmium, lead and mercury from high temperature processes in power generation and industry. In *Lead, Mercury, Cadmium and Arsenic in the Environment*. (ed Hutchinson, T.C. and Meema, K.M.), John Wiley and Sons, New York.

Pascoe G. A., McLaren P., and Soldate M. (2002) Impact of offsite sediment transport and toxicity on remediation of a contaminated estuarine bay. *Marine Pollution Bulletin* **44**, 1184-1193.

Pavelka C., Loehr R. C., and Haikola B. (1993) Hazardous waste landfill leachate characteristics. *Waste Management* **13**, 573-580.

Pearson R. G. (1966) Acid and Bases. *Science* **151**, 172-177

Pearson R. G. (1988) Absolute electronegativity and hardness: application to inorganic chemistry. *Inorg. Chem*. **27**, 734-740.

Pelletier E. (1995) Environmental organometallic chemistry of mercury, tin and lead: present status and perspectives. In *Metal Speciation and Bioavailability in Aquatic Systems*. (ed Tessier, A and Turner, D.R.), John Wiley and Sons, New York.

Pettine M., Campanella L., and Millero F. (1999) Arsenite oxidation by H_2O_2 in aqueous solutions. *Geochim. Cosmochim. Acta* **63**, 2727-2735.

Pokrovski G., Gout R., Schott J., Zotov A., and Harrichoury J. C. (1996) Thermodynamic properties and stoichiometry of As (III) hydroxide complexes at hydrothermal conditions. *Geochim. Cosmochim. Acta* **60**, 737-749.

Prosi F. (1989) Factors controlling biological availability and toxic effects of lead in aquatic organisms. *The Science of the Total Environment* **79**, 157-169.

Purcell T. and Peters J. (1998) Sources of silver in the environment. *Environ. Toxicology and Chemistry* **17**, 539-546.

Radner K. J., Dombrowski P. M., Farley K. J., Mahony J. D., and Di Toro D. M. (2004) Effect of thioarsenite formation on arsenic(III) toxicity. *Environ. Toxicology and Chemistry* **23**, 1649-1654.

Rattte H. T.. (1999) Bioaccumulation and Toxicity of silver compounds: A review. Environ. *Toxicology and Chemistry* **18**, 89-108.

Ridley W. P., Dizikes L. J., and Wood J. M. (1977) Biomethylation of toxic elements in the environment. *Science* **197**, 329-332.

Robie R. A. and Hemingway B. S. (1995) Thermodynamic properties of minerals and related substances at 298.15K and 1 bar (105 pascals) pressure and at higher temperatures. *U. S. Geological Survey Bulletin* **2131**, 148.

Roland G. W. (1970) Phase relations below 575°C in the system Ag-As-S. *Economic Geology* **65**, 241-252.

Rose J. (ed.) (1998) *Environmental Toxicology Current Developments*. Gordon and Breach Science Publishers, Australia. pp 171-180.

Rozen T. and Luther G. (2002) Voltammetric evidence suggesting Ag speciation in dominated by sulfide complexation in river water. In *Environmental Electrochemistry Analysis of Trace Element Biogeochemistry*. (ed. Taillefert, M. and Rozan, T.), American Chemical Society, Washington D.C.

Sanudo-Wilhelmy S. A. and Gill G. A. (1999) Impact of the clean water act on the levels of toxic metals on Urban estuaries: The Hudson River estuary revisited. *Environ. Sci. Technol*. **33**, 3477-3481.

Saxena R. S. and Bhatnagar C. S. (1960) Potentiometric studies on mercuric arsenites. *Z. anorg. U. allgem. Chemie* **303**, 12-18.

Schildkraut D., Dao P., Twist J., Davis A., and Robillard K. (1998) Determination of silver ions at submicrogram-per-liter levels using anodic square-wave stripping voltammetry. *Environ. Toxicology and Chemistry* **17**, 642-649.

Schonau K. A. and Redfern S. A. (2002) High-temperature phase transitions, dielectric relaxation, and ionic mobility of proustite, Ag_3AsS_3, and pyrargyrite, Ag_3SbS_3. *J. of Applied Physics* **92**, 7415-7424.

Schwarzenbach G. and Widmer M. (1963) Solubility of metal sulfides. I. Mercuric sulfides. *Helv. Chim. Acta* **46**, 2613-2628.

Shea D. and Helz G. R. (1988) The solubility of copper in sulfidic waters: Sulfide and polysulfide complexes in equilibrium with covellite. *Geochimica et Cosmochimica Acta* **52**, 1815-25.

Smith G. J. and Flegal A. R. (1993) Silver in San Francisco Bay estuarine waters. *Estuaries* **16**, 547-558.

Spycher N. F. and Reed M. H. (1989) As(III) and Sb(III) sulfide complexes: An evaluation of stoichiometry and stability from existing experimental data. *Geochimica et Cosmochimica Acta* **53**, 2185-2194.

Stefansson A. and Seward T. M. (2003) Experimental determination of the stability and stoichiometry of sulphide complexes of silver(I) in hydrothermal solutions to 400°C. *Geochimica et Cosmochimica Acta* **67**, 1395-1413.

Stranski I. N., Plieth K., and Zoll I. (1958) Uber die Auflosung, die Loslichkeit und die Umwandlung der beiden Arsenik Modifikationen in Wasser und wa∃rigen Losungen. *Zeit. Electrochem*. **62**, 366-372.

Stumm W. and Morgan J.J. (1996) *Aquatic Chemistry-Chemical Equilibria and Rates in Natural Waters, 3rd edition*, John Wiley & Sons Inc., New York.

Sugaki A., Scott S. D., Hayashi K., and Kitakaze A. (1987) Ag_2S solubility in sulfide solutions up to 250°C. *Geochemical Journal* **21**, 291-305.

Sundelin B. and Eriksson A. (2001) Mobility and bioavailability of trace metals in sulfidic coastal sediments. *Env. Toxicol. And Chem.* **20**, 748-756.

Tamas M. and Wysocki R. (2001) Mechanisms involved on metalloid transport and tolerance acquisition. *Curr. Genet.* **40**, 2-12.

Tossell J. A. (2000) Theoretical studies on metal thioarsenites and thioantimonides: Synergistic interactions between transition metals and heavy metalloids. *Geochemical Transactions* article 3.

Tossell J. A. (2000a) Metal-thiometalate transport of biologically active trace elements in sulfidic environments. 2. Theoretical evidence for copper thioarsenite complexing. *Environ. Sci. Technol.* **34**, 1483-1488.

Tossell J. A. (2001) Calculation of the UV absorption spectra of As(III) oxo- and thio- acids and anions in aqueous solution and of PF_3 in the gas-phase. *Aquatic Geochemistry* **7**, 239-254

Tossell J. A. (2001a) Calculation of the structure, stabilities, and properties of mercury sulfide species in aqueous solution. *J. Phys. Chem. A* **105**, 935-941.

Tossell J. A. (2004) Calculations of the interaction of bicarbonate ion with arsenites in aqueous solution and with the surfaces of Al hydroxide mineral. In *Advances in Arsenic Research* American Chemical Society (in press).

Ullrich S. M., Tanton T. W., and Abdrashitova S. A. (2001) Mercury in the aquatic environment: A review of factors affecting methylation. Critical Reviews in *Environ. Sci and Tech.* **31**, 241-293.

Uhler A. D. and Helz G. R. (1984) Solubility product of galena at 298°K: A possible explanation for apparent supersaturation in nature. *Geochimica et Cosmochimica Acta* **48**, 1155-1160.

USGS (1995) Mercury contamination of Aquatic Ecosystems. U.S. Department of the Interior-U.S. Geological Survey Fact Sheet FS-216-95.

Vorob'eva S.V., Ivakin A. A., Gorelov A. M., and Getrman E. M. (1977) Thio-complexes of arsenic(III) in solution. *Russian J. of Inorganic Chemistry* **22**, 1479-1481.

Wagemann R. (1978) Some theoretical aspects of stability and solubility of inorganic arsenic in freshwater environments. *Water Research* **12**, 139-145.

Wagman D. D., Evans W. H., Parker V. B., Schumm R. H., Halow I., Bailey S. M., Churney K. L., and Nuttall R. L. (1982) The NBS tables of chemical and thermodynamic properties. Selected values for inorganic and C1 and C2 organic substances in SI units. *J. Phys. Chem. Ref. Data* **11**, Supplement No. 2, National Bureau of Standards, Washington, D.C.

Webster J. G. (1990) The solubility of As_2S_3 and speciation of As in dilute and sulphide-bearing fluids at 25 and 90°C. *Geochimica et Cosmochimica Acta* **54**, 1009-1017.

Weissberg B. G., Dickson F. W., and Tunell G. (1966) Solubility of orpiment (As_2S_3) in Na_2S-H_2O at 50-200°C and 100-1500 bars, with geological applications. *Geochimica et Cosmochimica Acta* **30**, 815-827.

Welz B. and Sperling M. (1999) *Atomic Absorption Spectrometry*. Wiley-VCH, Weinheim. Pp 170.

Wilken R. T., Wallschlager D., and Ford R. G. (2003) Speciation of arsenic in sulfidic waters. *Geochem. Trans*. **4**, 1-7.

Winder C. (1993) Toxicity of Metals, Ch. 9. In *Occupational Toxicology*. (ed. Stacey, N.H.). Taylor and Francis, Bristol, PA. Pp 165-175.

Winter M. "WebElements^{TM} Periodic table." (1993) The University of Sheffield and WebElements Ltd, UK. 18 Oct. 2004 <webelements.com>.

Wood S. A., Tait C. D., and Janecky D. R. (2002) A raman spectroscopic study of arsenite and thioarsenite species in aqueous solution at 25^{o}C. *Geochem. Trans*. **3**, 31-39.

Zheng Y., Stute M., van Geen A., Gavrieli I., Dhar R., Simpson H. J., Schlosser P., and Ahmed K.M. (2004) Redox controls of arsenic mobilization in Bangladesh groundwater. *Applied Geochemistry* **19**, 201-214.

Zotov A.V., Levin K. A., Kotova Z. Y., and Volchenkova V. A. (1982) An experimental study of the stability of silver hydroxychloride complexes in hydrothermal solution. *Geokhimiya* **8**, 1123-1136.

Zotov A.V., Levin K. A., Khodakovskiy I. L., and Kozlov V.K. (1986) Thermodynamic parameters of Ag(I) chloride complexes in aqueous solution at 273-623 K. *Geokhimiya* **5**, 690-702.